PREDICTION OF EXTREME RUNOFF FREQUENCY EVENTS IN SOUTHERN CALIFORNIA

by

Bennington J Willardson

A Dissertation Presented to the
FACULTY OF THE USC GRADUATE SCHOOL
UNIVERSITY OF SOUTHERN CALIFORNIA
In Partial Fulfillment of the
Requirements for the Degree
DOCTOR OF PHILOSOPHY
(CIVIL ENGINEERING)

August 2011

Dedication

I would like to dedicate this dissertation to several people who have encouraged and supported me throughout the long journey through my Ph.D. program. First of all, I dedicate this dissertation to my wife, Rachael H. Willardson. She has been the bedrock of our home and has kept things together through many long and lonely days, nights, and weekends as I have taken classes and pursued my research. Her constant encouragement has kept me moving forward through difficult times. I love you!

Second, I would like to dedicate this dissertation to my Grandfather, Dr. Lyman Sessions Willardson. His example inspired me to study engineering, as he brought home pictures and treasures from exotic places where he had worked on drainage and irrigation problems. Along with Rachael, he provided guidance and counsel about pursuing a PhD program. Although he did not live to see the completion of my studies, he played a pivotal role in my advanced education.

And lastly, I would like to dedicate this dissertation to my children, Logan, Luke, Liam, and Karlie. Their love and enthusiasm for life has kept me excited about each step of the journey and provided a fullness of experiences that have been unimaginable until experienced. Remember, patience and hard work will bring great results.

Acknowledgements

I am so thankful for the opportunity I have had to pursue a PhD at the University of Southern California. I would like to acknowledge Dr. Jiin-Jen Lee for his example of hard work, his encouragement, and his dedication to improving the understanding of his students. His well-rounded approach and deep dedication to his students has increased my knowledge in many areas.

I would like to acknowledge the Foundation for Cross-Connection Control and Hydraulic Research and the Sonny Astani Department of Civil and Environmental Engineering for funding my graduate studies. Without the support, I would not have been able to attend the University of Southern California. I am very thankful for the opportunity that I was provided.

I would like to acknowledge Dr. Iraj Nasseri, who has been a mentor for me professionally and has encouraged me to incorporate some of the extensive data that I worked with at Los Angeles County Department of Public Works into this research. His patience and care have been valuable to me as I have worked through my PhD program.

Table of Contents

Dedication....ii

Acknowledgements. iii

List of Tables viii

List of Figures x

Chapter 1 – Introduction 1
1.1 Frequency Distribution Analysis of Extreme Events 4
1.2 Probable Maximum Precipitation Analysis 5
1.3 Soil Characteristics 6
1.4 Fire Factor Analysis 6
1.5 Monte Carlo Simulation Model Development and Output.... 7

Chapter 2 – Runoff Frequency Analysis for Gaged Watersheds 9
2.1 A Brief History of Flood Frequency Analysis 10
2.2 Data Sources for Extreme Flood Event Evaluation 11
2.2.1 Systematic Streamflow Data 12
2.2.2 Historic Streamflow Data 13
2.2.3 Paleoflood Data 14
2.2.4 Climate Data 15
2.3 Probability Distribution Functions for Flood Frequency Analysis 17
2.3.1 General Extreme Event Distributions 17
2.3.2 Parameter Estimation Methods 18
2.4 Selection of Flood Frequency Analysis Distributions 30
2.4.1 Improvement of Site Data Using Regional Approaches 32
2.4.2 Evaluation of Hydrologic Frequency Analysis Using Different Distributions and Parameter Estimation Methods 35
2.5 Evaluation of Gage Records Using a Moving Time Window 37
2.6 Bootstrap Analysis of Data Using MLM, MOM, and L-Moments 45
2.7 Chapter Summary and Conclusions 59

Chapter 3 – Rain Gage Frequency Analysis and Comparison to Probable Maximum Precipitation Frequencies 60
3.1 Introduction to Extreme Rainfall Data, Frequencies, and Predictions of the Probable Maximum Precipitation 61
3.2 General Analysis of Rainfall Variables 66
3.3 Rainfall Data in Los Angeles County 75
3.4 Analysis of Rainfall Frequencies in Los Angeles County 79
3.5 HMR 58 PMP Values Within Los Angeles County 84

3.6 Hershfield PMP Values Within Los Angeles County 90
3.7 Chapter Summary and Conclusions..... 104

Chapter 4 – Rainfall to Runoff – The Watershed Influence 106
4.1 Soil Classifications for Soil Loss Analysis in Los Angeles County.... 107
4.2 Constant Loss Method 111
4.3 Runoff Coefficient Methods..... 117
4.4 Clark Method of Hydrograph Routing..... 127
4.5 Chapter Summary and Conclusions..... 144

Chapter 5 – Fire Effects in Watersheds..... 146
5.1 Wildfire in the Western U.S. and in Los Angeles County 147
5.2 Changes to Vegetation During Fires 151
5.3 Changes to Soils During Fires..... 153
5.4 Changes to Runoff After Fires..... 154
5.5 Watershed Recovery From Fires 159
5.6 Fire Factor Development..... 162
5.7 Fire Factor Frequency Analysis..... 167
5.8 Chapter Summary and Conclusions..... 184

Chapter 6 – Monte Carlo Analysis of Probable Maximum Precipitation Translation to Probable Maximum Flood..... 186
6.1 Introduction to Monte Carlo Simulation 187
6.2 Rainfall – PMP and LACDPW Hyetographs..... 190
6.3 Soils – LACDPW and SSURGO/STATSGO Data Sets..... 192
6.4 Fire Factor Generation for use with LACDPW Soil Data 194
6.5 Clark UH Model Analysis..... 197
6.6 Chapter Summary and Conclusions..... 203

Chapter 7 – Analysis of Monte Carlo Analysis and Measured Runoff Frequencies 204
7.1 Runoff Coefficient to Rainfall Frequency Analysis..... 205
7.2 PMF Frequency Analysis of the Dams 214
7.3 Chapter Summary and Conclusions..... 222

Chapter 8 – Conclusions and Recommendations for Future Studies 224
8.1 Specific Findings 224
8.2 General Findings..... 229
8.3 Recommendations 231
8.4 Future Studies..... 232

References..... 235

Appendices

Appendix A – Rain Gage Location and Record Length 246
Appendix B – Rain Gage Statistics, PMPs, and AEPs 251
Appendix C – Los Angeles Soil Equations and Variables..... 261
Appendix D – LACDPW Style Analysis of Gridded Fire Factor Data 268
Appendix E – Grid Frequency Analysis of Fire Factors by Size..... 272

List of Tables

Table 2.1 Limits of Extrapolation for Varied Data Sets and Methods..... 30

Table 2.2 Stream Gage Data for Hartford, Connecticut USGS Gage 36

Table 2.3 Recurrence Intervals from Entire Record Set - Hartford, CT Gage.... 38

Table 2.4 Recurrence Intervals for the Hartford, CT Gage – 100-yr Time Window 44

Table 2.5 Regional Bootstrap Analysis - Flow Rates for Estimation Methods 49

Table 2.6 Regional Bootstrap Analysis - Comparison of Estimation Methods 50

Table 2.7 At-Site Analysis - Flow Rates for Estimation Methods 53

Table 2.8 At-Site Analysis - Comparison of Estimation Methods..... 54

Table 2.8 At-Site Analysis - Comparison of Estimation Methods..... 57

Table 3.1 Alternating Block Method of Hyetograph Development 72

Table 3.2 Rainfall Regions of Los Angeles County..... 77

Table 4.1 Infiltration Rates for NRCS Soil Texture Classifications..... 109

Table 4.2 Infiltration Rates for Soil Classifications..... 111

Table 4.3 Application of Constant Loss Method 112

Table 4.3 Area-Weighted Constant Loss and Imperviousness Calculations 115

Table 4.4 Constant Loss Infiltration Rates - Los Angeles Watersheds 117

Table 4.5 Application of Runoff Coefficient Method..... 122

Table 4.6 Runoff coefficients at Dams for Extreme Historic Storm Events 124

Table 4.7 Regression Parameters Analyzed for R Coefficient Correlation 134

Table 4.8 Peak Flow Rates and Volumes for Deer DB..... 141

Table 4.9 Calibrated Watershed Characteristics 142

Table 5.1 Vegetation Regrowth Rate for Burned Watersheds 161

Table 5.2 1965 - 1970 Fire History Data for the South Fork Watershed 166

Table 5.3 Analysis of 25 Square Mile Grid in Antelope Valley-Grid #130 169

Table 5.4 Percentile Analysis of Fire Factor Data..... 171

Table 5.5 Grid Data Summary Analysis..... 172

Table 5.6 Analysis of FF Annual Exceedence Probabilities..... 178

Table 5.7 Comparison of Average Design Values 180

Table 5.8 AEP and Recurrence Interval for Grid Analysis Fire Factors 182

Table 6.1 FF Probability Density Function Determination..... 195

Table 6.2 Monte Carlo Analysis Cases..... 198

Table 6.3 Watershed Characteristics for Monte Carlo Models 201

Table 6.4 Area Weighted PMP and PMP Frequency Data 202

Table 7.1 Comparison of Actual and Monte Carlo Maximum Runoff Rates to PMF 216

Table 7.2 Summary of Actual and Monte Carlo Model Dam Runoff Frequencies 217

List of Figures

Figure 2.1 Normal Distribution – Record Length Effects on Peak Flow Estimates 40

Figure 2.2 Log-Normal Dist. – Record Length Effects on Peak Flow Estimates 41

Figure 2.3 LP3 Distribution – Record Length Effects on Peak Flow Estimates 42

Figure 2.4 GEV1 Distribution – Record Length Effects on Peak Flow Estimates 42

Figure 2.5 Gamma Distribution – Record Length Effects on Peak Flow Estimates 43

Figure 2.6 Recurrence Interval Range Comparison for Various Parameter Estimation Methods with Different Distributions for the Bootstrapped Samples 51

Figure 2.7 Range of Recurrence Intervals Using Various Parameter Estimation Methods and Distributions 55

Figure 2.8 Comparison of At-Site Parameter Estimation to Regional Bootstrapping Parameter Estimation 58

Figure 3.1 Summary of Procedures Used to Derive Design Rainfall Depths ... 64

Figure 3.2 ANSCOLD Recommended Values of PMP Event AEPs 65

Figure 3.3 Alternating Block Hyetograph Example 72

Figure 3.4 Hyetographs for Different Weightings on Alternating Block Method 75

Figure 3.5 Rain Gages and Regions Used in PMP Analysis 78

Figure 3.6 L-Moment Ratio Analysis for all Analyzed Gages 80

Figure 3.7 L-Moment Ratio Analysis for Gages with Over 50 Years of Record 81

Figure 3.8 L-Moment Ratio Analysis of Regional Averages 83

Figure 3.9 Close-up of L-Moment Ratio Analysis for Regional Averages 83

Figure 3.10 Isohyetal Distribution of PMP Based on HMR 58 and 59. 85

Figure 3.11 Recurrence Interval for PMP Estimates within Los Angeles County 86

Figure 3.12 Probability Distribution of Recurrence Interval by Region 87

Figure 3.13 Probability of Recurrence Intervals Based on Record Length 88

Figure 3.14 Probability of Recurrence Intervals Based on Adjusted Record Length Groupings 89

Figure 3.15 Curve for Estimating K-Factor for Hershfield Method of PMP Analysis 91

Figure 3.16 Augmented f_1 Factor for Hershfield Analysis 94

Figure 3.17 Augmented f_2 Factor for Hershfield Analysis 94

Figure 3.18 Augmented f_3 Factor for Hershfield Analysis 95

Figure 3.19 Hershfield PMP Recurrence Interval Distribution by Order of Magnitude 97

Figure 3.20 Distribution of Order of Magnitude Differences in PMP Estimates 98

Figure 3.21 Spatial Analysis of Order of Magnitude Difference in Methodology 99

Figure 3.22 Hershfield Method PMP Contours for Los Angeles County 100

Figure 3.23 Comparison of Los Angeles Watersheds to ANSCOLD PMP Criteria 103

Figure 4.1 USDA Soil Texture Classification Nomograph 110

Figure 4.2 Rainfall Hyetograph and Constant Loss Excess Precipitation 113

Figure 4.3 Los Angeles County Runoff Coefficient Curve (LACDPW, 2006) . 121

Figure 4.4 Mean Annual Precipitation in Los Angeles County 125

Figure 4.5 Los Angeles County Runoff Coefficients Related to Frequency ... 126

Figure 5.1 Fires Within Los Angeles County (1878 – 2009) 150

Figure 5.2 Annual Area of County Burned by Wildfires 151

Figure 5.3 Burned Runoff Coefficients (C_{ba}) for Specific Soil in Los Angeles County 164

Figure 5.4 Santa Clara River South Fork Watershed Boundaries 166

Figure 5.5 Fire Analysis Grids (1, 5, 10, and 20 mile)..... 168

Figure 5.6 Major Watersheds Within Los Angeles County 174

Figure 5.7 Average Fire Factor by Watershed and Grid Size 175

Figure 5.8 Fire Factor Frequency Curves for Various Watershed Sizes..... 183

Figure 6.1 Monte Carlo Analysis Simulation Flow Chart for Each Realization..... 188

Figure 6.2 Thiessen Polygon Analysis of Rain Gages Within Los Angeles County 191

Figure 6.3 Monte Carlo Watershed Locations Within Los Angeles County 200

Figure 7.1 Case 1 – Runoff Coefficient vs. Rainfall Recurrence Interval Analysis 207

Figure 7.2 Case 2 – Runoff Coefficient vs. Rainfall Recurrence Interval Analysis 207

Figure 7.3 Case 3 – Runoff Coefficient vs. Rainfall Recurrence Interval Analysis 208

Figure 7.4 Case 4 – Runoff Coefficient vs. Rainfall Recurrence Interval Analysis 208

Figure 7.5 Case 5 – Runoff Coefficient vs. Rainfall Recurrence Interval Analysis 209

Figure 7.6 Case 6 – Runoff Coefficient vs. Rainfall Recurrence Interval Analysis 209

Figure 7.7 Comparison of Los Angeles and NRCS Soil Model Runoff Coefficients 210

Figure 7.8 Comparison of Monte Carlo Runoff Coefficients to Other Methods 211

Figure 7.9 Comparison of NRCS Models with MAP Requirements by DSOD 213

Figure 7.10 Range of Runoff Coefficients for Monte Carlo Analysis Models ... 214

Figure 7.11 L-Moments Frequency Distribution Analysis - Historic Data 220

Figure 7.12 L-Moment Plots Using Six Monte Carlo Models 220

Figure 7.13 Average L-Moment Ratios for Monte Carlo Cases and Actual Runoff 222

Chapter 1 – Introduction

The design and construction of public infrastructure, including roads, dams, channels, and buildings requires design criteria based on the purpose and life expectancy of the project. The design criteria determine the cost and risk associated with infrastructure construction. Major flood control projects normally require the capacity to carry runoff peak flows with a recurrence interval of once in 100 years, or an annual exceedence probability (AEP) of 0.01.

Runoff from watersheds is the result of several parameters, including: rainfall, soil type, antecedent moisture conditions, vegetation, slope, watershed shape, watershed size, and the degree of urbanization. Dams throughout the United States are designed to safely pass flow rates from the Probable Maximum Flood (PMF) in order to protect communities from catastrophic property damage and loss of life. The Bureau of Reclamation defines the PMF as “the maximum runoff condition resulting from the most severe combination of hydrologic and meteorologic conditions that are considered reasonably possible for the drainage basin under study” (Cudworth, 1989). Design of dam spillways often utilizes the PMF as the design event. Although this is standard practice, the PMF has no assigned recurrence interval.

Since the 1930s, engineers have been seeking methods to determine the probability of extreme runoff events and the associated risks. These studies have investigated the types of probability distributions needed for extreme event modeling, use of limited data sets, and regionalization of probability distribution parameters. The Interagency Committee on Water Data (IACWD, 1982) published Bulletin 17B to standardize the approach used by engineers working on Federal projects. Recently, focus has been directed at updating this document to use advances in the frequency analysis of extreme events. Most of the research into updating Bulletin 17B has been directed at frequency analysis of watersheds with data in the form of systematic runoff gage records, historical flood levels, and paleoflood data.

Bulletin 17B recommended further research needs. A major research need suggested by Bulletin 17B was the application of flood frequency analyses to watersheds with little or no systematic runoff gage data. Several types of models have been investigated as methods to transform measured rainfall into runoff volumes and peak flows using physical processes, statistical analysis, or artificial intelligence theories. These models normally rely on runoff gage data for calibration. In order to apply data from gaged watersheds to ungaged watersheds, regional relationships must be established. Studies have been conducted to find these correlations on an as needed basis (Calzacia and Fitzpatrick, 1989; Dooge, 1959; Hodge and Tasker, 1995; Hosking and Wallace,

1997; Mayer, 1987). However, watershed response often depends on antecedent conditions and the magnitude of the event. Regional relationships comparing the frequency of the rainfall and runoff events are often not determined due to limitations in data, budget, and time constraints.

Evaluation of extreme events often relies on statistical distributions with thin upper tails. Use of statistical distributions to determine the 100-year design peak flow often yields varied results, even when the analyzed gage data set contains over 100 years of record. Use of different estimators for statistical variables also influences the values produced by the statistical distributions. The most common variable estimators are the method of moments, probability weighted moments, and the maximum likelihood method.

In an effort to improve cost effectiveness and risk management for engineering structures, this dissertation evaluated hydrologic frequency analysis for extreme events to find out whether use of the Probable Maximum Precipitation (PMP) frequency could help anchor PMF runoff frequency distributions to produce similar runoff estimates for engineering design time frames ranging from 50 to 500 years.

The studies involved in this dissertation evaluated rainfall frequencies, soil characteristics, the effects of fire on vegetation and soils, and how those inputs

affected runoff frequency. Monte Carlo simulation was completed for several cases and compared to actual runoff data for 27 watersheds. Twelve of the watersheds were controlled by dams, the others were uncontrolled. Each of the major components of the study are briefly described below and the appropriate section with detailed information is called out.

1.1 Frequency Distribution Analysis of Extreme Events

In an effort to evaluate the PMF runoff frequencies comprehensively, the effects of record length, probability distribution, and parameter estimation methods were investigated. Chapter 2 provides analysis results on peak flow prediction using various distributions and distribution parameter estimation methods for a large data set. The section utilizes records from the Hartford, Connecticut runoff gage, which has records dating back to the 1600s. The section evaluates the effects of utilizing different portions of the record to estimate extreme event values, and the impact associated with utilizing different methodologies. The results presented in Section 2 provide useful information for understanding the limitations of flood frequency analysis.

1.2 Probable Maximum Precipitation Analysis

Rainfall is the most critical element in generating runoff in a watershed. The most extreme rainfall possible is defined as the Probable Maximum Precipitation (PMP). The definition of the PMP is the maximum amount of rainfall that may fall in a region based on the meteorological and orographic characteristics. The World Meteorological Organization and the United States National Oceanic and Atmospheric Administration developed procedures for determining the Probable Maximum Precipitation. The PMP then becomes input to hydrologic models used to develop PMF estimates in gaged and ungaged watersheds. Conversion of the PMP total volume into a rainfall hyetograph requires a temporal distribution. The two hyetographs used to represent temporal distribution of the PMP rainfall are discussed in Chapter 3, Section 3.1.

Chapter 3 contains analysis and comparison of rain gage data within Los Angeles County to PMP estimates based on two methods. The two methods for developing PMP estimates in this study were the method outlined in Hydrometeorological Reports (HMR) 58 and 59 developed by the National Oceanic and Atmospheric Administration (NOAA) and the Hershfield Method. The estimated rainfall frequencies generated by these methodologies and results of the comparison are presented.

1.3 Soil Characteristics

Storm runoff from a watershed is influenced by many factors. These include watershed shape, slope, soil type, antecedent soil moisture conditions, vegetation, storage, etc... The Monte Carlo models required soil input parameters to transform rainfall into excess precipitation. Two methods of soil parameter estimation are presented, the constant loss method, and the runoff coefficient method. Chapter 4 discusses how soil losses and watershed storage and shape are factored into the analysis of the PMF. The section also discusses how values were determined for the 27 watersheds studied.

1.4 Fire Factor Analysis

In many areas throughout the world, runoff is affected by wildfires. Watersheds in Southern California are very susceptible to fire due to the arid climate, chaparral covered foothills, and large populations. Chapter 5 discusses how fire affects watershed soils and vegetation, watershed recovery periods, and how watershed size relates to the probability of being partially or completely burned during a given year. The section also discusses how this probability can be factored into the analysis of the PMF.

1.5 Monte Carlo Simulation Model Development and Output

Chapter 6 provides discussion on the Monte Carlo simulation model developed to evaluate PMF runoff frequencies for watersheds within Los Angeles County. The model incorporates standard hydrologic methods along with the PMP, local soil data, wildfire impacts, watershed characteristics to generate runoff frequency curves for specific watersheds.

The model is used to evaluate six different cases, which include two soil methods, two hyetograph methods, and two fire factor scenarios. The Monte Carlo modeling evaluated 27 watersheds using all six cases to evaluate the impacts of different modeling methods on results.

Chapter 7 contains the results of the Monte Carlo simulation, runoff frequency analysis, and comparison to requirements of the California Department of Water Resources Division of Safety of Dams (DSOD) and others. Different modeling approaches yield different ranges of output. These ranges are discussed and analyzed to determine the applicability of modeling approaches.

This study investigated methods to improve the prediction of rare hydrologic events to help quantify risks in the design of hydraulic structures more accurately. The study evaluated variations in predicted risk based on the

statistical distributions and estimation techniques. It also evaluated the relationship between watershed area and the recurrence of fire within the watershed. The study evaluated several methodologies in modeling watersheds to determine the impacts of parameter selection on runoff frequencies. The PMP and PMF recurrence intervals were evaluated as a possibility to provide an anchor to extreme limit predictions in the 100-year to 500-year floods needed for design of critical infrastructure.

Chapter 2 – Runoff Frequency Analysis for Gaged Watersheds

Hydrologists apply frequency analysis to estimate the probabilities associated with design events (Kite, 1988). There are advantages and disadvantages when conducting frequency analysis to determine engineering projects risks. Although many criticize the methods and assumptions used for frequency analysis, it is one of the few tools available for defining project risks.

This chapter will provide a brief introduction to flood frequency analysis before going on to cover data sources used for runoff frequency analysis, their importance, and limitations. It will also cover several probability distribution functions currently used to predict extreme events in hydrologic engineering.

After the discussion of the distributions and parameter estimation methods, the methods for selecting a distribution for use in a study will be discussed in Section 2.4. The effects of gage record length on the distribution parameters and resulting estimation of probabilities will be discussed in Section 2.5. The final section in this chapter, Section 2.6, covers a bootstrap analysis of one data set to evaluate parameter estimation methods in developing probability estimates.

2.1 A Brief History of Flood Frequency Analysis

The use of statistical methods to analyze runoff began early in the 20th century. Public works agencies employed statistical methods for evaluating risks on construction of power generation, water supply, and flood control facilities. From the 1940s to 1950s, funding was secured through the Bureau of the Budget and a need arose for standard procedures to estimate risks in water resources projects. The Water Resources Council (WRC) published Bulletin 15, A Uniform Technique for Determining Flood Flow Frequency, as a first attempt to address flood frequency analysis.

The WRC revised the bulletin several times after the initial publication. The current version is Bulletin 17B, Guidelines for Determining Flood Flow Frequency, published in 1982. Bulletin 17B contains a section discussing research needs in several areas. The last twenty years have added research papers to many of the areas, but resolution of the issues remains elusive.

Continued research and development to solve the frequency analysis problems is needed due to the range of uncertainty in the analyses (IACWD, 1982; Kite, 1988). The Interagency Water Resources Council currently has a Hydrologic Frequency Analysis Work Group investigating changes to Bulletin 17B.

2.2 Data Sources for Extreme Flood Event Evaluation

All methods of frequency analysis are completely data dependent (Kite, 1988). Physically based models require information on the physical characteristics of the watershed including soil properties, slopes, land use, rainfall values, area, etc. Statistical analysis requires adequate data to represent the true distribution characteristics for the actual event population. Artificial intelligence methods, such as genetic algorithms, artificial neural networks, and fuzzy logic require enough data to train the model or compare results to actual events.

In the event that data at a site is limited, regional data provides a way to substitute space for time. Two main reasons exist for determining regional flood frequency relationships. The first reason is that single station sample variation is subject to large errors. The second reason is that there are more sites requiring data collection than there are sites with measured data. All frequency analyses, regional and site-specific, involve risks. In determining the design flood for a project, the length of records available, the project life expectancy, and the permissible probability of failure are all factors to be considered (Kite, 1988).

Engineers should investigate all types and sources of data before performing a frequency analysis to reduce the uncertainties in the analysis. The following paragraphs provide a brief discussion on data types used for frequency analysis,

even though this information is available in many engineering texts and research articles (Maidment, 1993; Hosking and Wallace, 1997, Rao and Hamed, 2000, Linsley, Kohler, and Paulhus, 1982).

2.2.1 Systematic Streamflow Data

Systematic streamflow data are normally used as the most reliable data source for frequency analysis studies. Systematic streamflow data is usually collected and archived by Federal, State, and local government agencies. Some data is also collected by non-government organizations. Streamflow records consist of data collected at established gaging stations operated and maintained over a continuous time period. The systematic data collected at these sites is based on the river water surface elevations, which are compared to rating curves developed by flow measurement at the site. Systematic streamflow records can include continuous flow data, estimates of peak discharge, and average or mean discharge for various time periods. Most systematic streamflow measurements on U.S. streams began after 1900 with only a few records dating back that far. Systematic records at a single site normally contain 20 to 60 years of record. The completeness of the data set varies from station to station.

2.2.2 Historic Streamflow Data

Historic streamflow data can extend the record length for many types of data, especially for extreme event frequency analysis (Swain et al, 1998). These data are most commonly used to extend peak discharge records to time periods prior to establishment of systematic stream gaging records. This type of data usually comes from measured high water marks indicating maximum levels, or knowledge that no flood has ever reached a certain level such as a bridge deck. Historic flood information should be obtained and documented whenever possible, particularly where the systematic record is relatively short. Use of historic data assures that estimates fit community experience and improves the frequency determinations (IACWD, 1982).

Historic observations also provide information about weather patterns, the frequency of extreme storm events, and changes in land use or vegetation that may be significant to runoff modeling calculations. However, use of historical data requires assessing the accuracy and validity of the observations. Historic data must be compared to the other types of data used in the analysis. Data that is much more extreme than the systematic data range should be evaluated carefully before use in frequency analysis.

2.2.3 Paleoflood Data

Paleoflood hydrology is the study of past or ancient flood events that occurred prior to the time of human observation or direct measurement by modern hydrological procedures (Baker, 1987). Unlike historic data, paleoflood data does not involve direct human observation of the flood events. Instead, the paleoflood investigator studies geomorphic and stratigraphic records (various indicators) of past floods, as well as the evidence of past floods and streamflow derived from historical, archeological, dendrochronologic, or other sources.

Paleoflood data generally includes records of the largest floods, or the largest floods stage limits over long time periods. This information can be converted to peak discharges using a hydraulic flow model. Generally, paleoflood data consist of two independent components, a peak discharge estimate and the time period or age over which the peak discharge estimate applies (Swain et al, 1998). Paleoflood studies can provide estimates of peak discharge for specific floods in the past, or they can provide exceedance and non-exceedance bounds for extended time periods. These differing types of paleoflood data must be appropriately treated in flood frequency analyses.

The addition of historical and paleoflood data to frequency analysis helps obtain realistic estimates of extreme flood quantiles (England et. al, 2003). Use of paleoflood data often extends records lengths by a factor of 10 to 100 times

longer than conventional or historical records. The extension occurs because paleoflood data is often the largest flood that has occurred in an area over an extremely long time period, indicating a recurrence interval roughly the same age as the date of the event. This is especially true in the western United States. In addition, the paleoflood record is a long-term measure of the tendency of a river to produce large floods (Swain et al, 1998).

Paleoflood data can improve understanding of the magnitude, occurrence, and distribution of extreme floods. Paleoflood data also aids testing of flood frequency analysis assumptions, such as homogeneity and stationarity, the adequacy of distributions for fitting extreme quantiles, and the possible use of tail modeling procedures (England et. al, 2003). In many cases, paleoflood studies can provide a long-term perspective, which can put exceptional annual peak discharge estimates in context and assist in reconciliation of conflicting historical records (Swain et al, 1998).

2.2.4 Climate Data

Climate data is not used directly in flood frequency analysis. Precipitation and weather data are used as input variables for hydrologic models that then simulate runoff based on the input variables. Input to hydrologic models can include

rainfall, snowfall, snow water equivalent, temperature, solar radiation, and wind speed and direction from individual weather stations. Data is now also available for broader regions through remote sensing and radar data collection.

The available climate data varies greatly in record length and quality throughout the United States. Snowfall, snow water equivalent, solar radiation, and wind data are usually limited to record lengths of less than about 30 years. Basic rainfall and temperature data are available for some stations for up to 150 years, but in most cases are limited to less than 100 years (Swain et al, 1998).

The PMP event is a special case of extrapolated climate data (FEMA, 2001). The National Weather Service provides PMP estimates for the United States. Other organizations provide data for locations worldwide. These estimates are based on generalized methods recommended by the World Meteorological Organization (World Meteorological Organization, 1986).

The generalized methods used to determine probable maximum precipitation require data from a large region and make adjustments for moisture availability and topographic effects on extreme rainfall depths. Estimates of design rainfall depths between the credible limit of extrapolation and the PMP are based on interpolation procedures. These procedures attempt to link estimates from

different methods and data sets. However, the use of atmospheric models has begun to be explored for developing PMP estimates.

2.3 Probability Distribution Functions for Flood Frequency Analysis

Fitting a distribution to data sets produces compact and smoothed representations of the frequency distribution from the available data. Distribution fitting also provides a systematic procedure for extrapolation to frequencies beyond the range of the data set (Swain et al, 1998). The choice of an appropriate probability distribution function is often based upon examination of the data using probability plots, the physical origins of the data, previous experience, and prescriptive guidelines. Given a family of distributions, estimates of the distribution parameters are determined and used to calculate quantiles and expectations with the "fitted" model.

2.3.1 General Extreme Event Distributions

Several probability distribution function families exist for extreme event evaluations of hydrologic phenomenon. The families and the family specific distributions are provided below:

1. Normal: Normal, Log-Normal (2), Log-Normal (3)
2. Gamma: Exponential, Gamma (2), Pearson III, Log-Pearson III

3. Extreme Value: General Extreme Value, Extreme Value Type 1, Weibull
4. Wakeby: Wakeby (5), Wakeby (4), Generalized Pareto
5. Logistic: Logistic, Generalized Logistic

Each of these probability models has properties that lend themselves to the evaluation of extreme event data. However, they also have limitations. Some distributions exhibit boundedness under certain conditions. Some distributions produce negative values that are not observed in hydrologic data. The distributions with many parameters are very sensitive to data set size. These limitations require careful consideration when selecting a distribution. Currently, for flood frequency analysis, the United States Federal Government requires use of the Log-Pearson III distribution with specific instructions given in Bulletin 17B. Analysis of other hydrologic data sets and problems have no standard practice defined. Some practicioners and researchers still question the specification of one distribution and method for flood frequency analysis.

2.3.2 Parameter Estimation Methods

Fitting a probability distribution function requires estimating parameters from the measured data that represents the sample set. There are many methods available for parameter estimation, including: the method of moments (MOM), the maximum likelihood method (MLM), the probability weighted moments method

(PWM), the least squares method (LS), maximum entropy (ENT), mixed moments (MIX), the generalized method of moments (GMM), and incomplete means method (ICM). The three most commonly used methods for estimating flood frequency parameters are the method of moments (MOM), the maximum likelihood method (MLM) and probability weighted moments (PWM) (Rao and Hamed, 2000).

Method of Moments

One of the simplest and most commonly used parameter estimation approaches is the method of moments. However, MOM estimates are usually inferior in quality and generally are not as efficient as the MLM estimates. Method of Moments estimates for distributions with three or more parameters are very sensitive to sample size because higher order moments are more likely to be highly biased in relatively small samples (Rao and Hamed, 2000). Moments about the origin are the expected values of powers of a random variable. The r^{th} moment about the origin for a probability distribution with a probability density function f(x) is given by Equation 2.1:

$$\mu'_r = \int_{-\infty}^{\infty} x^r f(x)dx \qquad \text{for r=1} \qquad \mu'_r = \mu_1 = \text{mean} \tag{2.1}$$

The central moments μ_r are computed using Equation 2.2:

$$\mu'_r = \int_{-\infty}^{\infty} (x - \mu_1)^r f(x)dx \qquad \mu_1 = 0 \tag{2.2}$$

Sample moments m'_r and m_r are calculated using equations 2.3 and 2.4.

$$m'_r = \frac{1}{n}\sum_{i=1}^{n} x_i^r \qquad m'_1 = \bar{x} = \text{sample mean} \tag{2.3}$$

$$m_r = \frac{1}{n}\sum_{i=1}^{n} (x_i - \bar{x})^r \qquad m_1 = 0 \tag{2.4}$$

Cunnane (1989) showed that these sample moments are often biased and should be corrected. Equations 2.5, 2.6, and 2.7 show some of the corrected central moments.

$$\hat{m}_2 = \frac{1}{n-1}\sum_{i=1}^{n} (x_i - \bar{x})^2 \tag{2.5}$$

$$\hat{m}_3 = \frac{n}{(n-1)(n-2)}\sum_{i=1}^{n} (x_i - \bar{x})^3 \tag{2.6}$$

$$\hat{m}_4 = \frac{n^2}{(n-1)(n-2)(n-3)}\sum_{i=1}^{n} (x_i - \bar{x})^4 \tag{2.7}$$

However, bias correction using simple expressions of n may not adequately correct the bias when the sample size is small. Moment ratios are often used to describe statistical distributions and moment ratio diagrams can be used to determine how well a sample set matches a parent distribution. Conventional moment ratios include the coefficient of variation C_v, the coefficient of skewness C_s, and the coefficient of kurtosis C_k (Rao and Hamed, 2000). These ratios are provided in equations 2.8, 2.9, and 2.10. The sample set moment ratios are calculated by substituting m_r for μ_r.

$$C_v = \frac{(\mu_2)^{1/2}}{\mu_1'} \tag{2.8}$$

$$C_s = \frac{\mu_3}{(\mu_2)^{3/2}} \tag{2.9}$$

$$C_k = \frac{\mu_4}{(\mu_2)^2} \tag{2.10}$$

Wallis (1974) indicated that although the sample moments have been corrected for bias, further bias correction is required for the sample moment ratios based on the sample size, and the skewness and form of the parent population. Kirby (1974) showed that the bounds on the skewness coefficient and coefficient of

variation of positive data, the maximum standardized variate, and the standardized range are related only to the sample size.

Method of Maximum Likelihood

The maximum likelihood method is considered the most efficient parameter estimation method since it provides the smallest sampling variance of the estimated parameters, and hence of the estimated quantiles, compared to other methods (Rao and Hamed, 2000). Experience has shown MLM parameter estimates have very good statistical properties in large samples and generally work well with analysis of hydrologic records (Swain et al, 1998).

The MLM involves the choice of parameter estimates that produce a maximum probability of occurrence of the observations. The likelihood function is the joint probability density function (pdf) of the observations conditional on given values of the parameters. Equation 2.11 shows the form of the relationship for a function with a pdf f(x) and parameters α_1, α_2, α_k.

$$L(\alpha_1, \alpha_2 .... \alpha_k) = \prod_{i=1}^{n} f(x_i; \alpha_1, \alpha_2 .... \alpha_k) \qquad (2.11)$$

The values for α_1, α_2,..α_κ that maximize the likelihood function are computed by partial differentiation with respect to α_1, α_2, ... α_κ and setting the partial derivatives

equal to zero. The resulting equations are then solved simultaneously to obtain the parameter values. Often it is easier to maximize the natural logarithm of the likelihood function (Rao and Hamed, 2000). Reducing the MLM estimates to solvable formulas is not possible and only use of numerical methods provides estimates for the parameters (Stedinger et al., 1988; O'Connell, 1997).

However, for special cases, such as the Pearson Type III distribution, the optimality of the MLM is only asymptotic and small sample estimates may lead to estimates of inferior quality (Bobee and Ashkar, 1991). Although the MLM frequently gives biased estimates, these biases can be corrected. However, with small samples it may not be possible to get MLM estimates if the number of parameters is large (Rao and Hamed, 2000).

Probability Weighted Moments

Some distributions, such as the Wakeby distribution, are difficult to estimate by conventional methods such as MLM or MOM, and the desirability of obtaining a closed form estimate led Greenwood et. al (1979) to devise probability weighted moments (Hosking and Wallis, 1997). The Probability Weighted Moments method (Greenwood et. al, 1979; Hosking, 1986) gives parameter estimates comparable to MLM estimates, yet in some cases the estimation procedures are much less complicated and the computations are simpler (Rao and Hamed,

2000). Parameter estimates from small samples using PWM are sometimes more accurate than MLM estimates (Landwehr et al., 1979). In some cases, explicit expressions for the parameters can be obtained using PWM, which is not the case with MOM or MLM.

Obtaining PWM parameter estimates requires equating the parent distribution moments with the corresponding sample moments, as in the MOM. For a distribution with k parameters, $\alpha_1, \alpha_2, \ldots \alpha_\kappa$, the first k sample moments are set equal to the corresponding population moments. The resulting equations are solved simultaneously for the unknown parameters.

Greenwood et al. (1979) defined PWMs:

$$M_{p,r,s} = E\left[x^p F^r (1-F)^s\right] = \int_0^1 [x(F)]^p F^r (1-F)^s \, dF \qquad (2.12)$$

Equations 2.13 and 2.14 provide the most commonly considered moments used in frequency analyses.

$$M_{1,0,s} = \alpha_s = \int_0^1 x(F)(1-F)^s \, dF \qquad (2.13)$$

$$M_{1,r,0} = \beta_r = \int_0^1 x(F) F^r \, dF \qquad (2.14)$$

In the equations, p, r, and s are real numbers. When r and s equal zero and p is a non-negative number, $M_{p,0,0}$ represents the conventional moment of order p about the origin, μ'_p. When p=1 and either r or s is equal to zero, then $M_{1,r,0} = \beta_r$ and $M_{1,0,s} = \alpha_s$ are linear in x and of sufficient generality for parameter estimation (Hosking, 1986). As x only takes the power of 1, simpler relationships are obtained between the distribution parameters and the probability weighted moments than the corresponding relationships using conventional moments. For an ordered sample $x_1 \le ... \le X_N, N > r, N > s,$ unbiased sample PWMs are given by equations 2.15 and 2.16 (Rao and Hamed, 2000).

$$a_s = \hat{\alpha}_s = \hat{M}_{1,0,s} = \frac{1}{N}\sum_{i=1}^{N}\binom{N-i}{s} x_i \Big/ \binom{N-1}{s} \tag{2.15}$$

$$b_r = \hat{\beta}_r = \hat{M}_{1,r,0} = \frac{1}{N}\sum_{i=1}^{N}\binom{i-1}{r} x_i \Big/ \binom{N-1}{r} \tag{2.16}$$

Special cases of these estimators include the sample mean $\bar{x} = N^{-1}\sum x_i = a_0 = b_0$ and the extreme data values $x_1 = Na_{N-1}$ and $x_N = Nb_{N-1}$. Alternatively, consistent but biased estimators of PWMs may be obtained by using the plotting position $F_i = (i - 0.35))/N$. Practical experience shows that plotting position estimators sometimes yield better estimates, even though there is no theoretical reason for

preferring plotting position over unbiased estimators. Plotting position estimates are given by equations 2.17 and 2.18 (Rao and Hamed, 2000).

$$a_s = \hat{\alpha}_s = \hat{M}_{1,0,s} = \frac{1}{N}\sum_{i=1}^{N}(1-F_i)^s\, x_i \tag{2.17}$$

$$b_r = \hat{\beta}_r = \hat{M}_{1,r,0} = \frac{1}{N}\sum_{i=1}^{N}F_i^r\, x_i \tag{2.18}$$

The PWMs α_s and β_r are related as shown in equation 2.19.

$$\alpha_s = \sum_{i=1}^{s}\binom{s}{i}(-1)^i\beta_i\,,\ \beta_r = \sum_{i=1}^{r}\binom{r}{i}(-1)^i\alpha_i \tag{2.19}$$

These relationships provide the following particular relationships between α_s and β_r.

$$\alpha_0 = \beta_0 \qquad \beta_0 = \alpha_0$$

$$\alpha_1 = \beta_0 - \beta_1 \qquad \beta_1 = \alpha_0 - \alpha_1$$

$$\alpha_2 = \beta_0 - 2\beta_1 + \beta_2 \qquad \beta_2 = \alpha_0 - 2\alpha_1 + \alpha_2$$

$$\alpha_3 = \beta_0 - 3\beta_1 + 3\beta_2 - \beta_3 \qquad \beta_3 = \alpha_0 - 3\alpha_1 + 3\alpha_2 - \alpha_3$$

L-Moments

PWMs were found to perform well for other distributions, but were hard to interpret (Hosking and Wallis, 1997). L-moments are statistical quantities that are derived from PWMs and increase the accuracy and ease of use of PWM-based analysis (Hosking and Wallis, 1997).

L-moments are analogous to conventional moments but can be estimated by linear combinations of the elements of an ordered sample, that is, by L-statistics. L-moments have the theoretical advantages over conventional moments of being able to characterize a wider range of distributions and, when estimated from a sample, of being more robust to the presence of outliers in the data. L-moments are less subject to bias in estimation than other moment methods (Hosking and Wallis, 1997).

Hosking (1990) found that certain linear combinations of probability weighted moments, which he called L-moments, could be interpreted as measures of the location, scale, and shape of probability distributions and formed the basis for a comprehensive theory of the description, identification, and estimation of distributions (Hosking and Wallis, 1997). L-moments do not involve squaring or cubing the observed values, as do the product-moment estimators. As a result, L-moment estimators of the dimensionless coefficients of variation and skewness

are almost unbiased and have very nearly a normal distribution (Hosking and Wallis, 1997).

The L-moments are defined by Hosking in terms of the PWMs α and β as shown in equation 2.20.

$$\lambda_{r+1} = (-1)^r \sum_{k=0}^{r} p^*_{r,k} \alpha_k = \sum_{k=0}^{r} p^*_{r,k} \beta_k \tag{2.20}$$

where:

$$p^*_{r,k} = (-1)^{r-k} \binom{r}{k} \binom{r+k}{k} \tag{2.21}$$

Particular relationships between PWMs and L-moments are:

$$\lambda_1 = \alpha_0 \qquad \lambda_1 = \beta_0$$

$$\lambda_2 = \alpha_0 - 2\alpha_1 \qquad \lambda_2 = 2\beta_1 - \beta_0$$

$$\lambda_3 = \alpha_0 - 6\alpha_1 + 6\alpha_2 \qquad \lambda_3 = 6\beta_2 - 6\beta_1 + \beta_0$$

$$\lambda_4 = \alpha_0 - 12\alpha_1 + 30\alpha_2 - 20\alpha_3 \qquad \lambda_4 = 20\beta_3 - 30\beta_2 + 12\beta_1 - \beta_0$$

Sample L-moments (l_r) are calculated by replacing α and β with the sample estimates a and b. L-moment ratios, which are analogous to conventional moment ratios are defined by Hosking (1990) as in equations 2.22 and 2.23.

$$\tau = \lambda_2 / \lambda_1 \tag{2.22}$$

$$\tau_r = \lambda_r / \lambda_2 , r \geq 3 \tag{2.23}$$

In the L-moment analyses, λ_1 is a measure of location, τ is a measure of scale and dispersion (LC_v), τ_3 is a measure of skewness (LC_s), and τ_4 is a measure of kurtosis (LC_k). Sample L-moment ratios, t and t_r, are calculated by substituting l_r for λ_r. Hosking (1990) showed that for r greater than or equal to 3, the absolute value of τ_r is less than one. If $x \geq 0$, then τ the LC_v of x satisfies $0<\tau<1$. This boundedness of L-moment ratios is an advantage because it is easier to interpret a measure such as τ_3, which is constrained to lie within the interval (-1,1), than the conventional skewness coefficient which can take arbitrarily large numbers (Rao and Hamed, 2000). Vogel and Fennessey (1993) discuss the advantages of L-moments compared to product moments.

2.4 Selection of Flood Frequency Analysis Distributions

Frequency analysis is an information problem. With a sufficiently large data set of flood flows or rainfall for a basin, an accurate frequency distribution for a site could be determined. However, this assumes that anthropogenic or natural processes did not alter the distribution of floods over time. In most situations, available data are insufficient to define adequately the annual exceedance probability of large floods (Swain et al, 1998). Lack of data forces hydrologists to develop estimates using practical knowledge of the physical watershed processes with efficient and robust statistical techniques when determining runoff frequency analyses (Stedinger et al., 1993). Table 2.1 developed by Swain et al (1998) provides information on the credible probabilities of data sets based on the data pool available.

Table 2.1 Limits of Extrapolation for Varied Data Sets and Methods

Type of Data Used for Flood Frequency Analysis	Limit of Credible Extrapolation for Annual Exceedence Probability	
	Typical	Optimal
At-Site Streamflow Data	1 in 100	1 in 200
Regional Streamflow Data	1 in 750	1 in 1,000
At-Site Streamflow and At-Site Paleoflood Data	1 in 4,000	1 in 10,000
Regional Precipitation Data	1 in 2,000	1 in 10,000
Regional Streamflow and Paleoflood Data	1 in 15,000	1 in 40,000
Regional Data and Extrapolations	1 in 40,000	1 in 100,000

Swain et. al. (1998) provide the following discussion regarding Table 2.1.

> Many factors can affect the equivalent independent record length for the optimal case. For example, gaged streamflow records in the western United States only rarely exceed 100 years, and extrapolation beyond twice the length of record, or to about 1 in 200 AEP, is generally not recommended (Interagency Advisory Committee on Water Data [IACWD], 1982). Likewise, for regional streamflow data the optimal limit of credible extrapolation is established at 1 in 1,000 AEP by considering the number of stations in the region, lengths of record, and degree of independence of these data (Hosking and Wallis, 1997). For paleoflood data, only in the Holocene epoch (or the past 10,000 years) is climate judged to be sufficiently like that of the present climate for these types of records to have meaning in estimating extreme floods for dam safety risk assessment. This climatic constraint indicates that an optimal limit for extrapolation from paleoflood data, when combined with at-site gaged data, for a single stream should be about 1 in 10,000 AEP. For regional precipitation data, a similar limit is imposed because of the difficulty in collecting sufficient station-years of clearly independent precipitation records in the orographically complex regions of the western United States. Combined data sets of regional gaged and regional paleoflood data can be extended to smaller AEPs, perhaps to about 1 in 40,000, in regions with abundant paleoflood data. Analysis approaches that combine all types of data are judged to be capable of providing credible estimates to an AEP limit of about 1 in 100,000 under optimal conditions.

The Federal guidelines published in Bulletin 17B (IACWD, 1982) recommend fitting a Pearson type 3 distribution to the common base 10 logarithms of the peak discharges. It uses at-site data to estimate the sample mean and variance of the logarithms of the flood flows, and a combination of at-site and regional information to estimate skewness (Swain et al, 1998).

Many other studies have shown that the distributions in the section on general extreme events work in different regions and for different types of hydrologic studies (Gunasekara and Cunnane, 1992; Vogel et al, 1993). The limits of data

extrapolation cause serious concern for hydrologists, especially when the data set being evaluated is relatively short, consisting of ten to twenty-five years of data.

2.4.1 Improvement of Site Data Using Regional Approaches

In a study performed under the guidance of the National Research Council (1988), several strategies were proposed in an effort to improve at-site data sets. These included substituting space for time to estimate extreme floods. Substituting space for time requires using hydrologic information at different locations in a region to compensate for short records at a single site. Cudworth (1989) detailed three procedures considered for regional flood frequency analysis. The approaches include the average parameter approach; the index flood approach; and the specific frequency approach. With the average parameter approach, some parameters are assigned average values based upon regional analyses, such as the log-space skew or standard deviation. Other parameters are estimated using at-site data, or regression on physiographic basin characteristics**,** perhaps the real or log-space mean. The index flood method is a special case of the average parameter approach. The specific frequency approach employs regression relationships between drainage basin characteristics and particular quantiles of a flood frequency distribution (Cudworth, 1989).

Swain et al, (1998) summarized the three approaches discussed by Cudworth. The summary of each is provided below:

Index Flood Method – The index flood procedure is a simple regionalization technique with a long history in hydrology and flood frequency analysis (Dalrymple, 1960). It uses data sets from several sites in an effort to construct more reliable flood-quantile estimators. A similar regionalization approach in precipitation frequency analysis is the station-year method, which combines precipitation data from several sites without adjustment to obtain a large composite record to support frequency analyses. The concept underlying the index flood method is that the distributions of floods at different sites in a "region" are the same except for a scale or index-flood parameter which reflects the size, rainfall and runoff characteristics of each watershed. The mean is generally employed as the index flood.

Average Shape Parameter – As at-site records increase in length, procedures that estimate two parameters, with at-site data to be used with a regional shape parameter, have been shown to perform better than index flood methods in many cases. For record lengths of even 100 years, 2-parameter estimators with a good estimate of the third shape parameter**,** are generally more accurate than are 3-parameter estimators. However, whether or not it is better to also regionalize the coefficient of variation depends upon the heterogeneity of the regions and the

coefficients of variability of the flows. In regions with high coefficients of variation (and high coefficients of skewness) index flood methods are more attractive.

Regional Regression – Regional regression analysis is used to derive predictive equations for values of various hydrologic statistics such as means, standard deviations, quantiles, and normalized regional flood quantiles based on physiographic watershed characteristics and other independent parameters. A specialized Generalized Least Squares (GLS) regression methodology was developed by Stedinger and Tasker (1985, 1986a, 1986b) to address regionalization of hydrologic statistics. Advantages of the GLS procedure include more efficient parameter estimates when some sites have short records, an unbiased model-error estimator, and a better description of the relationship between hydrologic data and information for hydrologic network analysis and design.

Law and Tasker (2000) summarized work on another method for augmenting short records at a site. The region-of-influence method uses multivariable regression equations for each recurrence-interval peak flow based on explanatory data to produce information for ungaged watersheds. The data set is derived from a unique group of similar gaging stations selected from a larger group of stations within the study area The unique group of stations that are most similar to the site of interest is called the “region-of-influence” by Burn (1990a, b).

Gaging station similarity to the site of interest is measured by the similarity in basin characteristics rather than by the physical distance between the sites.

2.4.2 Evaluation of Hydrologic Frequency Analysis Using Different Distributions and Parameter Estimation Methods

In order to provide a foundation for further discussion, three evaluations were conducted on data from the Hartford, Connecticut runoff gage maintained by the United States Geologic Survey. This gage was selected due to the extensive systematic record length and the incorporation of 4 historic events which extend the set from 1683 through 2005. The USGS collected systematic runoff data at the gage from 1838 to the present. Besides the systematic data, the data record contains four historic floods from 1683, 1692, 1801, and 1828. Table 2.2 contains the peak flow data for this station. Notes from the USGS records indicate that until 1956, the system was not greatly influenced by regulation and diversions. After 1956, the gage records indicate measurement of peak flows could be influenced by regulation and diversion. It is interesting to note that the largest peak flow rate recorded occurred before the time affected by regulation. The highest magnitude of 313,000 cfs was recorded in 1936 and the second highest runoff was 251,000 cfs recorded in 1938.

Table 2.2 Stream Gage Data for Hartford, Connecticut USGS Gage

Year	Flow Rate (cfs)	Year	Flow Rate (cfs)	Year	Flow Rate (cfs)	QC	Year	Flow Rate (cfs)	QC
1683	145,000	1879	102,000	1922	129,000		1964	80,000	6
1692	146,000	1880	60,000	1923	107,000		1965	36,000	6
1801	160,000	1881	66,000	1924	95,000		1966	57,000	6
1828	112,000	1882	57,000	1925	94,000		1967	79,000	6
1838	115,000	1883	95,000	1926	96,000		1968	97,000	6
1839	126,000	1884	103,000	1927	78,000		1969	114,000	6
1841	147,000	1885	76,000	1928	180,000		1970	73,000	6
1843	157,000	1886	105,000	1929	82,000		1971	75,000	6
1844	86,000	1887	111,000	1930	53,000		1972	92,000	6
1845	83,000	1888	85,000	1931	76,000		1973	99,000	6
1846	82,000	1889	42,000	1932	94,000		1974	73,000	6
1847	100,000	1890	62,000	1932	94,000		1975	76,000	6
1848	63,000	1891	88,000	1933	145,000		1976	109,000	6
1849	73,000	1892	78,000	1934	115,000		1977	113,000	6
1850	106,000	1893	124,000	1935	95,000		1978	68,000	6
1851	54,000	1894	51,000	1936	313,000		1979	101,000	6
1852	116,000	1895	142,000	1937	61,000		1980	87,000	6
1853	63,000	1896	144,000	1938	251,000		1981	105,000	6
1854	185,000	1897	96,000	1939	98,000		1982	101,000	6
1855	102,000	1898	100,000	1940	116,000		1983	94,000	2,6
1856	117,000	1899	106,000	1941	47,000		1984	192,000	6
1857	86,000	1900	118,000	1942	70,000		1985	40,000	6
1858	77,000	1901	148,000	1943	75,000		1986	83,000	6
1859	148,000	1902	139,000	1944	76,000		1987	139,000	6
1860	63,000	1903	117,000	1945	89,000		1988	71,000	6
1861	102,000	1904	101,000	1946	72,000		1989	85,200	6
1862	173,000	1905	123,000	1947	89,000		1990	93,200	6
1863	108,000	1906	91,000	1948	125,000		1991	72,800	6
1864	71,000	1907	94,000	1949	133,000		1992	68,200	6
1865	132,000	1908	78,000	1950	83,000		1995	45,500	5
1866	96,000	1909	131,000	1951	106,000		1996	106,000	5
1867	90,000	1910	93,000	1952	105,000		1997	79,900	6
1868	102,000	1911	63,000	1953	132,000		1998	102,000	6
1869	152,000	1912	100,000	1954	82,000		1999	74,500	6
1870	148,000	1913	144,000	1955	198,000		2000	72,100	6
1871	81,000	1914	105,000	1956	110,000	6	2001	100,000	6
1872	98,000	1915	95,000	1957	38,000	6	2002	69,800	6
1873	99,000	1916	88,000	1958	105,000	6	2003	92,000	6
1874	123,000	1917	78,000	1959	95,000	6	2004	98,100	5
1875	81,000	1918	82,000	1960	157,000	6	2005	113,000	5
1876	106,000	1919	89,000	1961	73,000	6			
1877	113,000	1920	110,000	1962	94,000	6			
1878	79,000	1921	90,000	1963	85,000	6			

The quality codes shown in the columns labeled “QC” in Table 2.2 indicate issues related to the data collection. Quality code 2 indicates that the discharge is an estimate and was not measured by the instrumentation due to the magnitude of the flows or damage to the equipment. Quality code 5 deals with the development of a river system. As urbanization occurs, dams and diversions are added to the system, which influence releases and magnitudes of storm flows. Quality code 6 indicates that upstream regulation and diversion are known to affect flow rates.

2.5 Evaluation of Gage Records Using a Moving Time Window

Record length influences the estimation of distribution variables such as the mean and standard deviation. To demonstrate the effects of record length on frequency analysis, a moving time window was used to divide the original record set into multiple data sets of a specific length. The data sets evaluated included record lengths of 10, 25, 50, and 100 years. The number of data sets investigated for each record length size can be determined by the equation n=x-l, where n is the number of tested sets, x is the number of record years, and l is the number of records in each data set. For example, 156 different data sets with a 10 year long record were evaluated with x=166, l=10, and n=166-10=156.

The record length evaluation utilized the MOM parameter estimators for five different statistical distributions. These included the normal, Log-normal (2), Extreme Value 1 (Gumbel), Log-Pearson III, and Gamma frequency distributions.

The evaluation with the moving time window was conducted to determine the effects of record length and the period of systematic data on the estimated runoff values for recurrence intervals of 10, 25, 50, 100, 200, 500, 1,000, and 10,000 years. Table 2.3 contains the estimations of extreme events for the listed recurrence intervals using the listed probability distributions. The estimations utilized the entire data set from the systematic record, but excluded the historical events.

Table 2.3 Recurrence Intervals from Entire Record Set - Hartford, CT Gage

Recurrence Interval	**Extreme Value Probability Distributions**				
T	**Normal**	**Log-Normal**	**Log-Pearson III**	**GEV1/Gumbel**	**Gamma**
1.25	69,662	71,513	71,408	70,412	77,757
2	100,411	94,848	94,308	94,409	104,979
5	131,160	125,797	125,560	126,696	137,939
10	147,233	145,806	146,319	148,074	157,583
25	164,373	170,663	172,639	175,084	180,430
50	175,445	188,931	192,337	195,121	196,257
100	185,405	207,027	212,207	215,011	211,223
200	194,520	225,103	232,329	234,828	225,533
500	205,566	249,136	259,513	260,973	243,670
1,000	213,314	267,510	302,353	280,733	256,919
10,000	236,287	330,345	355,118	346,339	298,790

Table 2.3 shows the difference in estimation of flow rates varies based on the distribution used. For example, although the systematic record used had 166 years of data, the estimate for the 100 year event is inconsistent, ranging from 185,405 to 215,011 cfs. As the recurrence interval of the event being estimated becomes more extreme, the difference between probability distributions becomes more extreme. When record lengths are limited, the differences also become more extreme. The moving time window analysis was conducted to systematically evaluate how extreme these differences become.

The analysis of the data for the Hartford, CT gage using the moving time window is summarized in five figures showing the range of average, minimum, and maximum values calculated for the different time window representing a specific period in the gage data. Figures 2.1 through 2.5 represent a graphical summary of the moving time window analysis. The graphs plot the results on the same scale, with the same legend, to facilitate visual comparison between different distributions. The data for specific recurrence intervals on the figures can be compared to Table 2.3 to evaluate the effects of a short record on the estimation of peak flow rates for a watershed using extensive records.

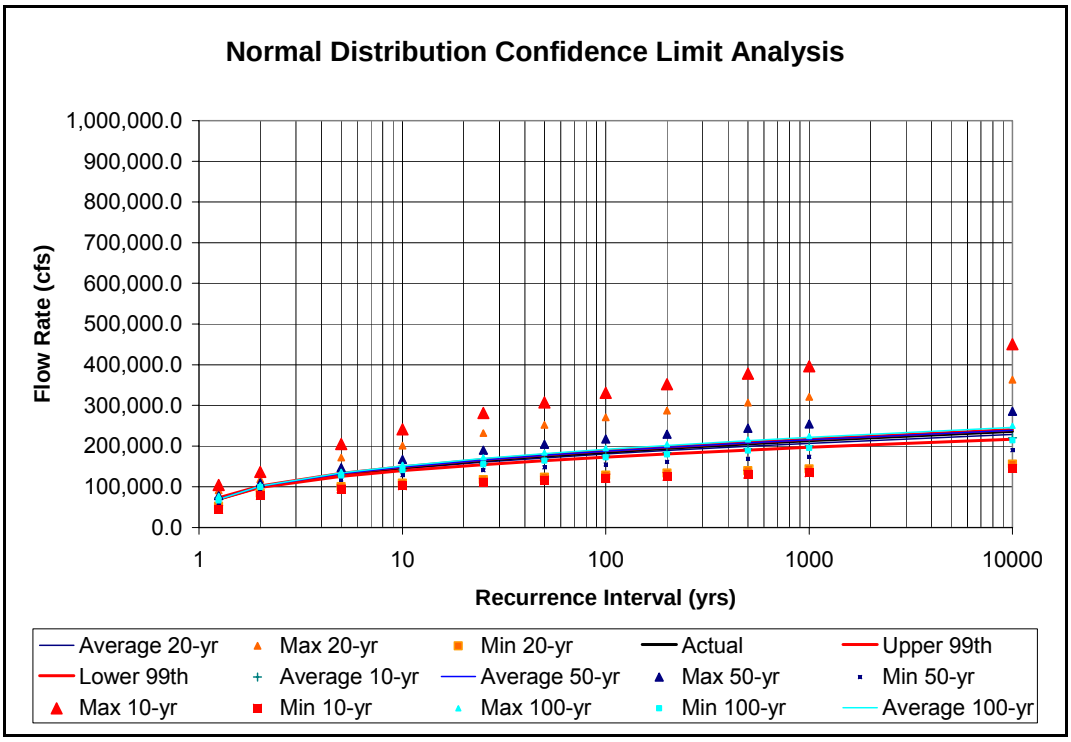

Figure 2.1 Normal Distribution – Record Length Effects on Peak Flow Estimates

Figure 2.1 shows the analysis results for the 10, 20, 50, and 100 year record lengths in a graphical format. As can be seen, the maximum and minimum values for the 10 year record sets are much larger and smaller respectively. For example, when looking at the 100-year estimated flow rate, the lowest 10 year record set produced a runoff estimate of approximately 100,000 cfs, while the largest estimate from a 10 year record set estimated 350,000 cfs. The range of values using the 166 year record set as shown in Table 2.3 ranges from 185,405 to 215,011 cfs.

For a 100 year record length moving time window, the minimum 100-year flow rate was 175,000 cfs, while the maximum was 195,000 cfs. Comparison to

Table 2.3 shows that use of the entire record set results in a range from 185,405 to 215,011 cfs as noted above. This information is very important. It shows how an estimated flow rate can vary, even when using the same record set over a different time period. Even with 100 years of data, the 100-year runoff estimate can still vary 20,000 cfs, which represents a 10 percent difference. As the record length decreases, the error in estimation increases greatly. The same trends can be seen in Figures 2.2 through 2.5.

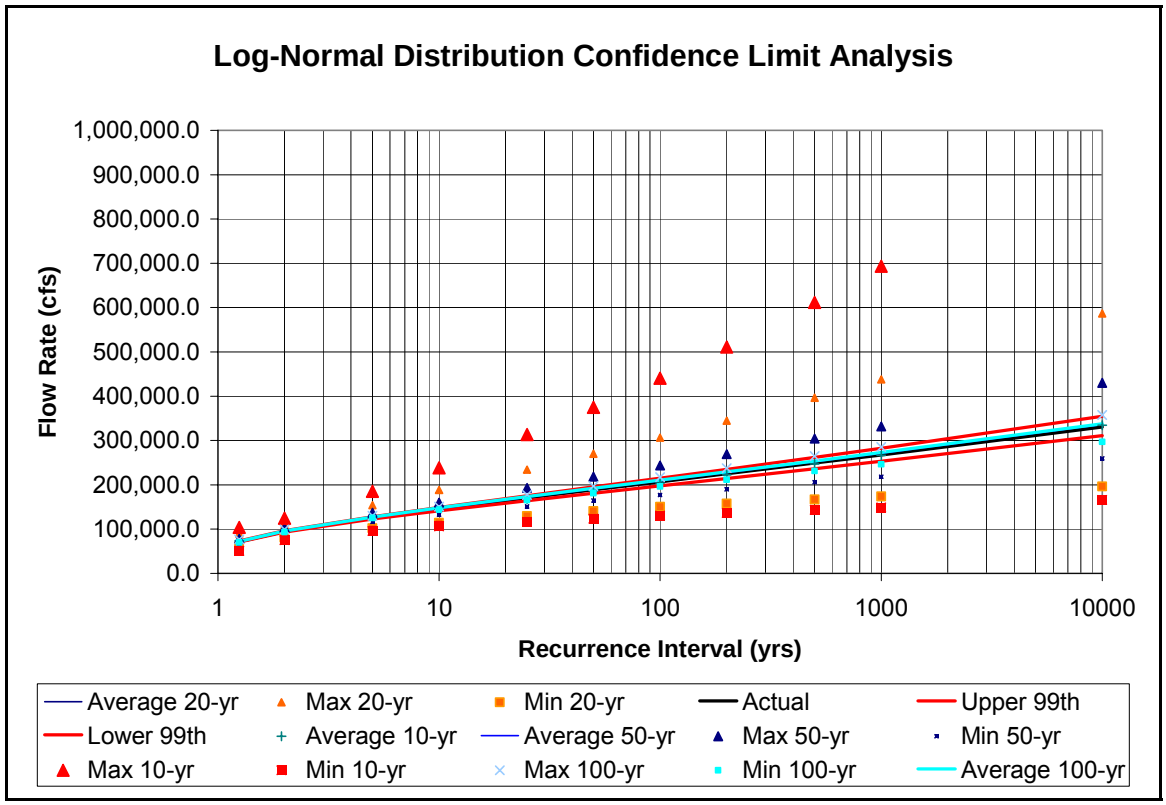

Figure 2.2 Log-Normal Dist. – Record Length Effects on Peak Flow Estimates

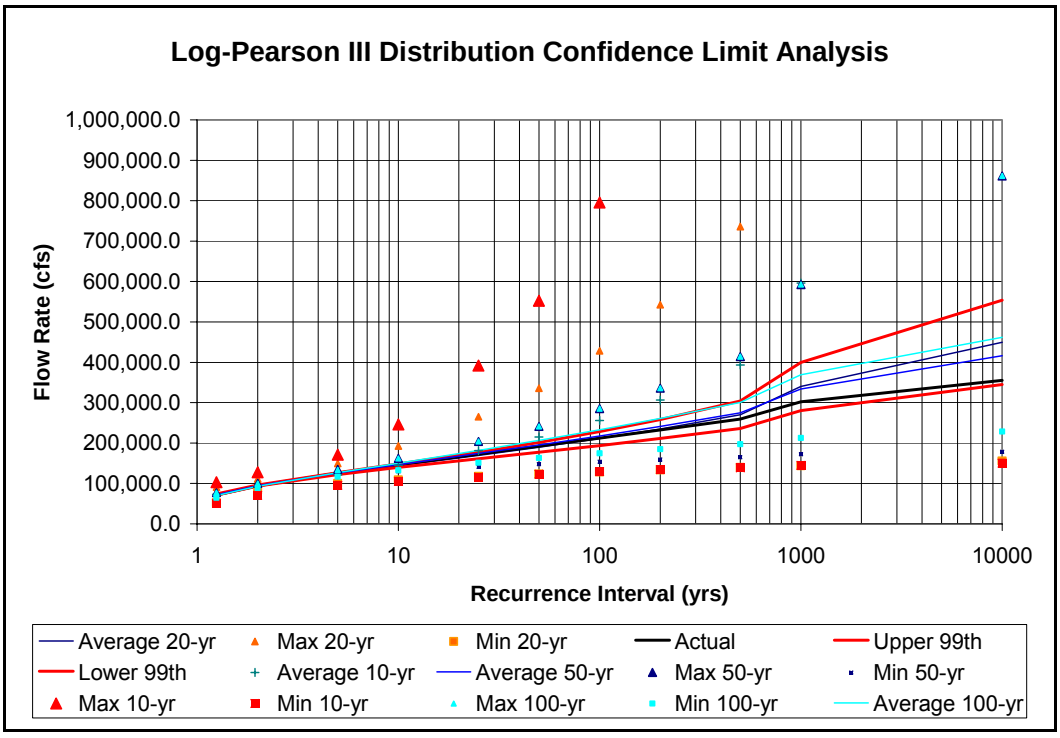

Figure 2.3 LP3 Distribution – Record Length Effects on Peak Flow Estimates

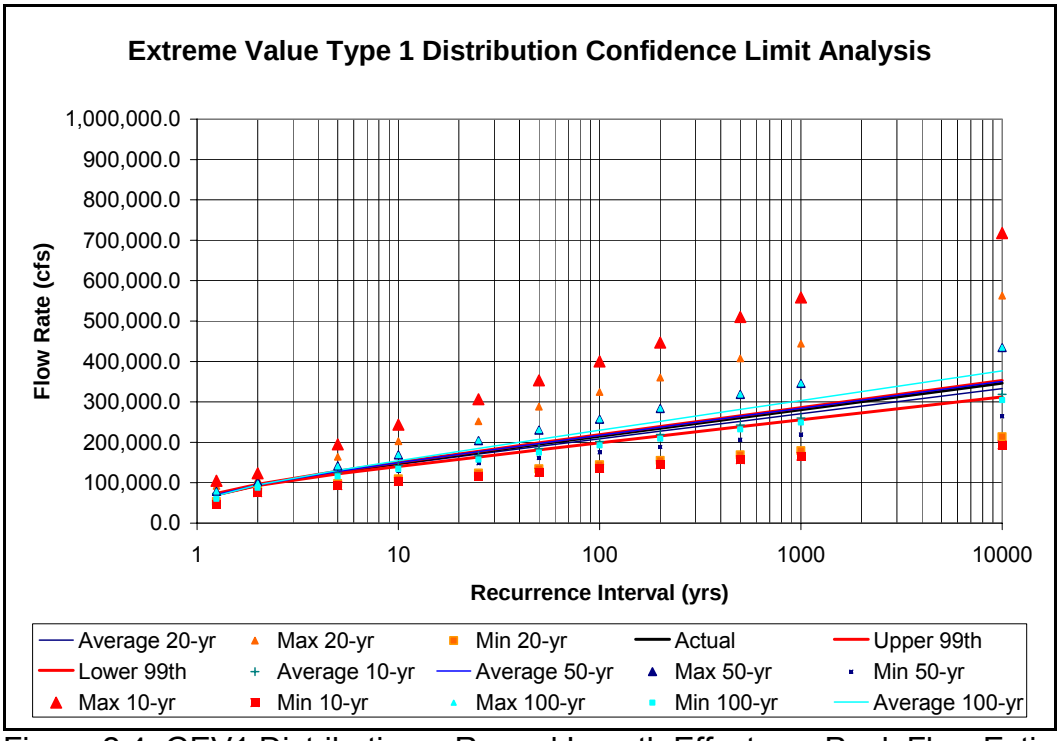

Figure 2.4 GEV1 Distribution – Record Length Effects on Peak Flow Estimates

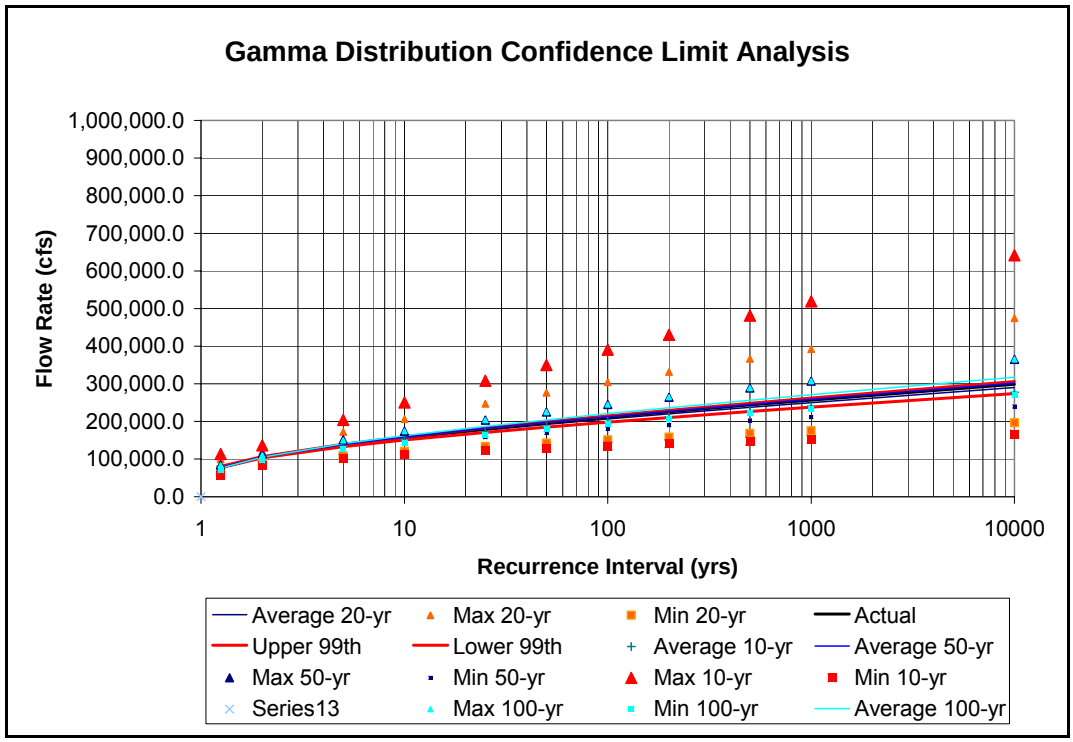

Figure 2.5 Gamma Distribution – Record Length Effects on Peak Flow Estimates

Comparing the maximum and minimum values from the 10, 20, 50, and 100 year record length and each probability distribution function showed that each record length and distribution produced a different value for a specific recurrence interval. Table 2.4 provides an example for the 100-yr recurrence interval and shows the maximum and minimum values for each moving time window. The table shows what can be seen in the figures above. Selection of the distribution is only one part of the issue related to estimating runoff of extreme events with records sets less than or equal to the actual runoff frequency desired for design. Many engineers assume that if you have a 100-year long record, there is limited risk in using the 100-year runoff estimated using probability distributions. This

study has shown that is incorrect. There will still be variation based on the actual time series collected.

Table 2.4 Recurrence Intervals for the Hartford, CT Gage – 100-yr Time Window

Record Length	Runoff Generated by Record Length for 100-yr Recurrence Interval				
Yrs	Normal	Log-Normal	Log-Pearson III	GEV1/Gumbel	Gamma
10 Min	111,003	114,600	106,900	109,200	120,600
10 Max	330,712	188,500	193,100	202,700	205,900
20 Min	117,800	129,800	110,900	123,500	133,600
20 Max	232,300	234,600	265,000	251,700	247,100
50 Min	123,600	140,700	112,700	134,000	142,400
50 Max	252,400	270,162	335,800	288,158	276,300
100 Min	128,900	150,100	113,800	144,500	150,700
100 Max	270,500	306,800	428,136	324,300	304,300

These findings led to the need for a second evaluation of the systematic gage records and the estimated flow rates from probability distribution analysis. The flow rates estimated using probability distributions are sensitive to the distribution selected and to the record length. Although a record set may be statistically sound for evaluating runoff frequency, one event can often change the entire outcome of the analysis. These values may be considered outliers statistically, but provide important insight into behavior of the watershed. It is important to be able to use the information collected at the gage even if it is a statistical outlier.

The literature review also indicated that the peak flow estimates were influenced by the method of estimating parameters for the distributions. Koutsoyiannis (2009) evaluated differences in rainfall estimates using the GEV2 distribution and

various variable estimation techniques, including method-of-moments, L-moments, and Maximum Likelihood. He used the Annual Exceedence Probability (AEP), which is the inverse of the recurrence interval, to quantify the probability of the PMP. For a gage with over 100 years of data, he noted that the PMP AEP ranged from 10^{-4} to 10^{-5}, depending on the method of parameter estimation.

In an effort to assess the effects of parameter estimation techniques on probability distribution results, and understand the full range of uncertainty found in the hydrologic analysis procedures, several probability distributions were tested for variations based on parameter estimation methods. The analysis evaluated frequency distributions on sets of data taken from the Hartford, CT gage data provided above through utilization of the bootstrap method. The analysis is discussed in more detail in the following section.

2.6 Bootstrap Analysis of Data Using MLM, MOM, and L-Moments

Evaluation of the data using a moving window was a good estimate of the behavior of the probability distribution estimates using different gage record lengths. However, it was felt that one time series may not adequately represent the behavior of the gage statistically. In order to expand the data set and

evaluate the parent distributions, it was felt that more samples should be generated and that a bootstrap analysis of the gage record be conducted.

Bootstrapping refers to a method of evaluating sample parameters. The data set is only one possible combination of the data. The data set is sampled with replacement many times to develop multiple sets of data from the original data set. The data sets are then analyzed to determine statistics such as mean, standard deviation, skewness, etc. These statistics can then be analyzed to determine the most probable statistics for the original data set. The results of the analysis on each individual data set are compared to evaluate how much variation may be possible in the original data set.

For this study, the full record length from the Hartford, CT gage of 156 years was sampled with replacement 200,000 times to create a set of data that could be divided into 2,000 bootstrap samples with 100 data points each. The parameter statistics were then calculated for each sample set for the following distributions: Normal, Log-Normal (2), Log-Normal (3), Exponential, Gamma (2), Pearson III, Log-Pearson III, General Extreme Value, Extreme Value Type 1, Weibull, Logistic, Generalized Logistic, and General Pareto.

Once the mean, standard deviation, and skewness from the 2,000 data sets were determined, the regional value for the original data set was determined by taking

the average of each of these parameters. These average values were used as the regional value for determining each distribution parameter in the distributions listed above. This is the classical approach to bootstrap analysis. The regional parameters were then used to evaluate specific recurrence intervals ranging from the 10-year to 10,000-year events. The regional parameters were used to the estimate runoff rates using three parameter estimation methods, the PWM, MOM, and MLM.

The results of using the regional values from the bootstrap analysis in developing estimated runoff rates are presented in Tables 2.5 and 2.6. Table 2.5 presents the estimates of flow rates based on the regional probability distribution parameters for the 13 distributions listed above. On the far right side of the table, there is a column showing the minimum, maximum, and average estimated flow rates, as well as the range of flow rates between the lowest and highest values estimated using the different probability distributions. Looking through the data shows significant variations between the distributions chosen for the bootstrap analysis.

Table 2.6 shows a percentage based comparison between the flow rates generated by the different parameter estimation methods. The first section contains the percent difference between PWM and MOM estimations, the second provides differences between MOM and MLM, and the third show differences

between PWM and MLM. The columns at the end of each set of rows shows minimum, maximum, average percent differences for each recurrence interval, along with the range of differences.

Table 2.5 Regional Bootstrap Analysis - Flow Rates for Estimation Methods

Regional Analysis on 2000 Bootstrapped Samples of 100 Data Points - MOM																		
T	Probability	GEV	Pearson III	Log Normal-3	Gen. Logistic	EV1	Gen. Pareto	Weibull	Normal	Exponential	Logistic	Log Normal-2	Gamma	Log Pearson III	Maximum	Minimum	Average	Range
10	0.1	151,240	153,377	151,923	148,575	153,009	155,163	154,357	152,143	152,935	149,500	152,829	154,114	150,720	155,163	148,575	152,299	6,588
20	0.05	174,198	177,237	175,095	169,730	174,147	179,944	178,575	165,826	179,040	165,016	173,473	172,568	174,253	179,944	165,016	173,777	14,928
50	0.02	205,712	208,466	206,450	200,340	201,508	210,912	209,560	181,226	213,550	184,688	200,060	194,960	207,022	213,550	181,226	201,881	32,325
100	0.01	230,732	232,035	231,014	226,165	222,011	233,056	232,394	191,492	239,656	199,291	220,013	210,862	233,481	239,656	191,492	223,246	48,164
200	0.005	256,927	255,641	256,467	254,755	242,439	254,153	254,807	200,888	265,762	213,789	240,012	226,109	261,650	265,762	200,888	244,877	64,873
500	0.002	293,526	286,980	291,653	297,459	269,391	280,517	283,890	212,275	300,271	232,877	266,700	245,488	301,872	301,872	212,275	274,069	89,597
1000	0.001	322,814	310,824	319,536	334,001	289,760	299,369	305,537	220,262	326,377	247,291	287,172	259,678	334,817	334,817	220,262	296,726	114,555
10000	0.0001	431,084	391,091	420,868	487,842	357,389	355,823	375,671	243,944	413,098	295,121	357,583	304,697	462,567	487,842	243,944	376,675	243,898
Regional Analysis on 2000 Bootstrapped Samples of 100 Data Points - PWM or L-moments																		
T	Probability	GEV	Pearson III	Log Normal-3	Gen. Logistic	EV1	Gen. Pareto	Weibull	Normal	Exponential	Logistic	Log Normal-2	Gamma	Log Pearson III	Maximum	Minimum	Average	Range
10	0.1	150,014	150,929	150,360	147,120	150,054	154,850	152,010	147,331	153,714	145,910	150,065	149,641	151,144	154,850	145,910	150,242	8,940
20	0.05	171,038	170,827	170,982	169,164	169,921	171,400	171,091	159,649	180,234	160,204	169,141	166,111	170,332	180,234	159,649	169,238	20,585
50	0.02	199,031	195,971	198,036	202,071	195,636	187,866	194,162	173,514	215,292	178,328	193,526	185,988	194,901	215,292	173,514	193,410	41,778
100	0.01	220,600	214,437	218,667	230,678	214,906	197,206	210,413	182,757	241,812	191,782	211,706	200,042	213,249	241,812	182,757	211,404	59,055
200	0.005	242,608	232,583	239,604	263,169	234,106	204,506	225,858	191,216	268,332	205,139	229,838	213,477	231,572	268,332	191,216	229,385	77,116
500	0.002	272,455	256,229	267,915	313,166	259,437	211,768	245,268	201,468	303,390	222,725	253,904	230,499	255,930	313,166	201,468	253,396	111,698
1000	0.001	295,642	273,934	289,897	357,220	278,581	215,887	259,315	208,659	329,911	236,005	272,273	242,931	274,551	357,220	208,659	271,908	148,561
10000	0.0001	376,689	332,118	367,068	553,627	342,143	224,127	302,916	229,979	418,009	280,071	334,927	282,211	338,244	553,627	224,127	337,067	329,501
Regional Analysis on 2000 Bootstrapped Samples of 100 Data Points - MLM																		
T	Probability	GEV	Pearson III	Log Normal-3	Gen. Logistic	EV1	Gen. Pareto	Weibull	Normal	Exponential	Logistic	Log Normal-2	Gamma	Log Pearson III	Maximum	Minimum	Average	Range
10	0.1	151,465	Invalid	150,386	146,369	151,135	179,939	174,202	151,901	195,355	141,443	150,720	150,115	150,826	195,355	141,443	157,821	53,912
20	0.05	172,105		169,427	167,682	171,386	209,270	189,633	165,515	244,034	155,472	170,218	166,793	170,541	244,034	155,472	179,340	88,562
50	0.02	199,000		193,669	199,217	197,600	240,703	205,282	180,838	308,383	173,258	195,195	186,932	195,898	308,383	173,258	206,331	135,125
100	0.01	219,285		211,678	226,401	217,243	259,940	214,848	191,053	357,062	186,463	213,851	201,178	214,910	357,062	186,463	226,159	170,600
200	0.005	239,610		229,590	257,052	236,815	275,960	223,069	200,402	405,741	199,571	232,483	214,800	233,956	405,741	199,571	245,756	206,170
500	0.002	266,598		253,296	303,823	262,636	293,169	232,423	211,732	470,091	216,830	257,252	232,066	259,363	470,091	211,732	271,607	258,359
1000	0.001	287,128		271,342	344,695	282,151	303,669	238,624	219,679	518,769	229,863	276,184	244,679	278,848	518,769	219,679	291,304	299,090
10000	0.0001	356,112		332,617	523,974	346,944	327,614	255,493	243,242	680,477	273,110	340,910	284,551	345,864	680,477	243,242	359,242	437,235

Table 2.6 Regional Bootstrap Analysis - Comparison of Estimation Methods

Difference Between Regional Analysis MOM and PWM																		
T	Probability	GEV	Pearson III	Log Normal-3	Gen. Logistic	EV1	Gen. Pareto	Weibull	Normal	Exponential	Logistic	Log Normal-2	Gamma	Log Pearson III	Maximum	Minimum	Average	Range
10	0.1	0.8%	1.6%	1.0%	1.0%	1.9%	0.2%	1.5%	3.2%	-0.5%	2.4%	1.8%	2.9%	-0.3%	3.2%	-0.5%	1.4%	3.7%
20	0.05	1.8%	3.6%	2.3%	0.3%	2.4%	4.7%	4.2%	3.7%	-0.7%	2.9%	2.5%	3.7%	2.3%	4.7%	-0.7%	2.6%	5.4%
50	0.02	3.2%	6.0%	4.1%	-0.9%	2.9%	10.9%	7.3%	4.3%	-0.8%	3.4%	3.3%	4.6%	5.9%	10.9%	-0.9%	4.2%	11.8%
100	0.01	4.4%	7.6%	5.3%	-2.0%	3.2%	15.4%	9.5%	4.6%	-0.9%	3.8%	3.8%	5.1%	8.7%	15.4%	-2.0%	5.3%	17.4%
200	0.005	5.6%	9.0%	6.6%	-3.3%	3.4%	19.5%	11.4%	4.8%	-1.0%	4.0%	4.2%	5.6%	11.5%	19.5%	-3.3%	6.3%	22.8%
500	0.002	7.2%	10.7%	8.1%	-5.3%	3.7%	24.5%	13.6%	5.1%	-1.0%	4.4%	4.8%	6.1%	15.2%	24.5%	-5.3%	7.5%	29.8%
1000	0.001	8.4%	11.9%	9.3%	-7.0%	3.9%	27.9%	15.1%	5.3%	-1.1%	4.6%	5.2%	6.4%	18.0%	27.9%	-7.0%	8.3%	34.8%
10000	0.0001	12.6%	15.1%	12.8%	-13.5%	4.3%	37.0%	19.4%	5.7%	-1.2%	5.1%	6.3%	7.4%	26.9%	37.0%	-13.5%	10.6%	50.5%
Difference Between Regional Analysis MOM and MLM																		
T	Probability	GEV	Pearson III	Log Normal-3	Gen. Logistic	EV1	Gen. Pareto	Weibull	Normal	Exponential	Logistic	Log Normal-2	Gamma	Log Pearson III	Maximum	Minimum	Average	Range
10	0.1	-0.1%		1.0%	1.5%	1.2%	-16.0%	-12.9%	0.2%	-27.7%	5.4%	1.4%	2.6%	-0.1%	5.4%	-27.7%	-3.6%	33.1%
20	0.05	1.2%		3.2%	1.2%	1.6%	-16.3%	-6.2%	0.2%	-36.3%	5.8%	1.9%	3.3%	2.1%	5.8%	-36.3%	-3.2%	42.1%
50	0.02	3.3%		6.2%	0.6%	1.9%	-14.1%	2.0%	0.2%	-44.4%	6.2%	2.4%	4.1%	5.4%	6.2%	-44.4%	-2.2%	50.6%
100	0.01	5.0%		8.4%	-0.1%	2.1%	-11.5%	7.6%	0.2%	-49.0%	6.4%	2.8%	4.6%	8.0%	8.4%	-49.0%	-1.3%	57.4%
200	0.005	6.7%		10.5%	-0.9%	2.3%	-8.6%	12.5%	0.2%	-52.7%	6.7%	3.1%	5.0%	10.6%	12.5%	-52.7%	-0.4%	65.1%
500	0.002	9.2%		13.2%	-2.1%	2.5%	-4.5%	18.1%	0.3%	-56.6%	6.9%	3.5%	5.5%	14.1%	18.1%	-56.6%	0.8%	74.7%
1000	0.001	11.1%		15.1%	-3.2%	2.6%	-1.4%	21.9%	0.3%	-58.9%	7.0%	3.8%	5.8%	16.7%	21.9%	-58.9%	1.7%	80.8%
10000	0.0001	17.4%		21.0%	-7.4%	2.9%	7.9%	32.0%	0.3%	-64.7%	7.5%	4.7%	6.6%	25.2%	32.0%	-64.7%	4.4%	96.7%
Difference Between Regional Analysis PWM and MLM																		
T	Probability	GEV	Pearson III	Log Normal-3	Gen. Logistic	EV1	Gen. Pareto	Weibull	Normal	Exponential	Logistic	Log Normal-2	Gamma	Log Pearson III	Maximum	Minimum	Average	Range
10	0.1	-1.0%		0.0%	0.5%	-0.7%	-16.2%	-14.6%	-3.1%	-27.1%	3.1%	-0.4%	-0.3%	0.2%	3.1%	-27.1%	-5.0%	30.2%
20	0.05	-0.6%		0.9%	0.9%	-0.9%	-22.1%	-10.8%	-3.7%	-35.4%	3.0%	-0.6%	-0.4%	-0.1%	3.0%	-35.4%	-5.8%	38.4%
50	0.02	0.0%		2.2%	1.4%	-1.0%	-28.1%	-5.7%	-4.2%	-43.2%	2.8%	-0.9%	-0.5%	-0.5%	2.8%	-43.2%	-6.5%	46.1%
100	0.01	0.6%		3.2%	1.9%	-1.1%	-31.8%	-2.1%	-4.5%	-47.7%	2.8%	-1.0%	-0.6%	-0.8%	3.2%	-47.7%	-6.8%	50.9%
200	0.005	1.2%		4.2%	2.3%	-1.2%	-34.9%	1.2%	-4.8%	-51.2%	2.7%	-1.2%	-0.6%	-1.0%	4.2%	-51.2%	-6.9%	55.4%
500	0.002	2.1%		5.5%	3.0%	-1.2%	-38.4%	5.2%	-5.1%	-54.9%	2.6%	-1.3%	-0.7%	-1.3%	5.5%	-54.9%	-7.0%	60.4%
1000	0.001	2.9%		6.4%	3.5%	-1.3%	-40.7%	8.0%	-5.3%	-57.2%	2.6%	-1.4%	-0.7%	-1.6%	8.0%	-57.2%	-7.1%	65.2%
10000	0.0001	5.5%		9.4%	5.4%	-1.4%	-46.2%	15.7%	-5.8%	-62.8%	2.5%	-1.8%	-0.8%	-2.3%	15.7%	-62.8%	-6.9%	78.4%

The data shown in Table 2.6 is provided in a graphical format in Figure 2.6. The range of the values is shown to help show which estimation methods provide more similar results. As can be seen, the difference between the PWM and the MOM is much smaller than the difference between either PWM and MLM or MOM and MLM.

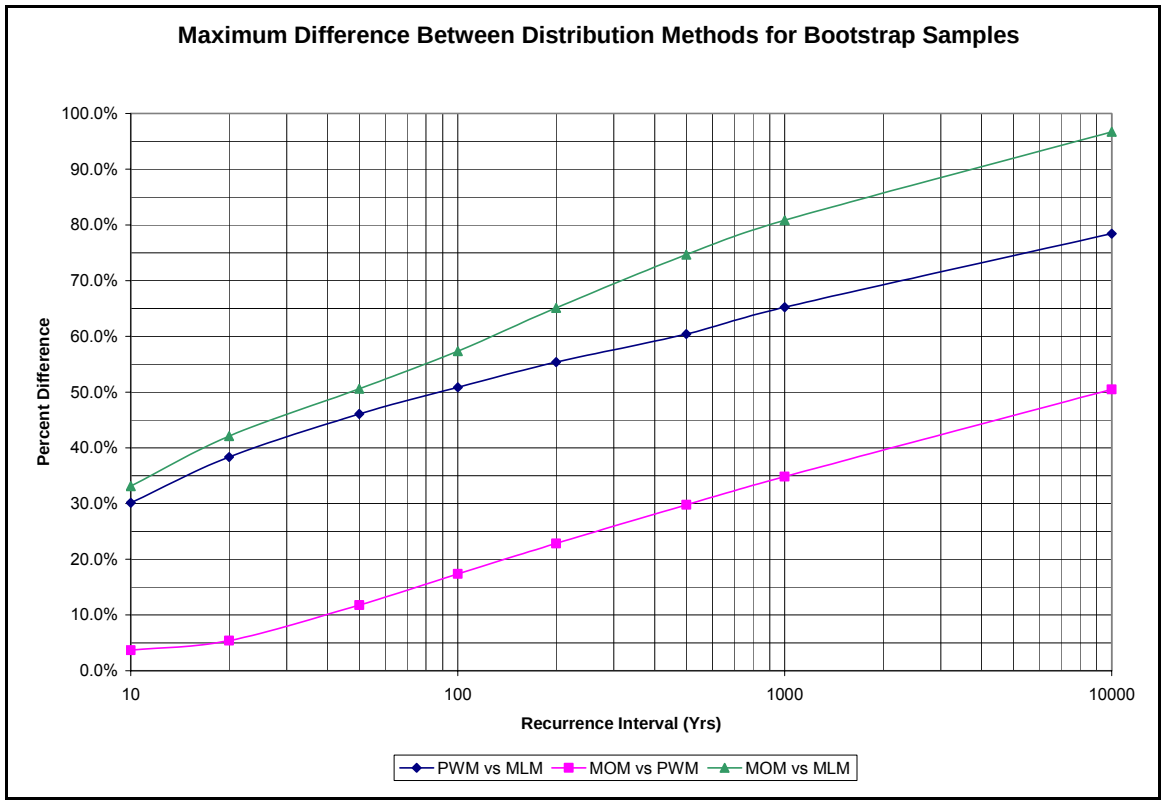

Figure 2.6 Recurrence Interval Range Comparison for Various Parameter Estimation Methods with Different Distributions for the Bootstrapped Samples

The next evaluation on the parameter estimation data sets utilized the original 156 years of data collected at the Hartford, CT runoff gage for the at-site flow data. The three parameter estimation methods were used to generate flow rates for the 13 distributions based on the gage record. This analysis is shown in Table 2.7.

Table 2.7 At-Site Analysis - Flow Rates for Estimation Methods

At-Site Analysis on Sample of 156 Data Points - MOM																		
T	Probability	GEV	Pearson III	Log Normal-3	Gen. Logistic	EV1	Gen. Pareto	Weibull	Normal	Exponential	Logistic	Log Normal-2	Gamma	Log Pearson III	Maximum	Minimum	Average	Range
10	0.1	145,496	147,853	146,151	144,017	149,391	147,589	147,866	148,589	149,322	146,141	149,717	150,341	145,948	150,341	144,017	147,571	6,324
20	0.05	167,971	173,028	169,566	164,525	168,972	172,448	173,367	161,264	173,506	160,514	168,599	167,117	168,679	173,506	160,514	168,427	12,992
50	0.02	200,527	207,433	202,962	195,168	194,319	206,607	208,038	175,530	205,474	178,737	192,714	187,380	201,279	208,038	175,530	196,628	32,508
100	0.01	227,770	234,255	230,349	221,831	213,312	233,465	234,858	185,041	229,658	192,265	210,677	201,718	228,325	234,858	185,041	218,733	49,818
200	0.005	257,611	261,720	259,750	252,136	232,236	261,232	262,112	193,745	253,841	205,695	228,581	215,430	257,771	262,112	193,745	241,682	68,367
500	0.002	301,551	298,963	301,953	298,813	257,203	299,386	298,717	204,293	285,809	223,378	252,330	232,812	300,893	301,953	204,293	273,546	97,660
1000	0.001	338,592	327,810	336,578	339,978	276,072	329,385	326,797	211,692	309,993	236,730	270,445	245,512	337,090	339,978	211,692	298,975	128,286
10000	0.0001	489,899	427,511	470,091	523,824	338,721	436,525	422,102	233,630	390,328	281,039	332,169	285,666	484,124	523,824	233,630	393,510	290,195
At-Site Analysis on Sample of 156 Data Points - PWM or L-moments																		
T	Probability	GEV	Pearson III	Log Normal-3	Gen. Logistic	EV1	Gen. Pareto	Weibull	Normal	Exponential	Logistic	Log Normal-2	Gamma	Log Pearson III	Maximum	Minimum	Average	Range
10	0.1	144,839	147,554	146,083	142,298	145,579	149,898	148,416	143,119	148,884	141,836	145,427	145,005	145,182	149,898	141,836	145,702	8,062
20	0.05	167,495	168,511	168,322	165,198	163,520	169,827	169,158	154,244	172,834	154,745	161,994	159,491	166,811	172,834	154,244	164,781	18,590
50	0.02	200,703	195,907	199,436	201,737	186,744	193,200	195,454	166,765	204,494	171,113	182,908	176,871	197,403	204,494	166,765	190,210	37,729
100	0.01	228,818	216,563	224,530	235,597	204,146	208,875	214,692	175,113	228,444	183,263	198,330	189,103	222,462	235,597	175,113	209,995	60,484
200	0.005	259,922	237,240	251,124	276,216	221,485	223,010	233,476	182,752	252,395	195,325	213,581	200,756	249,461	276,216	182,752	230,519	93,464
500	0.002	306,259	264,674	288,777	342,831	244,361	239,588	257,726	192,010	284,055	211,207	233,643	215,472	288,538	342,831	192,010	259,165	150,821
1000	0.001	345,772	285,535	319,281	405,312	261,650	250,705	275,693	198,504	308,005	223,200	248,830	226,188	320,970	405,312	198,504	282,280	206,808
10000	0.0001	510,818	355,707	434,381	720,733	319,051	280,374	333,503	217,758	387,565	262,995	299,913	259,897	449,941	720,733	217,758	371,741	502,974
At-Site Analysis on Sample of 156 Data Points - MLM																		
T	Probability	GEV	Pearson III	Log Normal-3	Gen. Logistic	EV1	Gen. Pareto	Weibull	Normal	Exponential	Logistic	Log Normal-2	Gamma	Log Pearson III	Maximum	Minimum	Average	Range
10	0.1	144,760	INVALID	145,719	144,769	140,931	160,732	171,933	148,589	165,331	136,611	143,287	144,646	145,305	171,933	136,611	149,384	35,323
20	0.05	167,418		167,081	170,810	157,283	185,568	186,967	161,264	198,032	149,264	158,950	158,981	167,084	198,032	149,264	169,058	48,768
50	0.02	200,670		196,585	214,113	178,449	214,680	202,212	175,530	241,262	165,308	178,636	176,172	197,945	241,262	165,308	195,130	75,954
100	0.01	228,856		220,115	255,852	194,310	234,193	211,531	185,041	273,964	177,217	193,097	188,266	223,268	273,964	177,217	215,476	96,746
200	0.005	260,069		244,836	307,644	210,113	251,781	219,541	193,745	306,665	189,041	207,355	199,785	250,588	307,644	189,041	236,764	118,603
500	0.002	306,625		279,513	396,002	230,962	272,397	228,654	204,293	349,895	204,609	226,052	214,328	290,193	396,002	204,293	266,960	191,709
1000	0.001	346,370		307,368	482,129	246,719	286,216	234,695	211,692	382,597	216,364	240,164	224,916	323,113	482,129	211,692	291,862	270,437
10000	0.0001	512,763		410,954	952,188	299,036	323,057	251,129	233,630	491,230	255,372	287,400	258,208	454,389	952,188	233,630	394,113	718,559

Table 2.8 At-Site Analysis - Comparison of Estimation Methods

Difference Between At-Site MOM and PWM																		
T	Probability	GEV	Pearson III	Log Normal-3	Gen. Logistic	EV1	Gen. Pareto	Weibull	Normal	Exponential	Logistic	Log Normal-2	Gamma	Log Pearson III	Maximum	Minimum	Average	Range
10	0.1	0.5%	0.2%	0.0%	1.2%	2.6%	-1.6%	-0.4%	3.7%	0.3%	2.9%	2.9%	3.5%	0.5%	3.7%	-1.6%	1.3%	5.2%
20	0.05	0.3%	2.6%	0.7%	-0.4%	3.2%	1.5%	2.4%	4.4%	0.4%	3.6%	3.9%	4.6%	1.1%	4.6%	-0.4%	2.2%	5.0%
50	0.02	-0.1%	5.6%	1.7%	-3.4%	3.9%	6.5%	6.0%	5.0%	0.5%	4.3%	5.1%	5.6%	1.9%	6.5%	-3.4%	3.3%	9.9%
100	0.01	-0.5%	7.6%	2.5%	-6.2%	4.3%	10.5%	8.6%	5.4%	0.5%	4.7%	5.9%	6.3%	2.6%	10.5%	-6.2%	4.0%	16.7%
200	0.005	-0.9%	9.4%	3.3%	-9.6%	4.6%	14.6%	10.9%	5.7%	0.6%	5.0%	6.6%	6.8%	3.2%	14.6%	-9.6%	4.6%	24.2%
500	0.002	-1.6%	11.5%	4.4%	-14.7%	5.0%	20.0%	13.7%	6.0%	0.6%	5.4%	7.4%	7.4%	4.1%	20.0%	-14.7%	5.3%	34.7%
1000	0.001	-2.1%	12.9%	5.1%	-19.2%	5.2%	23.9%	15.6%	6.2%	0.6%	5.7%	8.0%	7.9%	4.8%	23.9%	-19.2%	5.7%	43.1%
10000	0.0001	-4.3%	16.8%	7.6%	-37.6%	5.8%	35.8%	21.0%	6.8%	0.7%	6.4%	9.7%	9.0%	7.1%	35.8%	-37.6%	6.5%	73.4%
Difference Between At-Site MOM and MLM																		
T	Probability	GEV	Pearson III	Log Normal-3	Gen. Logistic	EV1	Gen. Pareto	Weibull	Normal	Exponential	Logistic	Log Normal-2	Gamma	Log Pearson III	Maximum	Minimum	Average	Range
10	0.1	0.5%		0.3%	-0.5%	5.7%	-8.9%	-16.3%	0.0%	-10.7%	6.5%	4.3%	3.8%	0.4%	6.5%	-16.3%	-1.2%	22.8%
20	0.05	0.3%		1.5%	-3.8%	6.9%	-7.6%	-7.8%	0.0%	-14.1%	7.0%	5.7%	4.9%	0.9%	7.0%	-14.1%	-0.5%	21.1%
50	0.02	-0.1%		3.1%	-9.7%	8.2%	-3.9%	2.8%	0.0%	-17.4%	7.5%	7.3%	6.0%	1.7%	8.2%	-17.4%	0.5%	25.6%
100	0.01	-0.5%		4.4%	-15.3%	8.9%	-0.3%	9.9%	0.0%	-19.3%	7.8%	8.3%	6.7%	2.2%	9.9%	-19.3%	1.1%	29.2%
200	0.005	-1.0%		5.7%	-22.0%	9.5%	3.6%	16.2%	0.0%	-20.8%	8.1%	9.3%	7.3%	2.8%	16.2%	-22.0%	1.6%	38.3%
500	0.002	-1.7%		7.4%	-32.5%	10.2%	9.0%	23.5%	0.0%	-22.4%	8.4%	10.4%	7.9%	3.6%	23.5%	-32.5%	2.0%	56.0%
1000	0.001	-2.3%		8.7%	-41.8%	10.6%	13.1%	28.2%	0.0%	-23.4%	8.6%	11.2%	8.4%	4.1%	28.2%	-41.8%	2.1%	70.0%
10000	0.0001	-4.7%		12.6%	-81.8%	11.7%	26.0%	40.5%	0.0%	-25.9%	9.1%	13.5%	9.6%	6.1%	40.5%	-81.8%	1.4%	122.3%
Difference Between At-Site PWM and MLM																		
T	Probability	GEV	Pearson III	Log Normal-3	Gen. Logistic	EV1	Gen. Pareto	Weibull	Normal	Exponential	Logistic	Log Normal-2	Gamma	Log Pearson III	Maximum	Minimum	Average	Range
10	0.1	0.1%		0.2%	-1.7%	3.2%	-7.2%	-15.8%	-3.8%	-11.0%	3.7%	1.5%	0.2%	-0.1%	3.7%	-15.8%	-2.6%	19.5%
20	0.05	0.0%		0.7%	-3.4%	3.8%	-9.3%	-10.5%	-4.6%	-14.6%	3.5%	1.9%	0.3%	-0.2%	3.8%	-14.6%	-2.7%	18.4%
50	0.02	0.0%		1.4%	-6.1%	4.4%	-11.1%	-3.5%	-5.3%	-18.0%	3.4%	2.3%	0.4%	-0.3%	4.4%	-18.0%	-2.7%	22.4%
100	0.01	0.0%		2.0%	-8.6%	4.8%	-12.1%	1.5%	-5.7%	-19.9%	3.3%	2.6%	0.4%	-0.4%	4.8%	-19.9%	-2.7%	24.7%
200	0.005	-0.1%		2.5%	-11.4%	5.1%	-12.9%	6.0%	-6.0%	-21.5%	3.2%	2.9%	0.5%	-0.5%	6.0%	-21.5%	-2.7%	27.5%
500	0.002	-0.1%		3.2%	-15.5%	5.5%	-13.7%	11.3%	-6.4%	-23.2%	3.1%	3.2%	0.5%	-0.6%	11.3%	-23.2%	-2.7%	34.5%
1000	0.001	-0.2%		3.7%	-19.0%	5.7%	-14.2%	14.9%	-6.6%	-24.2%	3.1%	3.5%	0.6%	-0.7%	14.9%	-24.2%	-2.8%	39.1%
10000	0.0001	-0.4%		5.4%	-32.1%	6.3%	-15.2%	24.7%	-7.3%	-26.7%	2.9%	4.2%	0.6%	-1.0%	24.7%	-32.1%	-3.2%	56.8%

Table 2.8 compares the different methodologies, similar to Table 2.6. As can be seen, there is a large range of variation between the methods. The MOM and PWM appear to give the most consistent results. This is shown in graphical format in Figure 2.7.

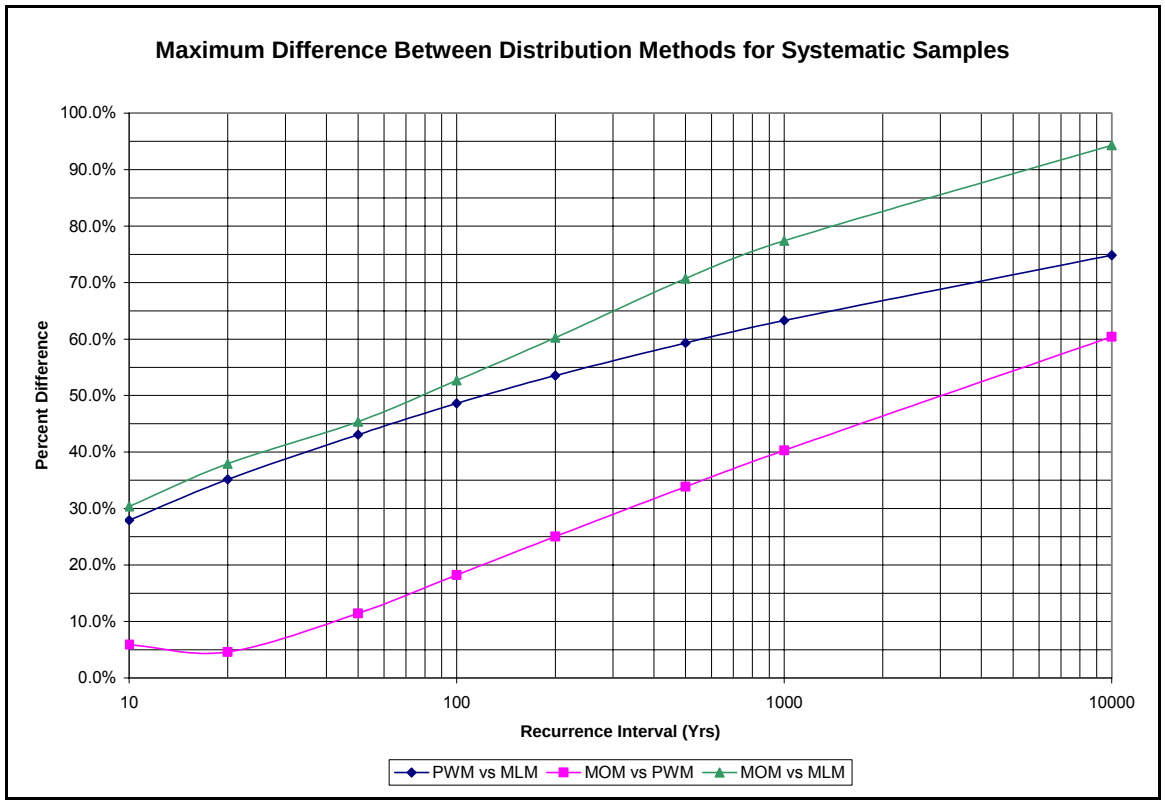

Figure 2.7 Range of Recurrence Intervals Using Various Parameter Estimation Methods and Distributions

For example, for the 10-yr recurrence interval, the range between the MOM and the MLM, shown by the green line is 30 percent. This indicates that if a hydrologist used the two of the distributions evaluated, and estimated the

parameters with the MOM and MLM methods, there would be a 30 percent difference in the estimated 10-yr peak flow rate.

Comparison between the MOM and MLM show the largest variation in the ratio between predicted flow rates. The difference between PWM and MOM ratios is consistently lower. It is interesting to note the range of ratios using different distributions and different parameter estimation methods. Depending on the method used for parameter estimation, one should expect a difference in estimates of 30 to 100 percent in estimates of extreme events.

The final comparison required for the analysis of distribution selection and parameter estimation methods was to compare the regional data from bootstrapping to the at-site data collected by the systematic gage. The data were compared to each other by taking the difference between the at-site and regional data and then dividing by the at-site data. A negative value indicates that the regional value was higher than the at-site value. This can be confirmed by looking at the same data point in Tables 2.5 and 2.7. The MOM appears to yield the most consistent results between the at-site and regional flow rate estimates, with the MLM yielding the widest range of flow rates. The information in Table 2.9 is presented in graphical format in Figure 2.8.

Table 2.8 At-Site Analysis - Comparison of Estimation Methods

Difference Between Regional and At-Site Analysis MOM																		
T	Probability	GEV	Pearson III	Log Normal-3	Gen. Logistic	EV1	Gen. Pareto	Weibull	Normal	Exponential	Logistic	Log Normal-2	Gamma	Log Pearson III	Maximum	Minimum	Average	Range
10	0.1	-4.1%	-4.2%	-4.1%	-4.0%	-4.4%	-4.2%	-4.2%	-4.4%	-4.4%	-4.2%	-4.2%	-4.6%	-4.1%	-4.0%	-4.6%	-4.2%	16%
20	0.05	-5.5%	-5.8%	-5.6%	-5.3%	-5.6%	-5.7%	-5.8%	-5.2%	-5.8%	-5.1%	-5.9%	-6.0%	-5.5%	-5.1%	-6.0%	-5.6%	1%
50	0.02	-7.0%	-7.4%	-7.2%	-6.8%	-6.8%	-7.3%	-7.4%	-5.9%	-7.2%	-6.1%	-7.9%	-7.5%	-7.0%	-5.9%	-7.9%	-7.0%	2%
100	0.01	-8.0%	-8.3%	-8.1%	-7.8%	-7.5%	-8.2%	-8.3%	-6.4%	-8.0%	-6.7%	-9.2%	-8.4%	-8.0%	-6.4%	-9.2%	-7.9%	3%
200	0.005	-8.9%	-9.1%	-9.0%	-8.7%	-8.0%	-9.0%	-9.1%	-6.8%	-8.6%	-7.2%	-10.4%	-9.2%	-8.9%	-6.8%	-10.4%	-8.7%	4%
500	0.002	-9.8%	-9.9%	-9.9%	-9.7%	-8.7%	-9.9%	-9.9%	-7.2%	-9.3%	-7.8%	-11.9%	-10.1%	-9.9%	-7.2%	-11.9%	-9.5%	5%
1000	0.001	-10.5%	-10.4%	-10.5%	-10.4%	-9.1%	-10.6%	-10.5%	-7.4%	-9.7%	-8.2%	-13.0%	-10.7%	-10.6%	-7.4%	-13.0%	-10.1%	6%
10000	0.0001	-12.3%	-11.7%	-12.1%	-12.2%	-10.1%	-12.2%	-11.8%	-8.1%	-10.7%	-9.2%	-16.2%	-12.4%	-12.6%	-8.1%	-16.2%	-11.6%	8%
Difference Between Regional and At-Site PWM																		
T	Probability	GEV	Pearson III	Log Normal-3	Gen. Logistic	EV1	Gen. Pareto	Weibull	Normal	Exponential	Logistic	Log Normal-2	Gamma	Log Pearson III	Maximum	Minimum	Average	Range
10	0.1	-3.9%	-3.2%	-3.6%	-3.7%	-3.6%	-4.0%	-3.4%	-3.4%	-3.8%	-3.3%	-3.7%	-3.7%	-4.3%	-3.2%	-4.3%	-3.7%	16%
20	0.05	-3.8%	-3.3%	-3.5%	-3.9%	-4.5%	-3.2%	-3.2%	-4.1%	-5.0%	-4.1%	-5.1%	-4.8%	-2.8%	-2.8%	-5.1%	-4.0%	2%
50	0.02	-2.9%	-3.2%	-2.9%	-3.4%	-5.5%	-1.7%	-2.8%	-4.7%	-6.1%	-4.9%	-6.8%	-6.0%	-0.2%	-0.2%	-6.8%	-3.9%	7%
100	0.01	-1.8%	-3.0%	-2.2%	-2.7%	-6.1%	-0.3%	-2.3%	-5.1%	-6.8%	-5.4%	-7.9%	-6.7%	2.2%	2.2%	-7.9%	-3.7%	10%
200	0.005	-0.3%	-2.8%	-1.4%	-1.6%	-6.6%	1.2%	-1.9%	-5.4%	-7.3%	-5.8%	-8.9%	-7.4%	4.7%	4.7%	-8.9%	-3.3%	14%
500	0.002	1.9%	-2.4%	-0.2%	0.2%	-7.2%	3.1%	-1.2%	-5.7%	-7.9%	-6.3%	-10.1%	-8.1%	8.2%	8.2%	-10.1%	-2.8%	18%
1000	0.001	3.7%	-2.1%	0.7%	1.8%	-7.5%	4.5%	-0.8%	-5.9%	-8.3%	-6.7%	-11.0%	-8.6%	10.9%	10.9%	-11.0%	-2.3%	22%
10000	0.0001	10.7%	-1.2%	4.0%	8.0%	-8.4%	8.6%	0.7%	-6.5%	-9.1%	-7.5%	-13.7%	-10.0%	19.9%	19.9%	-13.7%	-0.3%	34%
Difference Between Regional and At-Site Analysis MLM																		
T	Probability	GEV	Pearson III	Log Normal-3	Gen. Logistic	EV1	Gen. Pareto	Weibull	Normal	Exponential	Logistic	Log Normal-2	Gamma	Log Pearson III	Maximum	Minimum	Average	Range
10	0.1	-5.1%		-3.7%	-0.3%	-6.9%	-11.7%	-5.3%	-4.2%	-15.7%	-2.9%	-5.3%	-4.5%	-4.2%	-0.3%	-15.7%	-5.8%	16%
20	0.05	-3.9%		-2.4%	2.6%	-8.6%	-12.8%	-5.9%	-5.0%	-20.1%	-3.5%	-7.3%	-5.8%	-3.1%	2.6%	-20.1%	-6.3%	23%
50	0.02	-1.3%		-0.2%	7.6%	-10.3%	-12.7%	-6.4%	-5.7%	-24.1%	-4.2%	-9.6%	-7.3%	-0.8%	7.6%	-24.1%	-6.2%	32%
100	0.01	1.4%		1.8%	12.0%	-11.4%	-12.0%	-6.7%	-6.1%	-26.2%	-4.6%	-11.2%	-8.2%	1.4%	12.0%	-26.2%	-5.8%	38%
200	0.005	4.3%		3.8%	16.7%	-12.3%	-11.0%	-6.9%	-6.5%	-27.9%	-5.0%	-12.6%	-8.9%	3.7%	16.7%	-27.9%	-5.2%	45%
500	0.002	8.7%		6.4%	23.3%	-13.3%	-9.6%	-7.2%	-6.9%	-29.7%	-5.4%	-14.4%	-9.9%	7.0%	23.3%	-29.7%	-4.2%	53%
1000	0.001	12.1%		8.5%	28.4%	-13.9%	-8.4%	-7.3%	-7.1%	-30.8%	-5.7%	-15.7%	-10.5%	9.6%	28.4%	-30.8%	-3.4%	59%
10000	0.0001	24.1%		14.9%	44.3%	-15.5%	-4.6%	-7.7%	-7.8%	-33.3%	-6.4%	-19.5%	-12.2%	18.4%	44.3%	-33.3%	-0.4%	78%

Figure 2.8 provides insight into the comparison of the bootstrapped samples of 100 data points and the at-site parameters calculated from the actual 156-year record. The comparison between the MOM for bootstrapping versus at-site shows small differences, while the MLM shows a large range of variation for values estimated using the different distribution parameters. This indicates that bootstrapping does not add much in this instance to method of moment estimates, while there are significant variations in the estimates using bootstrapping for the maximum likelihood and probability weighted moments. The value of bootstrapping should increase as the sample size decreases.

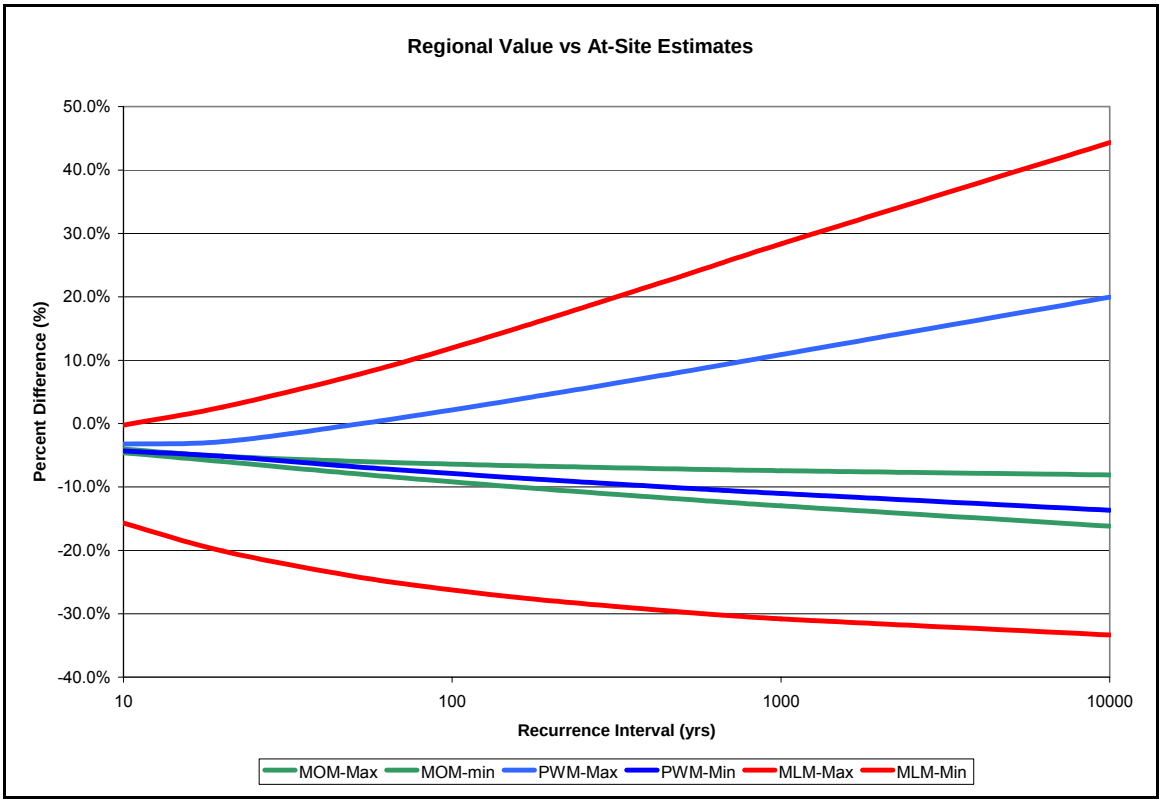

Figure 2.8 Comparison of At-Site Parameter Estimation to Regional Bootstrapping Parameter Estimation

2.7 Chapter Summary and Conclusions

This chapter has evaluated the effects of systematic sampling, record length, probability distribution selection, and distribution parameter estimation methods on the prediction of extreme runoff events. The conclusions that can be drawn from the research are:

1. Record length plays an important role in the fitting of probability distributions to the data set and in the predicted extreme values for runoff events.
2. The date when systematic sampling begins, and the exact data set captured, also influences probability distribution selection and the prediction of extreme values for runoff events.
3. Selection of a probability distribution affects the value for a specific recurrence interval, even if the record length is significantly longer than the recurrence interval of interest.
4. Selection of a parameter estimation method is important in the estimation of extreme runoff events using probability distributions. The use of probability weighted moments for shorter record lengths is suggested due to the linear nature of the method.

Chapter 3 – Rain Gage Frequency Analysis and Comparison to Probable Maximum Precipitation Frequencies

This chapter introduces the concepts of Probable Maximum Precipitation (PMP) and Probable Maximum Flood (PMF) as the design criteria for major hydraulic structures. After the introduction to these ideas in Section 3.1, an introduction into general rainfall analysis is covered in Section 3.2. This section covers the general ideas of temporal and spatial rainfall distributions, along with development of design storms.

After the general analysis, Section 3.3 discusses rain gages and climatic regions within Los Angeles County. Section 3.4 details the analysis of rainfall frequencies within Los Angeles County and the use of L-moment ratios to select a probability distribution. The GEV1 probability distribution, utilizing L-moment parameter estimation, was selected for all further analysis of rain gage data for this study.

Section 3.5 contains analysis and comparison of rain gage data within Los Angeles County, including the 24-hour PMP rainfall totals. The PMP is an important parameter utilized for determining PMF values for the design of

structures required to handle extreme events. PMP estimates for the region are determined based on the Hydrometeorological Reports (HMR) 58 and 59 developed by the National Oceanic and Atmospheric Administration (NOAA). Section 3.6 performs the same analysis on PMP estimates based on the Hershfield Method. The section discusses the methodology and the resulting PMP estimates. It also compares the two frequency estimates to determine if they are consistent.

3.1 Introduction to Extreme Rainfall Data, Frequencies, and Predictions of the Probable Maximum Precipitation

The analysis of flooding often utilizes watershed models to evaluate the effects of structures in changing flow peaks and timing, to determine the effects of urban development, or to develop runoff from design storm events. All models require data to represent temporal and spatial rainfall distributions, soil and vegetation parameters related to water loss, and watershed shape and slope characteristics that influence runoff storage and timing. These models are also used to develop Probable Maximum Flood (PMF) estimates from Probable Maximum Precipitation (PMP) estimates.

Debate over the PMF design standard continues and requires further research (FEMA, 2001). The National Research Council (1985) describes one of the most

significant initial reevaluations of this standard. The reevaluation explored base safety analysis using an incremental deterministic evaluation, and risk analysis as potential alternatives to the PMF criteria which is based on the PMP. Solutions to significant hydrologic problems in dam safety analysis still require further research.

Recent paleoflood evidence in the western United States indicates that the largest floods occurring in the past 10,000 years are significantly smaller than PMF estimates (FEMA, 2001). This difference between peak flow estimates might stem from modeling problems in trying to estimate peak flows from paleo-stage indicators or in area reduction factors used to convert point estimates of the probable maximum precipitation (PMP) to a total storm depth.

The National Research Council (1988) and IACWD (1986) addressed the problem of estimating exceedance probabilities for large floods, but did not provide guidance for extending estimates beyond the 1/1000 exceedance probability. Paleoflood information has extended flood distribution data to the 1/10,000 exceedance probability (FEMA, 2001). Further research needs to address how to incorporate different sources of information to obtain extreme flood exceedance probability estimates needed for risk assessment. The different data sources available include systematic gage records, stochastic precipitation and watershed models, and paleoflood information bounds.

FEMA (2001) recognized the need to develop simplified techniques since owners of small dams often do not have the resources to formulate/apply sophisticated meteorologic and hydrologic models. Opportunities for developing these simplifying techniques may reside in regional analyses.

Numerous methods have been used to develop discharge/frequency relationships for the range of possible reservoir inflows that could occur. Methods that have been employed to date have ranged from simple extrapolation of curves constructed based on finite periods of record, to the use of paleoflood hydrology, precipitation records, regional frequency analysis and stochastic hydrology to better estimate return periods that could serve as "anchor" points in extending the basic discharge/frequency curves. Paleofloods provide useful information for determining extreme tail probability locations with more confidence. However, many agencies lack the expertise, time, and/or money to investigate gaged and ungaged watersheds for evidence of paleofloods.

Estimation of the Annual Exceedence Probability (AEP) of the PMP is needed to define the upper end of the frequency curves shown in Figures 3.1 and 3.2. Figure 3.1 shows the concept of rainfall recurrence intervals. As the rainfall depth gets larger, the AEP, which is the inverse of recurrence interval gets smaller. The figure also shows the methods used to generate the AEP with a

certain degree of confidence. This corresponds with the data provided in Table 2.1. While assigning an AEP to the PMP is inconsistent with the "upper limiting" concept of the PMP, it is recognized that operational estimates of PMP are estimates only, and their accuracy is crucially dependent on the validity of both the method and the data used to derive them. Thus operational estimates of PMP may conceivably be exceeded (ANSCOLD, 2000).

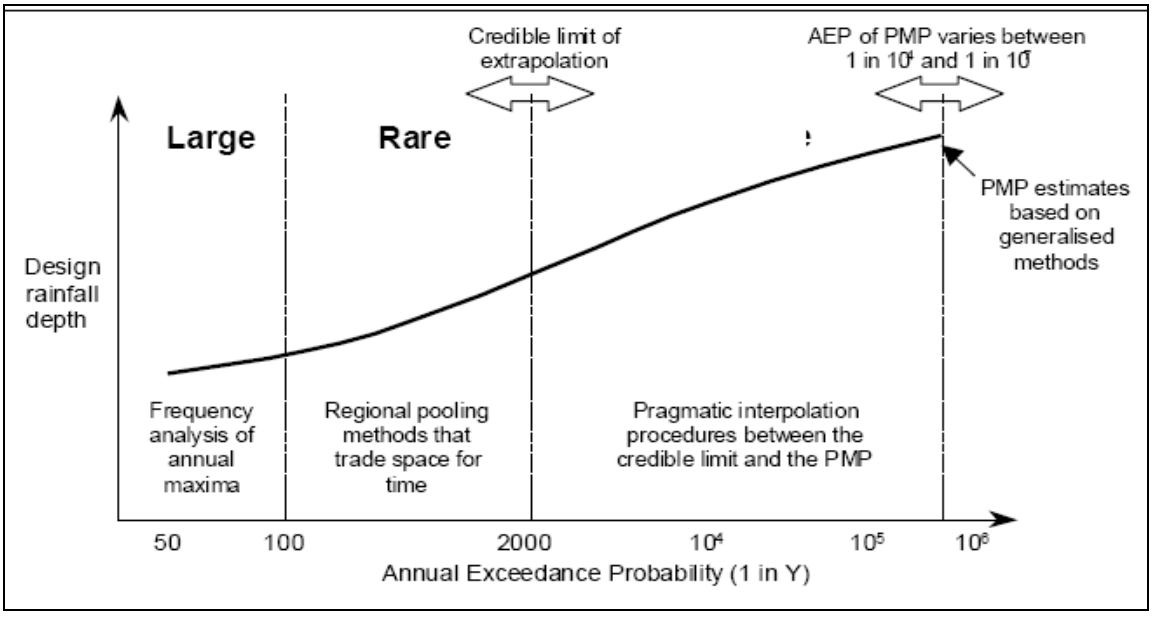

Figure 3.1 Summary of Procedures Used to Derive Design Rainfall Depths

The ANSCOLD paper recommended assigning an AEP to the PMP based on a review by Laurenson and Kuczera (1999). The method looked at procedures developed in Australia and other countries. The AEP of PMP estimates vary solely as a function of watershed area as shown in Figure 3.2. There is considerable uncertainty surrounding these recommendations based on methods

whose conceptual foundations are unclear and the events are outside the range of experience. The 75% confidence and upper and lower limits are very large, but are regarded as realistic. A probability mass function is provided to allow the incorporation of uncertainty into risk analysis. Although the probabilities are subjective, they reflect the uncertainty in the AEP estimates of PMP events (ANSCOLD, 2000).

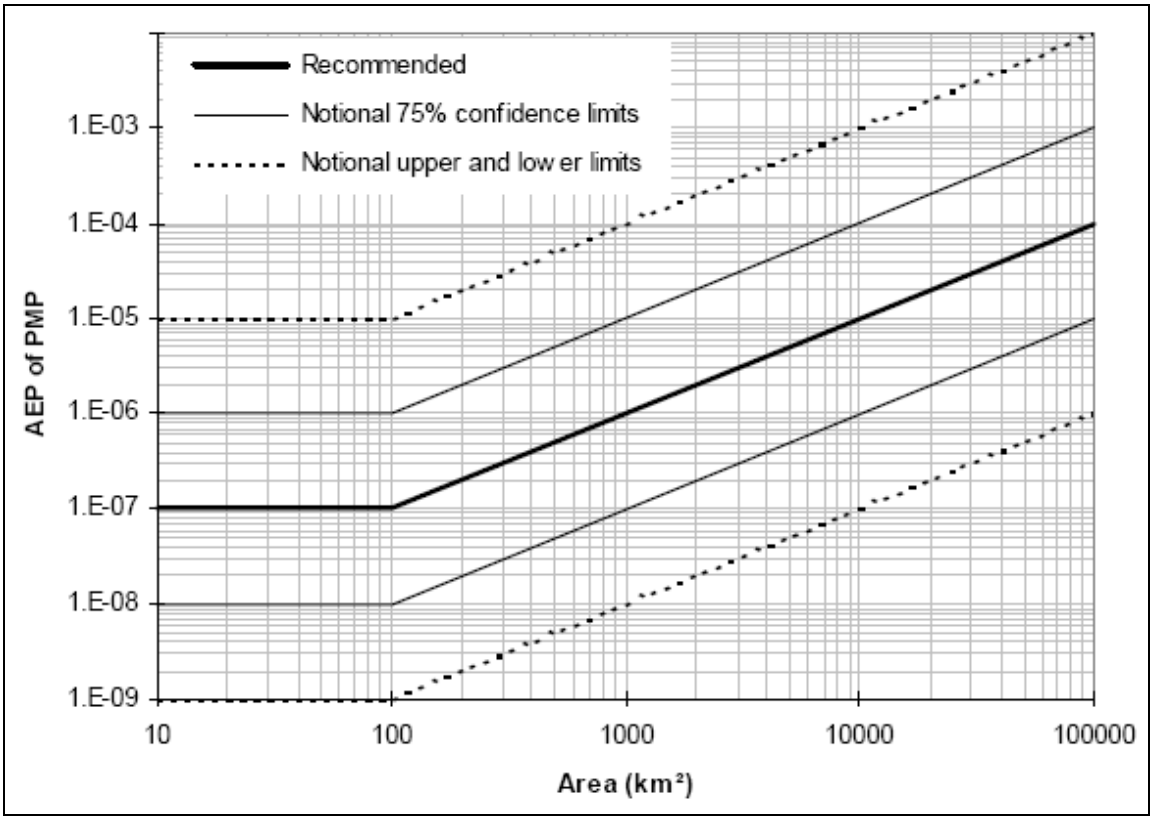

Figure 3.2 ANSCOLD Recommended Values of PMP Event AEPs

3.2 General Analysis of Rainfall Variables

Rainfall is a complex and ever changing driver of the hydrologic cycle within a region. Precipitation in the Western United States is influenced by the El Nino Southern Oscillation, the Madden-Julien Oscillation, the Pacific Decadal Oscillation, and many other factors. These meteorological phenomena are then coupled with topographic influences created by coastal mountain ranges which create orographic effects that increase rainfall on the windward side of the mountain and create rain shadows on the leeward side.

Spatial and temporal variations create a four dimensional reality that is often simplified for use in hydrologic models in the form of design storms. Design storms are also utilized due to difficulties in estimating flood frequency for ungaged watersheds where records are short (Linsley et. al, 1982). Design storms are usually developed for different recurrence intervals (AEP) and durations (time period). For example, a design storm could be a 50-yr 24-hr storm, or a 2-yr 1-hr storm.

Design storms require understanding regional storm types (Section 3.1.1), spatial distributions (Section 3.1.2), temporal distributions (Section 3.1.3), and total volumes of rainfall (Section 3.2). Storm type is dependent upon the region, the climate, and the topography. The rainfall spatial distribution is evaluated using area specific isohyets or through area-reduction relationships developed for the

region. The temporal distribution is often determined from the hyetographs of many historic storm events in the area of interest. Total volumes are determined using meteorologic data, modeling, and frequency analysis to determine the rainfall volume associated with a given AEP and duration.

3.2.1 Storm Type – Thunderstorm versus General Winter Storm

Evaluating rainfall characteristics for use with design storms and frequency analysis requires evaluating whether storm events are homogeneous. Rainfall within Los Angeles County falls within two general categories: convective storms and general winter storms. Runoff due to rainfall on snow covered mountains is not a very common occurrence in most of Southern California and is not considered in this study.

Convective storms, also known as thunderstorms, form as hot air rises and then rapidly cools. This causes precipitation in the form of rain or hail and also often results in thunder and lightning. This type of storm is often isolated to a small area within a region and has a short duration. Convective storms may also be embedded within general winter storms. HMR 58 uses the term “local storm” to describe short duration, high intensity rainfall events that influence small areas.

General winter storms are formed by weather systems that develop over the ocean and then move onto land. These systems have sustained moisture

available to keep feeding the storm system as it moves over land for several days. These storms often deliver consistent rainfall over a long period of time and may have durations of heavy rainfall embedded within the system. These types of systems, which tap into oceanic moisture and deliver large rainfall amounts to the western coast, have recently been classified as Atmospheric Rivers (Ralph et. al 2004, 2006; Neiman et. al 2008) and often bring widespread flooding to Southern California.

Local storms are defined by HMR 58 as a storm with a 6-hour duration. These events have high intensities but impact smaller areas within a larger region. Spatial and temporal analyses are required to determine the type of storm and how it should be used for frequency analysis and design storm creation.

3.2.2 Analysis of Spatial Rainfall Distributions - Development of the design storm requires evaluating the spatial and temporal distributions of measured rainfall events to generalize regional patterns. The spatial distribution requires evaluation of the scale of storm systems, orographic effects that may impact spatial distributions, and the type of storm generating the rainfall.

The World Meteorological Organization (WMO) has developed procedures for conducting depth-area-duration analyses (WMO, 1969). The process is summarized by Linsley et. al (1982) and is provided for understanding of

hydrologic processes. For storms with a single major center, the isohyets are taken as boundaries of individual areas. The average storm precipitation within each isohyet is computed and the storm total is distributed through successive increments of time. The time distribution is related to nearby gages for set time increments. Once the data is synchronized with the time distribution, the average rainfall over areas of varying sizes are determined. The maximum values for each area and duration are plotted and used to develop an enveloping curve. Storms with multiple storm centers are divided into regions for analysis.

Orographic effects often influence the amount of rainfall delivered to different areas within Southern California. The variation of precipitation has been studied with varying conclusions (Linsley et. al, 1982). Spreen (1947) studied the influences of elevation, slope, orientation, and exposure on seasonal precipitation in Western Colorado. Elevation accounted for 30 percent of the variation, while the four factors combined accounted for 85 percent of all variability. Some investigators only evaluate the precipitation-elevation relationship since elevation has been determined to be the greatest factor. Rainfall estimates in ungaged areas utilize these relationships to distribute rainfall appropriately between gaged locations.

Another method for utilizing rainfall spatial variations is to develop rainfall isohyets for different recurrence intervals and use the isohyets without depth

area reductions. Rainfall at gages within a region are analyzed using frequency analysis to determine rainfall totals for different AEPs and durations. The area weighted isohyetal value is used for modeling watershed subareas within a watershed model. These depths are matched to temporal distributions to generate the design storm.

3.2.3 Analysis of Temporal Rainfall Distributions – Once spatial relationships have been established for depth-area-duration, orographic effects, and the storm type to be used for the design storm, the temporal distribution must be developed for the design storm. The temporal distribution is usually provided as a hyetograph.

Alternating Block Analysis - Balanced Storm

The alternating block analysis method for developing a rainfall hyetograph requires development of an intensity-duration-frequency (IDF) curve which relates the intensity to a duration time for a specific AEP. Once the curve is developed, it can be used to develop a hyetograph for a design storm. Points on the IDF curve are read at a set time interval. For example, a curve could be broken into increments of ten minutes or of one hour.

For a balanced storm, the blocks of precipitation are then rearranged with the highest intensity placed in the middle of the storm time. In a 24-hour storm, the

largest block would be placed at the 13 hour mark. Assuming an hourly precipitation block, the next highest block would be placed at 12 hours and the third highest block would be placed at 14 hours. This alternating placement of blocks on either side of the center of the largest rainfall amount leads to a hyetograph for the design storm. Table 3.1 shows an alternating block analysis which is shown in graphical form in Figure 3.3.

Table 3.1 Alternating Block Method of Hyetograph Development

Rank (Block)	Time (hrs)	Intensity (in/hr)	Cumulative Precipitation	Block Positioning	Hyetograph Values
1	1	1.000	1.000	24	0.003
2	2	0.750	1.750	22	0.008
3	3	0.600	2.350	20	0.020
4	4	0.500	2.850	18	0.040
5	5	0.450	3.300	16	0.060
6	6	0.300	3.600	14	0.080
7	7	0.250	3.850	12	0.120
8	8	0.200	4.050	10	0.150
9	9	0.180	4.230	8	0.200
10	10	0.150	4.380	6	0.300
11	11	0.130	4.510	4	0.500
12	12	0.120	4.630	2	0.750
13	13	0.100	4.730	1	1.000
14	14	0.080	4.810	3	0.600
15	15	0.070	4.880	5	0.450
16	16	0.060	4.940	7	0.250
17	17	0.050	4.990	9	0.180
18	18	0.040	5.030	11	0.130
19	19	0.030	5.060	13	0.100
20	20	0.020	5.080	15	0.070
21	21	0.010	5.090	17	0.050
22	22	0.075	5.165	19	0.030
23	23	0.050	5.215	21	0.010
24	24	0.025	5.240	23	0.005

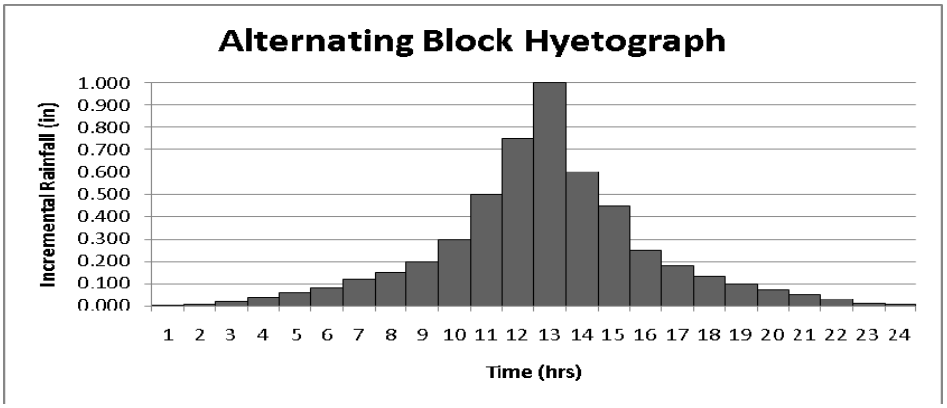

Figure 3.3 Alternating Block Hyetograph Example

Modified Alternating Block Analysis

Due to varying conditions throughout the country, other distribution methods have been developed to account for regional rainfall characteristics. Within Los Angeles County, two modified alternating block methods have been suggested for the development of design storms. The first modified alternating block method is the 2/3 rear weighted storm preferred by the Federal Energy Regulatory Commission (FERC) and the California Department of Safety of Dams (DSOD). The second is the 8/10 rear weighted storm preferred by the Los Angeles County Department of Public Works (LACDPW, 2006).

The 2/3 rear weighted storm shifts the center of the storm from the halfway point to a point at 2/3 of the time. For a 24-hr period, this corresponds to 16 hours instead of 12 hours through the storm. This is preferred by the regulators due to regional patterns of temporal rainfall distribution and also allows reservoirs to fill before the peak of the storm impacts the watershed. It is felt that this provides a safer design scenario for peak flow related designs.

The Los Angeles County Department of Public Works studied rainfall patterns throughout the County to determine rainfall temporal distributions. After analyzing many major storm events at many gages, it was determined that 80 percent of the rainfall occurred after 80 percent of the time had elapsed. Public Works utilizes a modified weighted alternating block method for 24-hour storms

where 80 percent of the rainfall occurs at approximately 19 hours (LACDPW, 2006). Figure 3.4 shows the difference between these three temporal distributions.

The figure represents balancing a 72-hour storm for the PMP using a balanced storm, a 2/3 weighted storm, and an 8/10 weighted storm with the same depth. The chart shows that the balancing of the alternating blocks around a specified time results in very different temporal distributions in the hyetograph. When developing a design storm, it is necessary to reconcile the design weightings to observed rainfall patterns in the region.

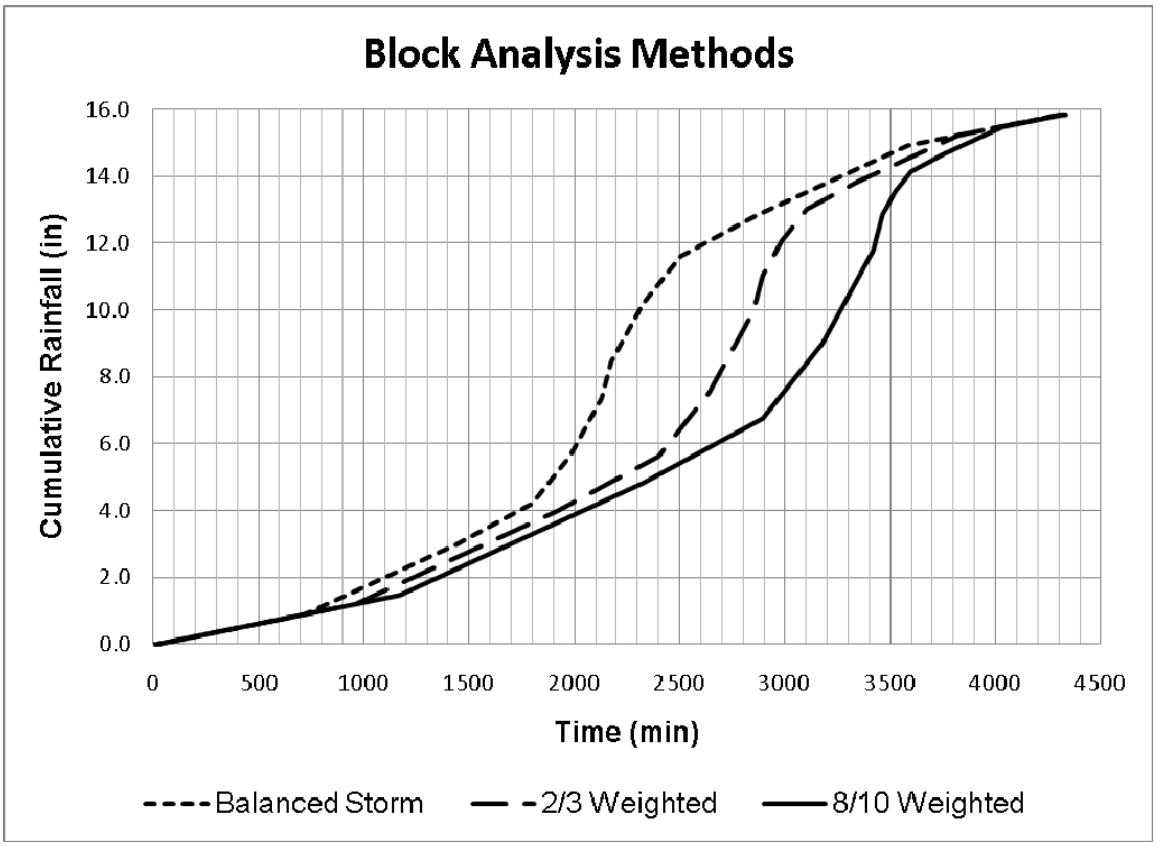

Figure 3.4 Hyetographs for Different Weightings on Alternating Block Method

The methods discussed above are used to develop design storms such as the PMP as discussed in HMR 58 and the rainfall used for determining the Capital Flood event used by Public Works. The next section discusses rainfall data availability within Los Angeles County and how it is used in this study.

3.3 Rainfall Data in Los Angeles County

Rainfall data is used to help forecast flooding, determine event frequency, develop design storms, and as input to models for the design of flood control and

water conservation facilities. Rainfall records have been diligently maintained since the late 1800's in the Los Angeles area. The Los Angeles County Flood Control District was formed in 1915 to deal with flooding within the County. The Flood Control District established a network of rain gages throughout the County and has monitored and expanded the network for the last 95 years. The National Weather Service, and its predecessor, the Bureau of Weather Services, also collected rainfall data. Currently, other agencies also collect rainfall data in certain areas of the County, including the Los Angeles County Fire Department, the City of Los Angeles, the California State Department of Water Resources, and the United States Army Corps of Engineers. Data for many of these gages are also collected by the Los Angeles County Department of Public Works in behalf of the Flood Control District.

Over the last 95 years, over one thousand gages have been installed throughout Los Angeles County. The history of each gage is unique. Some have remained in the same place for their entire period of record, others have been moved to nearby locations, and many have been abandoned. The current study utilized data from the active rain gages within Los Angeles County with annual records longer than 20 years. Appendix A contains the station number, name, region, elevation, location in latitude and longitude, and the years of record used in the analysis.

Figure 3.5 shows the location of the gage within the County, along with the station number. The figure shows eight regions within the County that were developed based on climate, elevation, and physical boundaries created by the mountains. The regions were defined by the Los Angeles County Flood Control District based on historical observations. The gage numbers in the figure correspond to the station number in Appendix A. Table 3.2 provides information about the regions shown in Figure 3.5.

Table 3.2 Rainfall Regions of Los Angeles County

Region	Name	Average Annual Rainfall (in)
A	Coastal Plain	13.71
B	San Fernando Valley	17.79
C	San Gabriel Valley	17.57
D	San Gabriel Mountains	27.24
E	Little Rock/Big Rock Canyons	18.76
F	Santa Monica Mountains	20.36
G	Santa Clarita	17.09
H	Antelope Valley	8.20

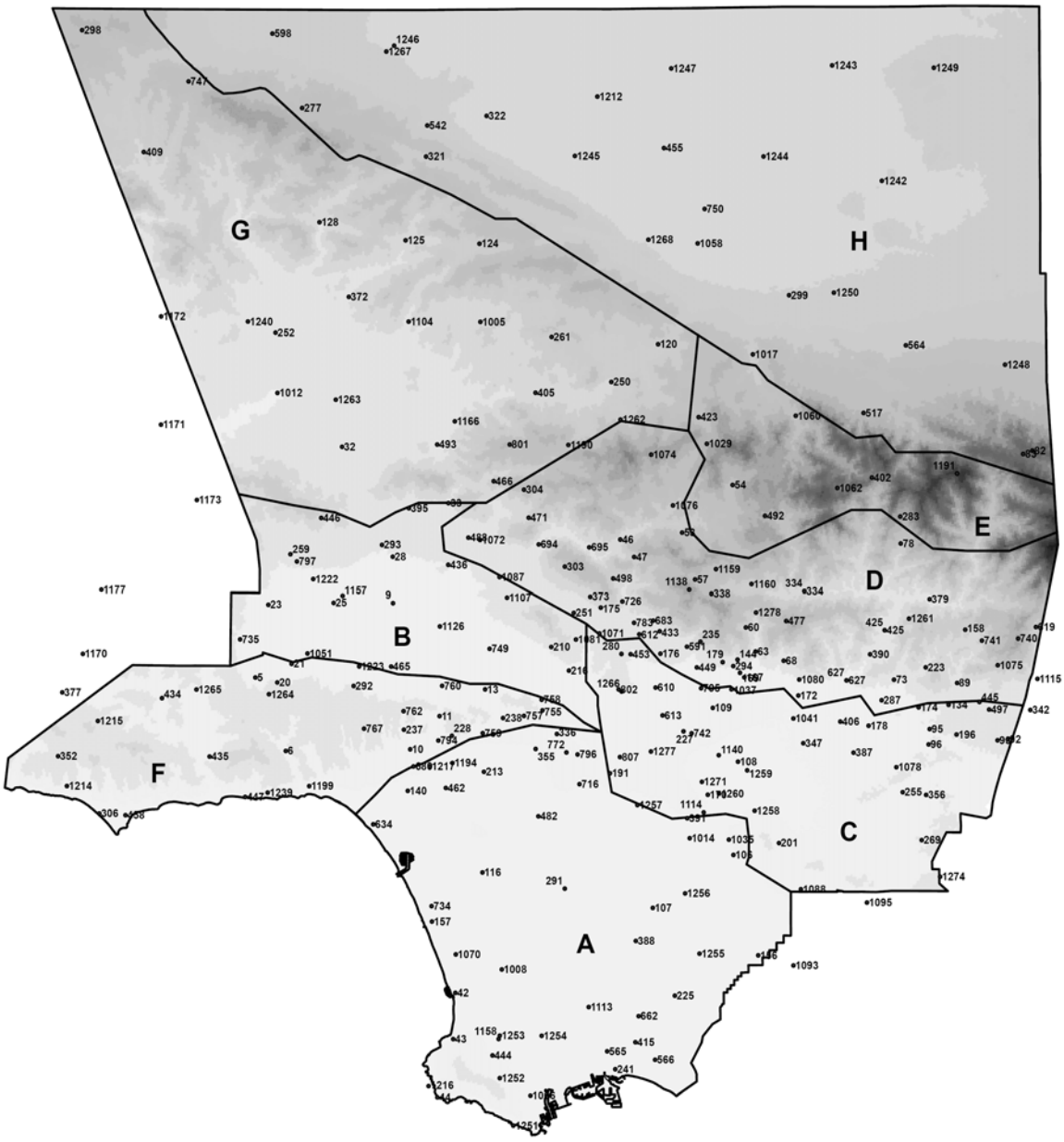

Figure 3.5 Rain Gages and Regions Used in PMP Analysis

3.4 Analysis of Rainfall Frequencies in Los Angeles County

The Los Angeles County Department of Public Works currently uses the GEV1 distribution to determine rainfall frequencies throughout the County. As seen in Chapter 2, selection of a valid frequency distribution plays an important role in the overall results of a study. In an effort to evaluate whether the GEV1 distribution fits the rainfall events in the County, a comparison chart using L-moment ratios was developed.

For a given distribution, moments can be expressed as functions of lower order moments (Rao and Hamed, 2000). Moment ratio diagrams show the relationship between sample estimates of a distribution and moments of the actual distribution. Two parameter distributions show up on the moment ratio diagram as a point, three parameter distributions plot as lines. Moment ratio diagrams provide graphical insight into which distributions may fit a certain data set. However, small sample sizes may introduce bias to the analysis. If more than one station or data set is being evaluated as a region, Rao and Hamed (2000) suggest plotting the regional average along with the individual station moment ratios.

The data from Los Angeles County was plotted on moment ratio diagrams to evaluate the appropriateness of distributions to be fit to the data. Figure 3.6

shows L-moment kurtosis (L-Ck) versus L-moment skew (L-Cs) diagrams for the entire rain gage data set. The distributions evaluated include the Log-Normal, Generalize Pareto, Generalized Logistic, General Extreme Value (GEV), Gumbel (GEV1), Normal, and Gamma-PIII. The moment ratios from the rain gages were plotted in Figure 3.6, along with the average moment ratio for all of the data sets.

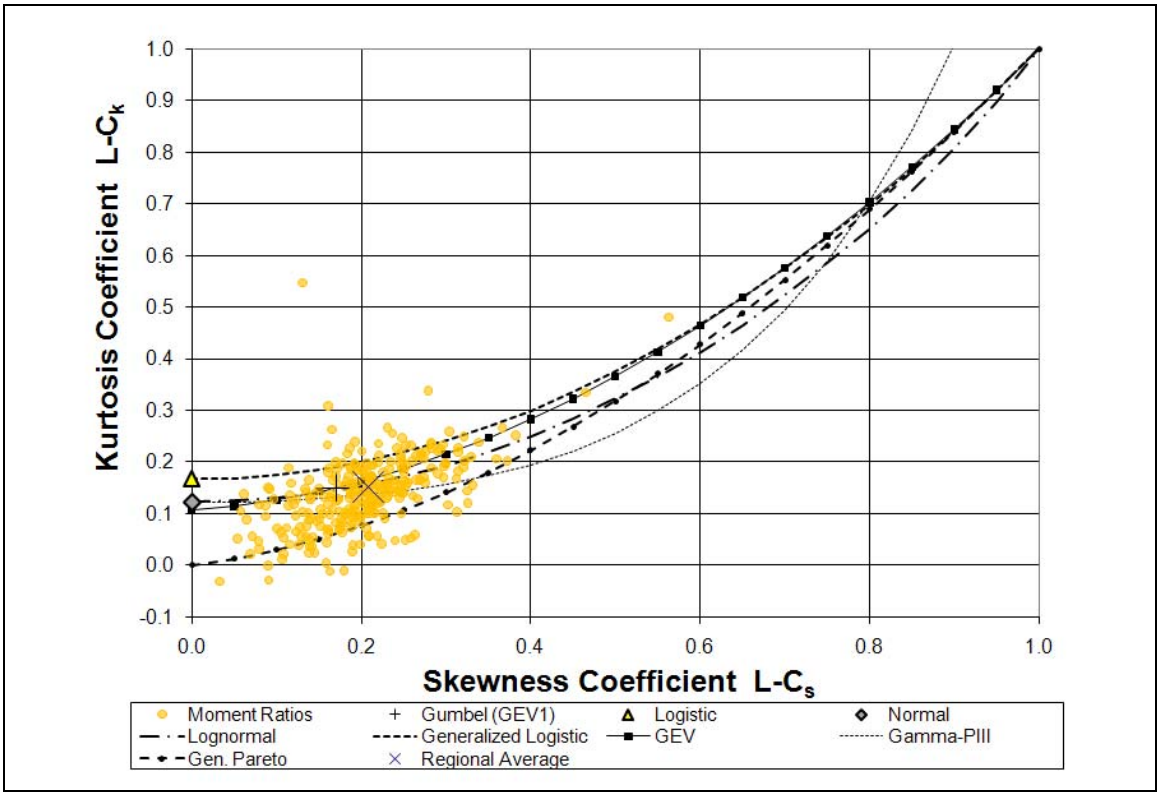

Figure 3.6 L-Moment Ratio Analysis for all Analyzed Gages

Figure 3.6 shows that many of the distributions would fit some portion of the rain gage data sets reasonably well. The Log-Normal and GEV appear to provide the best data fitting. As can be seen, the average moment for the entire data set as a region indicates that the Gumbel (GEV1) distribution is a reasonable

assumption. Figure 3.6 also shows that there are many outliers which are significantly different than many of the standard distributions used for extreme event modeling of data sets.

In an effort to investigate these outliers, only the data sets with records greater than 50 years were plotted in Figure 3.7. Setting the threshold at 50 years of record reduced the outliers that were above and below the standard parent distributions and also moved the data set regional average closer to the GEV1 distribution.

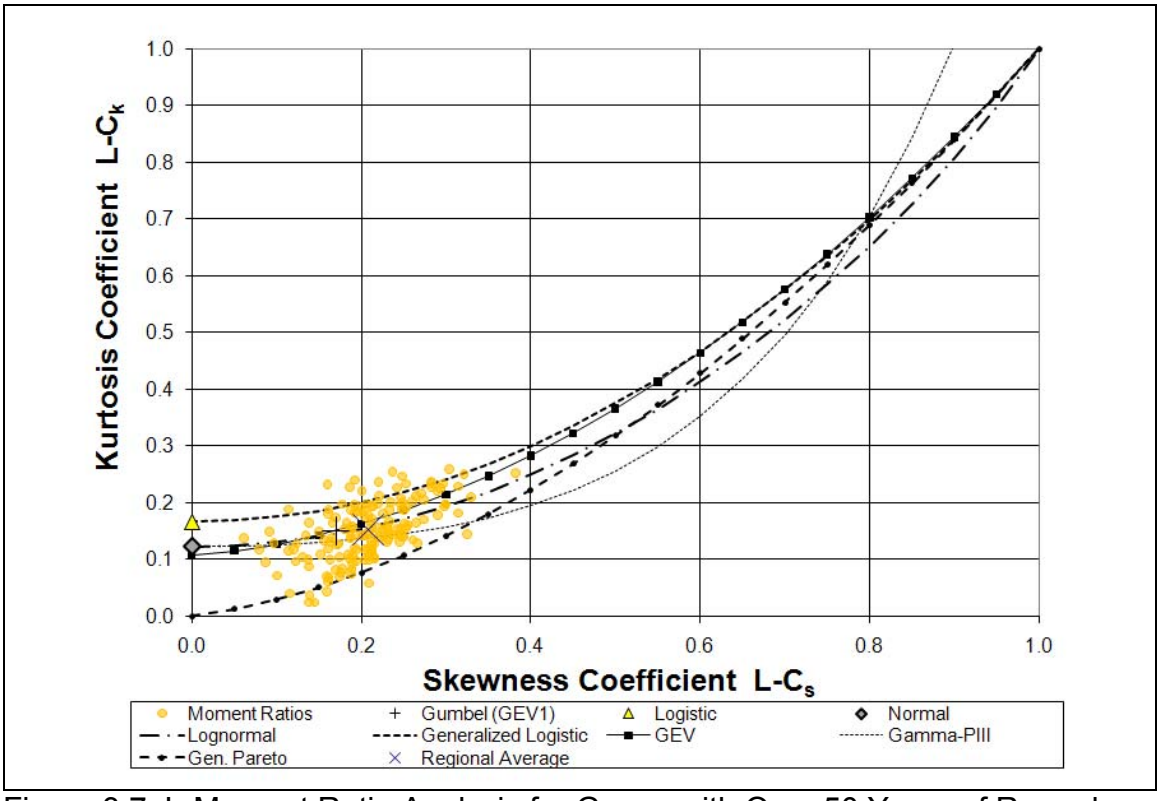

Figure 3.7 L-Moment Ratio Analysis for Gages with Over 50 Years of Record

As can be seen in Figure 3.7, both the GEV and Log-Normal distributions still fit the moment ratio data very well. This goodness-of-fit is due to the three parameter nature of the distribution allowing more flexibility to fit the data.

In an effort to determine whether the geographic regions established by the County (Table 3.1 and Figure 3.2) were significantly different with respect to selection of a frequency distribution, the average L-moment rations for Regions A – H were plotted in Figure 3.8. The regional average for the County was also plotted. The data was grouped so closely together that another plot with a tighter range was required to graphically evaluate goodness-of-fit. Figure 3.9 provides the plot with a more narrow range.

As can be seen, six of the regions fall between the County regional average and the GEV1 value. Regions G and H are right on top of each other. Two regions have higher skew, but this looks significant only when the axis range is significantly reduced and is a function of the plotting. Use of the GEV1 was considered appropriate for estimating extreme rainfall recurrence intervals and has been used for all rainfall frequency analysis in the remainder of this study.

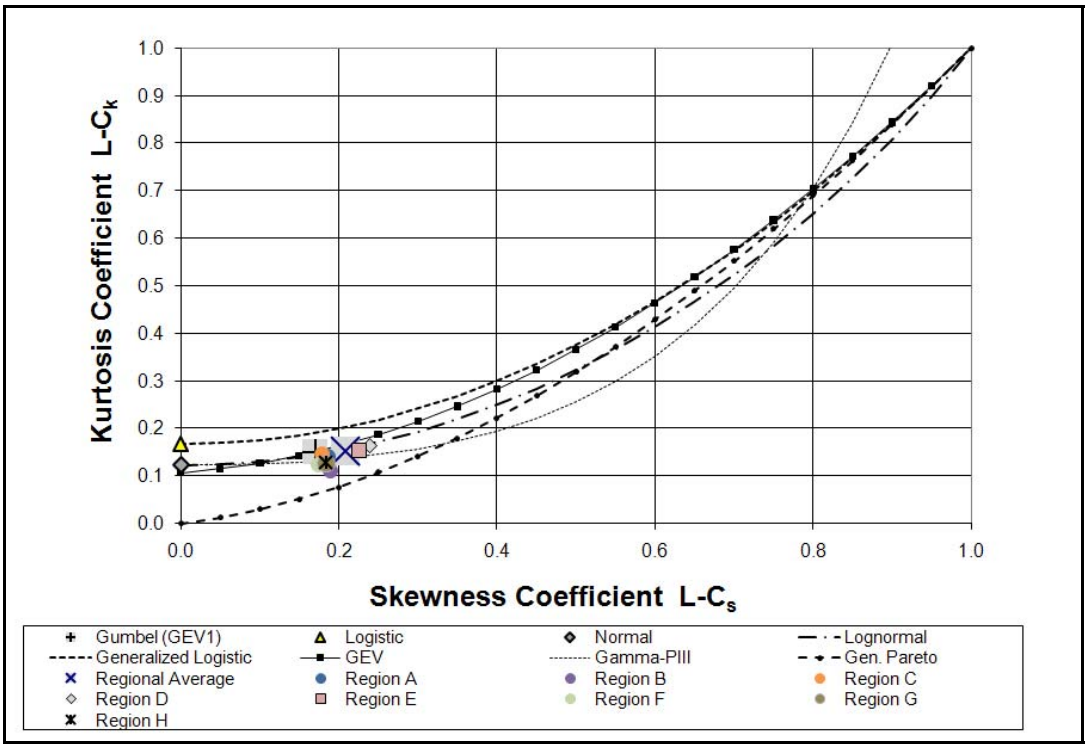

Figure 3.8 L-Moment Ratio Analysis of Regional Averages

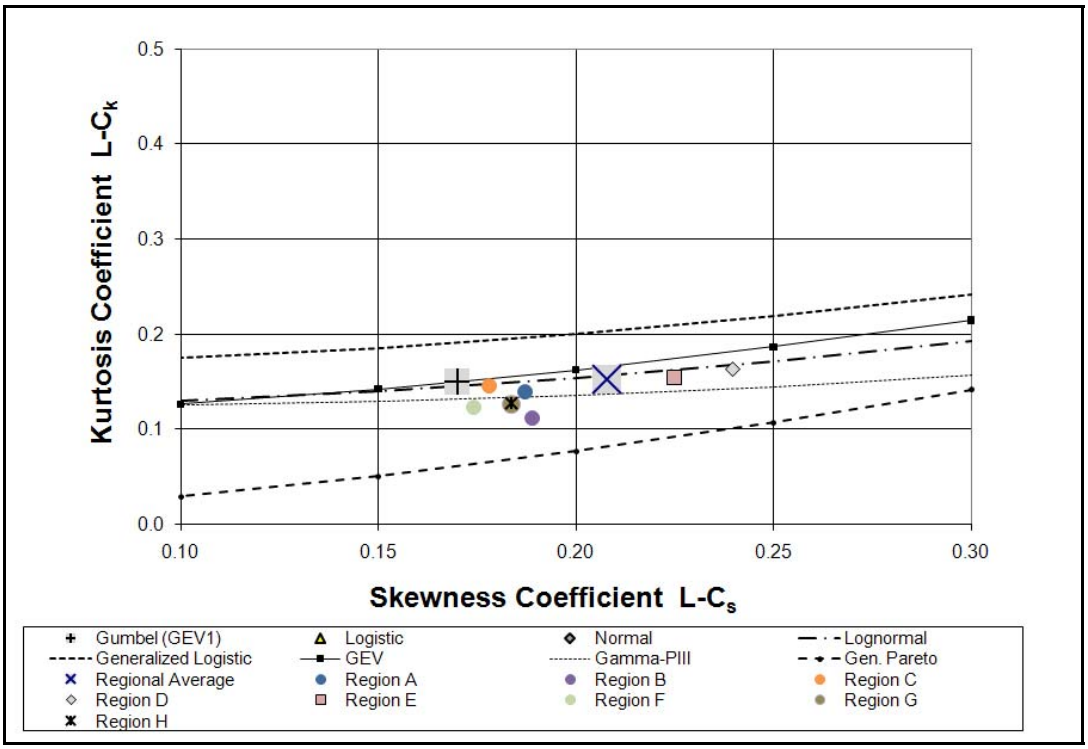

Figure 3.9 Close-up of L-Moment Ratio Analysis for Regional Averages

Appendix B contains rainfall frequency data for the rain gages based on the GEV1 distribution described in Chapter 2. The data includes the mean, standard deviation, and variables related to L-moment analysis discussed in Chapter 2. The last two columns contain the α and β variables used in the GEV1 distribution discussed in Chapter 2. Frequency analysis results for the 24-hour rainfall are also provided in the appendix for the following recurrence intervals: 10, 25, 50, 100, 200, 500, 10^3, 10^4, 10^5, 10^6, 10^7, 10^8, 10^9, 10^{10}, 10^{11}, and 10^{12}.

3.5 HMR 58 PMP Values Within Los Angeles County

With the determination of hydrologic frequencies discussed in Section 3.3, comparisons can be made between the official PMP values used for design throughout Southern California and rainfall frequencies at specific rain gages. The official PMP values are found in HMR 58 and are available in GIS format as shapefiles. Figure 3.10 is an isohyetal map of the PMP estimates developed for the HMR, along with regional boundaries for regions within Los Angeles County.

The isohyetal lines were converted to a raster image and merged with the gage shapefile to produce a table with the PMP value for each gage used in this study. Appendix B contains the HMR PMP value for each gage, along with the order of magnitude recurrence interval based on the GEV1 probability distribution. The

data in Appendix B provided enough input to evaluate frequencies of PMP estimates from HMR 58.

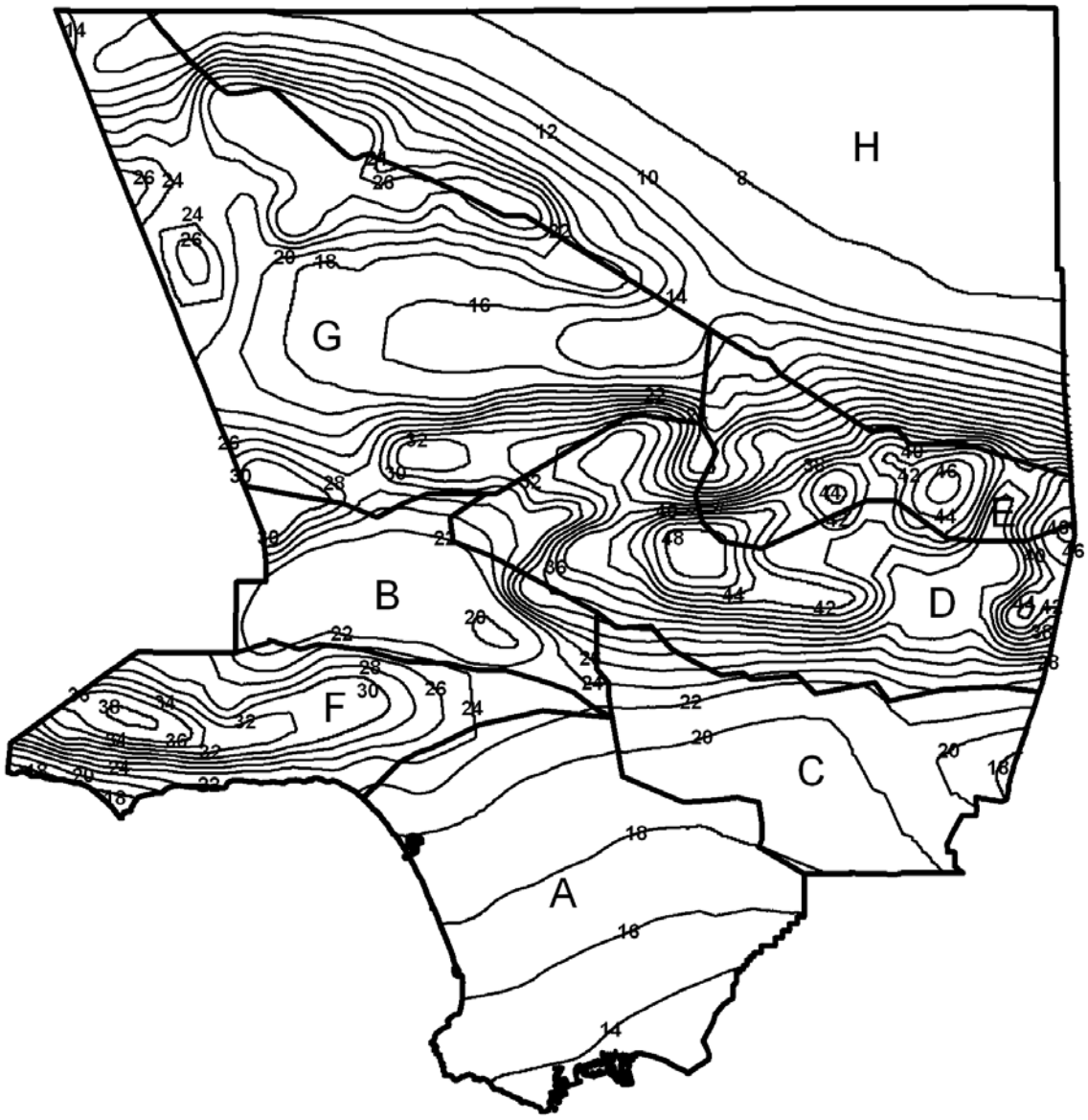

Figure 3.10 Isohyetal Distribution of PMP Based on HMR 58 and 59.

The National Research Council (1994) indicated that the PMP recurrence interval estimates across the United States generally range between 10^5 and 10^9. These values are fairly consistent with the data from within Los Angeles County, which generally centers around 10^8, with some outliers between 10^3 and 10^{13}. Figure 3.11 shows the distribution of recurrence intervals for the 269 Los Angeles County rain gages evaluated for this study.

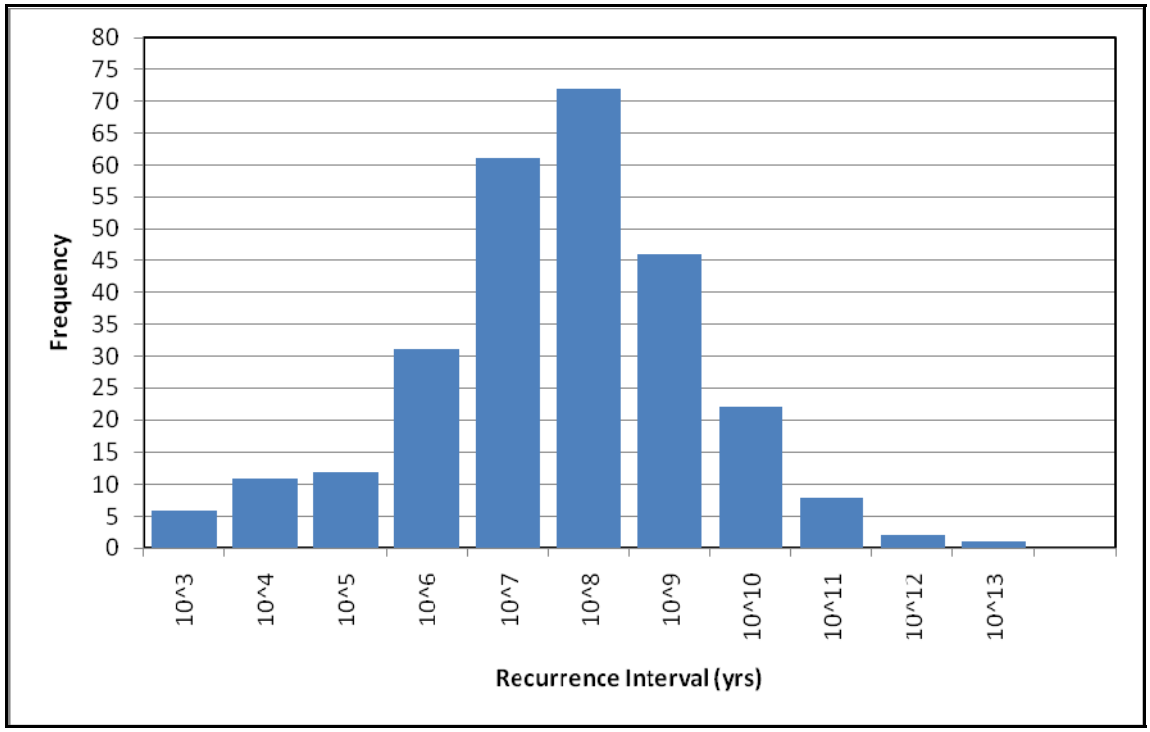

Figure 3.11 Recurrence Interval for PMP Estimates within Los Angeles County

Due to the wide distribution of recurrence intervals provided by the HMR for gages within the County, the data set was evaluated based on the hydrologic/climatic regions which are described in Table 3.2 and shown in Figure 3.5. The analysis evaluated whether different climate regions had different

ranges of recurrence intervals. Figure 3.12 presents a graph of the probability curves of each recurrence interval by region. Some regions had many more gages than other regions, which must be considered when evaluating the graph due to possible bias from limited data sets as discussed in Chapter 2. Regions with more gages had more well behaved probability curves. However, although there is some randomness in the plot, it is evident that the regional differences in climate do not explain the range of recurrence intervals for the PMP found within the HMR for Los Angeles County.

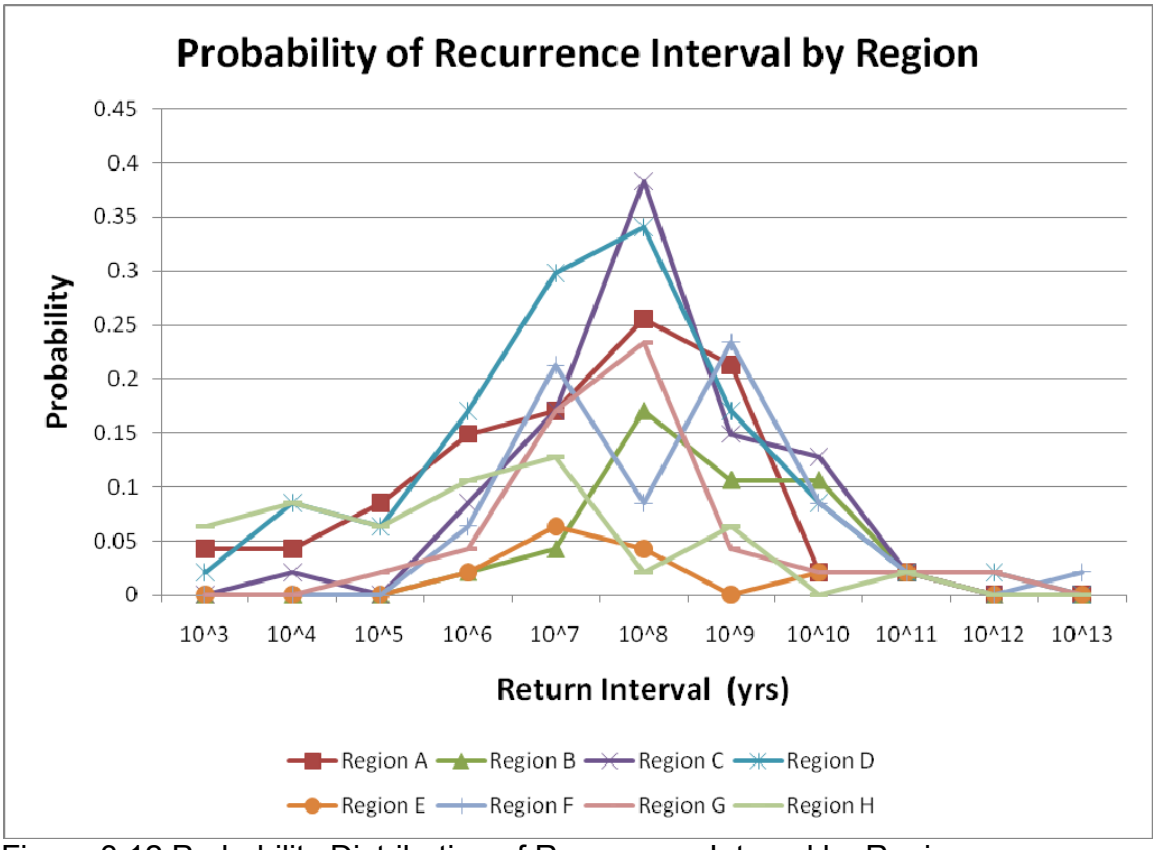

Figure 3.12 Probability Distribution of Recurrence Interval by Region

The rainfall gages were then separated into groups based on the length of recorded rainfall to determine whether record length had an influence on the estimate of recurrence interval. The data is plotted in Figure 3.13.

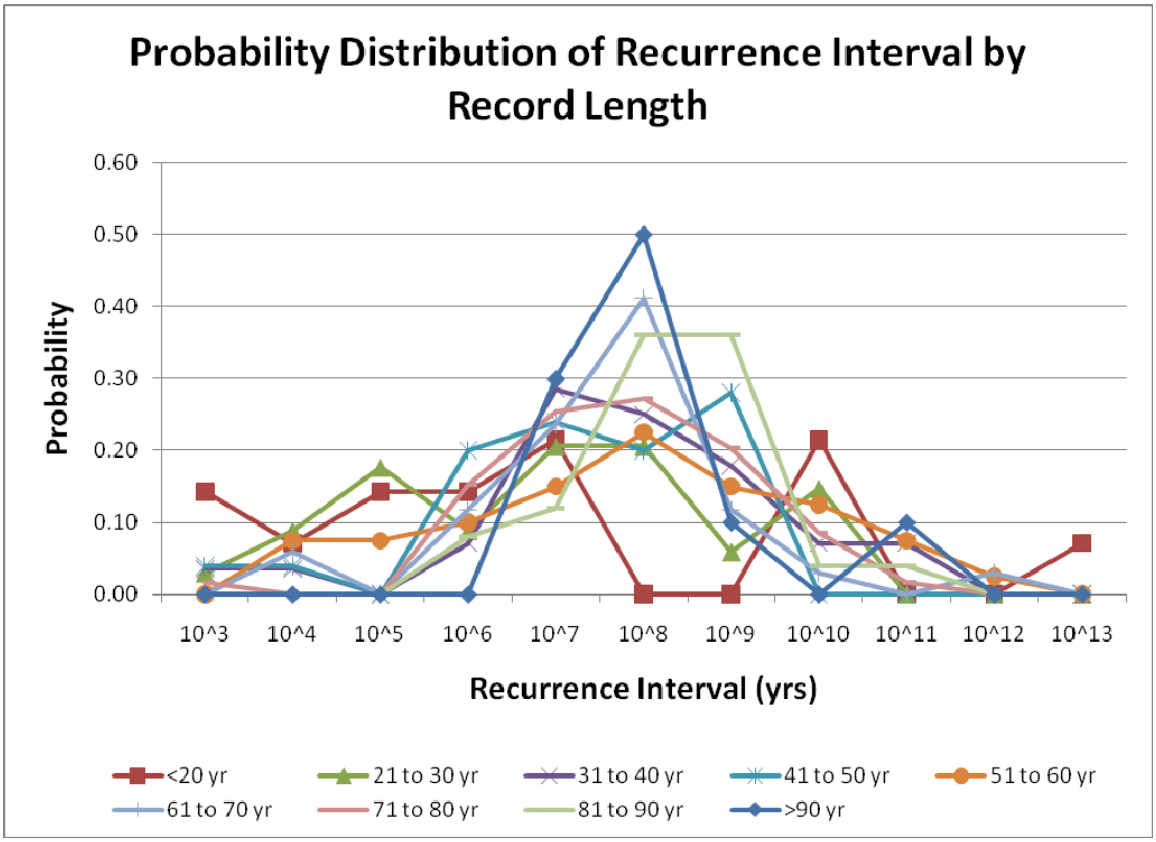

Figure 3.13 Probability of Recurrence Intervals Based on Record Length

Figure 3.13 shows the probability distribution of the rainfall recurrence intervals based on the years of record for the gage. The figure shows that for most gages, the probability distributions are fairly similar. The only distribution that is significantly different is the ">90 yr" set. After evaluating Figure 3.13, the variations appeared to be related to the limited number of gages with certain

gage periods. The effect of the small numbers of gages within the record length bins was then evaluated by combining data sets to create three data sets with 76 to 99 gages. Creating more evenly sized data sets resulted in Figure 3.14.

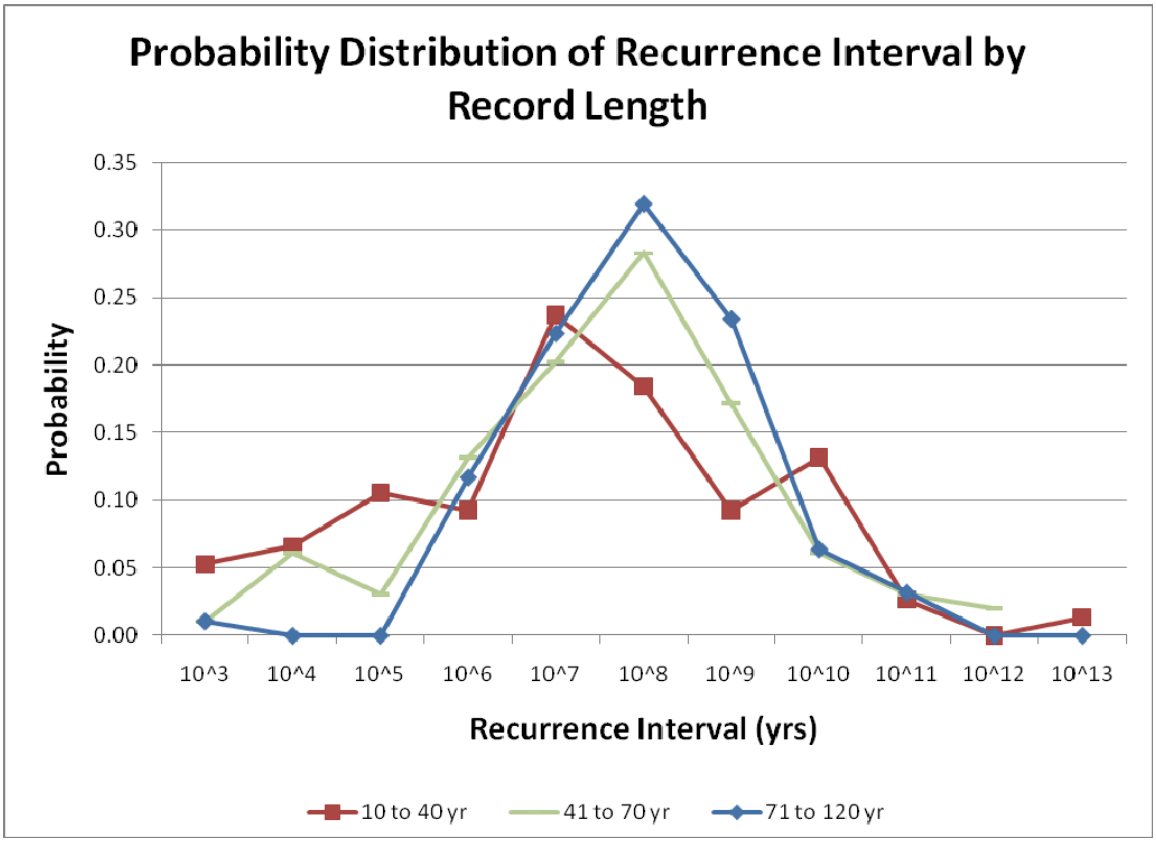

Figure 3.14 Probability of Recurrence Intervals Based on Adjusted Record Length Groupings

As shown in Figure 3.11, with three groups of similar size, the probability distributions for the PMP rainfall recurrence interval are very similar to the histogram shown in Figure 3.8. This indicates that although rainfall record length and regional climates and topographies vary throughout the county, estimates of the PMP follow a probability distribution roughly centered around

10^8 years. Each group of rain gages still showed a wide range of recurrence interval over approximately ten orders of magnitude. This range for PMP recurrence intervals over several orders of magnitude indicates that modeling of the PMF should also vary over several orders of magnitude since PMP is the major driver in runoff models. Use of an area-weighted PMP value in developing the PMF may tend to reduce the variation in recurrence interval over larger watersheds. However, smaller watersheds will be more sensitive to the local PMP values.

3.6 Hershfield PMP Values Within Los Angeles County

Hershfield (1960) developed an empirical method for estimating the PMP from gage records when only precipitation records were available for an area. He updated the method in 1965 and it was adopted by the World Meteorological Organization (WMO) and published in 1973 (WMO, 1973). The method has been widely used (Drobot, 2004; Koutsoyiannis, 2009; Eliasson, 1994) due to the ease and limited requirements for meteorological data that are needed for other methods of estimating PMPs. The method is based on Ven T. Chow's (Chow, 1961) developments on general frequency distribution analysis:

$$X_T = \overline{X}_n + K * S_n \qquad \text{Eq. 3.1}$$

Where:

X_T = rainfall recurrence intervals in years

$\overline{X}_n$ = mean of the series of n annual maxima

K = frequency variable that depends on distribution being fit

S_n = standard deviation of the series of n annual maxima

Hershfield used records from 2600 stations to determine an enveloping curve for the value of K needed to develop the PMP. The curve is provided by the WMO (1973) and reproduced here for reference in Figure 3.15.

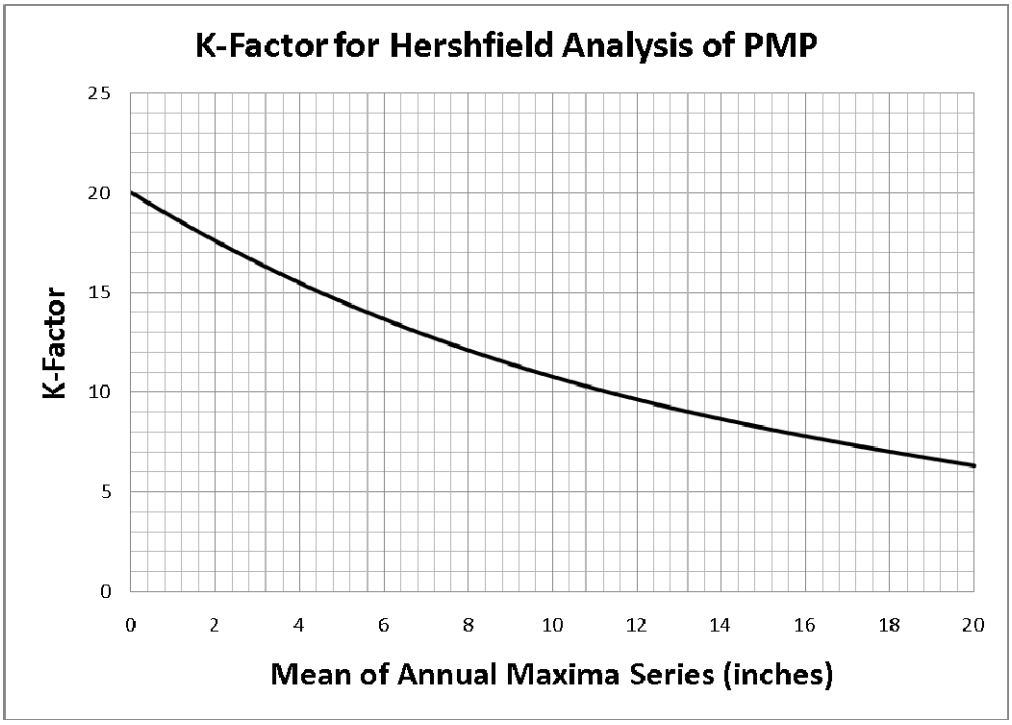

Figure 3.15 Curve for Estimating K-Factor for Hershfield Method of PMP Analysis

In an effort to aid computer calculations, an equation was fit to the curve and is labeled as Equation 3.2:

$$K = 20.0000 - 1.3037 * \overline{X}_n + 0.0449 * \overline{X}_n^{\,2} - 0.0007 * \overline{X}_n^{\,3} \qquad \text{Eq. 3.2}$$

As discussed in Section 2, short records have a higher probability of containing outliers that skew the data. Hershfield's method provides a way to adjust estimates for the PMP evaluation based on the number of years of record. The adjustment uses three factors to correct the mean and standard deviation as shown in Equations 3.3 and 3.4.

$$\overline{X}_n^{cor} = \overline{X}_n * f_1(\overline{X}_{n-m} / \overline{X}_n) * f_{3mean} \qquad \text{Eq. 3.3}$$

$$S_n^{cor} = S_n * f_1(S_{n-m} / S_n) * f_{3stdev} \qquad \text{Eq. 3.4}$$

Where:

$\overline{X}_n^{cor}$ = corrected mean of the series of n annual maxima

$\overline{X}_n$ = mean of the series of n annual maxima

$\overline{X}_{n-m}$ = mean of the series after excluding the highest annual maxima

S_n^{cor} = corrected standard deviation of the series of n annual maxima

S_n = standard deviation of the series of n annual maxima

S_{n-m} = standard deviation after excluding the highest annual maxima

f_1 = correction factor for the mean based on years of record and $\overline{X}_{n-m} / \overline{X}_n$

f_2 = correction factor for the mean based on years of record and S_{n-m} / S_n

f_{3mean} = correction factor for the mean based on years of record

f_{3stdev} = correction factor for the standard deviation based on years of record

Nomographs were provided in the WMO publication to help users determine the f_1, f_2, and f_3 adjustments for gages with up to 50 years of record. These nomographs were augmented to provide data for longer periods of record and are provided for reference as Figures 3.16, 3.17, and 3.18.

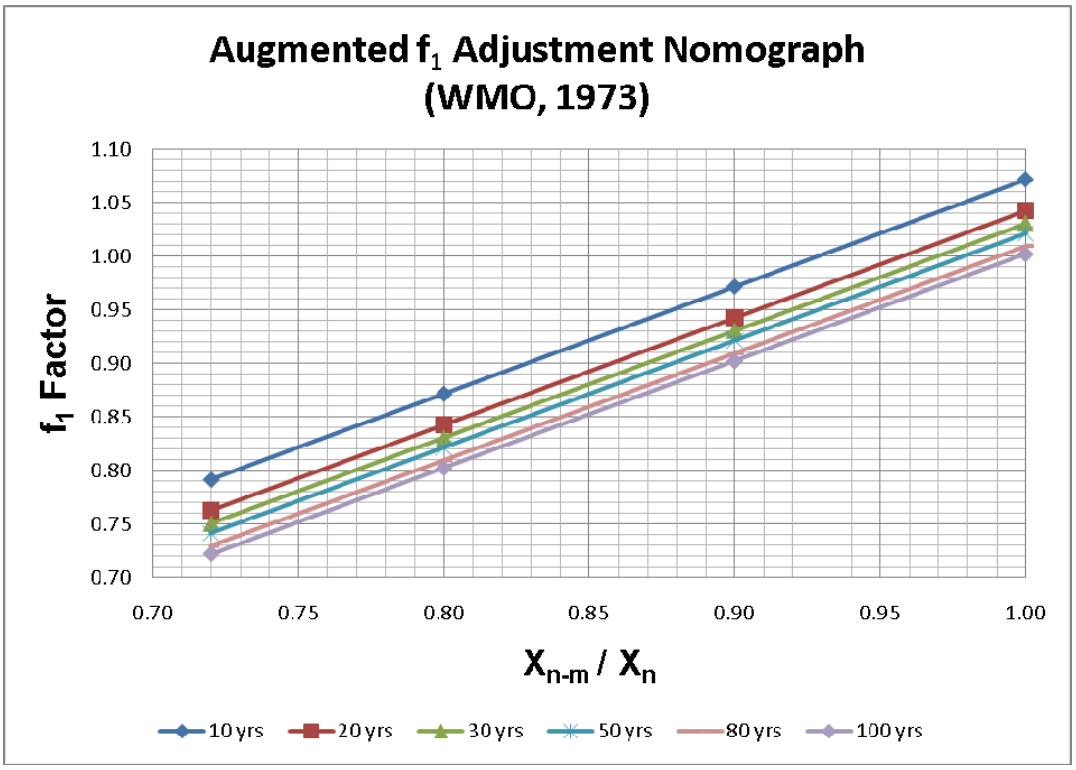

Figure 3.16 Augmented f_1 Factor for Hershfield Analysis

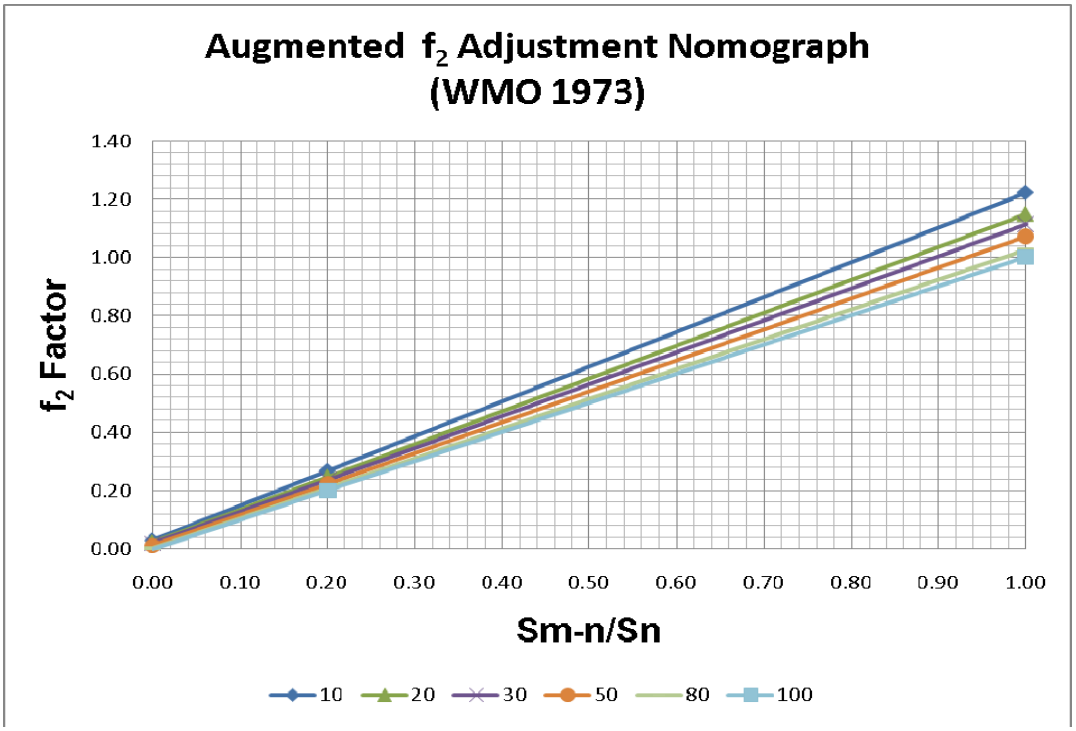

Figure 3.17 Augmented f_2 Factor for Hershfield Analysis

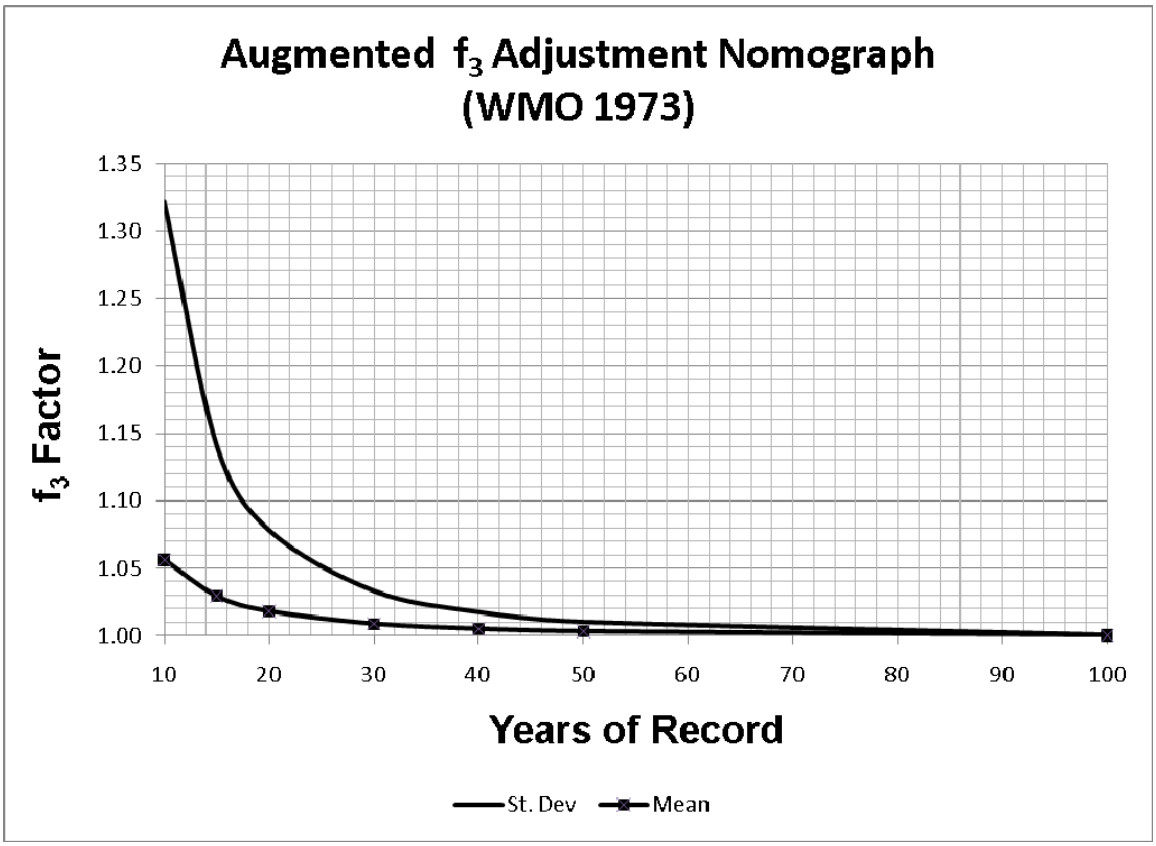

Figure 3.18 Augmented f_3 Factor for Hershfield Analysis

Equations have been developed which replicate values for the f_1, f_2, and f_3 nomographs to aid in computer calculations for large numbers of gage records. Equations 3.5 through 3.9 provide the information for the adjustment factors.

$$f_1 = \overline{X}_{n-m}/\overline{X}_n + \exp(-1.87286 - 0.09132n + 0.001583n^2 - 0.000011n) \quad \text{Eq. 3.5}$$

$$f_2 = (1.09 - 0.001n + 1.13/n) * S_{n-m}/S_n + (0.04 - 0.0019 * \ln(n)^2)) \quad \text{Eq. 3.6}$$

$$f_{3mean} = (0.998 + 5.1 * \ln(n)/(n^2))^{0.5} \quad \text{Eq. 3.7}$$

$$f_{3stdev} = 0.997 + 32.446/n^2 \quad \text{Eq. 3.8}$$

Where, n is the number of years of record and the other terms are described below Equations 3.3 and 3.4. These equations allow calculations to be carried out quickly by a computer rather than looking up the three values for each data set to be analyzed.

The Los Angeles County rain gage data sets were analyzed using the Hershfield method to determine the PMP rainfall estimate. A recurrence interval was determined for each gage using the same GEV1 distribution used to evaluate the PMP recurrence interval values based on rainfall totals from Hydrometeorolocial Report (HMR) 58. These Hershfield PMP recurrence interval values are also found in Appendix B. Once the Hershfield recurrence interval estimates were developed, the orders of magnitude range was evaluated to determine a probability distribution using the three gage groups based on years of record. Figure 3.19 shows the distributions, which are all centered around 10^8.

Although the distribution is similar to the recurrence interval distribution for HMR 58 shown in Figure 3.14, there are significant differences between the two data sets. Figure 3.20 plots the differences, in order of magnitude between the two data sets. The blue bars represent the actual distribution of differences, while the red bars represent a Normal distribution. The Hershfield method, based solely on gage record, does not match the HMR PMP values calculated

considering meteorology, topography, and transposition of extreme regional rainfall events.

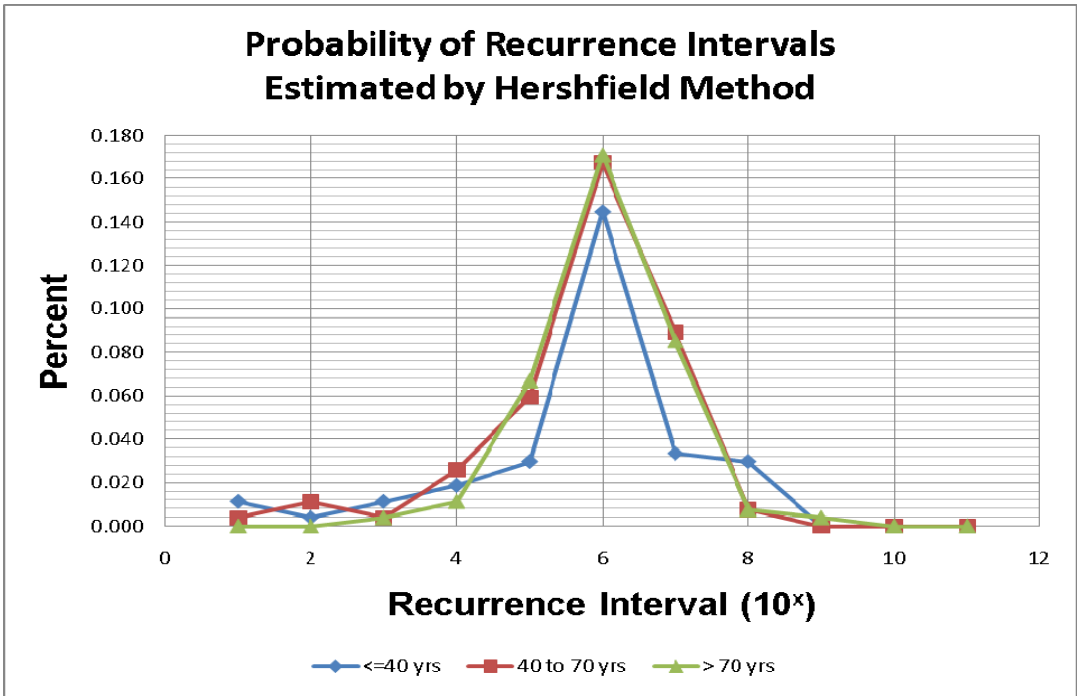

Figure 3.19 Hershfield PMP Recurrence Interval Distribution by Order of Magnitude

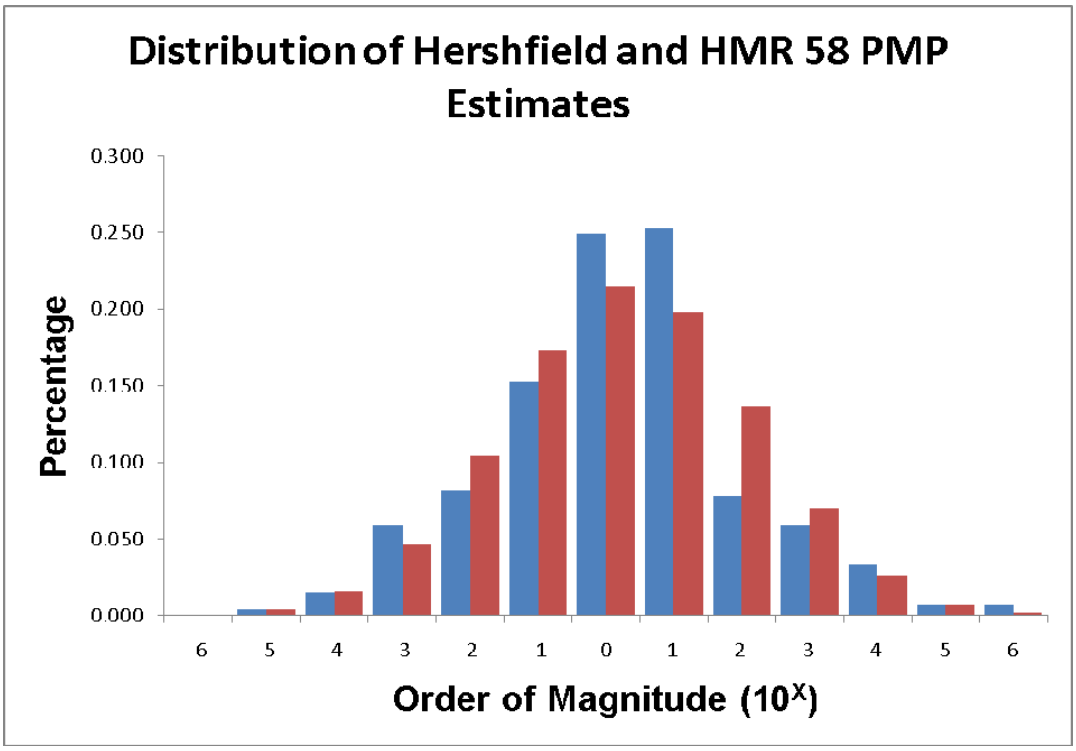

Figure 3.20 Distribution of Order of Magnitude Differences in PMP Estimates

Figure 3.20 shows the difference between the Hershfield and HMR 58 PMP estimates for the rain gages within Los Angeles County. The differences follow a Normal distribution pretty well as shown in the figure. In an effort to determine whether the differences were related to the different climatic regions within the County, ArcGIS was used to spatially locate the differences. Figure 3.21 shows the order of magnitude differences between the HMR 58 and the Hershfield PMP estimates. The larger circles around the gage show a larger difference in the estimates. A point with no ring indicates estimates of the same order of magnitude. As can be seen, the largest differences are scattered throughout the County, showing that region is not responsible for the difference.

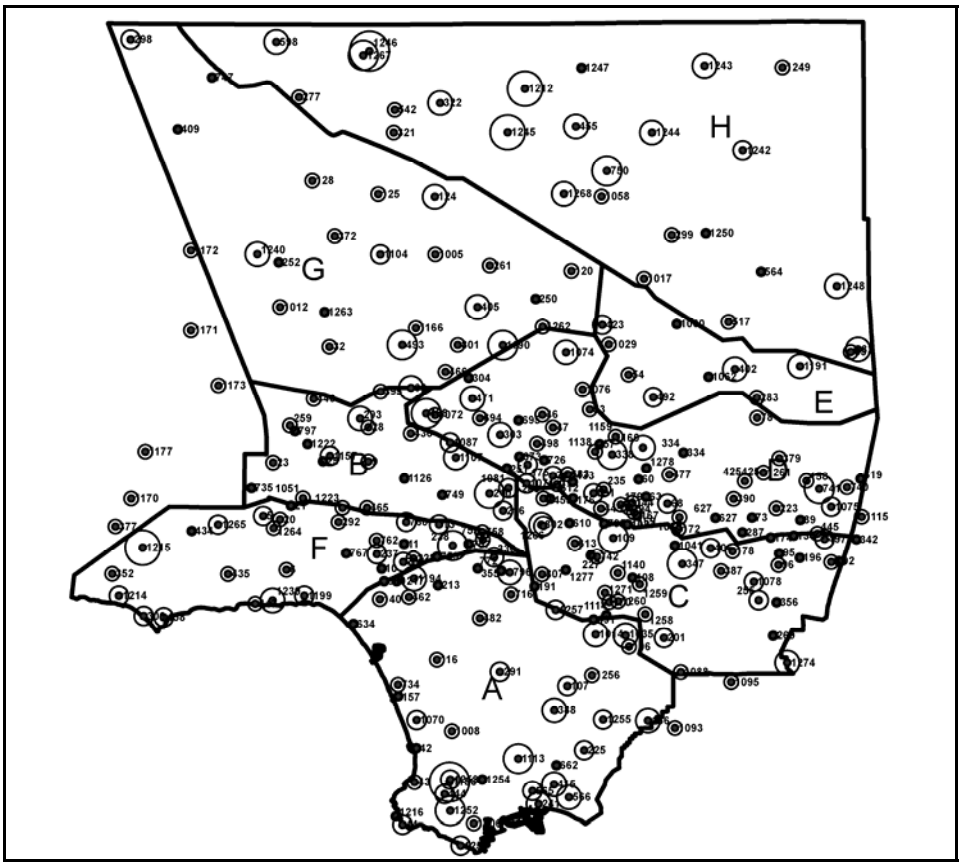

Figure 3.21 Spatial Analysis of Order of Magnitude Difference in Methodology

The Hershfield Method data in Appendix B was interpolated spatially using the Kriging method which is found within ArcGIS. Figure 3.22 shows the contours generated after the Kriging analysis spatially distributed the values from each of the Hershfield PMP estimates. Figure 3.22 can be compared to the contours shown in Figure 3.10 to evaluate similarities in spatial distributions.

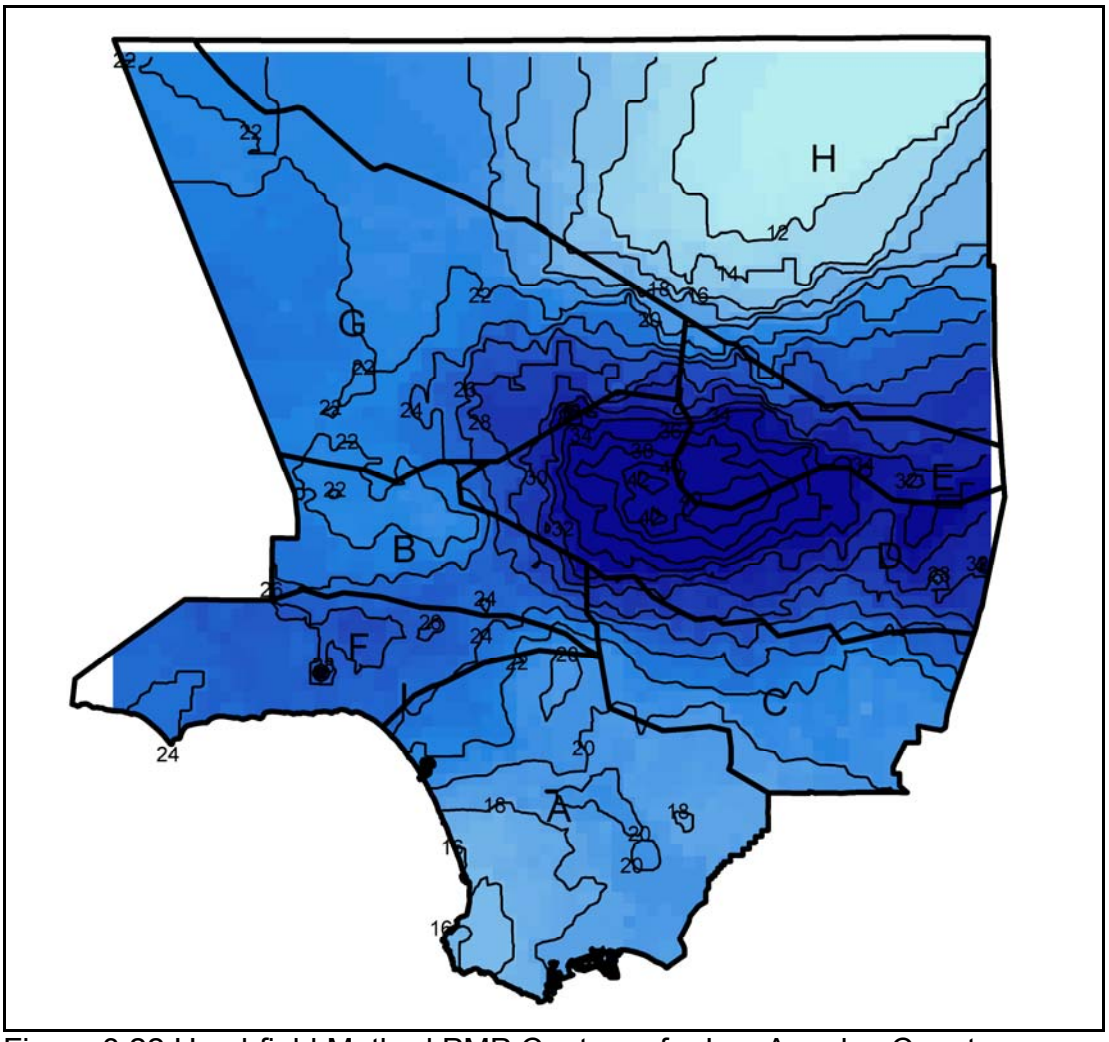

Figure 3.22 Hershfield Method PMP Contours for Los Angeles County

The darker shades on Figure 3.22 indicate higher intensity values for the 24-hr PMP calculated using the Hershfield Method. As can be seen, the areas with higher topography have higher rainfall values and there is a reasonable correlation between the spatial distribution of Hershfield Method and HMR 58 values. The highest value for PMP for the HMR is 48 inches. The highest for the Hershfield Method is 42 inches in the San Gabriel Mountains, Region D, in approximately the same location. The lowest value for the HMR PMP is 8 inches

in the Antelope Valley, Region H. The lowest PMP estimate using the Hershfield Method is 10.5 inches in the Antelope Valley.

As can be seen from the PMP frequency analysis, determining a recurrence interval for the PMP using either the HMR 58 or Hershfield method results in a wide range of results which vary from 10^3 to 10^{13}, with an average value of 10^8 based on the GEV1 distribution. Koutsoyiannis (2009) analyzed 169 rainfall stations with over 100 years of gage record in six geographical zones worldwide. He found that the PMP recurrence interval estimates were much smaller using a modified GEV2 distribution, but still ranged significantly based on the method of parameter estimation.

The HMR 58 method uses climate, topography, and transposition of historic rainfall events to develop PMP rainfall values. The Hershfield Method uses rain gage data and an empirical relationship to determine PMP estimates. In the end, both vary widely and are not easily classified based on recurrence intervals developed through extreme value distribution analysis.

The National Weather Service (NWS) is currently updating Atlas 14, which provides frequency analysis for California. They communicated with rain gage owners and engineers working in the area to ask whether the 1000-yr frequency values should be included in Atlas 14 (NWS, 2008). They got responses from

across the United States, with some engineers asking to discontinue the publication of 500-yr and 1000-yr estimates because they felt there was no practical need and the statistics were uncertain based on the limited record lengths currently available. Others wanted the information which is used for defining the 500-yr runoff for use in bridge scour and floodplain/insurance evaluations

The final analysis for the PMP compares the watersheds to be studied within Los Angeles County to the PMP estimates developed by ANSCOLD and presented in Figures 3.1 and 3.2. Figure 3.23 shows the range of PMPs for watersheds used in this study. The areas were converted to kilometers squared to make a direct comparison and then plotted on the proposed ANSCOLD PMP estimates. As can be seen in the figure, most watersheds fell within the very large bands. However, one watershed was outside their notional limits. The watershed points plotted in Figure 3.23 are based on an area weighting of the PMP at various gages throughout each watershed, which is discussed in Chapter 6 in more detail. Point gage estimates are much higher as has been seen in the previous figures.

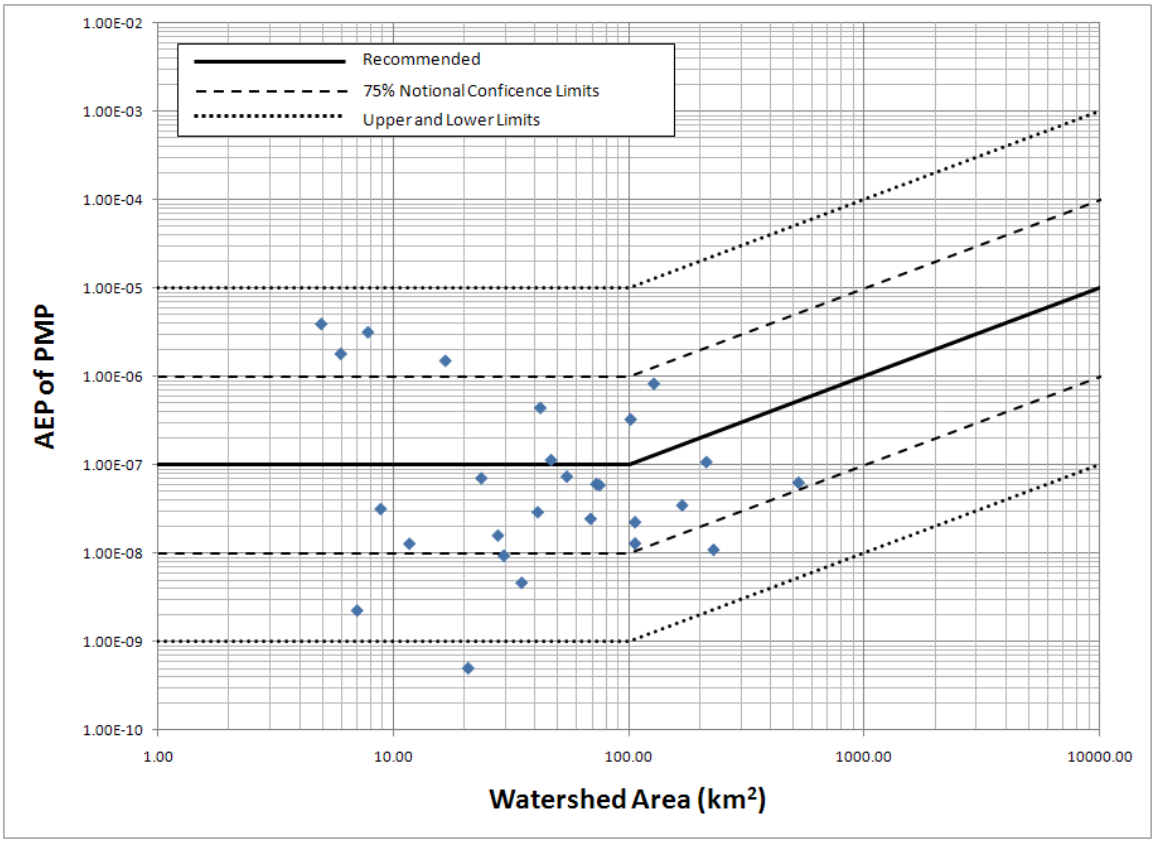

Figure 3.23 Comparison of Los Angeles Watersheds to ANSCOLD PMP Criteria

The results on this figure indicate that the assumptions are valid. It should be noted on the figure that as the watershed exceeds 100 km, the annual exceedence probability decreases. Intuitively, this can be explained by the spatial distribution of rainfall. As the area gets larger, the ability of the meteorology to deliver very significant rainfall, such as thunderstorms, decreases. The larger the area of the watershed, the less likely a sustained downpour becomes.

3.7 Chapter Summary and Conclusions

This chapter investigated extreme rainfall events used as input to generate the probable maximum flood. The use of design storms was discussed, and the HMR PMP and Los Angeles County temporal distributions were discussed as they will be used for the Monte Carlo modeling discussed in Chapters 6 and 7. Regions of different rainfall characteristics within Los Angeles County were presented and were used in the analysis of the HMR PMP and Hershfield PMP methodologies utilizing the GEV1 distribution using PWM parameter estimation (L-Moment). The results of the analysis were provided and led to the following findings and conclusions:

1. The GEV1 assumption for rainfall data evaluation within Los Angeles County is sound.
2. Gage record length does play a role in moment ratio analysis, leading the exclusion of some gages for further analysis due to their nature as statistical outliers.
3. The HMR PMP methodology results in inconsistent recurrence intervals ranging from 10^3 to 10^{13}. This range is consistent across gage record length and region.
4. The Hershfield PMP methodology results in inconsistent recurrence intervals ranging from 10^3 to 10^{13}. This range is consistent across gage record length and region.

5. The HMR PMP and Hershfield PMP methodologies are inconsistent with each other, providing consistent results for some gages and results ranging by orders of magnitude at others. This is consistent across regions.
6. The distribution of the PMP estimations appears to be normal with a center at approximately 10^8.
7. Due to the extreme range for the PMP, it is not suitable for a design standard, since it provides unequal protection in areas within the same area. This leads to unfair costs in the construction of major engineering facilities and unequal failure risks for communities.

Use of the PMP as an input for the Probable Maximum Flood design standard for dam spillways and other significant structures should be eliminated. Regulators should investigate the use of a standard rainfall recurrence interval that can be consistently applied across the County, State, and Nation in flood risk management. A possible suggestion is a precipitation with a recurrence interval of 10,000 years, i.e. 10^4.

Chapter 4 – Rainfall to Runoff – The Watershed Influence

Rainfall becomes runoff when all loss mechanisms are satisfied. Watershed losses include infiltration, surface storage, and evapotranspiration. Loss mechanisms and the methods used to model losses in this study will be discussed in Chapter 4.

Section 4.1 provides a general discussion on soil classifications and how they relate to loss of precipitation during rainfall events. Section 4.2 discusses the constant loss method of calculating rainfall losses to soil infiltration. Section 4.3 covers the general concept of runoff coefficient methods of determining infiltration losses to soils and then covers the specifics of the method developed by Los Angeles County.

Section 4.4 discusses watershed modeling using the Clark Unit Hydrograph method. Once losses are satisfied, storm runoff is influenced by several factors, which include watershed shape, slope, storage, etc...These factors can be lumped under two general concepts: transposition and diffusion. Transposition deals with the time it takes to move water through the watershed. Diffusion deals with the effects of storage on attenuating the peak of the runoff hydrograph. The Clark Unit Hydrograph method accounts for all of these aspects in a simple model.

4.1 Soil Classifications for Soil Loss Analysis in Los Angeles County

Of all the loss mechanisms during a rainfall event, soil Infiltration is the most significant, followed by surface storage, and then by evapotranspiration. All of these losses are subtracted from the total rainfall to determine the excess precipitation hyetograph. Once the excess precipitation is determined, it can be routed through the watershed using hydrologic and/or hydraulic principles to transform the rainfall into a runoff hydrograph.

Different methods have been developed to model soil losses. These include runoff coefficients, constant loss parameters, the Horton method, exponential loss calculations, and Green-Ampt losses (LACDPW, 2006). The maximum rate at which water can enter the soil is called the infiltration capacity (Linsley, 1982). The infiltration rate only reaches the infiltration capacity when the supply rate of rainfall exceeds the infiltration capacity. The most complex infiltration rate calculations involve moisture content, hydraulic conductivity, and capillary suction. Watershed properties such as slope and vegetative cover also influence infiltration rates.

Although the actual mechanics of infiltration are site specific and can be highly complex, engineers use different methods that range in complexity to estimate

the infiltration effects on runoff. The two methods that are most commonly used within Los Angeles County are the constant loss method and the runoff coefficient method. Both methods require classifying soils and assigning infiltration characteristics to the soil types.

The most used soil classification method used in the United States is the Natural Resources Conservation Services (NRCS) classification, formerly the Soil Conservation Service (SCS). The NRCS has mapped and classified over 20,000 soils across the nation. Soil formation depends on the parent material, climate, topography, biological factors, and time. Soils are named and classified on the basis of physical and chemical properties in their horizons (layers). “Soil Taxonomy” uses color, texture, structure, and other properties of first two meters of surface soil to key the soil into a soil classification system. This system also provides a common language for scientists (NRCS, 2010). A quick summary of general infiltration rates based on soil classification is provided by Rawls et. al. (1980) and is provided below in Table 4.1.

The NRCS has provided a nomograph for determining the soil texture classification. Sand refers to soil particles between 0.05 and 2.0 mm in size and can be further divided into coarse, medium, and fine sand with a sieve test. Silt is made up of soil particles between 0.002 mm and 0.05 mm. Clay is defined as

soil particles smaller than 0.002 mm (2 microns) in size. Figure 4.1 provides the nomograph developed by the NRCS, which is a branch of the US. Department of Agriculture (USDA). You enter the nomograph on the side where your soil has the highest percentage. Then follow the percentage line until it matches the ratio of the other two types. The confluence of the lines gives you the soil classification based on percent sand, clay, and silt.

Table 4.1 Infiltration Rates for NRCS Soil Texture Classifications

Soil texture class	Hydrologic soil group	Effective water capacity (C_w) (in/in)	Minimum infiltration rate (f) (in/hr)	Effective porosity, θ_e (in^3/in^3)
Sand	A	0.35	8.27	0.025 (0.022-0.029)
Loamy sand	A	0.31	2.41	0.024 (0.020-0.029)
Sandy loam	B	0.25	1.02	0.025 (0.017-0.033)
Loam	B	0.19	0.52 **	0.026 (0.020-0.033)
Silt loam	C	0.17	0.27	0.300 (0.024-0.035)
Sandy clay loam	C	0.14	0.17	0.020 (0.014-0.026)
Clay loam	D	0.14	0.09	0.019 (0.017-0.031)
Silty clay loam	D	0.11	0.06	0.026 (0.021-0.032)
Sandy clay	D	0.09	0.05	0.200 (0.013-0.027)
Silty clay	D	0.09	0.04	0.026 (0.020-0.031)
Clay	D	0.08	0.02	0.023 (0.016-0.031)

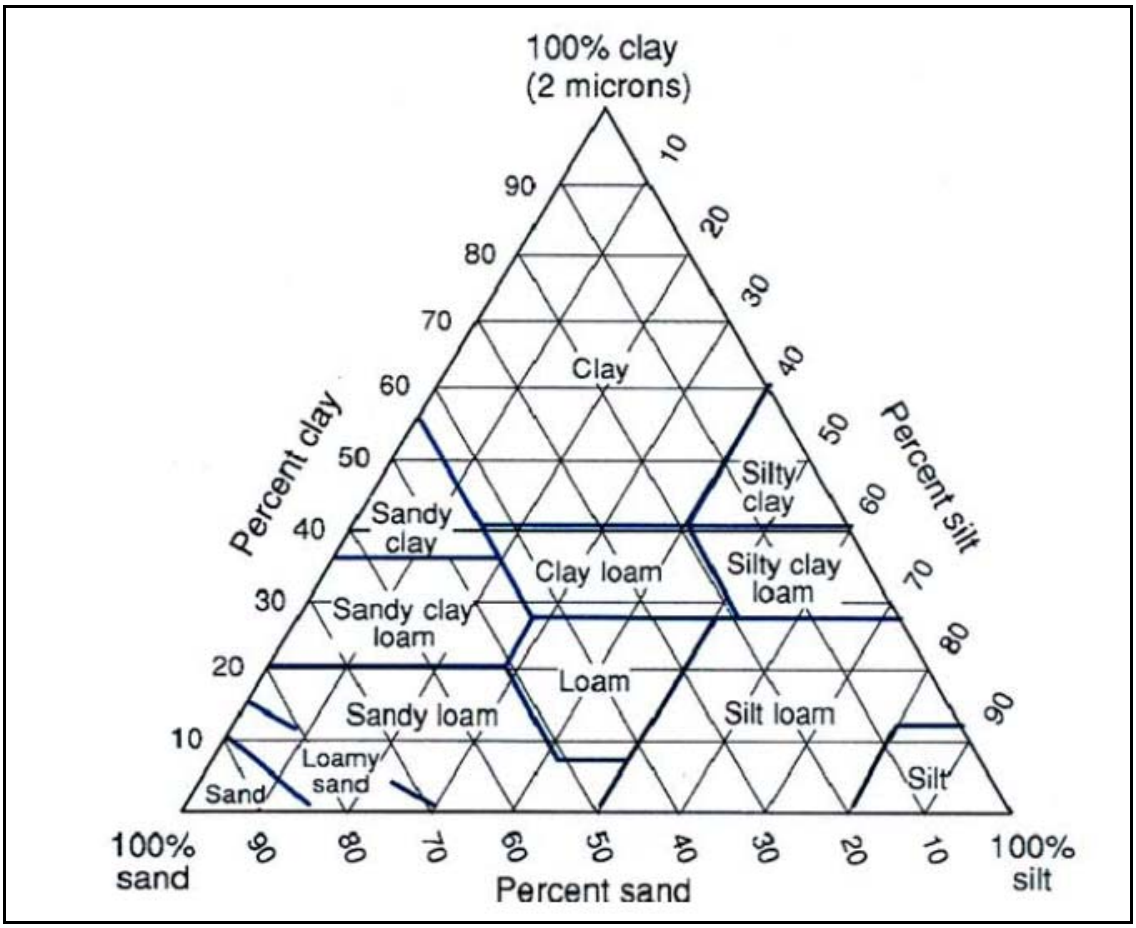

Figure 4.1 USDA Soil Texture Classification Nomograph

The NRCS simplified the soil types into four classifications A, B, C, and D. As shown in Table 4.1, there is correlation between soil types and textures. After classifying the soil type, the infiltration properties can be determined from tables. Maidmant (1993) provides estimates of infiltration rates based on texture and soil classification. These are provided in Table 4.2.

Table 4.2 Infiltration Rates for Soil Classifications

NRCS Classification	Low (in/hr)	High (in/hr)
A	0.30	9.28
B	0.15	0.30
C	0.05	0.15
D	0.00	0.05
USDA Soil Classification	**(cm/hr)**	**(in/hr)**
Sand	23.56	9.28
Loamy Sand	5.98	2.35
Sandy Loam	2.18	0.86
Loam	1.32	0.52
Silt Loam	0.68	0.27
Sandy Clay Loam	0.30	0.12
Clay Loam	0.20	0.08
Silty Clay Loam	0.20	0.08
Sandy Clay	0.12	0.05
Silty Clay	0.10	0.04
Clay	0.06	0.02

The USDA and NRCS have published many of their soil data sets in GIS format. The STATSGO and SSURGO GIS data provide the NRCS soil type (A to D), along with many soil characteristics, including low, medium, and high infiltration rates.

4.2 Constant Loss Method

One way to utilize the infiltration rates related to soil classifications is the Constant Loss Method, also known as the ϕ-index method. The Constant Loss

Method is a frequently used and generally accepted rainfall loss method for flood hydrology (LACDPW, 2006). When the rainfall rate is less than the constant loss rate, all rainfall is lost to infiltration. Runoff occurs when rainfall exceeds the constant loss infiltration rate. Table 4.3 shows direct runoff calculations for the constant loss method. The example uses a constant loss rate of 0.1 inches/hour for the soil loss, which is applied to an incremental rainfall series. Rainfall exceeding the loss rate becomes runoff.

Table 4.3 Application of Constant Loss Method

Time (hours)	Incremental Rainfall (in)	Loss (CL=0.10) in/hr)	Runoff
1	0.00	0.00	0.00
2	0.05	0.05	0.00
3	0.08	0.08	0.00
4	0.10	0.10	0.00
5	0.20	0.10	0.10
6	0.12	0.10	0.02
7	0.05	0.05	0.00

Figure 4.2 illustrates the relationship between the constant loss rate, the total rainfall, and the excess precipitation. The example shows 0.60 inches of rain falling in 7 hours. Infiltration accounted for 0.48 inches of the rain and 0.12 inches became runoff. Twenty percent of the rainfall became runoff for this rainfall event. This represents a total runoff coefficient of 0.2 for the event.

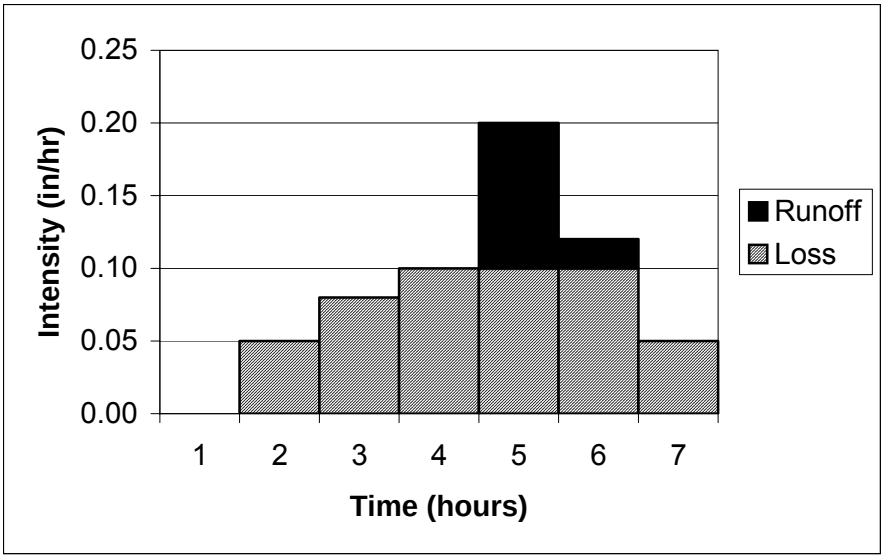

Figure 4.2 Rainfall Hyetograph and Constant Loss Excess Precipitation

The Constant Loss Method is used as a lumped model parameter. The different soil properties throughout a watershed subarea are area weighted to form an average constant loss value for the entire subarea.

Urbanization, rock outcroppings, and water bodies reduce the ability of the watershed to infiltrate rainfall since there is less soil area available for the rainfall to infiltrate. The constant loss method must account for these reductions in available infiltration area in order to model the watershed correctly. Equation 4.1 provides an equation to generate direct runoff using the constant loss method adjusted for imperviousness.

$P_e = ((Imp*0.9)*(i – CL))*t + 0.1*i*t$ Eq. 4.1

Where:

P_e = excess precipitation in inches

Imp = Imperviousness as a percentage

CL = Constant loss in inches/hr

I = intensity in inches/hr

t = time step for calculation in hrs

The equation assumes that the impervious area will result in 90 percent runoff, while 10 percent is stored on the surface area. This assumption is related to the two coefficients in the equation. For example, if an engineer wants to change this assumption to 95 percent runoff, the coefficients should be changed to 0.95 and 0.05 in Equation 4.1.

The constant loss and imperviousness for a watershed can be determined through area weighting if values for the soils are known. Area weighting can be done using Equation 4.2 below.

For example, if a watershed subarea had three soil types and a lake, as shown below in Table 4.3, with the associated areas, imperviousness, and constant losses, the calculations are shown in columns 5 and 6 of the table.

$$I_A = (\sum_j^n A_j * I_j) / \sum_j^n A_j \qquad \text{Eq. 4.2}$$

Where:

I_A = Area weighted imperviousness as a percentage

A_j = area of each soil or subarea imperviousness region

I_j = Subarea or soil region imperviousness in as a percentage

Table 4.3 Area-Weighted Constant Loss and Imperviousness Calculations

1 **Subarea**	**2** **Area (acres)**	**3** **Constant Loss (in/hr)**	**4** **Imperviousness (%)**	**5** **A_j*CL_j (in/hr)**	**6** **A_j*I_j (%)**
1	25	0.50	1	12.50	25
2	25	0.10	10	2.50	250
3	50	1.00	5	50.00	250
Lake	50	0.00	100	0.00	5000
$A_T = \Sigma A_j$	150			65	5525
$\Sigma CL_j/A_T$	0.433333		Divide	150	150
$\Sigma I_A/A_T$	36.83333			0.433333	36.83333

Use of the constant loss rate method requires either calibration to estimate the loss rate parameters or empirical relationships relating loss rates to soil types

and watershed factors. Constant loss rates are highly variable and depend on the degree of saturation, soil type, storm duration, and rainfall intensity (LACDPW, 2006). The Los Angeles County Department of Public Works researched constant loss rates for use in evaluation of PMP/PMF models. The unpublished report (Willardson, et. al, 2004b) describes research, analysis, and model calibration to determine constant loss values for several watersheds. The study also determined runoff coefficients for the watersheds for each storm period by comparing observed runoff to total rainfall.

Analysis of the storms linked the runoff coefficient to the recurrence interval of the storm and provided constant loss rates for each watershed studied. Table 4.4 contains the average constant loss value for the watersheds studied in the unpublished report. The table also contains low, medium, and high values for watershed infiltration rates obtained from the NRCS SSURGO and STATSGO data sets available for Los Angeles County. The values in the table are based on the area weighted values for all soils found in the watersheds.

The table shows that there is a wide range of infiltration values found by reviewing available information and through watershed studies. These values will be used for further analysis in the Monte Carlo Analysis model discussed in Chapters 6, 7, and 8. The watershed locations will also be provided.

Table 4.4 Constant Loss Infiltration Rates - Los Angeles Watersheds

Runoff Gage	Calibrated Model Infilt. (in/hr)	NRCS Low Infilt. (in/hr)	NRCS Med. Infilt. (in/hr)	NRCS High Infilt. (in/hr)	USDA Texture Infilt. (in/hr)
L1-R	0.092	0.051	0.102	0.152	0.643
F2B-R	0.308	0.000	0.030	0.050	0.839
P4B-R	0.340	0.021	0.060	0.100	1.450
U7-R	0.258	0.034	0.076	0.107	0.633
F19-R	0.282	0.063	0.116	0.167	0.784
F22-R	0.640	0.052	0.103	0.151	0.322
F53-R	0.202	0.000	0.030	0.050	0.858
F54B-R	0.289	0.000	0.030	0.050	0.629
F65B-R	0.366	0.105	0.171	0.230	0.545
F108-R	0.332	0.087	0.101	0.241	1.136
F111C-R	0.168	0.064	0.117	0.168	0.668
F122-R	0.283	0.080	0.137	0.187	4.337
F125-R	0.103	0.042	0.089	0.133	1.345
F135-R	0.376	0.090	0.151	0.203	0.929
F151-R	0.496	0.080	0.148	0.255	1.013

4.3 Runoff Coefficient Methods

Another way to define the relationship between rainfall and runoff is to develop a runoff coefficient. This can be done in several ways. The most used runoff coefficient method in the United States is the rational method, followed by the NRCS method. The rational method is limited to use within small watersheds (<200 acres) and only provides a peak flow rate. The rational method follows a simple formula shown in Equation 4.3:

$Q=C_U * i * A$ Eq. 4.3

Where:

Q = the volumetric flow rate, cfs

C_U = the runoff coefficient

i = rainfall intensity at a given point in time (inches/hour)

A = watershed area (acres)

Generation of excess precipitation, P_e, using the runoff coefficient method for a given time step is given by Equation 4.4.

$P_e = C_U * I$ Eq. 4.4

C_U, the undeveloped watershed runoff coefficient determines the percentage of rainfall that is converted to runoff based on intensity. The runoff coefficient for the rational method has an inverse relationship to the infiltration rate, the higher the runoff coefficient, the lower the infiltration rate.

The NRCS method assigns a curve number to the four soil types shown in Table 4.2. The curve number assigned depends on vegetation and development types.

Curve numbers are provided in many hydrology texts. There can be significant variation between the chosen coefficients based on the source of the tables.

Engineers within Los Angeles County utilize a variation of the Rational Method (LACDPW, 2006). The method generates runoff hydrographs from watershed subareas of approximately 40 acres and then utilizes level-pool or linear reservoir routing to move water through channels. Hydrographs are superimposed as the water moves through the watershed.

The Modified Rational Method (MODRAT) requires a relationship between rainfall intensity and a soil runoff coefficient to generate hydrographs. County engineers utilized a double-ring infiltrometer to test 179 soils types within the County and evaluated runoff coefficients based on rainfall intensity. The study resulted in runoff coefficient curves for all of the soil types relating the runoff coefficient to rainfall intensity. In 2004, the soil data was curve fit and the data sets were extended for use with PMP rainfall events (Willardson, 2004a.).

The Jandel Curve 2D program was used to analyze the runoff coefficient curve data and it was found that most of the data could be fit using Y-transformed rational equations. A few of the soil types could not be modeled accurately with

rational equations. One polynomial equation was selected to model these equations and fit all of the exceptions very well.

Appendix 1C provides the Los Angeles County Soil Number, the Jandel Equation Number, the equation, the equation coefficients, and the r^2 value for each curve fit. The average r^2 value was 0.997. The equations with the best r^2 value were not always used because they did not fit the data with a smooth continuous curve. In some cases, it was necessary to add a point to the data at the 20 in/hr intensity to constrain the equations to fit physical parameters of soil runoff conditions. It is impossible for a soil to have more runoff than the rainfall intensity which would be indicated by a runoff coefficient greater than 1.0.

In a few cases it was necessary to move the lowest Cu-I pair of data to meet the curve. In all cases this was done in the conservative direction by reducing the intensity at which the initial runoff coefficient became greater than 0.1. The lower limit for the runoff coefficient of 0.1 indicates that there is some runoff at all rainfall intensities. Moving the runoff coefficient to a lower intensity slightly increases the runoff.

Appendix C of the Los Angeles County Department of Public Works Hydrology Manual (2006) provides all of the runoff coefficient graphs that include 2004 study results. Figure 4.3 shows what these runoff coefficient curves entail.

Equation 4.2 can be used to generate excess precipitation hyetographs for different time steps. An example is provided utilizing 1-hr time steps to determine the rainfall intensity. Figure 4.3 provides the runoff coefficient for each time step. The excess precipitation for a given time interval is calculated using Equation 4.2. The total rainfall is equal to 1.00 inch over the seven hour storm, with a total storm runoff coefficient of 0.124. The maximum intensity/runoff coefficient of 0.16 can be read off Figure 4.3 at an intensity of 0.40 in/hr.

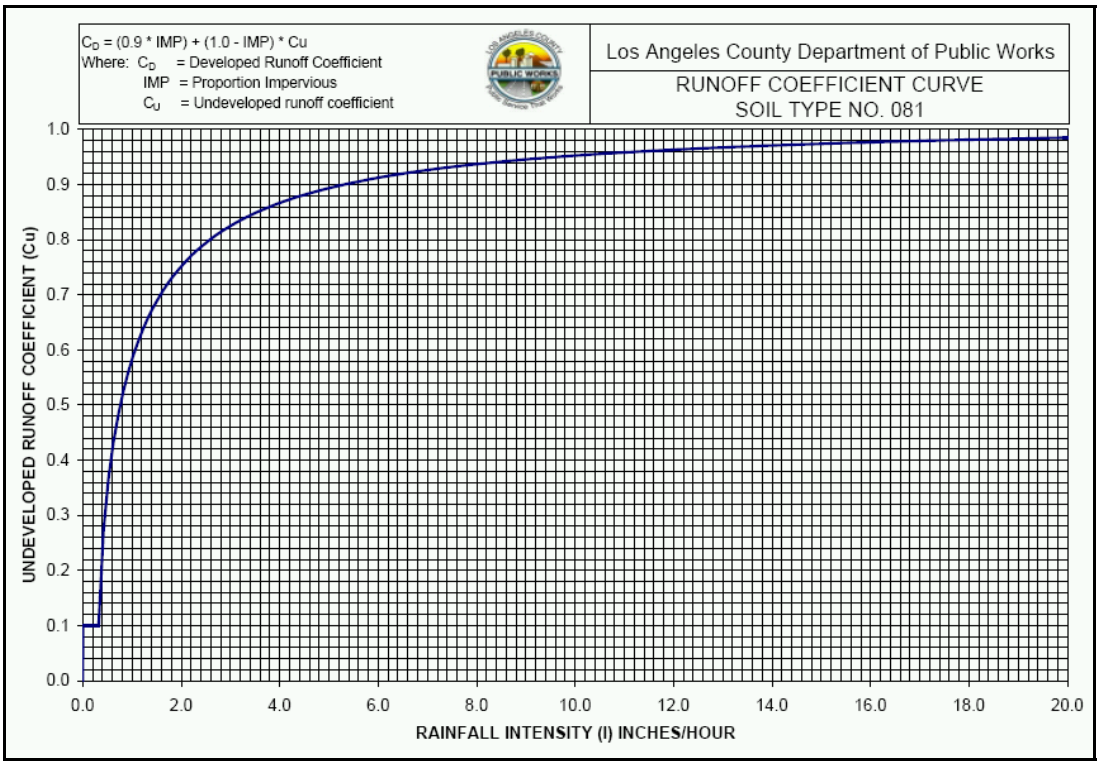

Figure 4.3 Los Angeles County Runoff Coefficient Curve (LACDPW, 2006)

Table 4.5 Application of Runoff Coefficient Method

Time (hours)	Incremental Rainfall (in)	Runoff Coeff.	Excess Precipitation (in)
1	0.00	0.10	0.000
2	0.05	0.10	0.005
3	0.15	0.10	0.015
4	0.20	0.10	0.020
5	0.40	0.16	0.064
6	0.15	0.10	0.015
7	0.05	0.10	0.005
Totals	1.00		0.124

Imperviousness within the watershed is corrected by using C_D, a runoff coefficient modified to represent the area weighted impact of impervious surface within the watershed. Equation 4.5 provides the area weighted relationship.

$$C_D = (0.9 * IMP) + (1 - IMP) * C_u \qquad \text{Eq. 4.5}$$

Where:

C_D = Developed area runoff coefficient

IMP = Percentage of watershed area that is impervious

C_u = Undeveloped area runoff coefficient

MODRAT utilizes a time of concentration to determine rainfall intensities for various time steps within a rainfall event. The resulting flow rate from each time

step is plotted to derive an excess precipitation hyetograph. An example from the LACDPW Hydrology Manual provides insight into how this is accomplished.

The Modified Rational Method also allows for changes to runoff characteristics due to fire burning the vegetation and changing the soil characteristics. This will be discussed in Chapter 5 in more detail.

Evaluating the range of runoff coefficients is important in determining reasonable runoff volumes and peak flows within watersheds. Willardson et. al. (2004b) modeled the Los Angeles County watersheds referenced in Table 4.4 to determine runoff coefficients for many storm events. They also researched work done by others on runoff coefficients. It was found that the watershed runoff coefficient was related to the rainfall frequency, where less frequent rainfall events have higher intensities, and usually have higher antecedent soil moisture conditions.

Historic records from reservoirs with well defined storage-elevation relationships provide runoff information for large rainfall events. Table 4.6 shows the rainfall/runoff ratios calculated for two extreme historic events. The Los Angeles County Storm Summary from 1938 and 1969 provided data for major storms occurring on March 2, 1938, and February 23-25, 1969. The resulting runoff coefficients are the highest recorded within the study area.

Table 4.6 Runoff coefficients at Dams for Extreme Historic Storm Events

Location	March 1938	February 1969
Big Tujunga Dam	0.56	0.54
Big Dalton Dam	0.40	0.49
Cogswell Dam	0.62	0.60
Live Oak Dam	0.27	0.35
Pacoima Dam	0.59	0.62
San Dimas Dam	0.33	0.32
Santa Anita Dam	0.47	0.59
Thompson Creek Dam	0.25	0.31

The February 1969 watershed conditions resulted in a high runoff coefficient due to a large storm in late January 1969, and minor storms that kept the soil moisture content in the watershed high (LACFCD, 1969). However, the February 1969 rainfall intensities are much smaller than expected from the PMP.

The California Department of Safety of Dams (DSOD) reviews most PMF studies within the State of California. Current DSOD standards are outlined by Calzascia and Fitzpatrick (1989) and in Mayer's thesis published in 1987. The DSOD relationship relates mean annual precipitation (MAP) to runoff coefficient and return period. DSOD's runoff coefficients for extreme events, as defined by Calzascia and Fitzpatrick, are related to MAP. DSOD states:

> It is assumed that antecedent storms have saturated the drainage basin so that loss rates are fairly low…. The general criteria is that the percent runoff should not be less than 70 when the mean annual precipitation (MAP) at the basin is greater than 25 inches and should not be less than 60 when the MAP is 25 inches or less.

Figure 4.4 presents the mean annual precipitation for the County of Los Angeles to provide a reference for the requirements of the DSOD.

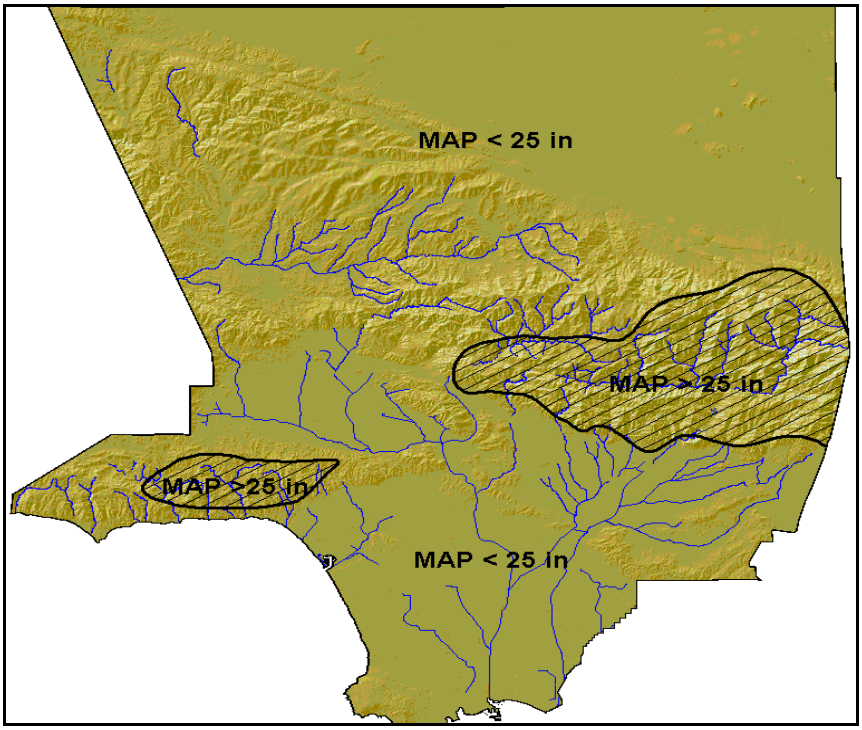

Figure 4.4 Mean Annual Precipitation in Los Angeles County

Drobot (2004) reports runoff coefficients exceeding 80 percent on steep slopes with high antecedent moisture conditions. Figure 4.5 presents a graph developed based on the research of different methods and regulatory requirements. The figure contains data from the model study conducted by Willardson et. al, design criteria from Maricopa County, Arizona (FCDMC, 2010), the California DSOD (Calzascia and Fitzpatrick, 1989), the American Society of Civil Engineers (Kibler, 1982), and prior design criteria from the LACFCD.

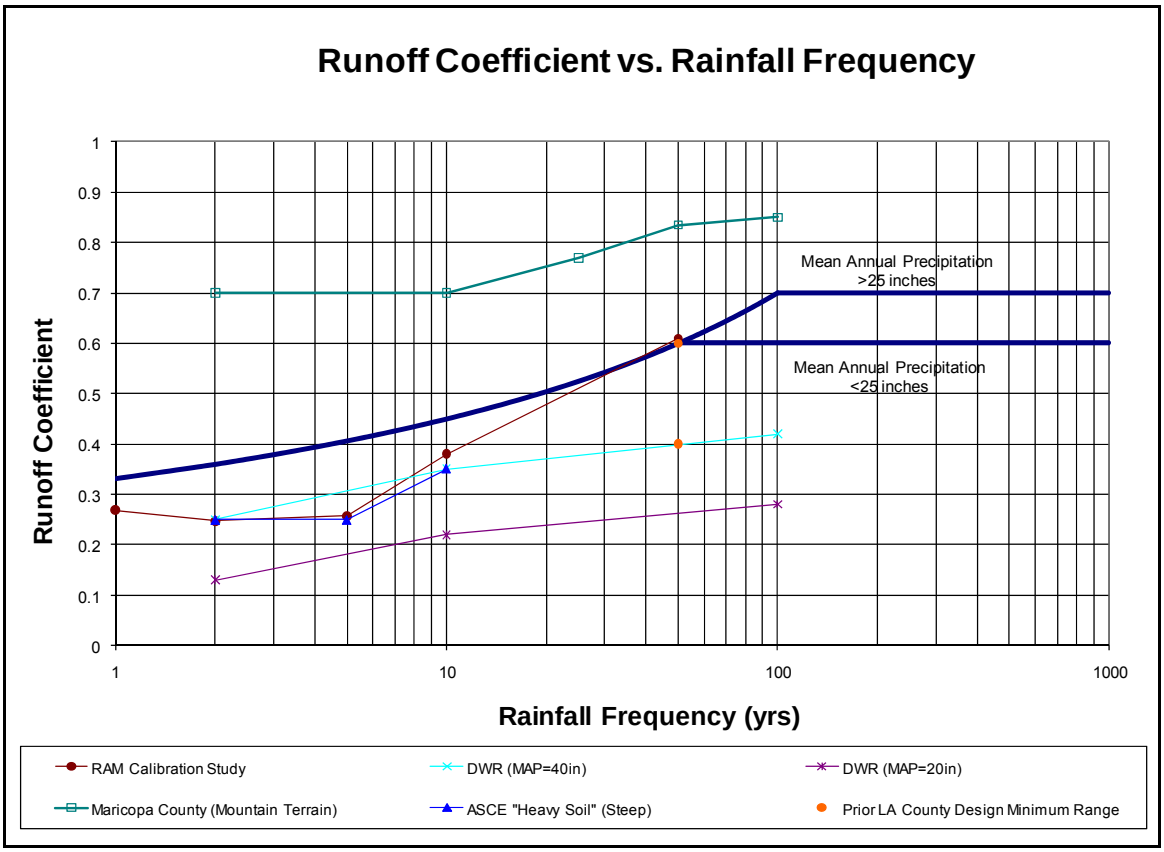

Figure 4.5 Los Angeles County Runoff Coefficients Related to Frequency

The soil runoff coefficients in Figure 4.5 will be compared to runoff coefficients from the Monte Carlo analysis presented in Section 6. Once rainfall excess has been determined, the rainfall must be routed through the watershed. Hydrologic routing has been approached in various ways. This study utilizes the Clark Unit Hydrograph to convert excess rainfall into a runoff hydrograph.

4.4 Clark Method of Hydrograph Routing

Once the excess precipitation in a watershed is determined based on a constant loss rate or runoff coefficient method, the hyetograph must be routed through the watershed to generate a runoff hydrograph. "The shape of the hydrograph from a basin depends on the travel time through the basin and on the shape and storage characteristics of the basin." (Linsley, 1982). The Clark Unit Hydrograph (CUH) method provides a method to route a hydrograph through gaged and ungaged watersheds.

The Hydrologic Modeling System HEC-HMS Technical Reference Manual (USACE, 2000) discusses how the CUH model derives a watershed UH by explicitly representing translation and attenuation. Translation deals with the movement of precipitation excess from where it falls in the watershed to the outlet. Attenuation is the peak flow rate reduction as the watershed stores the precipitation excess.

Short-term storage of water plays an important role in transforming excess rainfall to runoff. Storage occurs in soils, on the surface, and in the channels. A linear reservoir model is often used to represent the storage effects on peak attenuation. The linear reservoir combines all watershed storage effects. Therefore, the model can conceptually locate the reservoir at the watershed outlet. The linear reservoir model begins with the continuity equation:

$$\frac{dS}{dt} = I_t - O_t$$ Eq. 4.6

Where:

dS/dt = time rate of change of water in storage at time t

I_t = average inflow to storage at time t

O_t = outflow from storage at time t

With the linear reservoir model, storage at time *t* is related to outflow as:

$$S_t = RO_t$$ Eq. 4.7

Where:

R = a constant linear reservoir parameter, expressed in time in hours

Combining and solving the equations in a simple finite difference approximation yields two routing coefficients C_A and C_B:

$$O_t = C_A I_t + C_B O_{t-1}$$ Eq. 4.8

Where:

$$C_A = \frac{\Delta t}{R + 0.5\Delta t}$$ Eq. 4.9

$$C_B = 1 - C_A$$ Eq. 4.10

The average outflow during the period t is described by Equation 4.11:

$$\overline{O_t} = \frac{O_{t-1} + O_t}{2} \qquad \text{Eq. 4.11}$$

In the CUH model, the linear reservoir aggregates impacts of all watershed storage. Therefore, the reservoir may be considered to be located at the watershed outlet. The reservoir attenuates the peak flows and creates the dispersion effects on the hydrograph.

Besides the lumped storage model, the CUH model accounts for the time required for water to move to the watershed outlet using a linear channel model (Dooge, 1959). The water is routed from remote points to the linear reservoir with a translational delay but without attenuation. This delay is represented implicitly with a time-area histogram. The time-area histogram specifies the watershed area contributing to flow at the outlet as a function of time. If the area is multiplied by unit depth and divided by Δt, the computation time step, the result is inflow, I_t, to the linear reservoir.

Solving Equations 4.8 and 4.11 recursively, yields values of $\overline{O_t}$. However, if the inflow ordinates in Equation 4.8 are runoff from a unit of excess, the outflow ordinates equal the unit hydrograph.

Application of the Clark model requires knowing the time-area histogram properties and the storage coefficient, R. The time-area histogram implicitly defines the linear routing model properties. HEC studies show that a smooth function fitted to a typical time-area relationship based on the time of concentration represents the temporal distribution adequately for UH derivation for most watersheds. The HEC suggested relationship, included in HEC-HMS is found in Equation 4.12:

$$\frac{A_t}{A} = \begin{Bmatrix} 1.414\left(\frac{t}{t_c}\right)^{1.5} \; for\; t \le \frac{t_c}{2} \\ 1-1.414\left(1-\frac{t}{t_c}\right)^{1.5} \; for\; t \ge \frac{t_c}{2} \end{Bmatrix} \qquad \text{Eq. 4.12}$$

Where:

A_t = cumulative watershed area contributing at time t

A = total watershed area

t_c = time of concentration of watershed

The parameters t_c and R can be determined via calibration, or they can be estimated using other relationships (USACE, 2000). The time of concentration, t_c, represents the time for the entire watershed to contribute to runoff at the watershed outlet. The basin storage coefficient, R, is an index of the temporary storage of precipitation excess in the watershed as it drains to the outlet point.

Estimated travel time and storage characteristics for a basin are required to produce synthetic unit hydrographs from ungaged watersheds. This is accomplished through developing empirical relationships for the watershed time of concentration and storage coefficient. The time-area relationship developed by the USACE provides a sound relationship for modeling ungaged watersheds.

"In the Clark Unit Hydrograph, the time of concentration, t_c, is the time from the end of the effective precipitation to the inflection point of the recession limb of the runoff hydrograph." (Straub et. al, 2000). The inflection point corresponds to the point at which the last effective precipitation has reached the channel. All runoff after this time is the result of flow out of the channel storage.

The Modified Snyder Lag Time Equation was selected to estimate the Clark Method time of concentration. The U.S. Army Corps of Engineers modified the Snyder Lag Time Equation based on a study of watersheds in the Los Angeles area. The study determined a relationship between the equation variables and basin characteristics for mountain, valley, and foothill watersheds (Linsley, 1982; USACE, 1944). A Manning's n value of 0.05 corresponds to the mountain basin characteristics within Los Angeles County. Snyder's Lag Time Equation is provided as Equation 4.13.

$$T_{lag} = 24 * n * \left(\frac{(L * Lc)}{\sqrt{S}} \right)^{m}$$ Eq. 4.13

Where:

T_{lag} = The Snyder Lag Time (hrs)

n = Manning's roughness coefficient (0.05)

L = length of the longest flow path (miles)

L_c = length along the longest flow path to the watershed centroid (miles)

S = average slope of longest flow path (ft/mile)

m = lag exponent (0.38)

Various studies (Cudworth, 1989; USACE 1987) have proposed a relationship between the Snyder Lag Time (T_{lag}) and the time of concentration. The T_{lag} can be estimated as 50-75% of time of concentration. While T_{lag} was used directly as the t_c for these studies, understanding this relationship is useful for comparison with other studies.

The Clark Storage Coefficient, R (also shown as K in some texts), describes the channel storage within a watershed. A value for R was determined through model calibration for each analyzed storm event. An analysis was performed to determine relationships between R and various basin characteristics to allow engineers to approximate R for ungaged basins.

Several studies have proposed methods for estimating R for ungaged basins by using known watershed characteristics. Clark (1945) reported that "The average storage in hours…was found to be numerically equal to the reciprocal of the square root of the slope…from source to gage." He noted large variations between observed values and the average R values for some streams. Linsley, discussing Clark's paper, proposed a relationship that included area, and Clark agreed this relationship showed better correlation with the data. Equation 4.13 shows Linsley's relationship:

$$R = \frac{bL\sqrt{A}}{\sqrt{s}} \qquad \text{Eq. 4.13}$$

Where:

R = Clark Storage Coefficient

b = Watershed coefficient

L = Length along main channel (mi)

s = Average slope along main channel (ft/mi)

A = Drainage area (mi^2)

Linsley's relationship was evaluated using the data from the calibrated watersheds and was not well suited to developing a regional relationship for R within Los Angeles County. Watersheds with similar characteristics had vastly different values for the coefficient b, making an application of b to ungaged watersheds difficult.

Analysis of watershed characteristics was explored to create a regression equation to determine appropriate R values for Los Angeles County watersheds. Table 4.7 contains several fundamental watershed properties and related methods of measuring the characteristics. Watershed size and steepness measurements require no explanation. Watershed shape and elevation are discussed in more detail.

Table 4.7 Regression Parameters Analyzed for R Coefficient Correlation

Fundamental Property	Expected Relationship to Clark Coefficient (Property/R)	Measured Characteristic
Watershed Size	Increase/Increase	Area
	Increase/Increase	Length
	Increase/Increase	Length to Centroid
Watershed Steepness	Increase/Decrease	Slope (%)
	Increase/Decrease	Slope (feet per mile)
Watershed Shape	Increase/Decrease	Circularity Ratio
	Increase/Increase	Eccentricity
Watershed Elevation	Increase/Unknown	Mean Basin Elevation

Watershed shape characteristics explain the effect that the physical shape of the watershed has on the runoff hydrograph. The eccentricity of a watershed is a measure of how compact a watershed is about the outlet. Eccentricity is based on the formula for elliptical eccentricity:

$$\tau = \frac{\sqrt{\left|L_c^2 - W_L^2\right|}}{W_L}$$ Eq. 4.14

Where:

L_c = Length to Centroid

W_L = width perpendicular to L_c at centroid

High values of eccentricity indicate that a watershed is long and narrow. Channel storage is more pronounced for watersheds with high eccentricity values. Low eccentricity values indicate compact watersheds with fewer channel storage effects.

The circularity ratio measures the deviation of the watershed shape from that of a circle.

$$Circularity\ Ratio = \frac{Area\ of\ watershed}{Area\ of\ circle\ with\ same\ perimeter\ as\ watershed}$$ Eq. 4.15

The maximum circularity ratio for a watershed is one, indicating a perfect circle. As the circularity decreases from this value, the storage coefficient increases. The increase is related to the length of channel needed to convey the water to the outlet.

The mean basin elevation was used as an independent variable. Both Mayer (1987) and the USACE (1967) have used elevation as an independent variable to estimate unit hydrograph parameters. Watersheds at lower elevations in Los Angeles have different geomorphic characteristics than those at higher elevations.

Following the example of Mayer (1987), a regression analysis was undertaken to correlate R to watershed characteristics. The dependent variables investigated included R, as well as, T_{lag}+R, R/T_{lag}, and R/(T_{lag}+R). These parameters were regressed with the watershed characteristics shown in Table 4.6. A linear equation with multiple independent variables was adopted as the form of the equation. The regression analysis used eighty percent of the calibrated model data. A verification data set consisted of the remaining twenty percent of the calibrated model data.

The regression was performed using the statistical analysis package “SYSTAT” in a backwards stepwise procedure. Using this approach, a large number of possible combinations were quickly examined.

The characteristics shown in Table 4.6 are fundamental properties of the watersheds. Correlation between independent variables is undesirable in regression equations. Therefore, each regression trial used only one

characteristic from each fundamental property group. All possible combinations of characteristics were tested to determine the equation providing the optimal fit. Additionally, a similar regression analysis was completed for the natural log of each of the dependant and independent variables.

The regression analysis used the observed storage coefficients from the individual calibrated storms. However, regression analysis of this data produced large values of residual error. The source of these residuals was the large range of the observed R values for a given gage. To rectify this problem, the median value of R for each gage was determined and used in regressions to attain lower residual error. One effective relationship developed as shown in Eq. 4.16 and had a coefficient of determination of 0.90:

$$T_{lag} + R = -0.51529 + 0.00076 EL_{avg} + 0.49592 L_c + 1.01757 \tau \qquad \text{Eq. 4.16}$$

Where:

L_c = length to centroid

EL_{avg} = mean watershed elevation

τ = eccentricity

The validity of the regression equation was assessed by comparing the standard error of estimate of the regression data set to that of the data not used in producing the equation.

A direct comparison to the verification data set was attempted. The standard error of estimate for this data was much larger than for the regression data. This is explained by the nature of the data used for the regression. While a median was used for both the regression and validation sets, the regression set was larger and its median provided a better estimate of the actual median than the validation set median. The validation set was too small to provide a good estimate of the median R value.

Most of the calibrated watersheds analyzed were for dams. Problems arose when attempting to apply the equation to the smaller watersheds in the study. The equation predicted R's for these small basins which were higher than anticipated. In some cases, the R's were higher than those estimated by calibration for much larger basins. It was found that the regression equation approximation of the storage coefficient improved as the watershed size increased. Most hydrologic studies using the CUH Hydrology method will be much smaller than the average size of the watersheds used to create the regression equation. It was determined that another method for estimating R was needed to accommodate these smaller watersheds.

Analysis of T_{lag} and Linsley's R equations showed that both are functions of $L/s^{1/2}$. This commonality suggests the possibility of using a relationship between

R and T_{lag} to estimate R. Analysis of the calibrated watershed model results showed that Equation 4.17 provided a good estimate of R.

$$R=1.5*T_{lag} \qquad \text{Eq. 4.17}$$

Review of many studies showed that others have used similar relationships to compute the Clark Storage Coefficient from the time of concentration. The U.S. Army Corps of Engineers (1967) proposed that "the storage coefficient R equal 0.8 times the time of concentration, t_c" after failing to find a suitable regression equation for R. California's Division of Safety of Dams (Calzascia and Fitzpatrick, 1989) mentions that this method is suitable for developing CUH parameters within Southern California.

Russell, Keening, and Sunnell (1979) found that $R=c* t_c$, was appropriate in their study of watersheds around Vancouver, British Columbia. The calibrated value of c for the rural watersheds they studied ranged between 1.5 to 2.8. Mayer recommends using the relationship $R=3* t_c$ in Region 1 when there are few lakes within the watershed.

After converting t_c to T_{lag}, these values are similar to the value determined through analysis of the studied watersheds. The R calculated by Equation 4.17,

is similar to the R calculated using the regression equation, Equation 4.16, as shown in Figure 4.6.

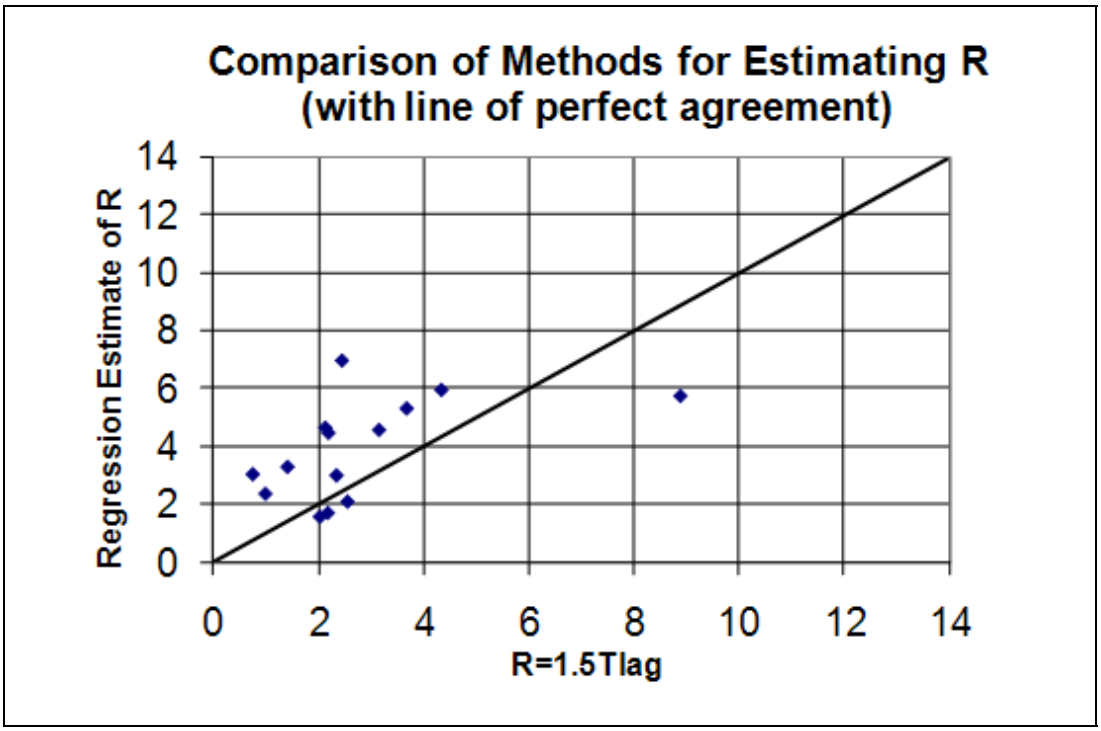

Figure 4.6 Comparison of Regression Equation and $R=1.5*T_{lag}$ Estimates of R

The computation of a runoff hydrograph using the CUH method and the relationship $R=1.5*T_{lag}$ to calculate R was tested against the modified rational method to compare peak flow rates. The $R=1.5*T_{lag}$ relationship provides results with peak flows similar to those of the modified rational and volumes that resemble historically measured volumes.

Table 4.8 and Figure 4.7 show a comparison of the hydrographs developed for a medium sized watershed where the CUH method might be applied. The

Modified Rational Method is compared to the two variations of the CUH method being considered. While both CUH methods use a synthetic unit hydrograph to develop the hydrograph, one uses the regression equation (Eq. 4.16) to estimate R while the other uses Equation 4.17.

The remaining element in the formulation of the CUH is the time-area relationship that specifies the amount of time for each portion of the watershed to contribute to runoff at the outlet.

Table 4.8 Peak Flow Rates and Volumes for Deer DB

Method	Peak Q (cfs)	Total Volume (ac-ft)
Modified Rational	785	56
R=1.5*Tlag (Eq. 4.17)	677	156
Regression Equation (Eq. 4.16)	362	151

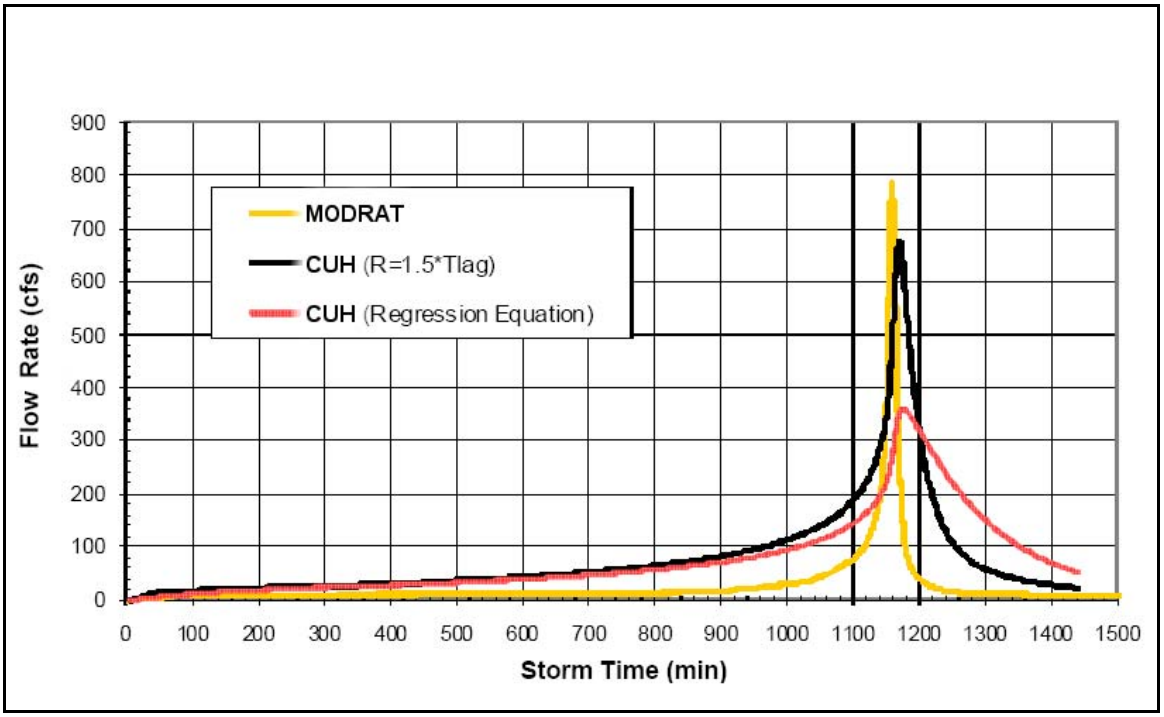

Figure 4.7 Comparison of Clark Unit Hydrograph to Modified Rational Method

The estimation procedures established were developed using a set of watersheds with certain characteristics. Use of the method provides reliable results when applied to watersheds within the same range of characteristics. Table 4.9 presents the range of watershed sizes where this method is applicable.

Table 4.9 Calibrated Watershed Characteristics

Characteristics	Range
Drainage Area	2 to 200 square miles
Flow Path Length	3 to 35 miles
Slope	300 to 1400 feet/mile

Many watersheds of interest within the County of Los Angeles have drainage areas smaller than the smallest gaged watershed studied. Comparison of hydrologic methods shows that the CUH Hydrology method is reasonable in these situations if the relationship $R=1.5*T_{lag}$ is used to determine the storage coefficient.

Hydrology studies of rural areas that are subject to brush fires must consider the drastic changes in the runoff/rainfall process that occur as a result of such fires. Section 5 will provide more information on burned watersheds and the effects on runoff.

The following discussion (FERC, 2001) puts the application of the results presented here in perspective as they relate to estimation of unit hydrograph parameters for ungaged watersheds:

> The means of estimating t_c and R are by no means infallible; it is extremely important that the hydrologic engineer doing this estimation have substantial experience and understand the hydrologic behavior of the basin. Although analytical techniques are indispensable when working on ungaged basins, the judgment of the experienced hydrologic engineers is important. The values selected for t_c and R should be justified.

4.5 Chapter Summary and Conclusions

Chapter 4 discusses the conversion of rainfall to runoff within a watershed system. Watersheds are complex and unique, due to their soil types, terrain, climate, and vegetation. Infiltration has the largest impact on how much rainfall becomes runoff. Two infiltration methods for use in watershed modeling were discussed in this chapter, the Constant Loss Method and the Runoff Coefficient Method. Both are widely used and will be evaluated in the Monte Carlo simulations discussed in Chapters 6 and 7.

Once infiltration has occurred, runoff is transported through the watershed. The runoff hydrograph is translated and diffused by overland flow, channel storage, channel characteristics, etc. The Clark Unit Hydrograph method was selected for hydrograph routing due to its simplicity and ability to accurately model watershed characteristics. It is also used by the California Division of Safety of Dams for PMF calculations and allows a direct comparison to the mandated PMFs at several dams within Los Angeles County. This chapter discussed the method and the development of regression equations to determine key input parameters. The key findings are as follows:

1. The constant loss and runoff coefficient methods are appropriate for use in watershed modeling for this study.

2. The Clark Unit Hydrograph method is a simple but effective tool for modeling watersheds and requires only a storage coefficient, a time of concentration, and a time-area relationship.
3. A synthetic CUH time-area developed by the U.S. Army Corps of Engineers is appropriate for use in Los Angeles County.
4. The Snyder Modified Lag Time is a reasonable estimation for time of concentration and takes into account physical watershed parameters such as flow path length, slope, watershed shape, and watershed roughness.
5. The CUH storage coefficient R, can be approximated by the equation $R=1.5*T_{lag}$ for watersheds within Los Angeles County.

Chapter 5 – Fire Effects in Watersheds

In many areas throughout the world, runoff is highly impacted by wildfires. Watersheds in Southern California are very susceptible to fire due to the arid climate, chaparral covered foothills, and large populations. Wildfires are a major influence on the structure and function of most Mediterranean-type ecosystems. This is certainly true for the brushland and forest communities of California (Keeley, 1981).

Chapter 5 discusses how fire affects watershed soils and vegetation, watershed recovery periods, and how watershed size relates to the probability of being partially or completely burned during a given year. Section 5.1 provides a general overview of how fire impacts hydrology in the Western United States and provides specific data for Los Angeles County. Section 5.2 discusses the changes to vegetation within the watershed and how that influences runoff. Section 5.3 discusses physical changes to soils that lie within a watershed affected by wildfire. Section 5.4 combines concepts from Sections 5.3 and 5.4 to discuss the changes to runoff after a fire. Section 5.5 discusses the recovery process for watersheds and discusses the time frames involved in hydrologic recovery.

Section 5.6 discusses the development of a fire factor (FF) for use in hydrologic analysis to include the effects of fire into runoff calculations. Section 5.7 provides

a detailed discussion on how Section 5.6 was implemented to determine FF probability density functions for watersheds of different sizes throughout Los Angeles County. The section also discusses how this probability can be factored into the analysis of the PMF.

5.1 Wildfire in the Western U.S. and in Los Angeles County

Fire plays an important role in most wildland ecosystems. In Mediterranean climates with chaparral systems, vegetation depends on fire to create a period of rebirth by removing dead materials and releasing nutrients back into the environment (Ainsworth and Doss, 1995).

Across the United States, over 130,000 wildfires burn more than 4 million acres annually, costing Federal agencies in excess of $768 million a year (1994-2002) in suppression alone (Butry et al., 2008). Some of the most well known fires have burned large sections of famous national parks such as Yellowstone and Yosemite.

Between the 1930s and 1970s, firefighting tactics and equipment became increasingly more sophisticated and effective fire suppression efforts increased dramatically, and the annual acreage consumed by wildfires in the lower 48 states dropped from 40 to 50 million acres a year (Laverty, 2001). Across the

Western United States, the aggressive fire suppression policies appeared to be successful. However, these policies have set the stage for the intense fires experienced over the last few decades.

Many wildland blazes of the interior mountains of California are caused by lightning. However, in the coastal ranges of California, where coastal sage scrub is a dominant community, the "Catalina eddy" and marine influence create conditions where summer lightning rarely occurs (Radtke 1983). Lightning or other natural causes may have played a major role in the creation of early to mid summer fires. Increased fire suppression has moved fire season into late fall and early winter, which coincides with the Santa Ana winds (Ainsworth and Doss, 1995). The fires later in the year differ in intensity from the summer blazes due to the Santa Ana conditions. Humidity levels are lower than normal and high wind speeds intensify a wildfire until it creates its own weather conditions. This is commonly known as a "*firestorm*". These fires are often too intense to control until fuels are either consumed, weather conditions change, or the fire reaches the sea (Ainsworth and Doss, 1995).

Full fire suppression gave forests and wildlands the opportunity to grow without the effects of fire, disrupting ecological cycles and changing the structure and make-up of the forests (Laverty, 2001; Pierson, Jr. et. al, 2003). Other vegetation that had been regularly eliminated from forests by periodic, low-intensity fires, became a dominant part of the forest. This vegetation became

susceptible to insects and disease, which left dead trees, mixed brush, and downed material to fill the forest floor. The accumulation of materials, when dried by extended periods of drought, creates the fuels that allow extremely large fires to burn across large areas of forest and wildland (Laverty, 2001).

From 2000 to 2002, almost 300,000 fires occurred in the western United States, burning 19 million acres, or approximately 30,000 square miles. The total area of the state of California, by comparison, is 167,300 square miles. In 2002, Colorado, Arizona, and Oregon recorded their largest forest fires in the last century (White, 2004). Keeley (1981) notes that in the 1970s, there were over 100,000 fires in California. Within Los Angeles County, fires have been mapped in GIS between 1878 and 2009. This data set contains both large and small fires and provides insight into which regions of Los Angeles County are impacted by fire. As can be seen in Figure 5.1, every area with open space has been impacted by fire. The areas in hash marks show the fire areas for 2008 and 2009. The Station Fire, which burned 160,000 acres, is the largest fire to occur within the 132 year history of fire records within the County. It is highlighted in Figure 5.1 and falls within Regions D, E, and G.

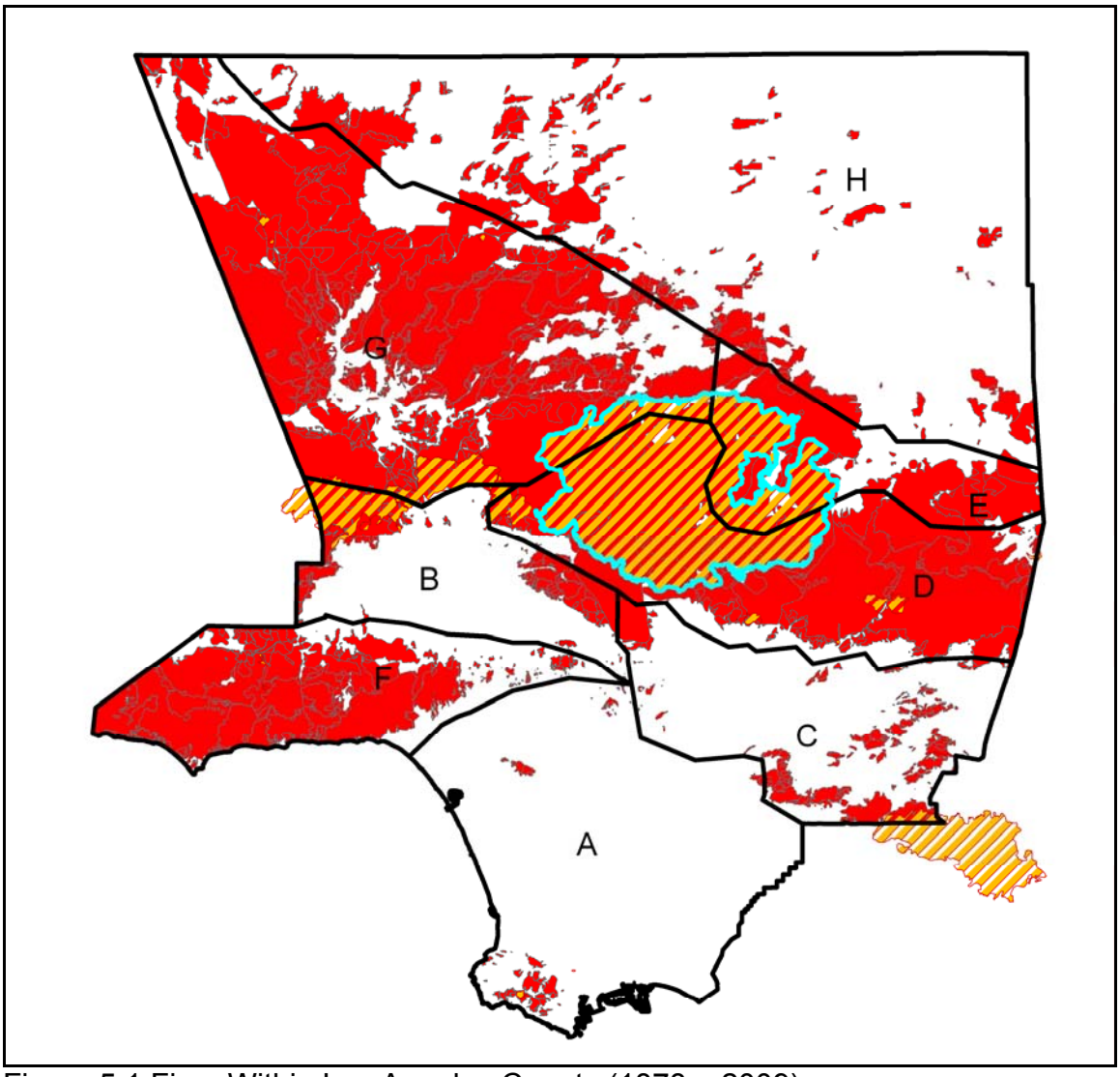

Figure 5.1 Fires Within Los Angeles County (1878 – 2009)

The annual area impacted by fire within Los Angeles County is shown in Figure 5.2. Each bar represents the area in square miles burned for a given year. The 50-year moving average shows the data has an increasing trend toward larger areas of land being burned. The fires in 2009 had the largest area of watershed burned and the largest fire on record.

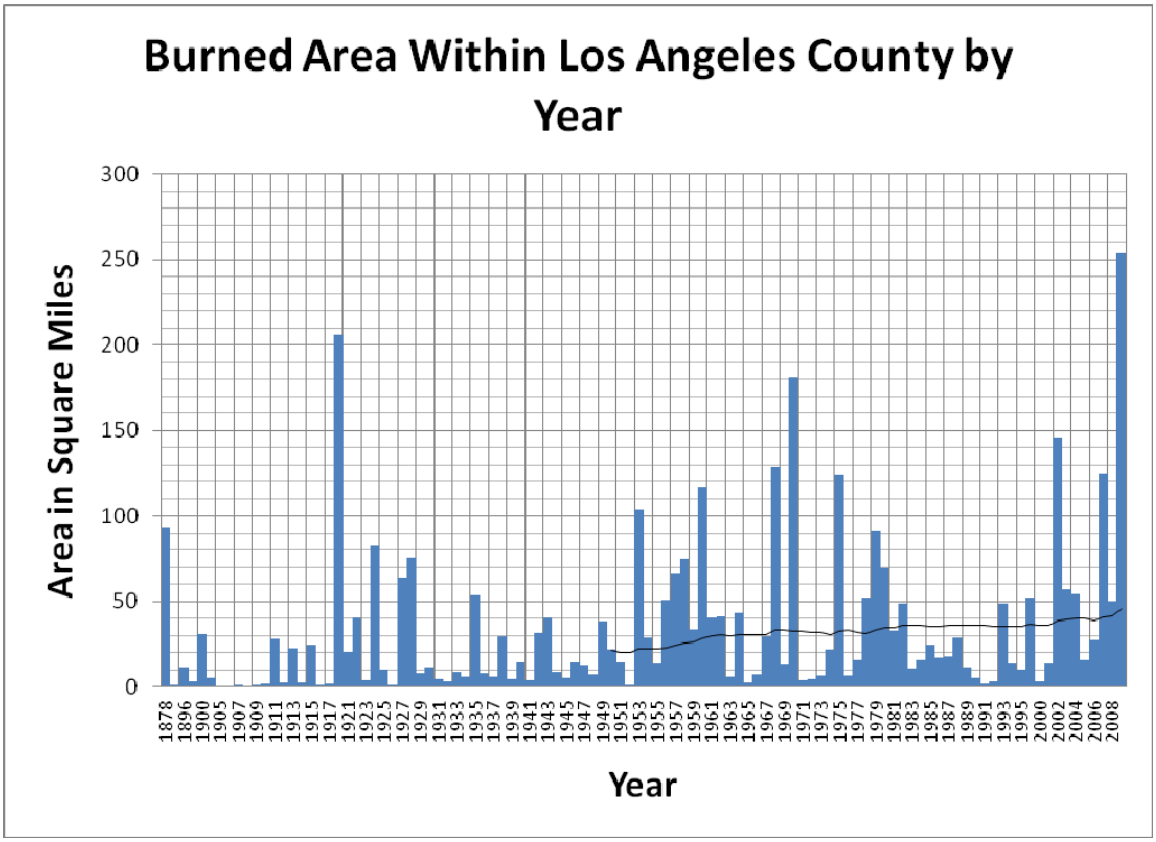

Figure 5.2 Annual Area of County Burned by Wildfires

5.2 Changes to Vegetation During Fires

Hanes (1987) notes that chaparral is considered to be the most characteristic vegetative community in the state. This is especially true in Southern California where chaparral communities experience long dry summers and receive most of their annual precipitation, from winter rains (Radtke 1983). Chaparral habitat covers approximately 8.5 percent of California, and ranges in elevation from near sea level to over 5,000' in Southern California. Two distinct chaparral

communities are found within Los Angeles County; hard chaparral and soft chaparral. These communities are more commonly referred to as chaparral and coastal sage scrub respectively (Ainsworth and Doss, 1995).

Fire in these forested areas is an important natural disturbance mechanism that plays a role of variable significance depending on climate, fire frequency, and geomorphic conditions. This is particularly true in regions where frequent fires, steep terrain, vegetation, and postfire seasonal precipitation interact to produce dramatic impacts (USDA, 2005).

The amount of vegetation consumed by a fire depends on the fire regime and fire severity (USDA, 2005). The USDA (2005) provides an in-depth discussion of fire regimes and severities. Low severity fires rarely produce adverse effects on watershed hydrologic conditions, while high severity fires generally result in higher runoff and erosion.

Wildfires can leave large areas devoid of vegetation and vulnerable to producing large volumes of runoff leading to flash floods, floods, or mudslides (NOAA, 2004). The high rate of runoff following brush fires may result from the combined effects of denudation and formation of a water-repellent soil layer beneath the ground surface (Nasseri, 1988). As discussed in Section 4, the type of vegetative cover on a soil changes the infiltration rates. This is due to the effects of vegetation on slowing surface runoff velocities. Loss of surface litter,

vegetative basal cover, and the associated microtopographic relief also reduce surface storage of water crucial for reducing runoff and increasing infiltration (Pierson, Jr. et. al, 2003).

The removal of vegetation due to fires increases runoff as surface runoff velocities increase, decreasing the time available for infiltration. Fires also change soil characteristics as discussed in Section 5.3.

5.3 Changes to Soils During Fires

Fires induce temperatures at ground level reaching six to seven hundred degrees centigrade. Burning vegetation, especially chaparral, releases oils, resins, and waxy fats stored in plants and plant litter as intense heat vaporizes the vegetation (McPhee, 1989). The soil acts as an insulator, keeping temperatures a few centimeters below the surface much cooler. This temperature difference allows condensation of vaporized substances, forming a *hydrophobic* layer. This layer is impermeable and prevents water from reaching all but the first few inches of soil. It also slows evaporation through the soil (Ainsworth and Doss, 1995). The extent and depth of a hydrophobic layer depends on the type of soil, the fire intensity, and antecedent soil moisture. Clay soils tend to resists the formation of a hydrophobic layer. Sandy and sandy loam soils are far more susceptible to hydrophobic conditions (DeBano 1987).

If a drop of water is placed on a pre-burn sample of sandy loam soil, the water will all but disappear. Yet, if water is placed upon a post-burn sample, the drop will ball up and may remain there for hours. The firestorms of Southern California typically occur just prior to the winter rains. Water quickly saturates the thin layer of permeable soil above the hydrophobic zone not being slowed by a vegetative canopy. Slower infiltration rates result in an increased intensity of surface runoff and erosion. (Ainsworth and Doss, 1995)

5.4 Changes to Runoff After Fires

As discussed in Sections 5.2 and 5.3, fire changes the soil and vegetation characteristics of a watershed. The changes result in higher runoff rates and more erosion within the watershed. Erosion of sediment leads to bulking of flows, where entrained sediment increases the volume of runoff. Vegetation, litter, rocks and other forms of ground cover create barriers that slow and spread water movement across the soil surface allowing more time for water to infiltrate over a larger surface area. Fire removes most of these barriers and allows the water to concentrate into rills. Rills allow increased flow depth and velocity. Higher flow depths and velocities significantly decreases runoff response time and increases runoff volume in streams (Pierson, Jr. et. al, 2003). Several studies have been conducted to determine the influence of fire on the volume and peak runoff from watersheds.

Veenhuis (2002) studied two burned watersheds in New Mexico. He noted that storm flows increased dramatically after the wildfire. Peak flows in each of these two watersheds increased to about 160 times the maximum-recorded flood prior to the fire. As vegetation reestablished itself in the second year, the annual maximum peak flow was reduced to approximately 10 to 15 times the pre-fire annual maximum peak flow. During the third year, maximum annual peak flows were reduced to about three to five times the pre-fire maximum peak flow. In the 22 years since the La Mesa wildfire, flood magnitudes have not completely returned to pre-fire magnitudes. The number of larger than normal peak flows seems to be most pronounced for 3 years after the fire. (Veenhuis, 2002). Other studies also indicate significant increases in runoff after fire (Pierson, Jr. et. al, 2003; Nasseri, 1988; Wondzell et. al, 2003).

Work by Davis (1977) suggests that many post fire flows are debris flows. In the watersheds that Davis studied he found bulking ratios in runoff ranged from 0.5% to 2.5% by volume for normal flows to 40% to 60% by volume for post fire flows. Bulking can increase runoff volumes and peaks significantly. However, it will not be further evaluated in this study.

Studies in the California chaparral wildlands demonstrate that dry ravel and, to a lesser extent, the formation of extensive rill networks account for most of the

increased sediment production following a fire (Wells, 1986). This process may even be more prominent in the post-fire environment due to creation of *hydrophobic* soil layers during a blaze. (Ainsworth and Doss, 1995)

Nasseri (1988) developed a model to evaluate effects of fires on hydrologic characteristics of watersheds. He determined that burning increased peak flows and volumes, shifting the annual exceedence probability of runoff generated from the same size rainfall event. He drew the conclusion "that flood control facilities serving watersheds that experience frequent brush fires should be designed for flow characteristics under burned conditions."

As discussed in Sections 4.2 and 4.3, two methods of soil losses can be used for determining loss relationships to convert rainfall to excess precipitation. The constant loss method utilizes a constant loss rate, while the runoff coefficient method takes a percentage of the rainfall to generate the excess precipitation. Within Los Angeles County, the runoff coefficient is tied to infiltration rates based rainfall intensity. Using a constant loss method for burned watersheds would require significant studies and would be very site specific.

Constant loss parameters are normally based only on soil type, and are then calibrated within a model to fit specific storms in order to develop a range of values for a particular watershed. Several researchers have been investigating

the effects of fire on hydrologic response in watersheds with coarse textured soils and sagebrush ecosystems (Pierson, et. al, 2008; Spaeth et. al, 2007). Spaeth et. al (2007) found that the presence or absence and magnitude of canopy cover of certain plant species seems to be associated with infiltration capacity, runoff, and sediment loss. However, further study is needed to determine the actual effects. No studies have been found to relate the infiltration rate to the soil types and textures discussed in Section 4.1.

The Los Angeles County Flood Control District (LACFCD) has adopted a fire response mechanism to the Modified Rational Method. Equation 4.4 is modified to reflect the effects of fire using C_{ba}, the burned runoff coefficient. Equation 5.1 provides this relationship.

$P_e = C_{ba} * I$ Eq. 5.1

Pe, the precipitation excess is equal to the burned runoff coefficient (C_b) multiplied by the rainfall intensity (I). In the case of a partially developed watershed, the developed runoff coefficient shown in Eq. 4.5 can be modified as shown in Equation 5.2.

$$C_D = (0.9 * IMP) + (1 - IMP) * C_{ba}$$ Eq. 5.2

Los Angeles County requires that watersheds with 15% or less urban development utilize the burned runoff coefficient.

As discussed in Section 4.3, double-ring infiltrometer tests were conducted to determine runoff based on rainfall intensity for soils within the County. Another set of testing was conducted on the same soils with the cover completely burned. This provided the basis for the burned watershed analysis, assuming that the watershed was completely burned. Equation 5.3 shows the LACDPW (2006) relationship for the C_{ba}.

$$C_{ba} = FF \times [(1-K) \times (1-C_u)] + C_u \qquad \text{Eq. 5.3}$$

Where:

C_{ba} = Adjusted burned soil runoff coefficient

FF = Fire Factor, the effectively burned percentage of watershed area

K = Ratio of burned to unburned infiltration rates for I, $0.677 \times I^{-0.102}$

I = Rainfall intensity, in/hr

C_u = Undeveloped runoff coefficient

The Fire Factor, FF, represents the hydrologic effects of a fire on the watershed based on a percentage of the watershed that is still impacted by loss of vegetation and changes to soil properties. Use of FF requires understanding the

relationship of fires to watershed recovery. The LACFCD requires use of the 50-year Fire Factor with the 50-year rainfall to determine the Capital Flood event used for design (LADPW, 2006).

The probability of a certain condition existing in the watershed should be factored into the evaluation of runoff frequency. Use of the average FF, or use of a probability distribution of FFs requires further analysis to determine the impacts related to runoff frequency distribution. Section 5.5 discusses watershed recovery from fire and the development of a fire factor based on the recovery.

5.5 Watershed Recovery From Fires

The vegetation of chaparral communities has evolved to a point it requires fire to spawn regeneration. Many studies have shown an increase in runoff and erosion rates the first year following fire, with recovery to pre-fire rates generally within five years (Wright and Bailey 1982). The timing and extent of recovery is highly dependent on precipitation, slope and vegetation type (Branson et al. 1981, Wright et al. 1982, Knight et al. 1983, Wilcox et al. 1988). Pierson, Jr. et. al (2003) noted that water repellency of the hydrophobic water layer deteriorates over time, resulting in a gradual recovery in the infiltration capacity of the soil.

Ainsworth and Doss (1995) discuss in detail the post-fire recovery of vegetation:

> "The recovery of a coastal sage occurs through a successional process in which various sub-communities of coastal sage are present at different time periods following the fire. During the first two years, herbaceous annual species dominate the landscape. Species such as California Poppies, Blue Dicks, Mariposa Lily, Fire Hearts, Lupines and many others carpet the post-burn environment. Among this colorful display is a rebirth of perennial chaparral species such as Chamise, Coastal Sage, California Buckwheat, Poison Oak, Bush Sun Flower, Ceanothus, Manzanita, Laurel Sumac, and Sugarbush begin to germinate from seed. Coast Live Oaks and Laurel Sumacs begin to recover through the processes of crown and stump sprouting.
>
> Two to three years following the blaze the fire annuals begin to disappear. They have produced vast quantities of seeds which are now stored in the soil until the next blaze comes along. The herbaceous community has succumbed to various factors such as a lack of fire scarified seeds, limited available sun light, due to a new canopy of perennial growth, and as the result of toxins, *allelopathogens*, released by perennials such as Chamise to reduce competition with other species. Many of the herbaceous species, such as Lupines, have laid the path to recovery by processing, or *fixing*, nutrients like nitrogen into a form which can be used by subsequent and more dominant perennial species. Other nitrogen fixing species like Deerweed have recovered as well, and it is at this time that perennial species begin to flower and thus start seed production once again.
>
> Four to ten years following a fire, the landscape is once again dominated by Chamise, Laurel Sumacs, Sugarbush, Buckwheat, Monkey Flowers, Live-Forevers, Toyon, and others. The community is reaching equilibrium and will begin the process of accumulating woody, dead, and organic materials rich in flammable oils until the next fire is allowed to burn, or escapes to the Santa Ana winds."

The Ainsworth and Doss (1995) qualitative summary has been numerically quantified by other studies. Pierson, Jr. et. al, (2003) studied two watersheds in Idaho which were severely burned. They note that virtually all vegetation and litter was consumed during the fire. Bare ground for all burned sites was greater

than 95% resulting in increased soil exposure to the erosive forces of raindrop impact and overland flow. It took two growing seasons and three winters for litter accumulation to reduce the amount of bare ground on the burned sites to near 50 percent.

Gradual watershed recovery must be considered when determining the annual hydrologic effects of fire and for developing a Fire Factor for use with MODRAT. The Los Angeles County Flood Control District studied vegetation recovery rates for watersheds within Los Angeles County (1959). Table 5.1 presents the recovery rates based on the number of years after the fire.

Table 5.1 Vegetation Regrowth Rate for Burned Watersheds

Years After Burn	Percent Recovered
0	R_0 = 10%
1	R_1 = 28%
2	R_2 = 52%
3	R_3 = 69%
4	R_4 = 80%
5	R_5 = 90%

Table 5.1 shows that watershed vegetation recovers to 90 percent of the pre-fire condition after five years. This is consistent with the results of the other

researchers, both quantitatively and qualitatively. The LACFCD data is used to develop Fire Factor information for watersheds within Los Angeles County. The Fire Factor (FF) represents the effectively burned percentage of the watershed area on an annual basis and can be used to adjust runoff coefficients for burned watershed hydrology.

5.6 Fire Factor Development

Many studies have been conducted to determine how frequently a fire impacts a watershed (Pierson, Jr. et. al, 2003; USDA, 2005). Barro and Conard (1990) noted that in a period of 750 years, fire occurs once every 65 years in coastal drainages, and once every 30 to 35 years inland. This is consistent with other studies cited by the USDA (2005). However, the number of times a fire occurs in a watershed does not fully describe the hydrologic impact that a fire has on the watershed.

The watershed recovery from fire must also be included in the analysis of fire effects on annual hydrologic conditions. Based on the recovery criteria discussed in Section 5.5, the fires within Los Angeles County were evaluated to see how often a watershed was impacted to some degree by fires, and what the probability was for the level of impact. The concept of a fire factor (FF) was developed to represent the effectively burned percentage of the watershed area.

The Fire Factor is used to adjust runoff coefficients for burned watershed hydrology as discussed in Section 5.4.

Runoff coefficients are adjusted to account for the effect of burns on a watershed (LACDPW, 2006). Figure 5.3 presents runoff coefficients modified using Eq. 5.3. The figure shows the runoff coefficient for an unburned watershed (FF=0.00), 50 percent burned (FF=0.50), and 100 percent burned (FF=1.00) soil runoff coefficients for a specific soil. The FF=1.00 represents the data collected by the double-ring infiltrometer test on soils within Los Angeles County.

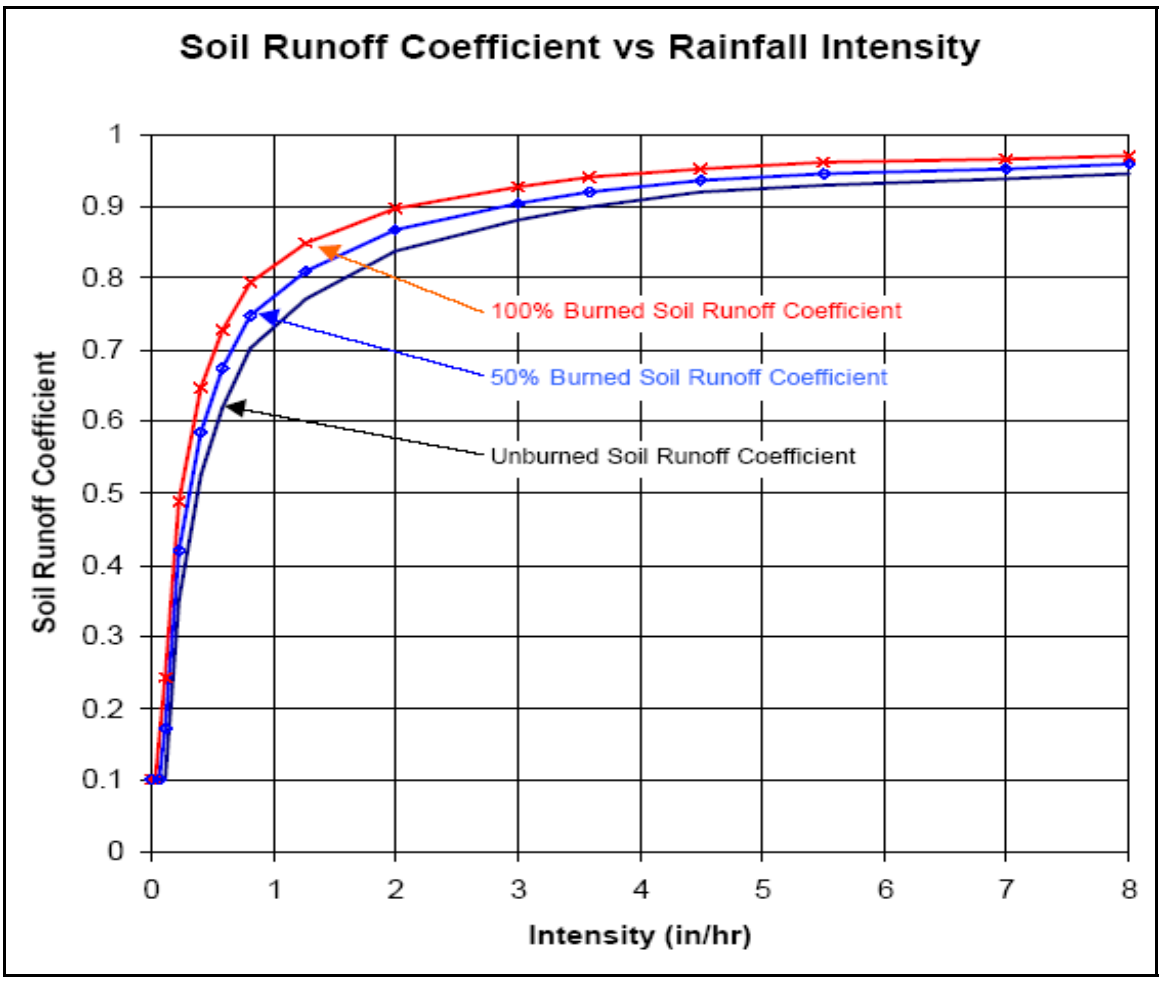

Figure 5.3 Burned Runoff Coefficients (C_{ba}) for Specific Soil in Los Angeles County

Table 5.1 shows that watershed vegetation recovers to 90 percent of the pre-fire condition after five years. The effectively burned area is determined by multiplying the burned areas from the last five years, expressed as a percentage, by the corresponding percent recovered from Table 5.1. The fire factor represents the effectively burned area expressed as the percentage of watershed

area. Walden and Willardson (2004) developed Equation 5.4 to determine the fire factor for a specific year.

$$FF = (B_i * (1 - R_i) + (B_{i-1} * (1 - R_{i-1}) + (B_{i-2} * (1 - R_{i-2}) + (B_{i-3} * (1 - R_{i-3}) + (B_{i-4} * (1 - R_{i-4}) + (B_{i-5} * (1 - R_{i-5})$$

Eq. 5.4

The subscripts in Equation 5.4 represent the number of years after a burn. B_i in Equation 5.4 represents the percentage of area burned and R_i represents the percentage of area recovered for the respective year. Walden and Willardson (2004) provide an example application of Equation 5.4 to the South Fork Watershed to demonstrate the calculation of the annual Fire Factor for the year 1970. Figure 5.4 shows the watershed divided into subareas for modeling, along with the fire boundaries for the five years prior to 1970. Table 5.2 summarizes the fire data, percentage of burned areas, and the percentage of recovery for five years prior to 1970.

A watershed with historical data can utilize Equation 5.4 to determine the annual fire factor for each year of record that covers fires within the area. Section 5.7 discusses the analysis of historical fire data within Los Angeles County to determine annual fire factors and the associated AEPs.

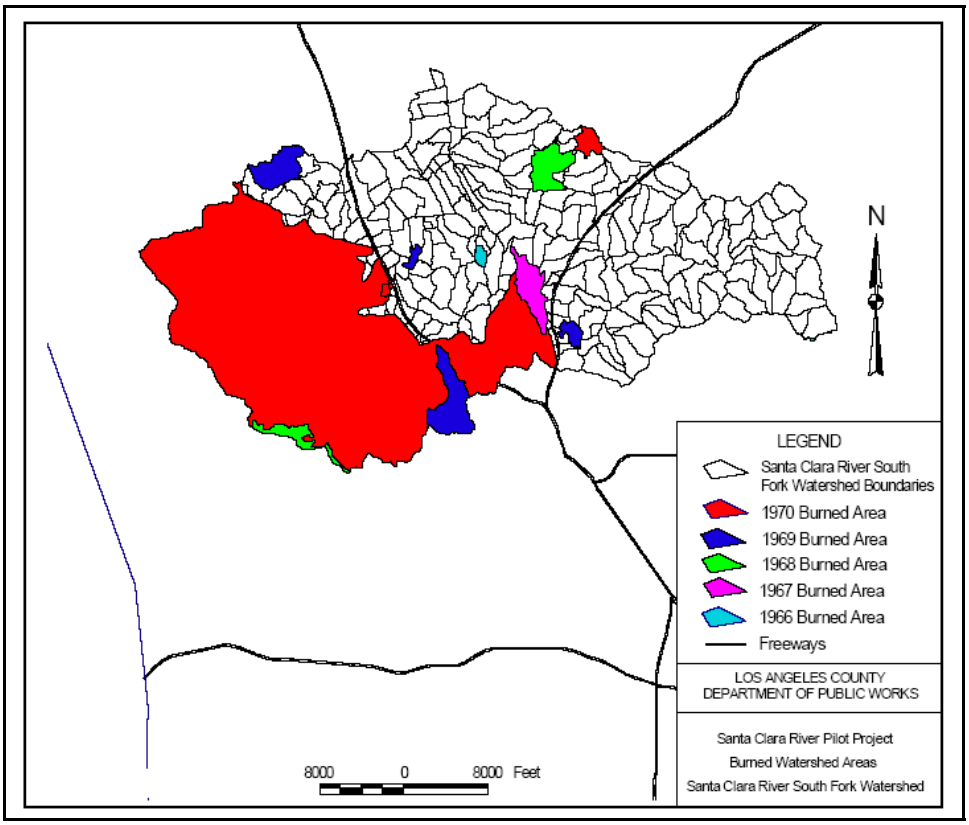

Figure 5.4 Santa Clara River South Fork Watershed Boundaries

Table 5.2 1965 - 1970 Fire History Data for the South Fork Watershed

Year	Total Burned Area (acres)	Percentage of Watershed Burned	Percentage Recovered	Percentage Still Effected
1965	0.0	0.00%	90.0%	10.0%
1966	41.3	0.18%	80.0%	20.0%
1967	273.6	1.21%	69.0%	31.0%
1968	422.6	1.87%	52.0%	48.0%
1969	763.4	3.37%	28.0%	72.0%
1970	11004.0	48.61%	10.0%	90.0%

FF = (0.0% * 0.10) + (0.18% * 0.20) + (1.21% * 0.31)
+ (1.87% * 0.48) + (3.37% * 0.72) + (48.61% * 0.90) = 47% or 0.47

5.7 Fire Factor Frequency Analysis

Historical fire data from 1878 through 2009 was analyzed to determine the percentage of the watershed affected by fires for each year of record. The analysis considered recovery from fires within the previous five years. The largest recorded fire within Los Angeles County occurred in August 2009. The Station Fire burned 165,000 acres, or 250 square miles. Studies by the LACDPW (Willardson and Walden, 2003; 2004) indicated that as watershed size increases, the probability of completely burning the watershed decreased.

In an effort to standardize an analysis, a GIS layer consisting of all areas impacted by fire over the last 132 years was delineated to represent areas with wildfire potential. The layer was then subdivided into grids, ranging in size from 0.1 to 1600 square miles. Figure 5.3 provides a map of several grid sizes and their distribution throughout the County. The figure shows 4 grid levels. The grids have side lengths of 1, 5, 10, and 20 miles, corresponding to grids with areas of 1, 25, 100, and 400 square miles. To reduce the number of calculations required, only areas that had experienced fire were evaluated to determine an annual fire factor. Use of areas where fire occurred excluded urban areas and areas with limited vegetation.

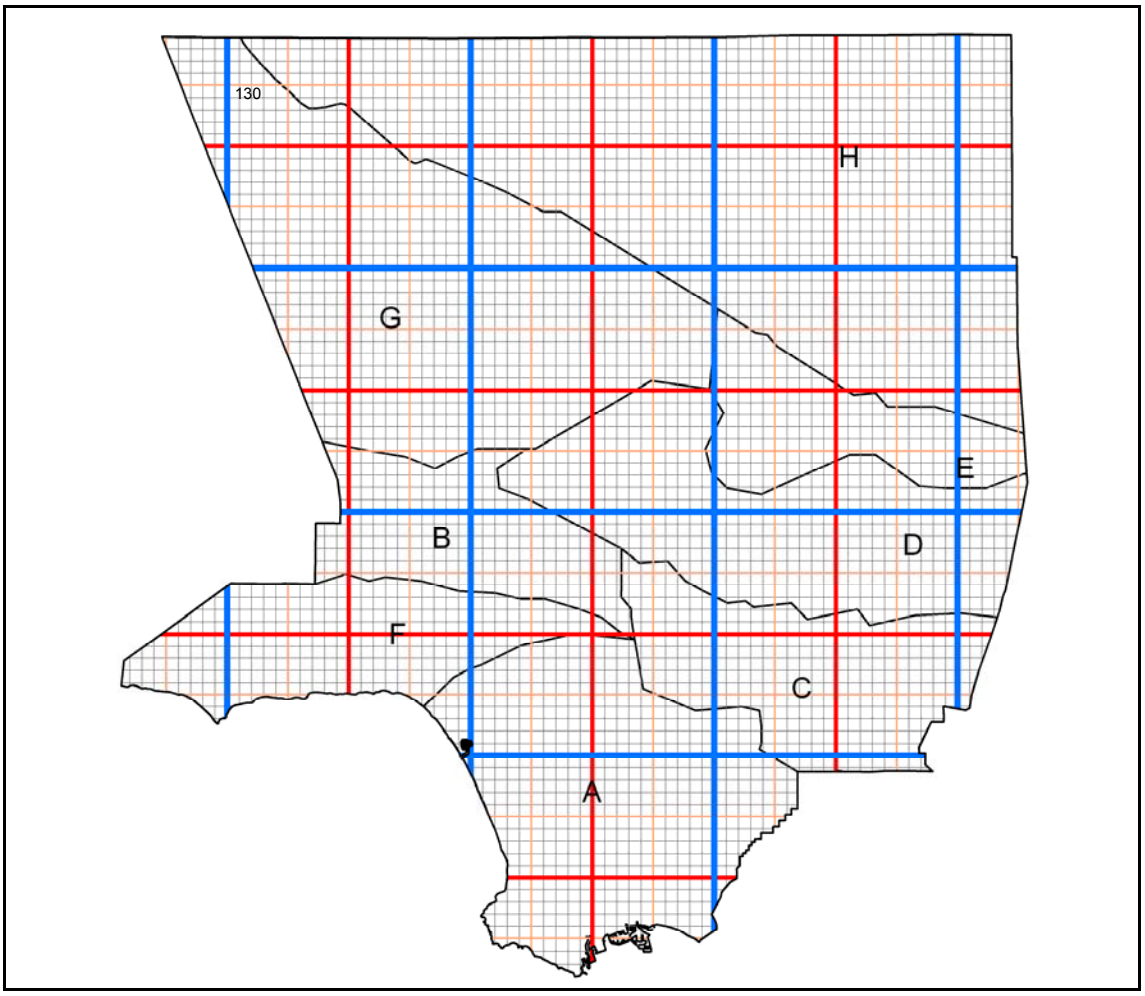

Figure 5.5 Fire Analysis Grids (1, 5, 10, and 20 mile)

The effectively burned area analysis for a single grid is shown in Table 5.3. Grid 130 is on the Antelope Valley/Santa Clara River boundary as shown in Figure 5.5. The yearly data for the area burned was developed using GIS to cut the fire layer using the grid shapefile as a boundary. Areas were recalculated and multiple burned areas within the grid were summed to determine a total area burned within the grid for a specific year.

Table 5.3 Analysis of 25 Square Mile Grid in Antelope Valley-Grid #130

1	2	3	4	5	6	7	8	9	10
Year	**Total Burned Area (acres)**	**Annual % of Watershed Burned**	**Effectively Burned Area After X Years of Recovery (Column 3*(1-Recovery Ratio))**						
			Years of Recovery						**Annual FF**
			0	**1**	**2**	**3**	**4**	**5**	
			0.10	0.28	0.52	0.69	0.80	0.90	
1879	.	.							
.	.	.							
.	.	.							
1920	0.0	0.00%							
1921	0.0	0.00%							
1922	0.0	0.00%							
1923	0.0	0.00%							
1924	0.0	0.00%							
1925	0.0	0.00%							
1926	26.9	0.17%	0.00						0.00
1927	5903.0	36.89%	0.33	0.00					0.33
1928	234.0	1.46%	0.01	0.27	0.00				0.28
1929	0.0	0.00%		0.01	0.18	0.00			0.19
1930	0.0	0.00%			0.01	0.11	0.00		0.12
1931	0.0	0.00%				0.00	0.07	0.00	0.08
1932	0.0	0.00%					0.00	0.04	0.04
1933	0.0	0.00%						0.00	0.00
.	.	.							.
.	.	.							.
1968	6694.7	41.84%	0.38						0.38
1969	0.0	0.00%		0.30					0.30
1970	62.0	0.39%	0.00		0.20				0.20
1971	0.0	0.00%		0.00		0.13			0.13
1972	0.0	0.00%			0.00		0.08		0.09
1973	0.0	0.00%				0.00		0.04	0.04
1974	0.0	0.00%					0.00		0.00
1975	0.0	0.00%						0.00	0.00
.	.	.							.
.	.	.							.
2004	5585.9	34.91%	0.31						0.31
2005	0.0	0.00%		0.25					0.25
2006	0.0	0.00%			0.17				0.17
2007	0.0	0.00%				0.11			0.11
2008	0.0	0.00%					0.07		0.07
2009	0.0	0.00%						0.03	0.03
2010	0.0	0.00%							0.00

Columns 1, 2, and 3 show the year of analysis, the annually burned area in acres, and the percent of the 25 square mile watershed burned during the year. Columns 4-9 show the year of recovery and also show the recovery ratio as a decimal. Column 10 provides the annual fire factor representing the effectively burned area within the watershed.

The area affected by the fire is equal to the sum of recovery ratio subtracted from unity (1-recovery ratio) for years 0-5. The effectively burned area for each year is determined using Equation 5.4, which is the sum of values across columns 4-9. Each year, the total area burned is adjusted using the recovery ratio. The fire impact in 1928, an annual fire factor of 0.18, is equal to (1-0.28)*0.3689 + (1-0.10)*0.0146.

The number and sizes of fires occurring with a watershed impact the watershed for several years. As an example, 3 fires occurred in Grid 130 in 1926, 1927, and 1928. The 1926 fire impact was so small, that it does not show up when percentages are rounded to two decimal places. All three fires impact the watershed in 1928, while the watershed is still recovering from the fires of 1926 and 1927. However, the annual fire factor for 1927 (0.33) is larger than the annual fire factor for 1928 (0.28) due to the magnitude of the 1927 fire and the recovery rates for each year.

Each grid cell was analyzed to determine annual fire factor statistics for each cell. These were then evaluated to determine overall statistics for the grid size. The resulting summary analysis is provided in Table 5.4.

Table 5.4 Percentile Analysis of Fire Factor Data

Grid Analysis Statistics on All Fire Factor Data											
Grid Level	**0**	**1**	**2**	**3**	**4**	**5**	**6**	**7**	**8**	**9**	**10**
Area (mi^2)	**0.1**	**0.25**	**1**	**4**	**16**	**25**	**64**	**100**	**256**	**400**	**1052**
μ	0.048	0.023	0.026	0.023	0.020	0.020	0.017	0.018	0.017	0.016	0.015
σ	0.393	0.117	0.115	0.101	0.084	0.079	0.067	0.060	0.052	0.044	0.042
γ	12.18	6.11	5.67	6.08	6.60	6.61	7.30	6.16	6.07	5.08	5.71
Fire Factor by Percentile Analysis											
99th	0.900	0.900	0.720	0.606	0.471	0.444	0.343	0.320	0.255	0.229	0.212
95th	0.229	0.231	0.155	0.127	0.110	0.110	0.087	0.094	0.093	0.084	0.085
90th	--	--	0.009	0.023	0.030	0.035	0.033	0.040	0.042	0.042	0.040
80th	--	--	--	--	0.002	0.004	0.006	0.010	0.013	0.016	0.014
70th	--	--	--	--	--	--	--	0.002	0.003	0.007	0.005
60th	--	--	--	--	--	--	--	--	--	0.002	0.001
50th	--	--	--	--	--	--	--	--	--	--	--
40th	--	--	--	--	--	--	--	--	--	--	--
30th	--	--	--	--	--	--	--	--	--	--	--
20th	--	--	--	--	--	--	--	--	--	--	--
10th	--	--	--	--	--	--	--	--	--	--	--
5th	--	--	--	--	--	--	--	--	--	--	--

Table 5.4 shows the percentile analysis of all fire factors, including a fire factor of 0. The table shows an interesting trend which is important to understand. As the watershed size increases, the percentage of watershed impacted drops. However, the opposite is true of the standard deviation. Small watersheds have high standard deviations, showing that when there is a fire in the watershed, it is significantly impacted by the fire. Large watersheds have lower standard deviations, reflecting the fact that most fires are contained prior to impacting

large areas of a watershed. Only extremely large fires, Like the Station Fire impact large geographic areas. The high skew indicates that there are a lot of 0 values for the fire factor in the data set, skewing the data towards the no fire affect.

Table 5.5 shows an analysis of the fire factors when the FF=0 values are removed from the data set. The table shows the Grid Level, which ranges from 0-11, the grid side length, and the grid area. The last column provides the number of annual fire factors evaluated for each grid level.

Table 5.5 Grid Data Summary Analysis

Level	Side Length	Area	Mean	Std. Dev.	5th Perc.	95th Perc.	Max	Min	# of Annual FFs
	(mi)	($mi.^2$)							
0	0.32	0.10	0.386	0.304	0.011	0.900	1.000	0.000	277374
1	0.50	0.25	0.350	0.306	0.005	0.960	1.000	0.000	130815
2	1.00	1.00	0.214	0.262	0.001	0.720	1.000	0.000	46851
3	2.00	4.00	0.136	0.211	0.000	0.480	1.000	0.000	19131
4	4.00	16.0	0.081	0.154	0.000	0.263	1.000	0.000	8474
5	5.00	25.0	0.069	0.136	0.000	0.253	1.000	0.000	6670
6	8.00	64.0	0.050	0.108	0.000	0.214	1.000	0.000	3898
7	10.00	100.0	0.042	0.087	0.000	0.171	0.824	0.000	2896
8	16.00	256.0	0.038	0.074	0.000	0.058	0.751	0.000	1837
9	20.00	400.0	0.030	0.057	0.000	0.078	0.562	0.000	2218
10	32.00	1024.0	0.031	0.057	0.000	0.065	0.562	0.000	981
11	40.00	1600.0	0.031	0.059	0.000	0.096	0.672	0.000	754

The grid level data sets were analyzed to determine the mean annual fire factor, the standard deviation, and the 5th and 95th percentile for each grid level. Although data was developed for grid sizes up to 1600 square miles, analysis of

the data indicated that representative samples of watersheds larger than 100 square miles were not realistic due to the spatial extent of the fire data and the size of the County.

The Los Angeles County Department of Public Works has developed fire factors using a similar method for the major watersheds within the County. The study utilized subwatersheds, but did not look at consistent sizes. Once annual fire factors were developed county-wide, the data was then divided by watershed to determine whether the fire factors varied significantly between watersheds.

Figure 5.6 shows the major watersheds within the county. The major watersheds include the San Gabriel River, Los Angeles River, Santa Clara River, and the Antelope Valley. Malibu Creek, North Santa Monica Bay, South Coast, and Compton Creek watersheds were all lumped into Coastal Watersheds.

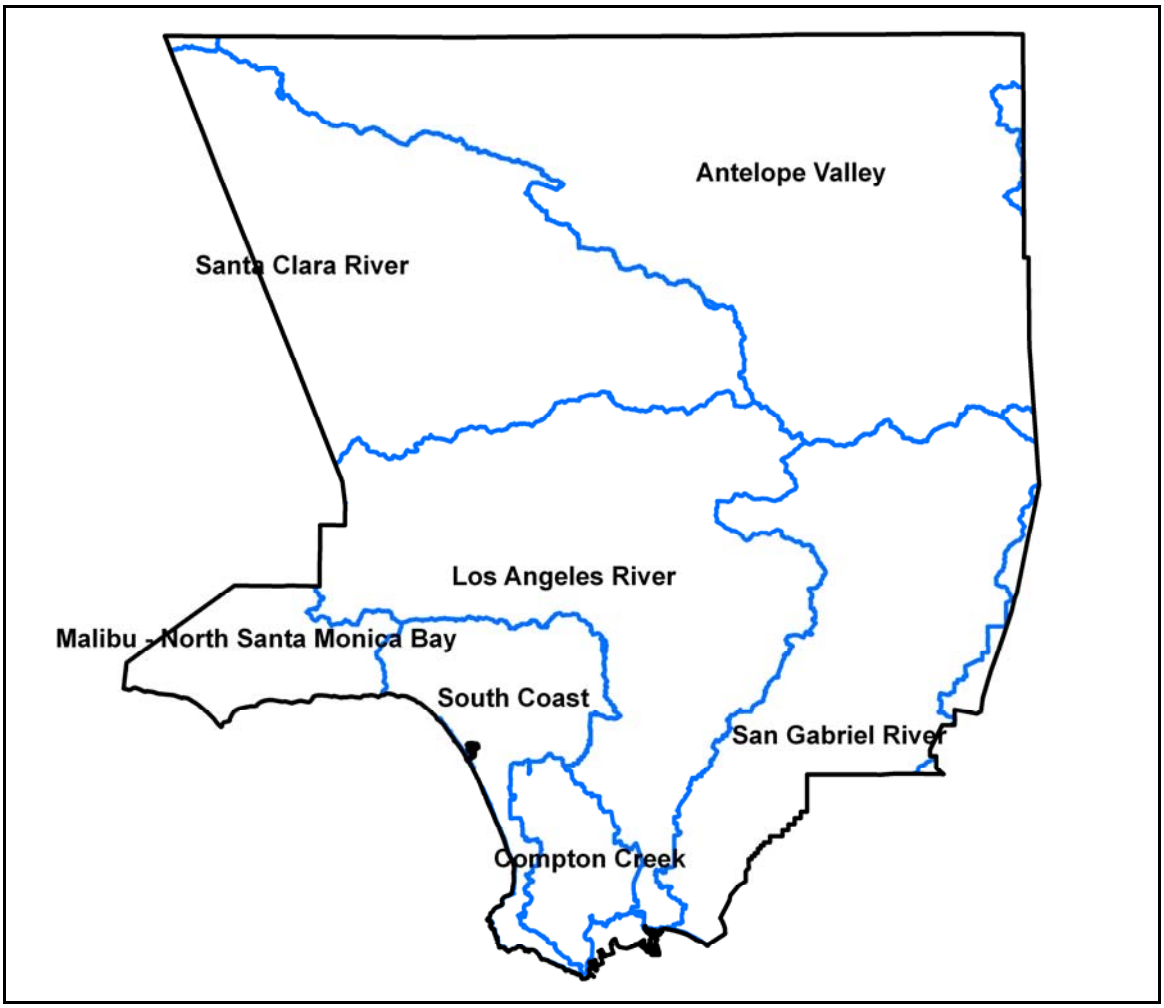

Figure 5.6 Major Watersheds Within Los Angeles County

Figure 5.7 shows a chart with the average fire factor broken down by watershed and grid size. The average 5th and 95th percentile values are also shown for each grid level using the data from all watersheds for a given grid level. These can be compared to the values in Table 5.5. As can be seen in the figure, there is little difference in the average fire factor value for each grid level based on the watershed. Review of the data showed that the size of the watershed is the driving factor in the annual fire factor.

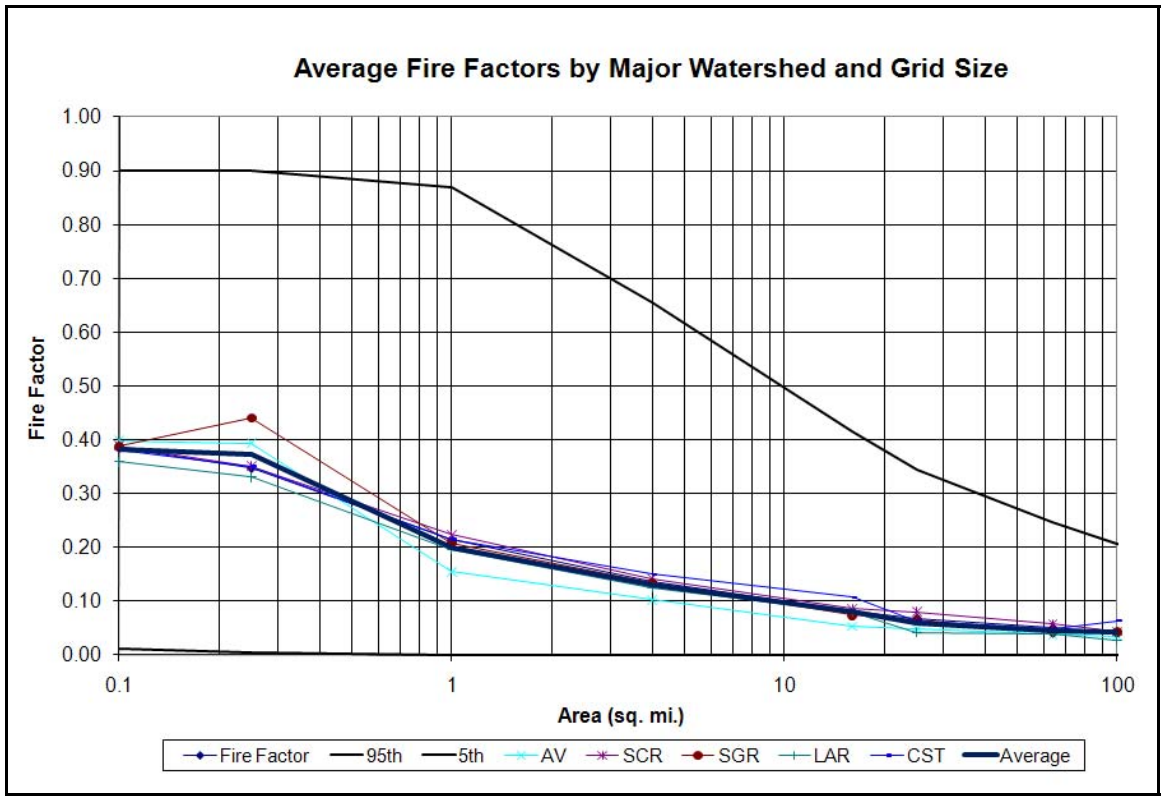

Figure 5.7 Average Fire Factor by Watershed and Grid Size

All of the average fire factors show a constant or decreasing trend from 0.1 square miles through 1.0 square miles, except for the San Gabriel River data set. The data was reprocessed using the same methods used for all other data sets and reanalyzed. The results were the same. The jump may be related to grid delineation or the occurrence of fire within the San Gabriel River watershed. The spike does not change the average trend at the 0.25 square mile grid level and appears to be sampling noise.

Once it was determined that the watershed size was more important than the location within the County, the next analysis involved determining the AEP for each grid level. Three methods of determining the AEP were selected. The first analysis method utilized the entire data set, which included FFs ranging from 0.00 to 1.00. Percentile analysis of the data set provided the FF corresponding to a set of predetermined AEPs. This is consistent with the data sets in Table 5.4.

The next analysis of the data set evaluated only FFs greater than 0.00 using percentile analysis. This data set represents only evaluating the annual values for impacted time frames. This resulted in higher values of FF for the same set of AEPs. This analysis is consistent with the data in Table 5.5.

The third method utilized the LACDPW methodology to determine the FF corresponding to various AEPs (LACDPW, 2006; Walden and Willardson, 2003; Walden, Willardson, and Conkle, 2004). The LACDPW Hydrology Manual (2006) requires the use of a 50-yr FF, AEP=0.02, for design hydrology studies. The 50-yr FF is specific to the major watersheds within Los Angeles County and ranges from 0.34 in the Santa Clara River Watershed to 0.83 in the Coastal Watersheds. The LACDPW FFs were developed by studying four subareas within each major watershed. The size of the studied watersheds ranged from 8.11 to 48.95 square miles.

The LACDPW method evaluates the frequency of FFs, the amount of time a watershed was affected by fire, and the amount of time it was unaffected by fire. The probability of exceeding a specific FF was determined and then was adjusted using the percentage of time a watershed was affected by fire. For example, if a watershed was affected by fire 10 percent of the time, and the probability of being burned between 10% to 20% was 0.20, the conditional probability would be FF*Percent of Time Effected by Fire = 0.20 * 0.10. This resulted in an AEP of 0.02, which corresponds to a 50-yr recurrence interval. The FF would then be 15% or 0.15. Appendix D contains the results of the frequency analysis for each of the grid sizes following the LACDPW methodology.

Table 5.6 shows the data from the analysis results from the three methods discussed above. The upper half of the table contains the data from the grid analysis. Column 1 shows the grid level, Column 2 shows the grid size in square miles, Columns 3 and 4 show the percent of time the watershed is affected or unaffected by fire. Column 5 is left blank to allow the upper and lower halves of the table to align for comparison.

Table 5.6 Analysis of FF Annual Exceedence Probabilities

Grid Analysis of 50-year Fire Factors							
Grid Level	Area Sq. Mi.	% of Time Burned	% of Time Unburned		50-yr FF All	50-yr FF > 0%	50-yr FF LACDPW
0	0.10	0.10	0.90		0.72	0.97	0.78
1	0.25	0.10	0.90		0.72	0.94	0.35
2	1.00	0.13	0.87		0.48	0.90	0.50
3	4.00	0.17	0.83		0.38	0.88	0.40
4	16.00	0.24	0.76		0.29	0.64	0.29
5	25.00	0.28	0.72		0.28	0.56	0.28
6	64.00	0.32	0.68		0.22	0.44	0.22
7	100.00	0.40	0.60		0.21	0.35	0.21
8	256.00	0.42	0.58		0.18	0.29	0.19
9	400.00	0.51	0.49		0.17	0.22	0.16
10	1,000.00	0.47	0.53		0.14	0.21	0.14
11	1,600.00	0.46	0.54		0.14	0.21	0.13
Analysis of LACDPW 50-year Fire Factors					**Comparison of Methods LACDPW vs. Grid**		
Watershed	Area Sq. Mi.	Time Burned	Time Unburned	50-yr FF	All	> 0%	LACDPW
Coastal Watersheds							
Rustic	12.60	0.29	0.71	0.34	0.32	0.71	0.32
Agoura	18.76	0.69	0.32	0.61	0.29	0.62	0.29
Las Virgines	17.84	0.71	0.29	**0.83**	0.29	0.63	0.29
Malibu Creek	26.74	0.64	0.36	0.41	0.27	0.55	0.27
Los Angeles River Watersheds							
Devils Gate	23.06	0.74	0.26	0.41	0.28	0.58	0.28
Pacoima	28.20	0.58	0.42	**0.71**	0.27	0.55	0.27
Chatsworth/West Hills	22.68	0.72	0.28	0.35	0.28	0.58	0.28
Verdugo Hills	11.76	0.59	0.41	0.39	0.32	0.73	0.33
Santa Clara River Watersheds							
Bouquet	48.95	0.91	0.09	0.24	0.24	0.49	0.24
Mint	26.44	0.83	0.17	0.21	0.28	0.55	0.27
South Fork	35.37	0.83	0.17	**0.34**	0.26	0.53	0.26
San Francisquito	46.84	0.79	0.21	**0.34**	0.24	0.49	0.24
San Gabriel River Watersheds							
Cogswell Dam	38.82	0.70	0.30	0.35	0.26	0.52	0.25
Morris Dam	8.11	0.47	0.53	0.54	0.35	0.80	0.36
Santa Anita Dam	10.59	0.38	0.62	**0.71**	0.33	0.75	0.34
San Dimas Dam	16.17	0.54	0.46	**0.71**	0.29	0.64	0.29

The lower half of the table provides a summary of the data used to determine the LACFCD Design Fire Factors for each major watershed (LACDPW, 2006;

Walden and Willardson, 2003; Walden, Willardson, and Conkle, 2004). Column 1 provides the subwatershed name by creek. Column 2 provides the size of watershed in square miles, for comparison with the grid data in the upper half of the table. Columns 3 and 4 show the time where the watershed is affected and unaffected by fire impacts. The average watershed size for the LACDPW study was 25.12 square miles. Taking the average for time burned and unburned from the LACDPW study resulted in an average percent of time burned of 0.65, and an unburned time of 0.35. This is fairly similar to the data for Grid Level 5, 25 square miles, of 0.72 and 0.28, respectively.

The 50-year FFs used for design hydrology within Los Angeles County are shown in Table 5.7. These correspond to the highest subwatershed 50-yr FF value determined during the LACDPW study for each major watershed and shown in Column 4 of Table 5.6. Column 3 of Table 5.7 shows the average of the four subwatershed 50-yr FF values shown in Column 4 of Table 5.6. Average values for the grid data sets shown in Columns 6-8 in the lower half of Table 5.6 are also provided for comparison in Columns 4-6 of Table 5.7. The last column of Table 5.7 shows the maximum grid analysis 50-yr FF for each major watershed based on the subwatershed sizes shown in the lower half of Table 5.5.

Table 5.7 Comparison of Average Design Values

Watershed	50-yr Design FF	LACDPW Average	Grid Analysis 50-yr FF			
			All	> 0%	Cond.	Max
Coastal	0.83	0.55	0.29	0.63	0.29	0.71
Los Angeles River	0.71	0.47	0.29	0.61	0.29	0.73
Santa Clara River	0.34	0.28	0.26	0.51	0.25	0.55
San Gabriel River	0.71	0.58	0.31	0.68	0.31	0.80

All of the maximum data found in Column 7 of Table 5.7 came from the data set using percentile analysis on FF values greater than 0.00. These values match the LACDPW methodology more closely than the other two sets. The conditional probability methodology used by LACDPW compares almost exactly with the percentile analysis of the entire data set including all FF=0.00 values. The LACDPW utilized the maximum 50-yr FF to provide a safety factor based on what had been experienced in actual watersheds. For the remainder of the study, only results from the > 0% data set will be used to maintain this margin of safety for determining the FF AEPs.

The >0% data set was analyzed using several distributions and plotting position methods. These included the Normal, Log-Normal, Log-Pearson III, and Gumbel frequency distributions, along with the Weibull, California, Cunnane, Gringorton, Adamowski, and Hazen plotting position methods. These methods are described in Rao and Hamed (2000). The results of the frequency distribution analyses varied significantly. The plotting position methods were within a very tight range. The average of the different plotting position methods was determined and

compared with percentile analysis of the data sets. The average of the plotting position values and the percentile analysis were almost identical. Problems with the frequency distribution fitting occurred because the distributions are unbounded on one or both ends, where the FF range is bounded between 0.0 and 1.0, which represent the physical limits of being unburned or completely burned. It was determined that percentile analysis would be used to determine the AEP for each grid level. Appendix E shows the results of the frequency distribution and plotting position analysis results.

The results of the AEP analysis are provided in Table 5.8. The table contains the FF associated with specific AEP/Recurrence Interval. Looking at the table, evaluating each column shows that the FF for any given AEP decreases as the grid size increases. Physically, this indicates that a fire of the same size burns a smaller percentage of the watershed as the watershed area increases.

Evaluation of the rows in Table 5.8 show that as the AEP decreases, corresponding to a larger recurrence interval, the FF also increases. This also makes sense physically, since smaller fires are more common. Fire and forestry departments make every effort to contain fires before they burn large land areas as discussed previously.

Table 5.8 AEP and Recurrence Interval for Grid Analysis Fire Factors

Grid Level	Area Sq. mi.	AEP / Recurrence Interval					
		0.9900 / 1.01-yr	0.8000 / 1.25-yr	0.5000 / 2-yr	0.2000 / 5-yr	0.1000 / 10-yr	0.0400 / 25-yr
0	0.1	0.0007	0.1000	0.3100	0.7200	0.9000	0.9000
1	0.25	0.0004	0.0719	0.2599	0.7200	0.9000	0.9035
2	1	0.0001	0.0118	0.1000	0.4000	0.6819	0.9000
3	4	0.0000	0.0044	0.0405	0.2192	0.4382	0.7180
4	16	0.0000	0.0019	0.0170	0.1109	0.2474	0.4739
5	25	0.0000	0.0018	0.0139	0.0897	0.1997	0.4034
6	64	0.0000	0.0013	0.0105	0.0610	0.1370	0.2938
7	100	0.0000	0.0013	0.0092	0.0521	0.1175	0.2420
8	256	0.0000	0.0015	0.0106	0.0517	0.1067	0.2071
9	400	0.0000	0.0013	0.0092	0.0410	0.0841	0.1542
10	1024	0.0000	0.0014	0.0093	0.0429	0.0879	0.1467
11	1600	0.0000	0.0023	0.0101	0.0498	0.0761	0.1358
Grid Level	**Area Sq. mi.**	**0.0200 / 50-yr**	**0.01000 / 100-yr**	**0.0050 / 200-yr**	**0.0020 / 500-yr**	**0.0010 / 1000-yr**	**0.0001 / 10000-yr**
0	0.1	0.9738	1.0000	1.0000	1.0000	1.0000	1.0000
1	0.25	0.9400	1.0000	1.0000	1.0000	1.0000	1.0000
2	1	0.9000	1.0000	1.0000	1.0000	1.0000	1.0000
3	4	0.8775	0.9000	1.0000	1.0000	1.0000	1.0000
4	16	0.6449	0.7870	0.9000	1.0000	1.0000	1.0000
5	25	0.5591	0.6990	0.8367	0.9612	1.0000	1.0000
6	64	0.4389	0.5581	0.7200	0.9000	0.9219	1.0000
7	100	0.3505	0.4528	0.5340	0.6374	0.7418	0.8141
8	256	0.2889	0.3423	0.4806	0.6156	0.6381	0.7363
9	400	0.2180	0.2874	0.3483	0.4297	0.4850	0.5541
10	1024	0.2145	0.2746	0.3531	0.4511	0.4962	0.5550
11	1600	0.2112	0.3238	0.3996	0.4702	0.5706	0.6617

Figure 5.8 graphically presents the data found in Table 5.8. The trends are easily noted in the chart. Each curve in the figure represents a specific AEP. The curve is designated using the recurrence interval, which is the reciprocal value of the AEP. As discussed in previous sections, the data sets for watersheds up to 100 square miles are felt to be more reliable due to the number of grids analyzed. The larger grids had relatively few annual fire factors for

review and so there is more uncertainty in the analysis of the FFs for larger areas.

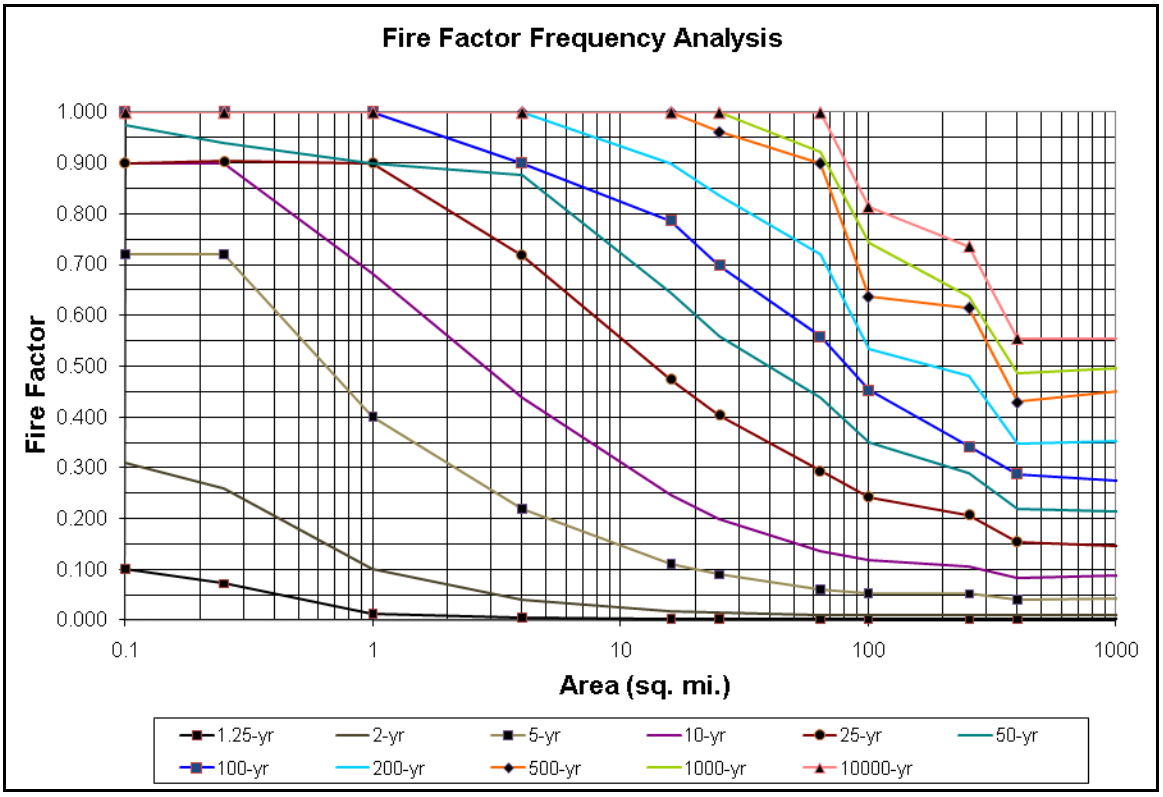

Figure 5.8 Fire Factor Frequency Curves for Various Watershed Sizes

Development of probability density functions for the FF allows the impacts of fire and watershed recovery to be investigated as a joint probability of occurrence within a watershed. The study of the joint probability of fire and extreme rainfall has been facilitated with a Monte Carlo analysis that is described in Chapter 6.

5.8 Chapter Summary and Conclusions

Chapter 5 discusses the important role fire plays in the hydrologic cycle in the western United States and particularly in Southern California. The effects on soils and vegetation result in increased runoff for several years after a fire. A method of quantifying the impacts of fire on runoff coefficients is provided using the concept of a fire factor.

The fire factor methodology utilizes the recovery rates of soils and vegetation from the impact of a fire to modify the runoff coefficient over several years. The method produces an annual fire factor ranging from 0 when a watershed is unaffected by fire, to 1.0, when a watershed has been completely burned. The annual fire factors can be evaluated using statistical methods to determine a recurrence interval. Watershed size was evaluated to determine whether the fire factor recurrence interval changed as the watershed size increased. The findings are summarized below:

1. Fires have a significant impact on hydrology within Los Angeles County.
2. The effects of fire on watershed hydrology can be quantified and a method has been developed for use with runoff coefficients within Los Angeles County.
3. The recurrence interval of annual fire factors is dependent on watershed size. The larger the watershed, the more likely there is to be a fire within

the boundaries. However, the larger a watershed gets, the less likely it is to burn completely. As a watershed gets smaller, the likelihood of burning decreases, but the probability of burning the entire area increases.

4. There is no discernible difference in fire factor recurrence interval within the major watersheds of Los Angeles County.
5. The method currently employed by Los Angeles County to incorporate the 50-year fire factor into hydrology studies is fairly consistent with the study conducted, but is conservative.
6. Fire Factor Area-Frequency curves were developed for the Los Angeles County data sets. It is felt that these curves should be fairly consistent throughout Southern California due to the similar topography and climate. Similar curves could be developed for other regions of the Western United States.

Chapter 6 – Monte Carlo Analysis of Probable Maximum Precipitation Translation to Probable Maximum Flood

Chapter 6 provides discussion on the Monte Carlo model developed to evaluate PMF runoff frequencies for watersheds within Los Angeles County. The model incorporates standard hydrologic methods along with the rainfall data, local soil data, wildfire impacts, and watershed characteristics to generate runoff frequency curves for specific watersheds.

Section 6.1 covers the general topic of Monte Carlo Simulation analysis and why it fits so well with this study of PMP and PMF estimation. The section also details the structure of the Monte Carlo model developed for this study. Section 6.2 discusses the development of the rainfall totals and hyetographs used as inputs for the Monte Carlo modeling. Section 6.3 discusses the methodology for incorporating the Los Angeles County Soils and NRCS Soils data into the Monte Carlo model.

Section 6.4 discusses fire factor generation for use with the Los Angeles County soil methodolgy during Monte Carlo simulation of the watersheds. Section 6.5 covers use of the Clark Unit Hydrograph within the Monte Carlo model and the cases used to evaluate the watersheds.

6.1 Introduction to Monte Carlo Simulation

Monte Carlo analysis utilizes repeated random sampling of input parameter probabilities to generate input data sets to be fed to a deterministic model. The input data sets are run through the deterministic model to generate output values. The output values can then be analyzed to determine the output value probability distribution. Monte Carlo models are normally utilized when there are complex problems with several coupled degrees of freedom for a given problem. Due to the highly intense computational requirements, Monte Carlo analysis is most suited for computer simulation.

A Monte Carlo model was developed to evaluate the conditional probability of peak annual runoff based on the independent rainfall and FF probability distributions. Figure 6.1 contains a flow chart for the Monte Carlo analysis model.

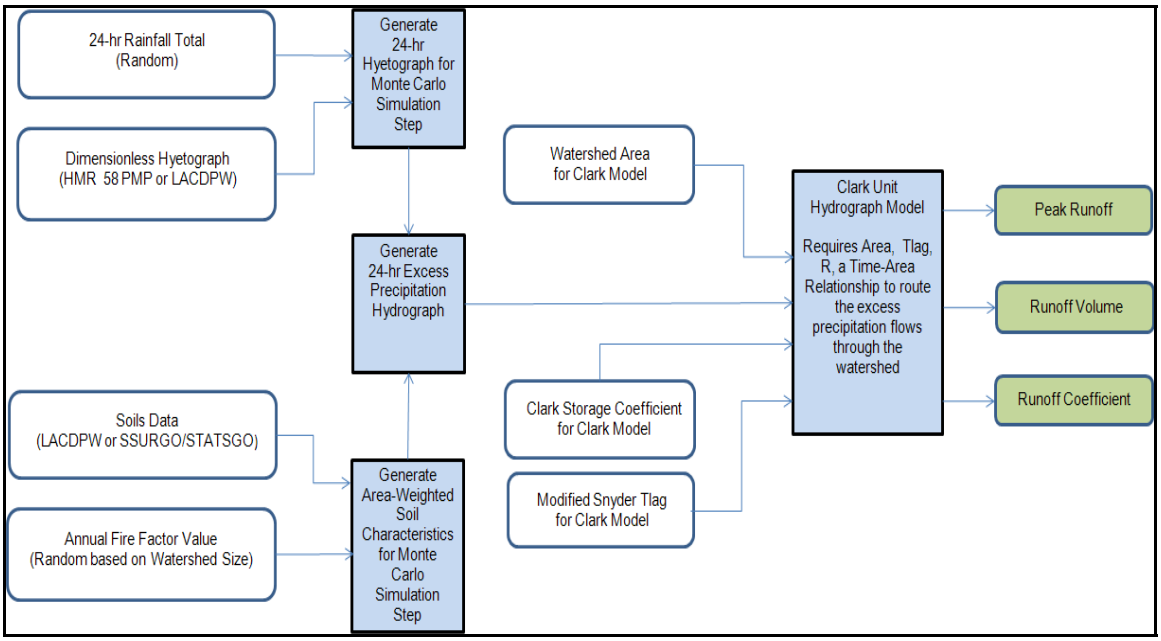

Figure 6.1 Monte Carlo Analysis Simulation Flow Chart for Each Realization

As shown in the flow chart in Figure 6.1, a total 24-hour rainfall total is combined with either the PMP or LACDPW unit hyetograph to develop a temporal distribution for a specific 24-hr maximum rainfall total. The scaled hyetograph becomes an input variable for the next step in the Monte Carlo Model. The 24-hour rainfall total is based on an area weighted probability distribution developed from gages capturing rainfall data near or in the watershed.

The soil data for each Monte Carlo watershed is developed as a lumped parameter. The area weighted characteristics of the soils, either runoff coefficient or constant loss rate, are determined using GIS data and then added together to get the lumped soil parameters. SSURGO/STATSGO constant loss values are analyzed with the same rainfall data as the LACDPW soils to

determine appropriateness of the approach for watershed modeling. The soil data from the LACDPW GIS data set is combined with the Fire Factor value for the watershed to determine the impacts on infiltration with a combination of fire effects. The FF probability distribution is based on watershed size as discussed in Section 5. No fire effects have been determined for use with the constant loss method. The use of FFs with the constant loss method requires further research.

Once the soil characteristics and scaled rainfall hyetograph are determined, the hyetograph is applied to the soil characteristics using the runoff coefficient method (LACDPW), or the constant loss method (SSURGO/STATSGO). The resultant output is an rainfall hyetograph, which becomes input to the deterministic Clark Unit Hydrograph model.

Inputs for the Clark Unit Hydrograph model are the excess precipitation hydrograph, the watershed area, the lag time (Eq. 4.13) and the Clark Storage Coefficient (Eq. 4.17). The time-area relationship was programmed into the Clark UH Model, utilizing Eq. 4.12. All of the parameters remain constant for each realization of the Monte Carlo simulations, except for the excess precipitation hydrograph.

The Clark UH Model outputs are the peak flow rate, runoff volume, and total runoff coefficient for the storm. These values are collected for each iteration of

the Monte Carlo Simulation, resulting in an output data set of a desired number of realizations. In the case of this study, 60,000 realizations were run for each combination of soil and hyetograph type.

6.2 Rainfall – PMP and LACDPW Hyetographs

The first probabilistic data set to be generated for the Monte Carlo Model is the rainfall data. Due to the size of the watersheds being analyzed, there are normally several rain gages within the watershed. The first step in analyzing the rainfall data is to determine the area-weighted parameters for the rain gages within the watershed. This is done using the Theissen Polygon Method. Figure 6.2 provides the Theissen polygon breakup for Los Angeles County.

The watershed area is subdivided based on which Thiessen polygons cover the watershed. The average and standard deviation for each set of gage data within the watershed is multiplied by the area weighting. The area weighted values are then added together to develop a composite gage average and standard deviation. This data is then entered into Matlab using the function GEVRND, which generates a set of random values based on the General Extreme Value frequency distribution. The function was restricted so that it produced a random sample that follows the Gumbel Extreme Value (GEV1) distribution. The Matlab

gevrnd function provided a sample of 60,000 24-hr rainfall volumes that were used as a random input for the Monte Carlo model watershed.

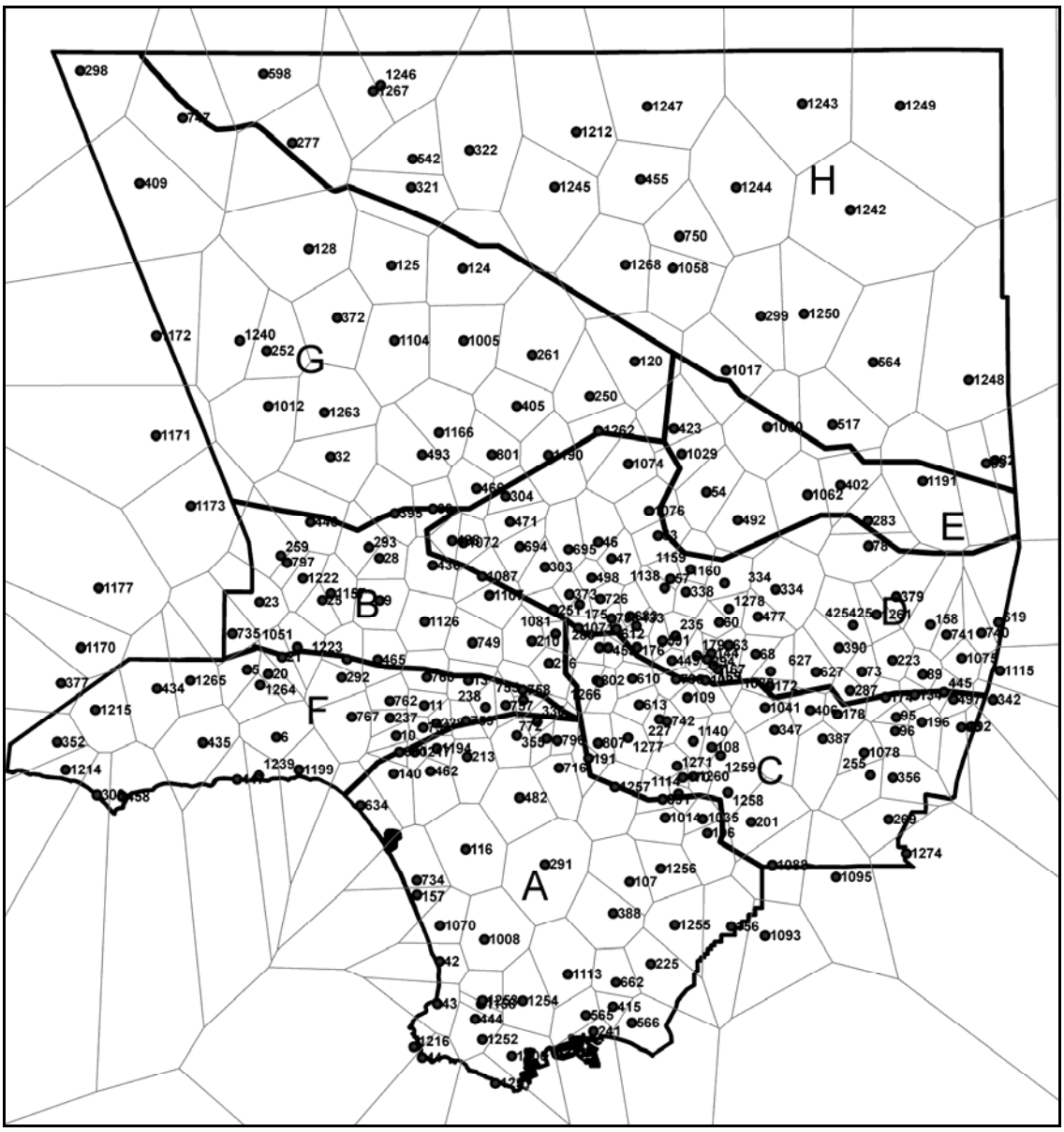

Figure 6.2 Thiessen Polygon Analysis of Rain Gages Within Los Angeles County

The 24-hr rainfall total is then divided into a temporal distribution utilizing either the Los Angeles County Unit Hyetograph, or the PMP Unit Hyetograph based on

HMR 58 and 59 procedures that are tied to watershed location and size. The rainfall temporal distribution is applied to the entire watershed since it is the average rainfall distribution based on the gages near the watershed. The time step used for the hyetographs in this study was 10 minutes.

6.3 Soils – LACDPW and SSURGO/STATSGO Data Sets

The next set of watershed inputs is related to the watershed soil characteristics. As discussed in Chapter 4, two soil/infiltration analysis methods have been used in Los Angeles County. The first is the LACDPW Soil Runoff Coefficient Curve method, which includes the use of fire factors. The second is the Constant Loss Method utilizing the SSURGO/STATSGO data sets provided by the NRCS and requiring calibration. The soil loss data sets provided in Table 4.4 will be used for the Monte Carlo Model.

The watershed soil data was determined using the GIS boundaries for soil types delineated by the watershed boundary. Each LACDPW soil curve was then area-weighted to develop a composite soil curve for each watershed. Some watersheds had only two soil types, while others had up to ten.

Los Angeles County Soil Method

Once the composite soil curve was developed, each time step of the rainfall hyetograph was applied to the LACDPW soil curve to develop an excess precipitation hydrograph. The intensity used for each time step was equal to the rainfall during the time step divided by the time step in units of hours, the resulting value was inches per hour. This intensity was then used to look up a value on the runoff coefficient curve and develop the appropriate runoff for the time step. Time steps were varied to determine what level provided the most accuracy, while providing reasonable computational time. A sensitivity analysis revealed that a time step of 10 minutes provided runoff values very similar to a 1 or 5 minute time step, but greatly decreased the processing time. The 10 minute time step is used throughout the testing to provide consistent comparison between all watersheds and methodologies.

Constant Loss Method

The SSURGO/STATSGO data was also delineated using GIS layers. The constant loss value for each watershed was determined through area weighting. Once an area weighted constant loss was determined, the rainfall hyetograph was reduced at each time step by the constant loss rate, as described in Chapter 4. This process resulted in an excess precipitation hydrograph for the watershed.

The runoff coefficients resulting from the model will be compared to the values provided in Figure 4.5 in Chapter 7, which discusses the results of the Monte Carlo simulation analysis.

6.4 Fire Factor Generation for use with LACDPW Soil Data

Since no relationship has been developed for use of fire factors with the constant loss method, the fire factor (FF) analysis is only conducted with the LACDPW soils method. The use of a fire factor requires determining the fire factor and then applying it to the runoff coefficient calculation as shown in Chapter 4. For all model runs that utilized the FF, the FF was calculated based on the watershed size, as a random variable.

The first step in generating the watershed specific FF required utilizing the FF probability density functions that were developed for specific grid sizes. The FF pdf values for a specific watershed size were then linearly interpolated based on the two grid sizes that bound the actual size of the watershed. Table 6.1 shows an example of the pdf for specific FFs for the grid sizes bounding the data for the watershed above F2B-R, Brown's Creek, which has an area of 13.5 square miles. A map showing all of the watersheds modeled is found below in Figure 6.3. The numbers for each watershed corresponding to the map are shown,

along with watershed data in Table 6.3. Brown's Creek is labeled with a 6 on the map.

Table 6.1 FF Probability Density Function Determination

Grid Level/Watershed	3	F2B-R Brown's Creek	4
Area (sq mi)	4.0	13.5	16.0
FF	Probability Density Functions		
1.000	0.001	0.001	0.001
0.950	0.001	0.001	0.001
0.900	0.001	0.001	0.001
0.850	0.001	0.001	0.001
0.800	0.001	0.001	0.001
0.750	0.002	0.002	0.001
0.700	0.001	0.001	0.001
0.650	0.002	0.002	0.001
0.600	0.001	0.001	0.001
0.550	0.002	0.002	0.001
0.500	0.003	0.003	0.002
0.450	0.003	0.003	0.003
0.400	0.003	0.003	0.003
0.350	0.005	0.005	0.003
0.300	0.005	0.005	0.005
0.250	0.006	0.006	0.006
0.200	0.008	0.008	0.009
0.150	0.012	0.012	0.014
0.100	0.022	0.022	0.026
0.050	0.081	0.081	0.147
0.001	0.009	0.009	0.022
0.000	0.830	0.830	0.752

Table 6.1 shows the FF in Column 1. The probability for the occurrence of a specific FF in a watershed with a 4.0 square mile watershed is shown in Column 2. Column 4 shows the probability for the occurrence of a specific FF in a watershed with a 16.0 square miles. The values in Column 3 are interpolated from Columns 2 and 4 to show the expected probability for recurrence of a

specific FF in Brown's Creek, a watershed of 13.5 square miles. This probability density function (pdf) is specific for Brown's Creek. Inspection of the table shows that some values occur more frequently than others. This is related to the percentage of watershed burned, and the percentage values used to measure recovery as presented in Chapter 5.

The FF pdf for each specific watershed was similarly developed and then used to develop a set of random FF data based on the pdf. The Matlab function RANDSAMP allows a user to specify data values and a weighting distribution to use in developing a data set. The data values are then randomly sampled with replacement based on the given parameters. A set of 60,000 random fire factors, ranging from 0 to 1, were developed for each watershed. Since the FF had already been weighted based on the watershed size, each watershed had a FF data set unique to its specific characteristics.

The output from the RANDSAMP -function was evaluated against an actual data set by simulating a watershed with a 1 square mile area. Multiple 60,000 data point sets were generated based on the FF pdf for the 1 square mile grid. The mean, standard deviation, and skew for the randomly generated values were compared to the original data set. The results showed that the randsamp function produced sample sets that statistically match the parent data set.

The Monte Carlo model then utilized one of the 60,000 randomly generated FF as an input to use with the LACDPW runoff coefficient method to modify the runoff coefficient based on the effects of a fire during each model run.

6.5 Clark UH Model Analysis

The Monte Carlo model required a deterministic model to simulate the watershed response functions. The Clark Unit Hydrograph (CUH) model was selected as the watershed model due to its simplicity and widespread use. More details on the method are provided in prior sections.

The specific variables needed for watershed analysis include the lag time, Clark Storage Coefficient, and a time area relationship. The time area relationship utilized a relationship developed by the US Army Corps of Engineers as discussed above. The other parameters were determined using GIS data sets.

For runoff frequency analysis at gages within Los Angeles County, several combinations were selected for evaluation. These combinations were selected to evaluate possible differences in results based on soil loss methods and different rainfall hyetograph methodologies. The combinations selected are referred to as cases, and are listed below in Table 6.2.

Table 6.2 Monte Carlo Analysis Cases

Case	Soil Loss Method	Rainfall Hyetograph	Use of Fire Factor
1	Constant Loss	HMR PMP	No
2	Constant Loss	Los Angeles	No
3	Los Angeles	HMR PMP	No
4	Los Angeles	HMR PMP	Yes
5	Los Angeles	Los Angeles	No
6	Los Angeles	Los Angeles	Yes

Utilizing the six cases above, the Monte Carlo Analysis method was used to evaluate twelve watersheds upstream of reservoirs within Los Angeles County and fifteen watersheds upstream of historic runoff gages with good records. The watershed characteristics used to model these watersheds are provided in Table 6.3. The watersheds range in size from 1.90 to 202.70 square miles.

The PMPs and PMP frequencies for each watershed were estimated using an area weighted average from gages near the watershed. The gage weighting utilized the Thiessen Polygons shown in Figure 6.2 above for evaluating gage influence on the watersheds shown in Figure 6.3 below. The information for each watershed area weighted PMP is provided in Table 6.4. The table includes a watershed number for reference to Figure 6.3, the watershed name based on the runoff station, the area weighted PMP, the area weighted PMP frequency, the area weighted mean and standard deviation used in Matlab as discussed above, the number of gages used for the area weighting analysis, and a list of the gage numbers for comparison to Appendices A and B.

As can be seen in Table 6.4, the watershed PMP frequencies range in value from 10^5 to 10^9, with most watershed PMP frequencies falling between 10^6 and 10^8. The watersheds had a varying number of gages utilized to get the area-weighted PMP values and frequencies. The number of gages ranged from 1 to 24, with most watersheds having 4 to 10 gages included in the analysis. As discussed in previous sections, the HMR 58 and 59 methodology for calculating PMPs differed significantly in many areas from the Hershfield methodology for PMP calculation. The value of the rainfall recurrence interval utilized for each PMP value was the average of the Hershfield and HMR 58 rainfall values. This was done giving equal weighting to each method, since both are used in practice and it is not possible to determine whether either provides a better estimate than the other. Both methods have large ranges for recurrence interval.

Once the data was developed for each of the model runs for every watershed, the Monte Carlo models were run to generate the output. Chapter 7 discusses the results of the model runs and how the Monte Carlo model output compares to runoff and runoff coefficient values discussed in previous sections.

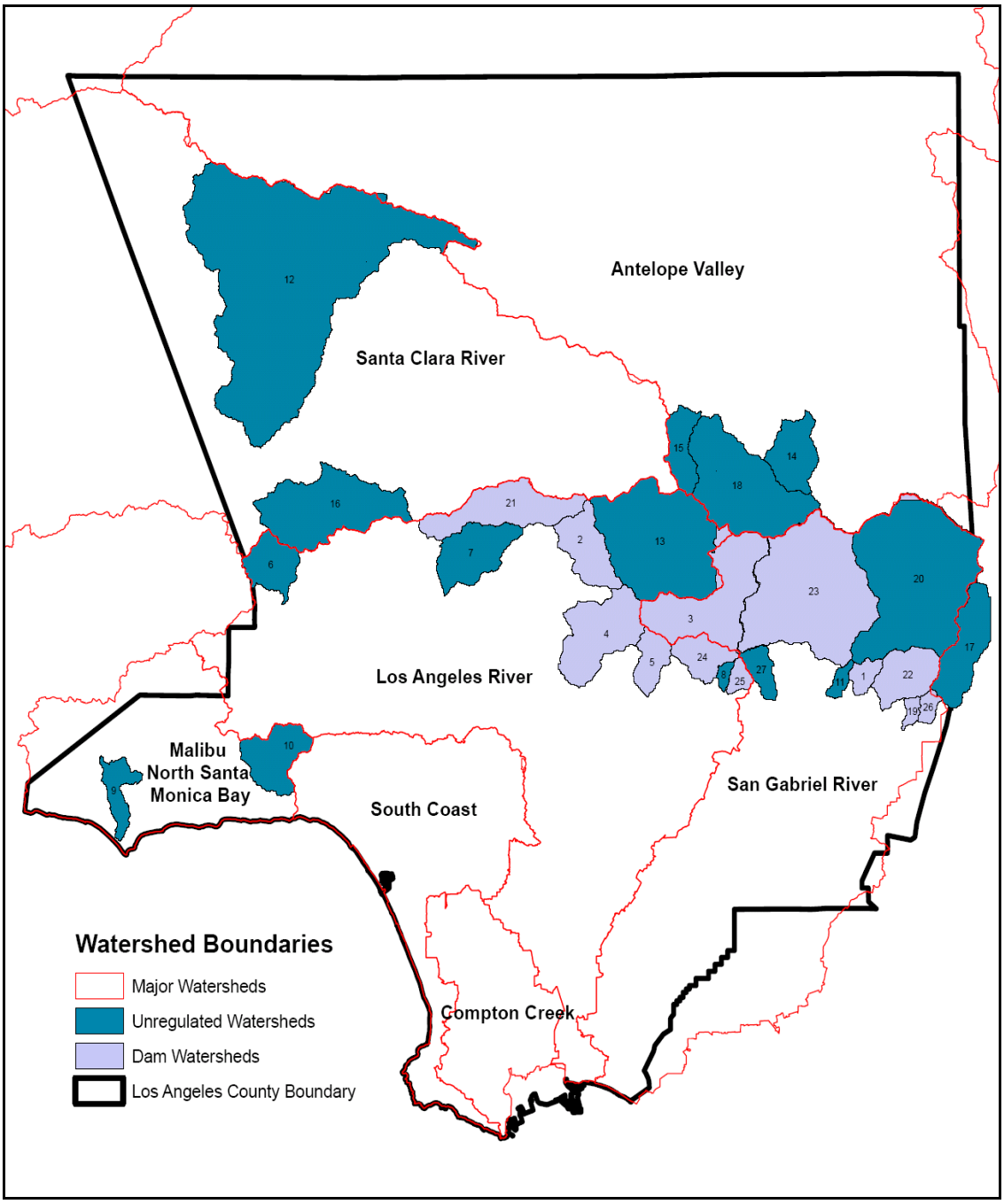

Figure 6.3 Monte Carlo Watershed Locations Within Los Angeles County

Table 6.3 Watershed Characteristics for Monte Carlo Models

Map #	Watershed Name	Watershed Size	Length of Channel	Length to Centroid	Snyder Exponent	Slope	Snyder Coef.	Snyder Lag Time	Clark UH Storage Coef.	Percent Imperv.	Const. Loss	Initial Loss
		Area	L	L_c	m	S	C_t	T_{lag}	R	Imp.	C_{loss}	I_{loss}
		(mi^2)	(mi)	(mi)		(ft/mi)		(hrs)	(hrs)	(%)	(in/hr)	(in)
1	Big Dalton Dam	4.50	3.83	1.77	0.38	140.82	1.20	0.97	1.46	1.00	0.14	0.00
2	Big Tujunga Dam	82.20	17.17	7.34	0.38	68.19	1.20	3.38	5.07	1.52	0.08	0.00
3	Cogswell Dam	39.20	11.29	4.57	0.038	149.00	1.20	1.38	2.08	1.72	0.10	0.00
4	Devils Gate Dam	28.90	14.35	7.50	0.38	106.37	1.20	2.93	4.39	9.21	0.09	0.00
5	Eaton Dam	9.10	7.62	4.43	0.38	209.98	1.20	1.65	2.48	5.39	0.09	0.00
6	F2B - Browns Creek	13.50	7.52	4.06	0.38	330.90	1.20	1.46	2.19	3.03	0.31	0.00
7	F19 - Little Tujunga Wash	21.00	9.61	4.39	0.38	428.25	1.20	1.57	2.36	2.49	0.28	0.00
8	F22 - Monrovia Creek	1.90	2.92	1.36	0.38	1409.19	1.20	0.51	0.77	1.00	0.64	0.00
9	F53 Dume Creek	8.00	7.91	3.74	0.38	300.96	1.20	1.47	2.20	3.01	0.20	0.00
10	F54 - Topanga Canyon	18.00	7.56	2.83	0.38	237.60	1.20	1.36	2.04	3.31	0.29	0.00
11	F65 - Little Dalton Creek	2.70	3.58	1.49	0.38	623.70	1.20	0.67	1.00	1.08	0.37	0.00
12	F108 - Castaic Creek	40.90	10.72	3.87	0.38	267.86	1.20	1.71	2.56	5.50	0.33	0.00
13	F111 - Big Tujunga Creek	64.90	12.84	6.19	0.38	321.69	1.20	2.11	3.17	1.00	0.17	0.00
14	F122 - Pallett Creek	15.80	8.12	4.40	0.38	516.00	1.20	1.43	2.14	1.67	0.28	0.00
15	F125 - Santiago Creek	11.34	8.20	3.97	0.38	436.42	1.20	1.42	2.13	1.00	0.10	0.00
16	F135 - SCR South Fork	40.90	10.72	3.87	0.38	267.86	1.20	1.71	2.56	12.42	0.38	0.00
17	F151 - San Antonio Creek	26.50	11.29	5.37	0.38	701.39	1.20	1.64	2.47	1.77	0.50	0.00
18	L1-R Little Rock Creek	49.20	16.04	7.08	0.38	293.60	1.20	2.46	3.69	1.00	0.09	0.00
19	Live Oak Dam	2.30	3.08	1.50	0.38	205.31	1.20	0.78	1.17	2.63	0.04	0.00
20	P4B - San Gabriel East Fork	88.20	20.24	9.90	0.38	384.72	1.20	2.90	4.35	1.03	0.34	0.00
21	Pacoima Dam	28.00	18.78	9.64	0.38	75.04	1.20	3.81	5.71	1.31	0.14	0.00
22	San Dimas Dam	16.20	8.42	4.47	0.38	150.23	1.20	1.84	2.76	1.37	0.12	0.00
23	San Gabriel Dam	202.70	25.53	9.50	0.38	95.06	1.20	4.07	6.10	1.58	0.10	0.00
24	Santa Anita Dam	10.70	5.60	2.60	0.38	226.25	1.20	1.19	1.78	1.93	0.06	0.00
25	Sawpit Dam	3.40	3.91	1.86	0.38	304.26	1.20	0.86	1.29	1.00	0.10	0.00
26	Thompson Creek Dam	3.00	3.15	1.50	0.38	287.92	1.20	0.74	1.11	1.00	0.05	0.00
27	U7- Fish Creek	6.40	5.57	2.78	0.38	805.00	1.20	0.95	1.43	1.00	0.26	0.00

Table 6.4 Area Weighted PMP and PMP Frequency Data

Map #	Watershed Name	Area Weighted PMP (in)	Area Weighted PMP Freq. (GEV1) (yrs)	Number of Rainfall Gages (#)	Area Weighted 24-hr Rainfall Average (μ)	Area Weighted 24-hr Rainfall St. Dev (σ)	Mean Annual Precip. (in)	Gages Influencing the Watershed
1	Big Dalton Dam	31.34	7.82E+07	4	4.004	1.009	30.00	223, 158, 1261, 379
2	Big Tujunga Dam	36.08	9.30E+06	15	4.233	1.318	28.00	1160, 57, 1159, 47, 695, 46, 53, 492, 1076, 54, 1074, 1190, 1029, 1262, 423
3	Cogswell Dam	40.97	3.06E+06	11	5.705	1.587	40.00	60, 477, 1278, 338, 334, 1138, 1160, 57, 1159, 492, 1062
4	Devils Gate Dam	39.57	1.70E+07	14	4.599	1.430	28.00	453, 280, 612, 1071, 433, 783, 683, 175, 726, 1138, 57, 498, 47, 53
5	Eaton Dam	32.60	1.42E+07	5	4.475	1.271	30.50	449, 591, 235, 338, 1138
6	F2B - Browns Creek	25.26	2.16E+08	4	2.937	0.765	18.50	797, 259, 446, 1173
7	F19 - Little Tujunga Wash	28.14	1.36E+07	7	3.958	1.172	21.50	1087, 1072, 488, 471, 33, 304, 466
8	F22 - Monrovia Creek	34.26	2.55E+05	3	5.183	1.625	28.50	68, 63, 477
9	F53 Dume Creek	29.07	2.01E+09	4	2.634	0.746	16.80	458, 306, 1214, 1215
10	F54 - Topanga Canyon	29.42	8.84E+06	7	4.035	1.190	22.00	1199, 6, 767, 1264, 292, 20, 21
11	F65 - Little Dalton Creek	30.82	4.46E+08	4	3.482	0.882	28.50	73, 223, 425, 1261
12	F108 - Castaic Creek	20.03	4.46E+07	15	2.799	0.739	20.00	1263, 1012, 252, 1240, 372, 124, 125, 128, 321, 409, 542, 322, 277, 747, 1267
13	F111 - Big Tujunga Creek	35.17	2.87E+07	10	4.164	1.289	29.00	1160, 57, 1159, 53, 492, 1076, 54, 1074, 1029, 423
14	F122 - Pallett Creek	28.35	3.44E+07	4	3.095	1.003	19.00	402, 1060, 517, 564
15	F125 - Santiago Creek	20.12	1.07E+08	5	2.571	0.703	17.00	54, 1029, 423, 1060, 1017
16	F135 - SCR South Fork	25.18	7.78E+07	7	3.142	0.839	19.00	446, 395, 33, 32, 493, 1263, 1012
17	F151 - San Antonio Creek	38.68	4.09E+07	4	4.879	1.323	27.00	1115, 1075, 740, 619
18	L1-R Little Rock Creek	32.76	1.21E+06	9	4.284	1.243	27.00	492, 1062, 54, 402, 1029, 423, 1060, 517, 1017
19	Live Oak Dam	28.96	5.54E+05	3	4.757	1.634	22.50	497, 445, 1075
20	P4B - San Gabriel East Fork	33.97	9.17E+07	11	4.205	1.092	28.00	741, 740, 158, 619, 1261, 379, 78, 283, 1191, 83, 82
21	Pacoima Dam	31.25	1.66E+07	7	4.260	1.284	21.00	33, 304, 466, 1074, 1190, 801, 1262
22	San Dimas Dam	35.02	2.27E+06	6	4.382	1.394	28.50	89, 223, 1075, 741, 740, 158
23	San Gabriel Dam	37.47	1.60E+07	24	4.972	1.331	30.00	741, 740, 425, 158, 60, 619, 477, 1261, 1278, 379, 338, 334, 1138, 1160, 57, 1159, 78, 283, 492, 1062, 402, 1191, 83, 82
24	Santa Anita Dam	36.33	6.31E+07	2	5.354	1.869	34.00	172, 176
25	Sawpit Dam	32.90	3.16E+07	1	4.944	1.507	27.50	172
26	Thompson Creek Dam	31.90	3.16E+05	4	5.521	1.945	22.50	342, 497, 1115, 1075
27	U7- Fish Creek	33.89	6.64E+05	6	5.297	1.578	27.50	627, 1080, 68, 390, 477, 334

6.6 Chapter Summary and Conclusions

Chapter 6 presents the methodology to be employed in Monte Carlo simulation of 27 watersheds within Los Angeles County. The use of random rainfall and fire factors generated from area-weighted rain gage analysis and the fire factor area-frequency curves is detailed, along with a flow chart showing the modeling steps used to generate multiple realizations for peak runoff, runoff volume, and runoff coefficients.

The watersheds to be modeled are introduced, and tables provide information on the key input parameters that are needed to run each model. Six modeling cases are laid out for each watershed to allow comparison of the impacts in changing the rainfall hyetograph methodology, the soil infiltration loss, and use of a fire factor. Each watershed model was run for the 6 cases, utilizing 60,000 realizations of unique rainfall and fire factor combinations. The results are discussed in Chapter 7.

Chapter 7 – Analysis of Monte Carlo Analysis and Measured Runoff Frequencies

Chapter 7 reviews the results from the six cases used in the Monte Carlo runoff modeling described in Chapter 6. Section 7.1 compares the runoff coefficient values to the corresponding rainfall frequency. These are then compared to various design criteria methodologies to determine the appropriateness of assigning runoff coefficients based on rainfall frequency. Section 7.2 compares peak runoff rate frequency analysis based on the Monte Carlo simulation to the PMF frequencies at 12 dams within Los Angeles County. The relationships are investigated utilizing multiple probability distributions for each dam watershed. The runoff frequencies are then compared to the area-weighted rain gage PMP frequency to see if there is any correlation. Table 6.2 is reprinted here for allowing quick reference to the differences in the different cases.

Case	Soil Loss Method	Rainfall Hyetograph	Use of Fire Factor
1	Constant Loss	HMR PMP	No
2	Constant Loss	Los Angeles	No
3	Los Angeles	HMR PMP	No
4	Los Angeles	HMR PMP	Yes
5	Los Angeles	Los Angeles	No
6	Los Angeles	Los Angeles	Yes

7.1 Runoff Coefficient to Rainfall Frequency Analysis

The first analysis completed on the Monte Carlo results was a comparison of runoff coefficient frequencies to rainfall frequencies to evaluate how runoff coefficient behaves compared to soil modeling method and rainfall recurrence interval. Each case was evaluated by itself. Figures 7.1 through 7.6 are summaries of the data sets for Monte Carlo Simulation Cases 1 through 6. Each figure summarizes over 1.6 million watershed conditions. The analysis represents 27 watersheds with 60,000 rainfall/FF conditions for each specific Monte Carlo Case. The figures show the average, maximum, minimum, and the 10th and 90th percentile runoff coefficient values for each case. The charts maintain the same scale so that it is easier to visually note that the range for the different cases varies significantly.

Figures 7.1 and 7.2 represent data that utilizes the NRCS constant loss soil models. Figure 7.1 represents the HMR PMP hyetograph, while Figure 7.2 represents the Los Angeles County hyetograph. The y-axis represents the runoff coefficient, which ranges from 0.0 to 1.0, representing the percentage of runoff generated. The x-axis shows the recurrence interval for the rainfall corresponding to the runoff coefficient. The data trendlines showing the minimum, maximum, average, and the 10th and 90th percentiles of the data for each recurrence interval demonstrate the range of runoff coefficients

encountered for the specific case. Comparison of Figures 7.1 and 7.2 shows that Case 1 had lower runoff coefficients than Case 2 by approximately 13 percent for the average values.

Figures 7.3 to 7.7 represent the Los Angeles County runoff coefficient method to account for infiltration losses. There is approximately a 10 percent difference in runoff coefficient values between Figures 7.3 and 7.4. This represents the effects of the fire factor on the runoff coefficient for cases that utilized the HMR PMP hyetograph. There is also an approximate 10 percent difference in runoff coefficients between Figures 7.5 and 7.6 that is related to the fire factor effect. It is interesting to note, that between Figures 7.3 and 7.5, and Figures 7.4 and 7.6, there is also a 10 percent difference. This difference is related to use of the HMR PMP versus the Los Angeles County hyetographs, consistent with the observations from Figures 7.1 and 7.2. The overall difference between the various cases underscores the importance of choosing the soil losses and rainfall parameters when modeling watersheds.

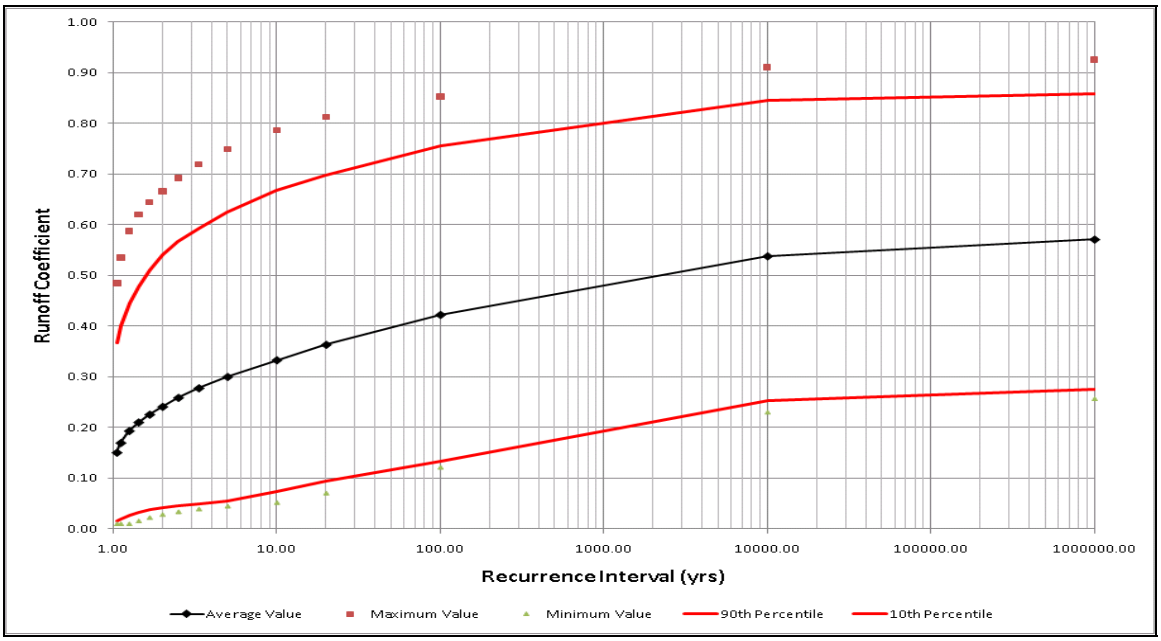

Figure 7.1 Case 1: Runoff Coefficient vs. Rainfall Recurrence Interval Analysis

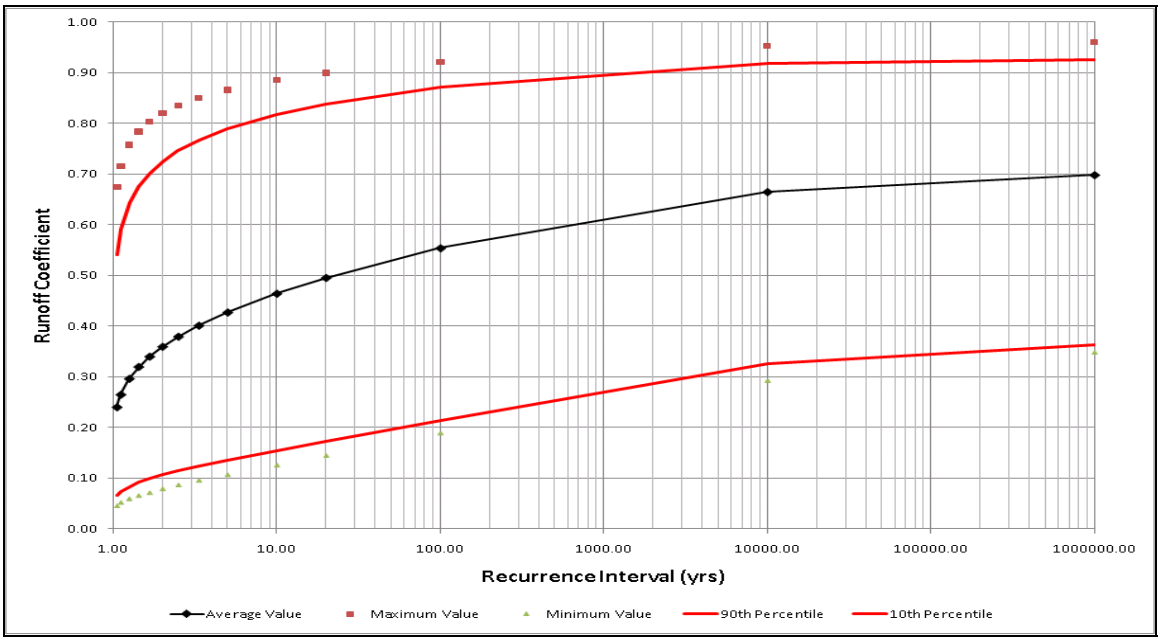

Figure 7.2 Case 2: Runoff Coefficient vs. Rainfall Recurrence Interval Analysis

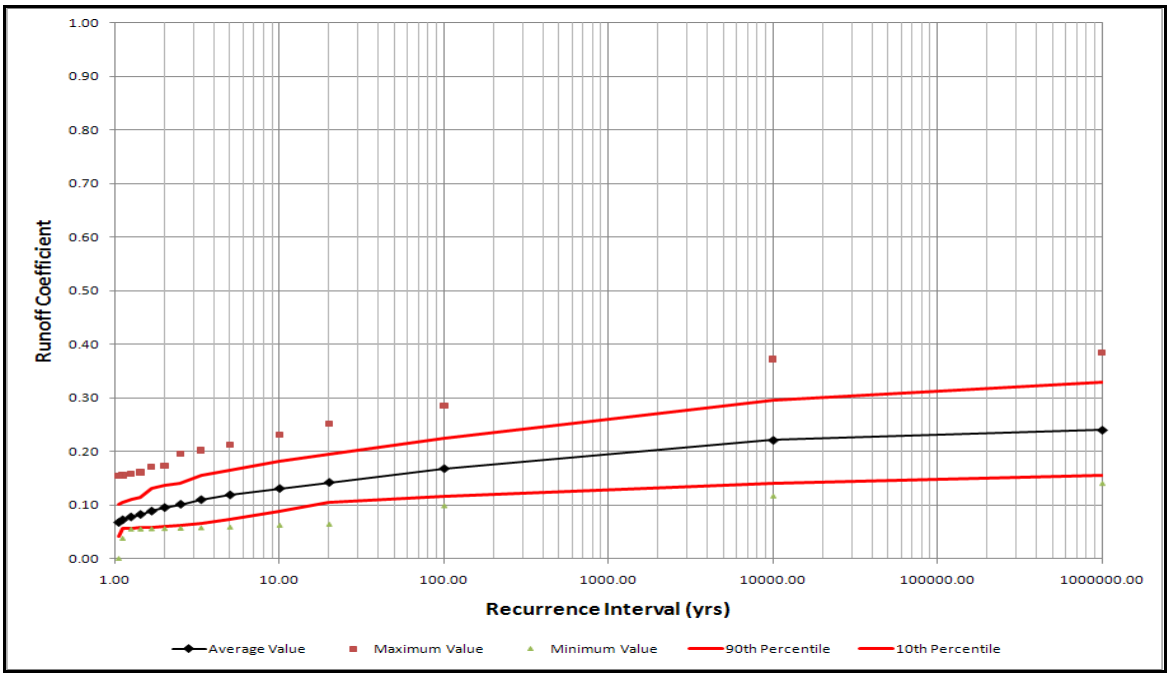

Figure 7.3 Case 3: Runoff Coefficient vs. Rainfall Recurrence Interval Analysis

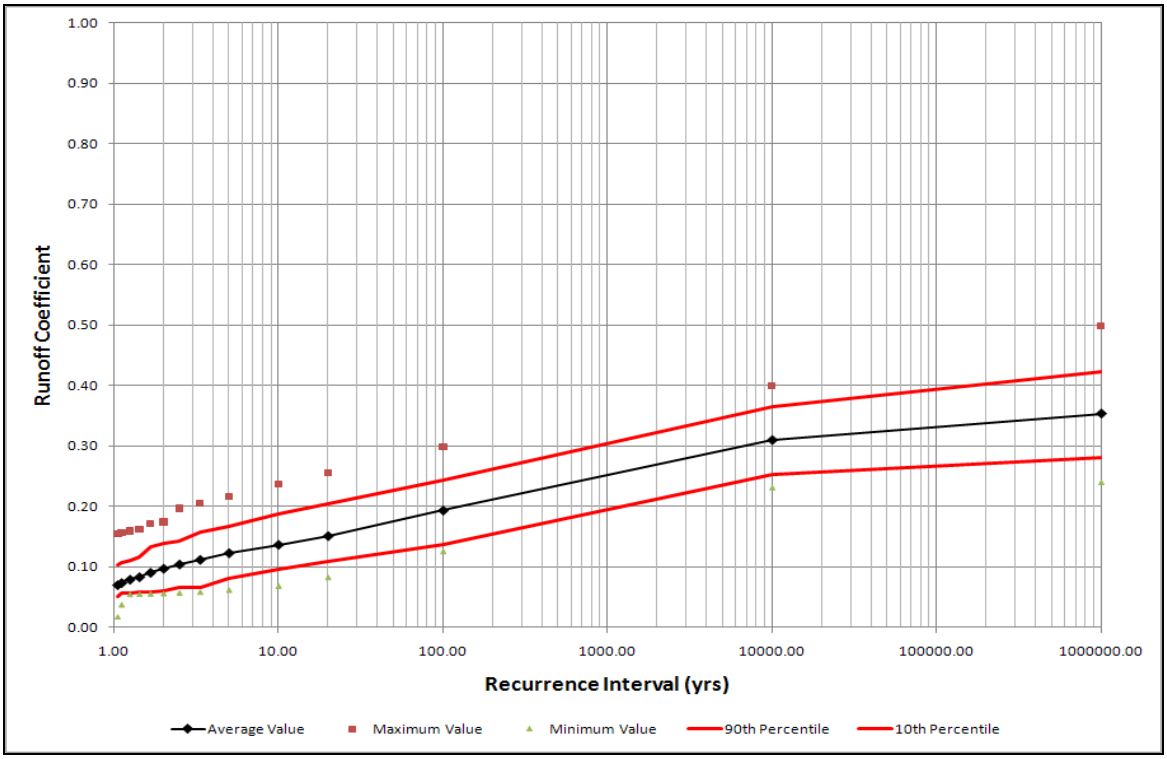

Figure 7.4 Case 4: Runoff Coefficient vs. Rainfall Recurrence Interval Analysis

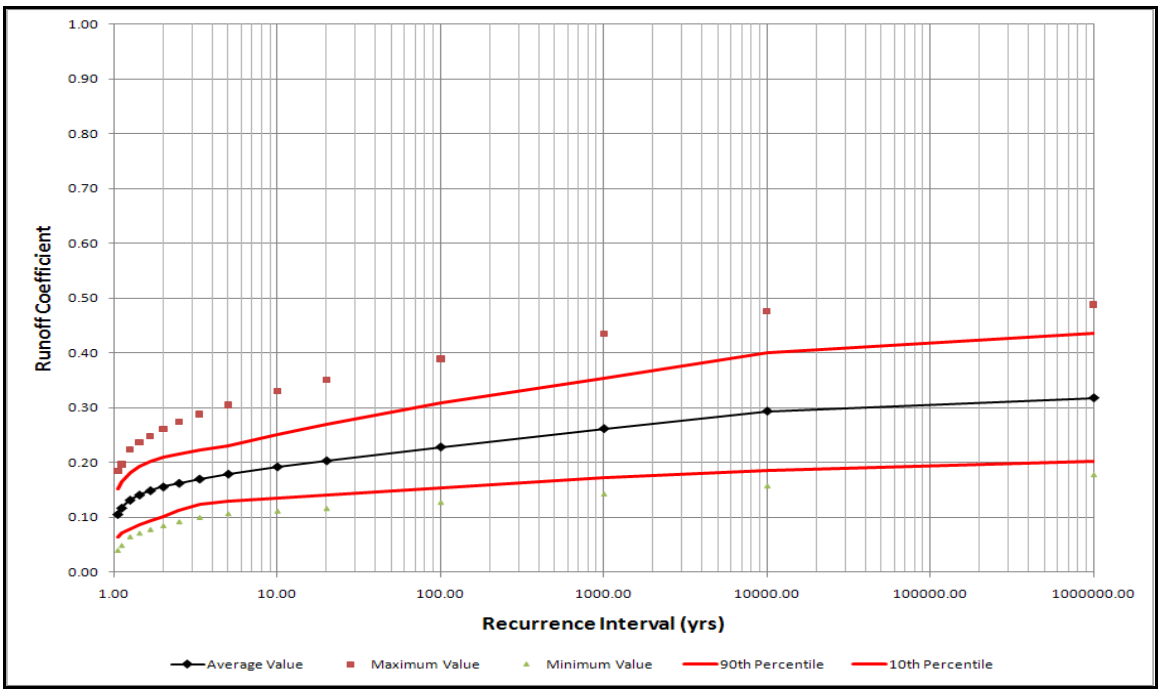

Figure 7.5 Case 5: Runoff Coefficient vs. Rainfall Recurrence Interval Analysis

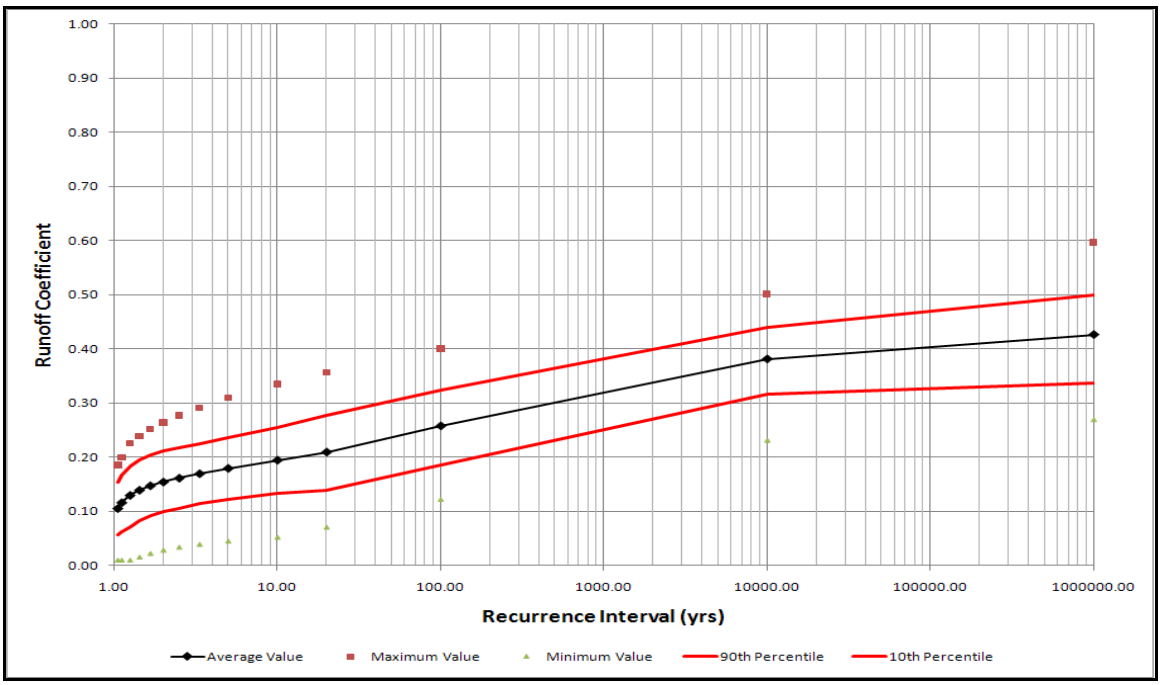

Figure 7.6 Case 6: Runoff Coefficient vs. Rainfall Recurrence Interval Analysis

Next, the average values for the cases was determined and plotted in a graph with a format similar to Figures 7.1 through 7.6. Figure 7.7 shows average and maximum values for the NRCS (Cases 1 and 2) and the Los Angeles Soil Models (Cases 3-6).

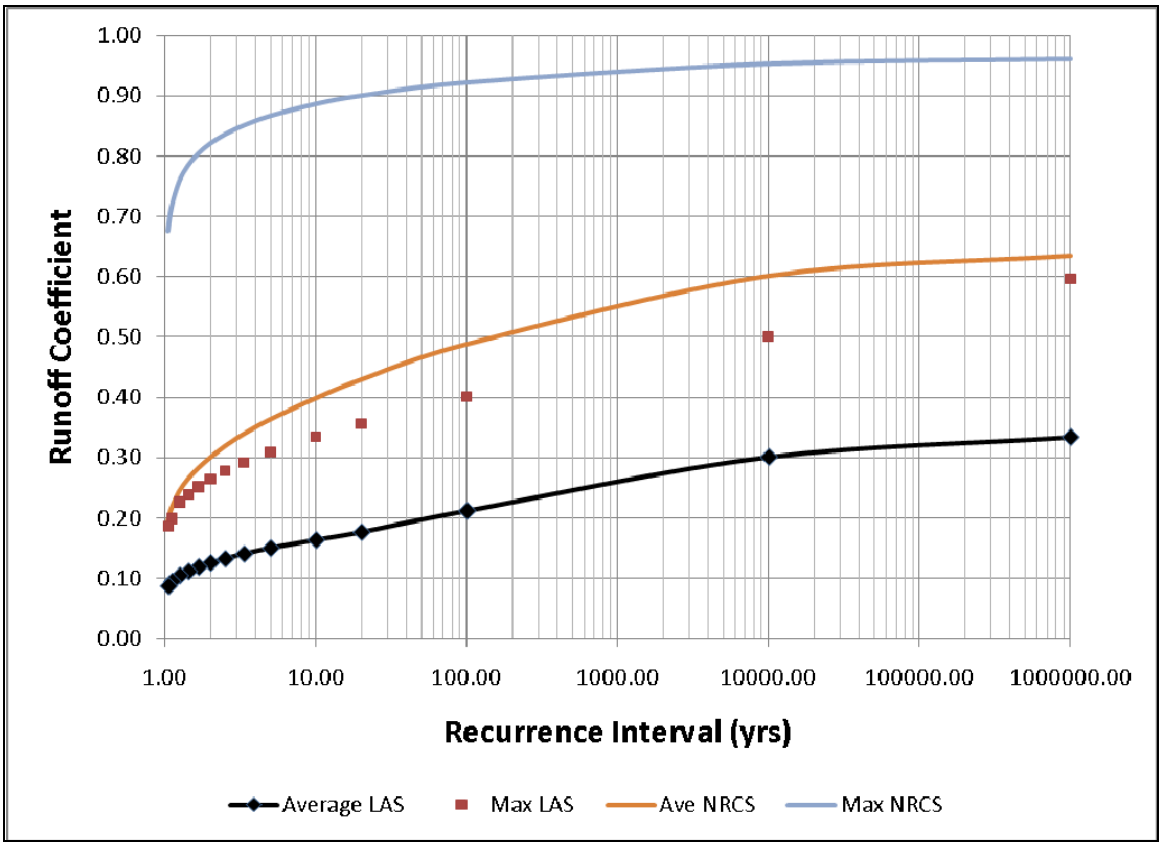

Figure 7.7 Comparison of Los Angeles and NRCS Soil Model Runoff Coefficients

Figure 7.7 shows the large difference between the two soil methods, even though the Los Angeles Soil method utilizes fire factors. This indicates that the method for determining runoff through the soil processes is very important. In an effort to

compare this study to other studies that have been done, and other runoff coefficient ranges that have been suggested, the Monte Carlo results were superimposed on Figure 4.3. Figure 7.8 provides the comparison of the Monte Carlo Analysis with the California DSOD, the California Department of Water Resources (DWR), the ASCE, Maricopa County, and previous Los Angeles County design ranges.

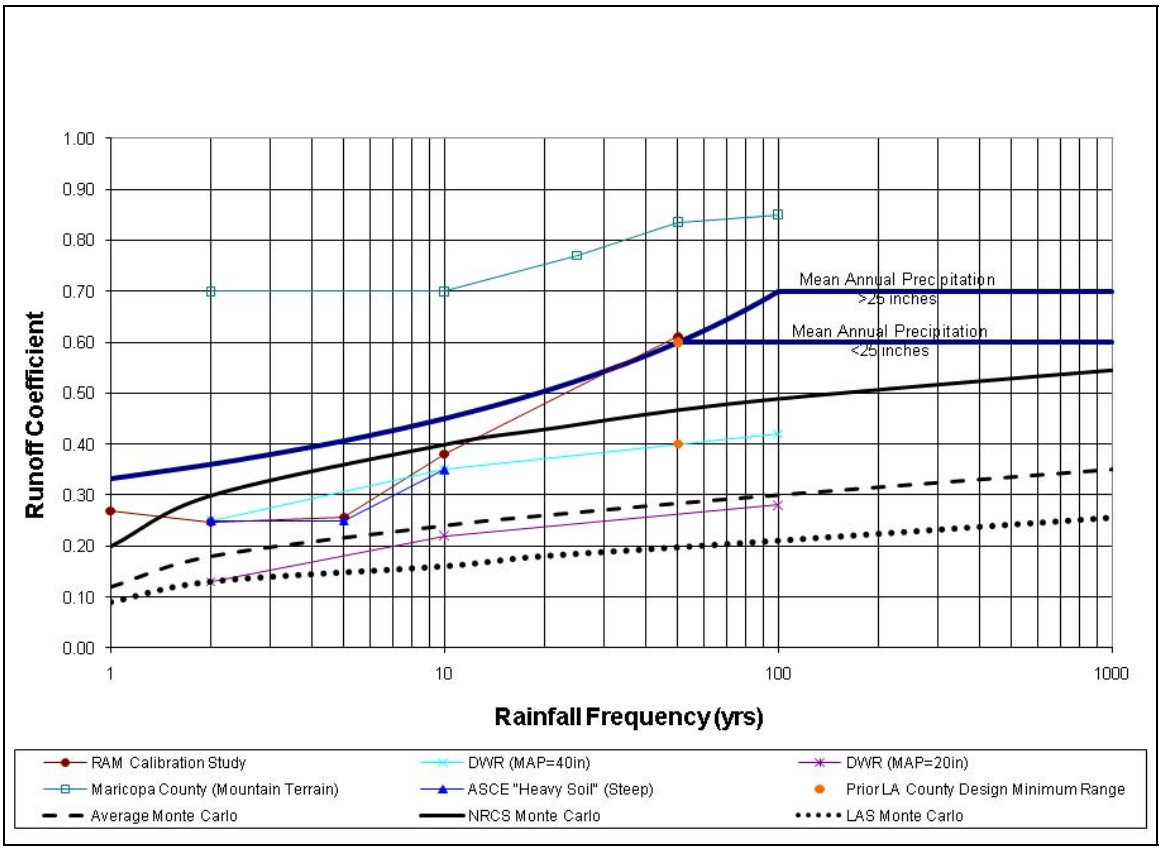

Figure 7.8 Comparison of Monte Carlo Runoff Coefficients to Other Methods

The solid black line in Figure 7.8 shows the average runoff coefficient values for the NRCS soils, while the dotted black line represents the Los Angeles Soil method. The dashed line is the average for all six cases. This chart indicates

that the NRCS soil model produced runoff coefficients more similar to other studies than the Los Angeles Soil method, but still significantly lower.

The next comparison was to evaluate the effect that the mean annual precipitation had on the runoff coefficients ranges as required by the California DSOD. There were 11 watersheds with a MAP less than 25 inches per year. The other 15 watersheds had MAPs greater than 25 inches per year. Since the DSOD utilizes an NRCS constant loss approach, the data from Cases 1 and 2 were used for comparison purposes. The analysis results based on the MAP regions are provided in Figure 7.9.

Figure 7.9 shows the range between the average and maximum values of runoff coefficients using the NRCS constant loss method for the Monte Carlo Models. The average values match DSOD requirements fairly well, but the analysis shows that the DSOD values do not match all watersheds. As shown in Figures 7.8 and 7.9, the DSOD values fall between the Maricopa County standards and the upper results of this study, and the DWR requirements for MAP of 20 to 40 inches and the lower results from this study. This indicates that the DSOD estimates work well on average, but that some watershed flow rates are overly conservative, while other watersheds are under protected. The DSOD requirements for recurrence intervals over 100 years are equal, indicating that they do not require increased runoff rates for events greater than 100 years.

This does not make sense intuitively since infiltration rate has a maximum value. Rainfall greater than the infiltration rate becomes runoff. The larger a storm becomes, the more likely it is to exceed the infiltration rate and generate higher runoff coefficients.

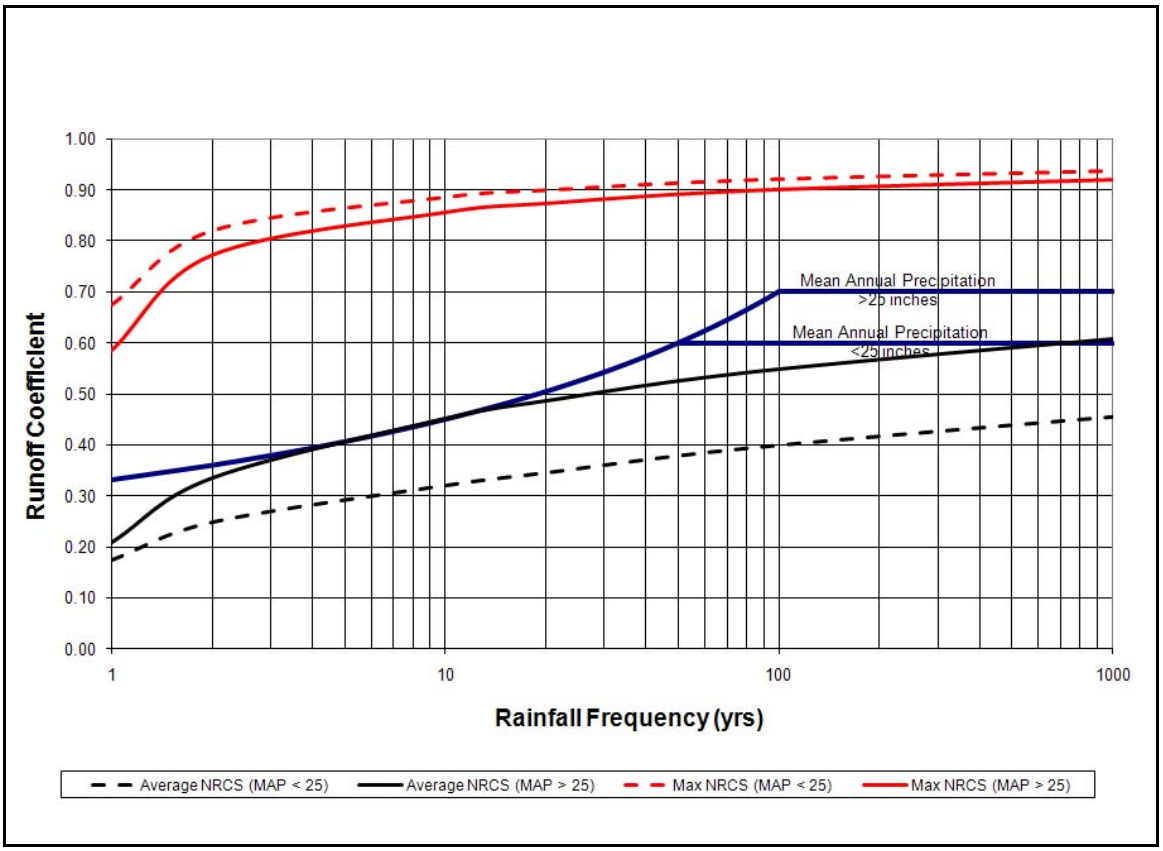

Figure 7.9 Comparison of NRCS Models with MAP Requirements by DSOD

Figure 7.10 shows the full range of runoff coefficients for all of watersheds and all of the cases to illustrate the highs, lows, and average values for the watersheds within Los Angeles County. The results of the Monte Carlo analysis show that the division of watersheds with different MAPs is a reasonable approach, but that

caution should be taken when assigning the specific runoff coefficient for design of engineering structures.

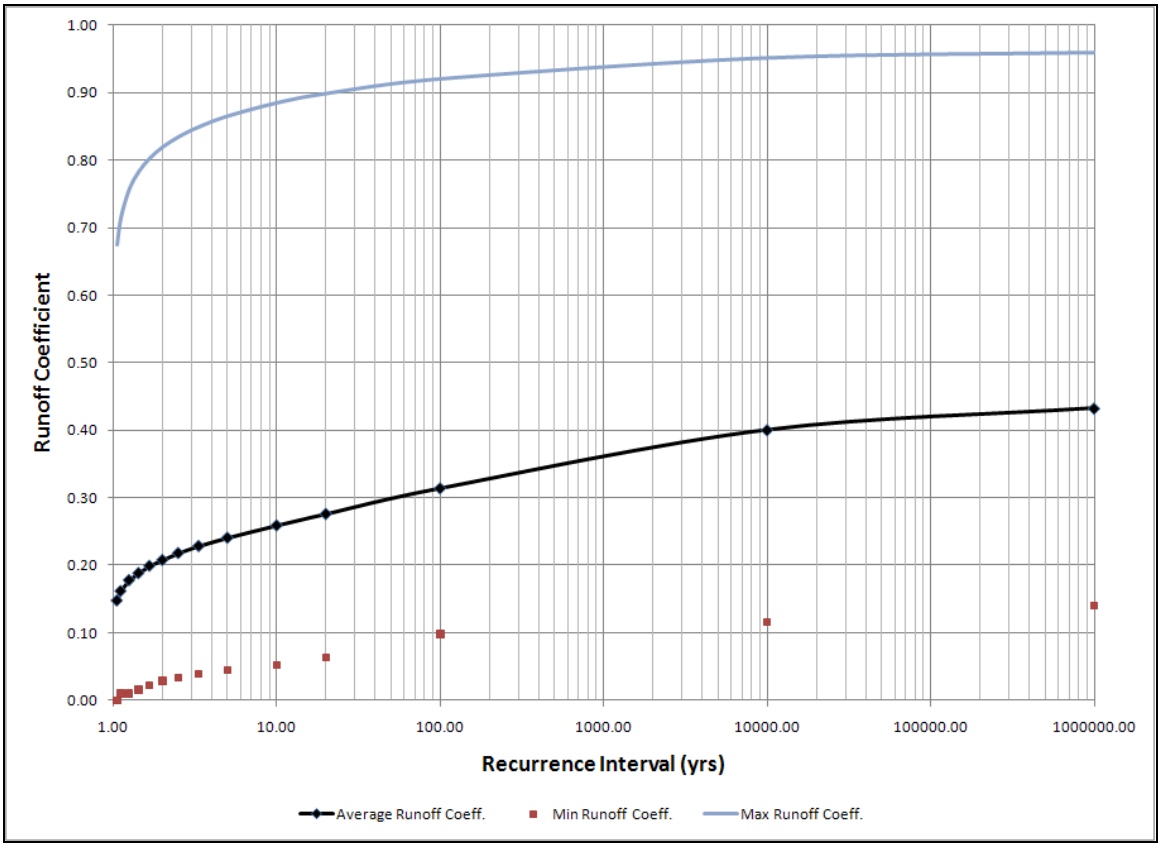

Figure 7.10 Range of Runoff Coefficients for Monte Carlo Analysis Models

7.2 PMF Frequency Analysis of the Dams

The next phase of the Monte Carlo model analysis requires evaluating the PMF of the dam watersheds to compare the Monte Carlo runoff coefficients to the official DSOD PMFs. Table 7.1 shows the PMF runoff data based on the DSOD model studies, the actual maximum flow rates measured at each of the 12 dams,

and the maximum flow rate from each of the six Monte Carlo model runs. It also shows these flow rates as a ratio of the DSOD PMF. As can be seen, the models resulted in a large range of ratios. The maximum model flow rate ratios range from 11.55% for Big Dalton Dam to 177.35% for Live Oak Dam. This information shows that use of plotting positions and percentile analysis for dam frequency analysis coupled with the Monte Carlo modeling will not work well on many of the dams, unless much longer input data sets are used. The event of interest is significantly outside the limits of the data sets.

In this case, evaluation of the PMF runoff frequency requires use of the probability distributions discussed in Chapter 2. The flow rate runoff frequency distributions were evaluated using the Log-Normal, Gumbel, Log-Pearson III, and Gamma probability distributions. Table 7.2 contains a summary of the PMF flow rate, the PMP rainfall, the PMP recurrence interval for the watershed, and the maximum precipitation generated for the Monte Carlo modeling. The table is then divided into the runoff frequency distributions and shows the recurrence interval of the PMF based on frequency analysis of the actual runoff gage and the models.

Table 7.1 Comparison of Actual and Monte Carlo Maximum Runoff Rates to PMF

Variable	Symbol	Big Dalton	Big Tujunga	Cogswell	DGD	Eaton	Live Oak	Pacoima	San Dimas	San Gabriel	Santa Anita	Sawpit	Thompson Creek
PMF (cfs)	cfs	16,800	111,570	59,900	36,000	14,400	2,200	24,000	28,600	245,805	26,100	5,700	6,290
Actual Max Flow	cfs	1,540	32,940	24,710	10,840	2,670	403	8,320	4,920	89,320	5,500	1,600	580
Case 1	cfs	3,516	56,800	33,693	25,776	8,553	3,078	15,302	14,364	109,307	15,731	4,574	5,601
Case 2	cfs	4,381	68,053	44,901	28,277	9,681	3,902	16,352	16,264	140,955	18,655	5,739	7,159
Case 3	cfs	1,940	22,048	15,534	10,970	3,039	1,860	5,643	9,613	47,847	6,100	2,229	3,980
Case 4	cfs	1,964	22,112	16,141	10,970	3,039	1,979	6,097	9,613	48,554	8,542	2,500	3,980
Case 5	cfs	2,753	30,855	21,540	13,421	4,272	2,707	6,725	11,541	73,353	9,078	3,320	5,567
Case 6	cfs	2,753	30,926	22,195	13,421	4,272	2,825	6,967	11,541	74,146	11,519	3,450	5,567
Percentage of PMF													
Actual Max Flow	%	9.17%	29.52%	41.25%	30.11%	18.54%	18.32%	34.67%	17.20%	36.34%	21.07%	28.07%	9.22%
Case 1	%	20.93%	50.91%	56.25%	71.60%	59.40%	139.92%	63.76%	50.22%	44.47%	60.27%	80.25%	89.04%
Case 2	%	26.08%	61.00%	74.96%	78.55%	67.23%	177.35%	68.13%	56.87%	57.34%	71.47%	100.69%	113.81%
Case 3	%	11.55%	19.76%	25.93%	30.47%	21.11%	84.56%	23.51%	33.61%	19.47%	23.37%	39.10%	63.27%
Case 4	%	11.69%	19.82%	26.95%	30.47%	21.11%	89.95%	25.40%	33.61%	19.75%	32.73%	43.87%	63.27%
Case 5	%	16.39%	27.66%	35.96%	37.28%	29.67%	123.03%	28.02%	40.35%	29.84%	34.78%	58.25%	88.50%
Case 6	%	16.39%	27.72%	37.05%	37.28%	29.67%	128.39%	29.03%	40.35%	30.16%	44.13%	60.53%	88.50%
Maximum	%	26.08%	61.00%	74.96%	78.55%	67.23%	177.35%	68.13%	56.87%	57.34%	71.47%	100.69%	113.81%
Minimum	%	9.17%	19.76%	25.93%	30.11%	18.54%	18.32%	23.51%	17.20%	19.47%	21.07%	28.07%	9.22%
Average	%	16.03%	33.77%	42.62%	45.11%	35.25%	108.79%	38.93%	38.89%	33.91%	41.12%	58.68%	73.66%

As can be seen in Table 7.1, the results for Big Dalton, Live Oak, and Thompson Creek Dams are different from the other dams. The average value as a percentage of the PMF shown in the last row of the table indicates that these watersheds are significantly different. These watersheds are much smaller than the other watersheds studied. Big Dalton is always the last to respond during major rain events. Thompson Creek is also slow to respond. These watersheds may be in rain shadows of other mountains.

Table 7.2 Summary of Actual and Monte Carlo Model Dam Runoff Frequencies

Variable	Big Dalton	Big Tujunga	Cogswell	DGD	Eaton	Live Oak	Pacoima	San Dimas	San Gabriel	Santa Anita	Sawpit	Thompson Creek
PMF (cfs)	16,800	111,570	59,900	36,000	14,400	2,200	24,000	28,600	245,805	26,100	5,700	6,290
PMP (in)	31.34	36.08	40.97	39.57	32.60	28.96	31.25	35.02	37.47	36.33	32.90	31.90
PMP Recurrence (yrs)	10^7	10^6	10^6	10^7	10^7	10^5	10^7	10^6	10^7	10^7	10^7	10^5
Maximum Model Precip. (in)	23.43	29.10	33.60	34.26	30.38	34.90	25.30	29.57	26.05	40.36	34.53	46.13
Log-Normal Distribution												
Historic Data	10^3	10^2	10^2	10^2	10^3	10^2	10^2	10^3	10^2	10^3	10^2	10^2
Case 1	>10e10	10^7	10^6	10^6	10^7	10^2	10^4	10^5	10^7	10^6	10^5	10^5
Case 2	>10^10	10^6	10^6	10^6	10^6	10^1	10^4	10^5	10^7	10^5	10^4	10^4
Case 3	>10^10	>10^10	>10^10	>10^10	>10^10	10^6	>10^10	10^7	>10^10	>10^10	10^9	10^5
Case 4	>10^10	>10^10	>10^10	>10^10	>10^10	10^5	>10^10	10^7	>10^10	>10^10	10^8	10^6
Case 5	>10^10	>10^10	>10^10	>10^10	>10^10	10^3	>10^10	10^7	>10^10	10^9	10^6	10^4
Case 6	>10^10	>10^10	10^9	>10^10	>10^10	10^3	>10^10	10^7	>10^10	10^9	10^6	10^4
Log-Pearson III Distribution												
Historic Data	10^3	10^2	10^2	10^4	10^4	10^3	10^2	10^3	10^2	10^3	10^3	10^3
Case 1	10^3	10^2	10^3	10^3	10^3	10^2	10^2	10^2	10^3	10^3	10^2	10^2
Case 2	10^4	10^2	10^3	10^3	10^3	10^1	10^3	10^2	10^2	10^2	10^2	10^2
Case 3	10^4	10^4	10^4	10^4	10^5	10^3	10^6	10^2	10^4	10^5	10^3	10^2
Case 4	10^4	10^4	10^4	10^6	10^5	10^2	10^5	10^3	10^4	10^3	10^3	10^2
Case 5	10^4	10^3	10^4	10^4	10^4	10^2	10^5	10^2	10^3	10^3	10^3	10^2
Case 6	10^4	10^4	10^4	10^4	10^4	10^2	10^5	10^2	10^3	10^3	10^2	10^2
General Extreme Value Type 1 Distribution												
Historic Data	>10^10	>10^10	10^8	10^9	>10^10	>10^10	10^9	>10^10	10^9	>10^10	>10^10	>10^10
Case 1	>10^10	>10^10	10^8	10^7	10^9	10^3	10^8	10^10	>10^10	10^9	10^6	10^6
Case 2	>10^10	10^9	10^6	10^6	10^9	10^2	10^6	10^8	10^9	10^7	10^4	10^4
Case 3	>10^10	>10^10	>10^10	>10^10	>10^10	>10^10	>10^10	>10^10	>10^10	>10^10	>10^10	>10^10
Case 4	>10^10	>10^10	>10^10	>10^10	>10^10	10^8	>10^10	>10^10	>10^10	>10^10	>10^10	>10^10
Case 5	>10^10	>10^10	>10^10	>10^10	>10^10	10^5	>10^10	>10^10	>10^10	>10^10	>10^10	>10^10
Case 6	>10^10	>10^10	>10^10	>10^10	>10^10	10^5	>10^10	>10^10	>10^10	>10^10	>10^10	10^7
Gamma Distribution												
Historic Data	>10^10	10^9	10^6	10^8	>10^10	10^9	10^7	>10^10	10^8	>10^10	10^9	>10^10
Case 1	>10^10	>10^10	>10^10	>10^10	>10^10	10^4	10^9	>10^10	>10^10	>10^10	10^9	10^9
Case 2	N/A	N/A	N/A	N/A	N/A	N/A	N/A	N/A	N/A	N/A	N/A	N/A
Case 3	>10^10	>10^10	>10^10	>10^10	>10^10	>10^10	>10^10	>10^10	>10^10	>10^10	>10^10	>10^10
Case 4	>10^10	>10^10	>10^10	>10^10	>10^10	>10^10	>10^10	>10^10	>10^10	>10^10	>10^10	>10^10
Case 5	>10^10	>10^10	>10^10	>10^10	>10^10	10^6	>10^10	>10^10	>10^10	>10^10	>10^10	10^9
Case 6	>10^10	>10^10	>10^10	>10^10	>10^10	10^5	>10^10	>10^10	>10^10	>10^10	>10^10	10^9

The first row in Table 7.2 shows the DSOD approved PMF flow for the dam in each column. The second row shows the area-weighted PMP for the watershed. The recurrence intervals based on the GEV1 probability distribution is provided in

the third row, while the fourth row shows the maximum modeled rainfall. In most cases, the modeled rainfall was less than the PMP. The exceptions were Live Oak, Santa Anita, Sawpit, and Thompson Creek Dams. The range of the area-weighted PMPs was from 10^5 through 10^7. The sections below the PMF and PMP information show the recurrence interval of the DSOD approved PMF based on comparison to recurrence intervals developed using probability distribution analysis for the historic gage data and data from each of the six Monte Carlo Simulation cases.

As an example, the approved DSOD PMF for Big Dalton Dam is 16,800 cfs. Analysis of the gage record data for Big Dalton using the Log-Normal distribution showed that this value fell in between the 1/1000 and 1/10,000 year recurrence interval values of 8,738 and 25,080 cfs. This resulted in a recurrence interval value of 10^3 in the row titled Historic Runoff under the Log-Normal distribution section, in row 7 of Table 7.2. This evaluation was conducted for each of the 7 possible cases for the four probability distributions listed in Table 7.2.

ANSCOLD (2000) recommended that if rainfalls are used in event-based models to estimate flood peaks, special attention is needed to ensure that the rainfall AEP is preserved in the consequent flood. For example, if an estimate of the 1:5000 AEP rainfall is available from regional pooling, then modeling considerations are required to ensure that the AEP of the resulting flood peak is

also at least 1:5000. There are a number of ways of ensuring that the AEP is preserved for frequent floods, but as the AEP of the flood decreases it becomes increasingly difficult to validate. The factors that influence the rainfall to flood conversion are many. The major factors include non-linearity of flood response in overland flow paths and channels, rainfall losses, temporal patterns, and initial snowpack. Some of these issues can be solved, some are tractable research problems, and some are unlikely to be resolved in the near future. Physically-based models provide a vehicle to explore ways of using physical reasoning to condition extrapolations of flood response. Paleo-hydrological techniques provide another avenue for extending the AEPs by an order of magnitude.

Based on the ANSCOLD recommendation, the PMF recurrence intervals shown in Table 7.2 should be equal to or greater than the PMP recurrence interval due to the joint probability of the PMP distribution with the soil and fire factor conditional probabilities. The table shows that the Log-Normal, Gumbel (GEV1), and Gamma distributions appear to meet expected range requirements for the PMF in most cases. However, there is a very large range in the results. The moment ratios for these data sets were plotted to determine which distribution might fit the results best. Figure 7.11 shows the moment ratio diagram for the dams based on analysis of the historic runoff data. The moments are spread across a large spectrum showing that some of the 3-parameter methods, such as Gamma, LP-III, and the GEV may provide the best fits.

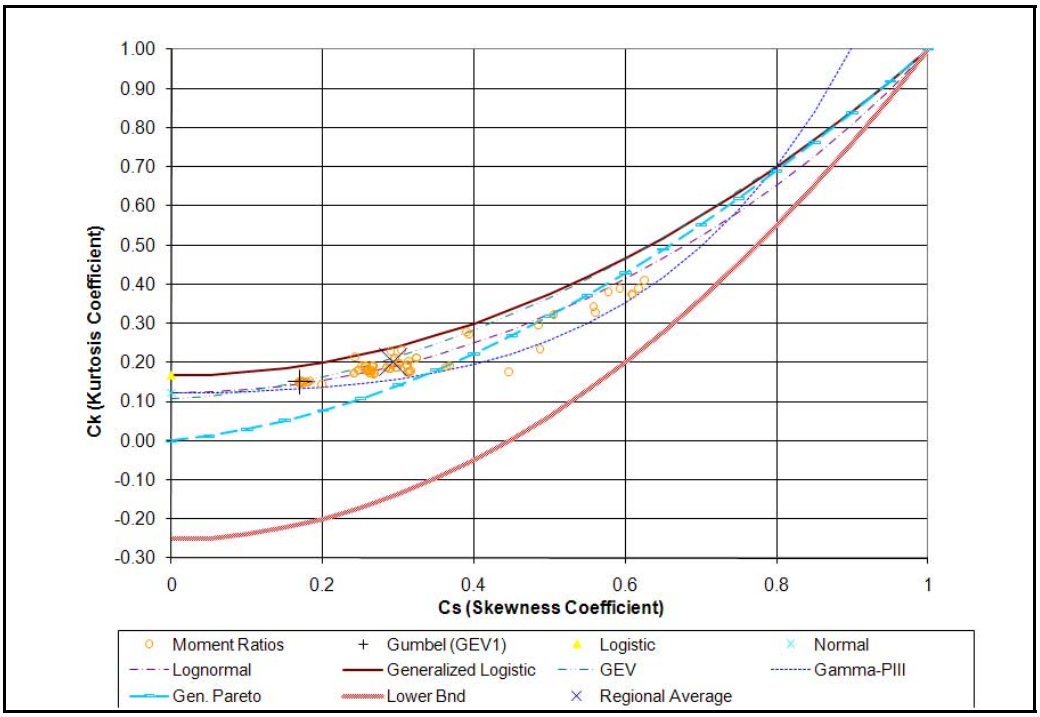

Figure 7.11 L-Moments Frequency Distribution Analysis - Historic Data

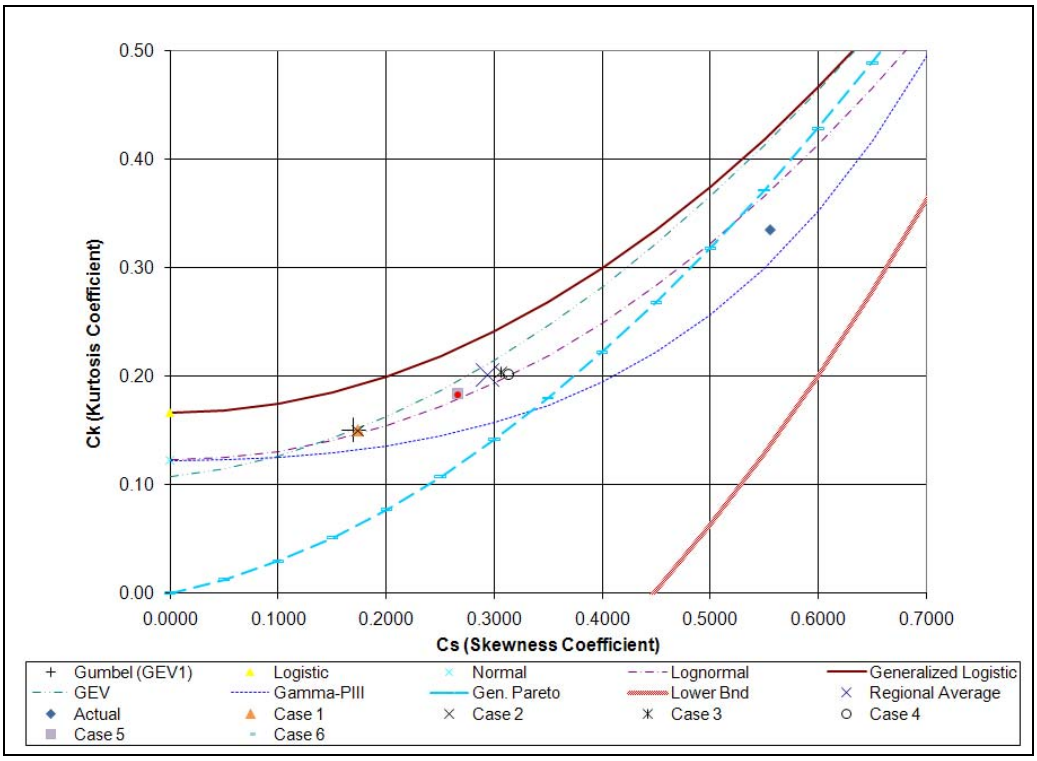

Figure 7.12 L-Moment Plots Using Six Monte Carlo Models

In order to evaluate the results of the Monte Carlo Analysis, the data from each of the 6 cases was plotted in Figure 7.12. Figure 7.12 shows that there is a large range in the moment ratios from the Monte Carlo simulations. The data for Cases 1 and 2 are clustered near the GEV1 distribution point. This is due to the fact that the rainfall distribution was GEV1 and the constant loss method was utilized. It appears that watershed routing and the constant loss method did not have much impact on the probability distribution for these two cases, and so the data remains clustered around the GEV1 moment ratio.

Cases 3-6 utilize the Los Angeles County runoff coefficient method, the GEV1 rainfall distribution, and probability distributions related to the impacts of fire in Cases 4 and 6. Figure 7.12 shows a large spread on these data sets, especially Case 4 and 6. However, none of the modeled cases resulted in a distribution of data sets similar to the data points generated by the actual runoff measurements for inflow into the dams. Figure 7.13 provides insight into the clustering of the case results versus the actual runoff. The average moment ratio for each case is plotted with the average moment ratio for the actual runoff gage measurements.

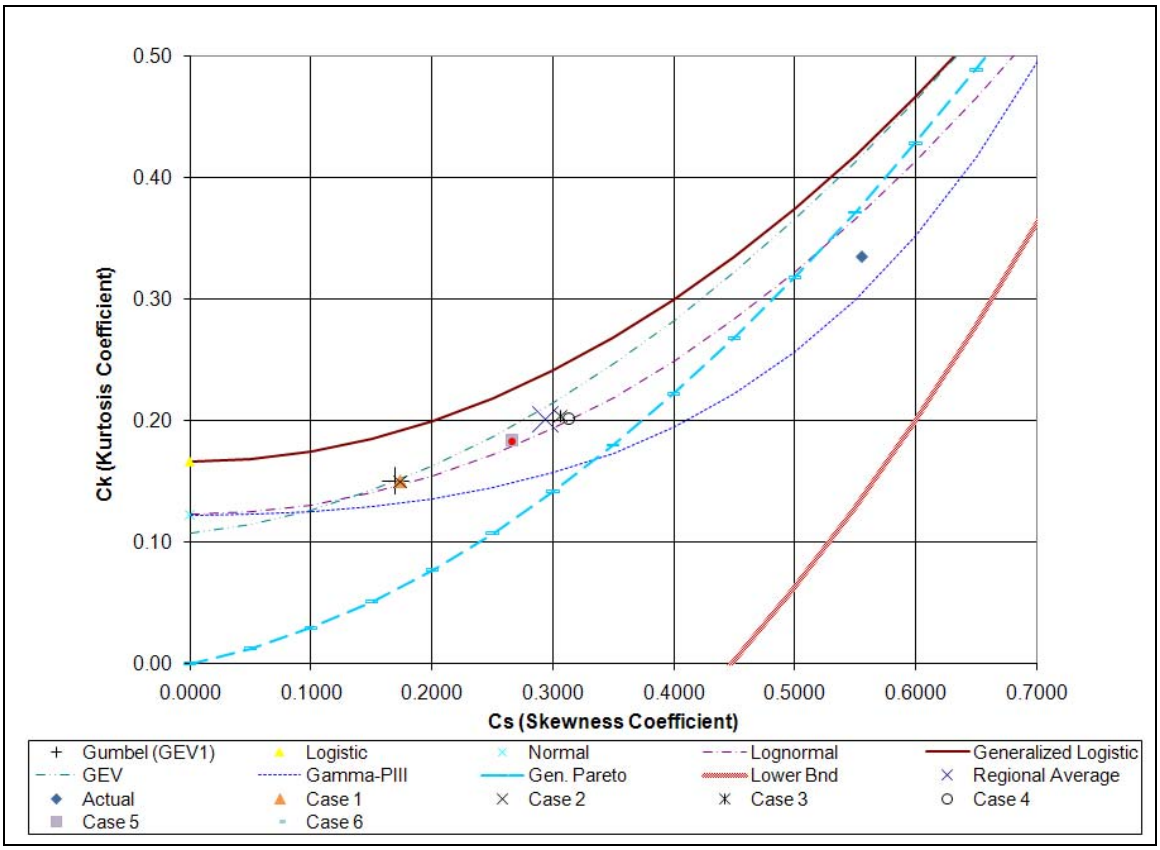

Figure 7.13 Average L-Moment Ratios for Monte Carlo Cases and Actual Runoff

7.3 Chapter Summary and Conclusions

This chapter discusses the results of the Monte Carlo simulation studies of watersheds to determine the impacts of rainfall, soil methodology, and fire factor analysis on extreme runoff events. The cases modeled do not provide the same moment ratio as the actual data set. Although the Monte Carlo model produced the same type of flow rates and coefficients as modeled for the official PMF studies, use of probability based inputs resulted in estimates of PMF values with recurrence intervals similar to the PMP recurrence intervals.

The Monte Carlo simulation methodology provided improved predictions of runoff frequency based on the joint probability of rainfall and fires within watersheds. Watershed models without fire factors will demonstrate probability distributions similar to the rainfall input probability distribution.

Use of the PMP recurrence interval as an anchor point for use with the actual gage data is not practical for use in establishing the runoff frequency of the PMF. The large range in orders of magnitude which may be ascribed to the PMP based on the method of determining the PMP makes it unreliable.

Chapter 8 – Conclusions and Recommendations for Future Studies

8.1 Specific Findings

The use of probability distributions to extend short records to engineering design time frames is a common practice in the engineering field. Although significant efforts are expended in these analyses, extension of these methods past a 100 to 200 year time frame becomes very unreliable due to the lack of data and changes in the climate over extremely long periods.

Regional analysis of data extends the data set for longer time frames. Use of bootstrapping also allows further development of possible data set combinations to improve estimates over at-site data. The results of this study indicate the following:

1. Record length plays an important role in the fitting of probability distributions to the data set and in the predicted extreme values for runoff events.

2. The date when systematic sampling begins, and the exact data set captured, also influences probability distribution selection and the prediction of extreme values for runoff events.

3. Selection of a probability distribution affects the value for a specific recurrence interval, even if the record length is significantly longer than the recurrence interval of interest.

4. Selection of a parameter estimation method is important in the estimation of extreme runoff events using probability distributions. The use of probability weighted moments for shorter record lengths is suggested due to the linear nature of the method.

Evaluation of rainfall within Los Angeles County, along with comparison to the Probable Maximum Precipitation (PMP) Methods suggested by Hershfield and the National Weather Service in Hydrometeorological Reports 58 and 59 led to the following conclusions:

5. The GEV1 assumption for rainfall data evaluation within Los Angeles County is sound.

6. Gage record length does play a role in moment ratio analysis, leading the exclusion of some gages for further analysis due to their nature as statistical outliers.

7. The HMR PMP methodology results in inconsistent recurrence intervals ranging from 10^3 to 10^{13}. This range is consistent across gage record length and region.

8. The Hershfield PMP methodology results in inconsistent recurrence intervals ranging from 10^3 to 10^{13}. This range is consistent across gage record length and region.

9. The HMR PMP and Hershfield PMP methodologies are inconsistent with each other, providing consistent results for some gages and results ranging by orders of magnitude at others. This is consistent across regions.

10. The distribution of the PMP estimations appears to be normal with a center at approximately 10^8.

11. Due to the extreme range for the PMP, it is not suitable for a design standard, since it provides unequal protection in areas within the same

area. This leads to unfair costs in the construction of major engineering facilities and unequal failure risks for communities.

Studies used to determine the watershed modeling requirements for this study found the following:

12. The constant loss and runoff coefficient methods are appropriate for use in watershed modeling for this study.

13. The Clark Unit Hydrograph method is a simple but effective tool for modeling watersheds and requires only a storage coefficient, a time of concentration, and a time-area relationship.

14. A synthetic CUH time-area developed by the U.S. Army Corps of Engineers is appropriate for use in Los Angeles County.

15. The Snyder Modified Lag Time is a reasonable estimation for time of concentration and takes into account physical watershed parameters such as flow path length, slope, watershed shape, and watershed roughness.

16. The CUH storage coefficient R, can be approximated by the equation $R=1.5*T_{lag}$ for watersheds within Los Angeles County.

Since fire plays such a significant role in the hydrologic cycle of Southern California, the impacts of fire were studied and a fire factor methodology was developed. The recurrence interval based on vegetation soil and recovery were investigated and the following conclusions were developed.

17. Fires have a significant impact on hydrology within Los Angeles County.

18. The effects of fire on watershed hydrology can be quantified and a method has been developed for use with runoff coefficients within Los Angeles County.

19. The recurrence interval of annual fire factors is dependent on watershed size. The larger the watershed, the more likely there is to be a fire within the boundaries. However, the larger a watershed gets, the less likely it is to burn completely. As a watershed gets smaller, the likelihood of burning decreases, but the probability of burning the entire area increases.

20. There is no discernible difference in fire factor recurrence interval within the major watersheds of Los Angeles County.

21. The method currently employed by Los Angeles County to incorporate the 50-year fire factor into hydrology studies is fairly consistent with the study conducted, but is conservative.

22. Fire Factor Area-Frequency curves were developed for the Los Angeles County data sets. It is felt that these curves should be fairly consistent throughout Southern California due to the similar topography and climate. Similar curves could be developed for other regions of the Western United States.

8.2 General Findings

Besides these specific findings, some general conclusions can be drawn. There is no way to verify the actual data distribution of either rainfall or runoff. In the end, many extreme value probability distribution methods may be used for estimating extreme values with recurrence intervals greater than 1000 years. However, this study showed that not all probability distribution methods provided

the expected results, with runoff recurrence intervals being greater than or equal to the recurrence interval of the rainfall used in modeling.

The use of probability distributions to determine what might happen during extreme events in engineered hydrologic and hydraulic systems ignores many of the rules related to the use of probability distributions including homogeneity, stationarity, and upper bounds imposed by physical processes that are not shown in available systematic data records. The following general conclusions were reached through the analyses conducted:

1. Anchoring a runoff frequency analysis on the PMP frequency is not possible since the PMP estimates range by 6 orders of magnitude within the County independent of the PMP estimation method. The two methods used in this study were the most common approaches used industry wide. The study showed inconsistent results between the HMR 58 and Hershfield methods. The distribution of the order of magnitude appears to fit a Normal Distribution with a center around a magnitude of 10^8.

2. Runoff coefficients based on the rainfall recurrence interval seem appropriate for use in watershed studies. Those proposed by the California Division of Safety of Dams (DSOD) and based on the Mean

Annual Precipitation (MAP) are reasonable for Los Angeles County, but will result in overly high runoff in some watersheds and lower than expected runoff in others.

3. Estimation of fire factor recurrence intervals based on the watershed area is a reasonable approach. Recurrence of fire within a watershed goes up as size increases, but the amount of watershed burned decreases as watershed size increases. The fire factor value approaches 1 as the size of the watershed decreases, but the probability of having a fire also decreases as size decreases.

4. Selection of soil methodologies and rainfall hyetographs significantly influence watershed models and must be chosen with care.

8.3 Recommendations

Two major finding will have significant impact on the civil engineering community. The inconsistency of the PMP methodology leads to a significant policy question on use of the PMP as a standard for design. Due to the significant variation in recurrence interval, this is a non-uniform standard and is open for challenges in the legal system. Policy makers should evaluate the inconsistencies and look for

a methodology that can be applied consistently across their jurisdictions. The recommendation of the author of this study is to select an extreme rainfall event based on a specified probability distribution as the set policy. A recommended starting place would be a rainfall event with a recurrence interval of 10^4, using the Gumbel (GEV1) probability distribution with L-moment parameter estimation.

The second major finding of the study relates to fire factors and the recurrence of fire within a watershed. The area of a watershed plays a significant role in the extent of damage caused by a fire. The larger the watershed, the less likely to burn the entire area. Use of the fire-factor area frequency curves for evaluating the fire risk within a watershed is recommended for Southern California. Due to the climate, topography, and urbanization within the region, it is felt that the curves developed are applicable to a wider area than Los Angeles.

8.4 Future Studies

This study found that more research is needed to relate soil and watershed properties to changes in runoff characteristics. The use of FF with constant loss or soil characteristic methodologies, will require more data collection and analysis. Parameters of this type of study should include soil type and characteristics pre- and post-fire, vegetation type, watershed slope, and fire

intensity. With this information, developing models of watersheds that account for changes in soil and watersheds due to fires can be improved.

After a fire, sediment is more easily removed from hills and channels within a watershed. Entrainment of sediment increases runoff volumes, even when the volume of water within the watershed may remain the same. Use of bulking factors is not prevalent in the hydrologic study of watersheds. More efforts need to be made to determine whether increased water runoff, increased sedimentation, or both result in the order of magnitude increases in flow runoff. The impacts of bulking should be advocated throughout the engineering communities and policies should be adopted to provide guidance on how to incorporate the increases in flow volumes in design of engineering structures. Currently, only a few counties in Southern California appear to have policies to implement bulking into hydrologic studies.

Protection of life and property requires use of statistics and engineering judgment to provide adequate safety to citizens living in areas affected by flooding and fires. Based on the results of this study, it is suggested that many appropriate methods would result in adequate protection. Use of the PMP rainfall provides extreme event protection, while use of other frequencies for design of key systems is appropriate. As long as a community sets a reasonable policy that

provides protection for more frequent recurrence intervals, use of statistics is justified. There will always be a risk of failure for any structure, regardless of the design extreme event. The cost benefit analysis eventually dictates what can be built and the level of protection that is provided. Other times, systems are built over time and the increase in risk happens gradually. A system that was adequate in the past becomes inadequate as the system changes, as watershed develop, as levees settle, etc. The expense of retrofitting is too high, and people live with lowered protection until an extreme event destroys the old system.

Engineers must plan for the future and prepare for what may be if they are ever to provide the protection that they calculate using risk assessment tools such as probability distributions.

References

Ainsworth, J. and Doss, T.A. 1995. Natural History of Fire & Flood Cycles. Post-Fire Hazard Assessment Planning and Mitigation Workshop at the University of California, Santa Barbara, August 18, 1995.

Asquith, W.H., and Slade, R.M., Jr., 1999, Site-specific estimation of peak-streamflow frequency using generalized least-squares regression for natural basins in Texas: U.S. Geological Survey Water-Resources Investigations Report 99-4172, 19 p.

ANSCOLD, Australian National Committee on Large Dams, Guidelines on Selection Flood Capacity for Dams. March 2000.

Baker, V.R., 1987. Paleoflood hydrology and extraordinary flood events: *Journal of Hydrology*, v. 96, p. 79-99.

Barbour, M.G., Burk, J.H., and Pitts, W.D. (1980), *Terrestrial Plant Ecology*, The Benjamin/Cummings Publishing Company, Menlo Park, California.

Barro, S.C., and Conard, S.G. (1990). *Fire Effects on California Chaparral*, Pacific Southwest Research Station, Riverside, California.

Branson, F.A., G.F. Gifford, K.G. Renard, and R.F. Hadley. 1981. Rangeland Hydrology, second edition. Kendall/Hunt Publishing, Dubuque, IA.

Bobee, B., and Ashkar, F. 1991. “The Gamma Family and Derived Distributions Applied in Hydrology. Water Resources Publications, Littleton, CO.

Burn, D.H., 1990a, An appraisal of the “region of influence” approach to flood frequency analysis: Hydrological Sciences Journal, v. 35, no. 2, p. 149-165.

Burn, D.H., 1990b, Evaluation of regional flood frequency analysis with a region of influence approach: Water Resources Research, v. 26, no. 10, p. 2257-2265.

Butry, D. T., Gumpertz, M. L., and Genton, M. G. (2008), "The production of large and small wildfires," *in Holmes, T. P., Prestemon, J. P., and Abt, K. L. (eds.), The Economics of Forest Disturbances: Wildfires, Storms, and Invasive Species, Springer: Dordrecht, The Netherlands,* **5,** 79-106.

Calzascia, E.R. and Fitzpatrick, J.A., “Hydrologic Analysis within California’s Dam Safety Program.” Western Regional Conference and Dam Safety Workshop, May 1-3, 1989 Sacramento, CA

Clark, C.O., 1945. Storage and the Unit Hydrograph. *Trans ASCE*, vol 110. pp 1442

Chow, V.T., Maidment, D.R., and Mays, L.W. (1988) *Applied Hydrology*, McGraw-Hill, New York, pp. 530-537.

Chow, V.T. 1961 – A general formula for hydrologic frequency analyses. Transactions American Geophysical union, Vol. 32, pp 231-237

Cohn, T.A., W.L. Lane, and W.G. Baier, 1997. An algorithm for computing moments-based flood quantile estimates when historical flood information is available, *Water Resources Research,* 33(9), p. 2089-96.

Cudworth, A.G. 1989. *Flood hydrology manual*. A water resources technical publication. Bureau of Reclamation, Denver, Colorado, 243 p.

Cunnane, C. 1989. Statistical Distributions for Flood Frequency Analysis. World Meteorological Organizations Operational Hydrology, Report No. 33, WMO-No. 718, Geneva, Switzerland.

Davis, J.P. (1977), *Southern California Reservoir Sedimentation, Fall Meeting & Exhibits*, American Society of Civil Engineers, San Francisco, California.

DeBano, L.F., J.F. Osborn, J.S. Krammes, and J. Letey, Jr. 1967. Soil wetability and wetting agents: Our current knowledge of the problem. USDA Forest Service Research Paper, Pacific Southwest Forest and Range Experimental Station, General Technical Report PSW-43, Berkeley, CA.

DeBano, L.F. (1987), *Chaparral Soils*, Pacific Southwest Forest and Range Experimental Station.

Dooge, J.C.I. 1959. A general theory of the unit hydrograph. *Journal of Geophysical Research,* 64(2), 241-256.

Drobot, R. (2004) Meteorological Baseline Report, Assessment of Rainfall Intensity, Frequency and Runoff for the Rosia Montana Project. S.C Rosia Montana Gold Corporation, S.A.

Eliasson, J. Statistical Estimates of PMP Values, *Nordic Hydrology, 25, 1994, 301-312*

England Jr., J.F., Jarrett, R.D., Salas, J.D., 2003a. Comparisons of two moments-based estimators that utilize historical and paleoflood data for the log Pearson type III distribution. Water Resources Research, Vol. 39, No. 9, 1243.

England Jr., J.F., Jarrett, R.D., Salas, J.D., 2003b. Data-based comparisons of moments estimators using historical and paleoflood data. Journal of Hydrology. v. 278, p. 172–196.

Federal Emergency Management Agency (FEMA), 2001. FEMA Workshop Proceedings: Hydrologic Research Needs for Dam Safety. Hydrologic Engineering Center, Davis, CA. November 14-15, 2001.

Federal Energy Regulatory Commission, September 2001. *Engineering Guidelines for the Evaluation of Hydropower Projects*, Chapter 8 Determination of the Probable Maximum Flood.

Flood Control District of Maricopa County. *Drainage Design Manual for Maricopa County, Hydrology*. June 2010.

Florsheim, J.L., Keller, E.A., & Best, D.W. (1991), *Fluvial Sediment Transport in Response to Moderate Storm Flows Following Chaparral Wildfire*, Southern California; Geologic Society of America Bulletin, v. 103, pg. 504-511.

Fontaine, T.A. (1995) Rainfall-runoff model accuracy for an extreme flood. J. Hyd. Engr., ASCE, 121(4), pp. 365-374.

Greenwood, J.A., Landwehr, J.M., Matalas, N.C., and Wallis, J.R. 1979. Probability Weighted Moments: Definition and Relation to Parameters of Several Distributions Expressible in Inverse Form. Water Resources Research, Vol. 15, No. 5, pp. 1049-1054.

Gifford, G.F. 1985. Cover allocation in rangeland watershed management (a review). In B. Jones and T. Ward, eds., Watershed Management in the Eighties, Denver, CO, April 30 - May 1, 1985., pp 23-31. American Society of Civil Engineers, New York.

Gunasekara, T.A.G., Cunnane, C. 1992 Split Sampling Technique for Selecting a Flood Frequency Analysis Procedure, Journal of Hydrology, vol. 130, pp, 189-200

Hanes, T.L. (1987), *The Vegetation Called Chaparral*, Department of Biological Science, California State University, Fullerton.

Hillel, D. 1980. Fundamentals of soil physics. Academic Press. New York, NY.

Holmes, T.P., Huggett, R.J., Westerling, A.L., 2008. Statistical Analysis of Large Wildfires, DOI: 10.1007/978-1-4020-4370-3_4

Hodge, S.A., and Tasker, G.D., 1995, Magnitude and frequency of floods in Arkansas: U.S. Geological Survey Water-Resources Investigations Report 95-4224, 52 p.

Hosking, J.R.M. 1986. "The Theory of Probability Weighted Moments". Res. Rep. RC 12210, IBM Research Division, Yorktown Heights, NY. 10598.

Hosking, J.R.M. 1990. L-Moments: Analysis and Estimation of Distributions using Linear Combinations of Order Statistics. Journal of Royal Statistical Society B, Vol 52, pp. 105-124.

Hosking, J.R.M., and J.R. Wallis, 1997. *Regional Frequency Analysis: An Approach Based on L-moments,* Cambridge Univ. Press, 224 pp.

Interagency Advisory Committee on Water Data (IACWD), 1982. *Guidelines for Determining Flood Flow Frequency,* Bulletin 17B, U.S. Department of the Interior, U.S. Geological Survey, Office of Water Data Coordination, Reston, Virginia.

Interagency Advisory Committee on Water Data (IACWD), 1986. "Feasibility of Assigning Probability to the Probable Maximum Flood", Office of Water Data Coordination, U.S. Department of the Interior, Geological Survey, Office of Water Data Coordination, Reston, VA.

Keeley, J.E., 1981. Distribution of Lightning- and Man-Caused Wildfires in California. Symposium on Dynamics and Management of Mediterranean Type Ecosystems. San Diego, CA

Kibler, D.F., Ed. *Urban Storm Water Hydrology*. American Geophysical Union. p 91, Washington D.C. 1982.

Kirby, W. 1974. Algebraic Boundedness of Small Samples, Water Resources Research, Vol. 10, No. 2, pp. 220-222.

Kite, G. W. (1988). *Frequency and risk analyses in hydrology*. Littleton, Colo., U.S.A: Water Resources Publications.

Knight, R.W., W.H. Blackburn, and C.J. Scifres. 1983. Infiltration rates and sediment production following herbicide/fire brush treatments. Journal of Range Management 36:154-157.

Koutsoyiannis, D. 2009. Statistics of Extremes and Estimation of Extreme Rainfall: II. Empirical Investigation of Long Rainfall Records.Hydrol. Sci. J. 49(4), 591-610.

Landwehr, J.M., Matalas, N.C., and Wallis, J.R. 1979. Probability Weighted Moments Compared with Some Traditional Techniques in Estimating Gumbel Parameters and Quantiles. Water Resources Research, 15, pp. 1055-1064.

Lane, W. L., and T. A. Cohn, Expected moments algorithm for flood frequency analysis, in North American Water and Environment Congress 1996 [CD-ROM], edited by C. T. Bathala, Am. Soc. of Civ. Eng., Reston, Va., 1996.

Laverty, L. 2001. A Report to the President in Response to the Wildfires of 2000, September 8, 2000.

Law, G.S., G.D. Tasker, 2000. Flood-Frequency Prediction Methods for Unregulated Streams of Tennessee: U.S. Geological Survey Water-Resources Investigations Report 03-4176, 79 p.

Linsley, R.K., Kohler, M.A. and Paulhus, J.L.H. 1982. *Hydrology for Engineers, Third Edition*. McGraw-Hill, New York.

Los Angeles County Flood Control District (LACFCD), Report on Debris Reduction Studies for Mountain Watersheds of Los Angeles County, November 1959.

Los Angeles County Flood Control District,1938. *Storm of March 2, 1938*. Table X

Maidment, D. R., ed. (1993), Handbook of Hydrology, McGraw Hill.

Mayer, R.G. M.S. Thesis. “Unit Hydrographs for Small Ungaged Watersheds in Southeastern California”. p 120. California State University, Sacramento, 1987

McPhee, J. (1989), *The Control of Nature*, The Noonday Press, Farrar, Straus and Giroux, New York.

Nasseri, I. 1988. Frequency of Floods from a Burned Chaparral Watershed. Symposium on Fire and Watershed Management, October 26-29, 1988, Sacramento, CA.

National Oceanographic and Atmospheric Administration (NOAA), July 2004. Service Assessment Southern California Wildfires October 20 to November 3, 2003.

National Research Council (NRC), 1985. Safety of Dams, Flood and Earthquake Criteria, Committee of Safety Criteria for Dams, National Academy Press, Washington, D.C., 321p.

National Research Council (NRC), 1988. "Estimating Probabilities of Extreme Floods, Methods and Recommended Research", ISBN 0-309-03791-3, National Academy Press, Washington, D.C. 141p.

National Research Council (NRC), 1994. "Estimating Bounds on Extreme Precipitation Events", National Academy Press, Washington, D.C.

NRCS, 2010. Soil Classification Website.
http://soils.usda.gov/education/facts/formation.html

National Weather Service, 2008. Personal Communication with Debbie Martin of the Hydrometeorological Design Studies Center, January 14, 2008.

Neiman, P. J., F. M. Ralph, G. A. Wick, J. D. Lundquist, and M. D. Dettinger, 2008: Meteorological characteristics and overland precipitation impacts of atmospheric rivers affecting the West Coast of North America based on eight years of SSM/I satellite observations. J. Hydromet., 9, 22-47.

O'Connell, D.R.H., 1997. FLFRQ3, Three-Parameter Maximum Likelihood Flood-Frequency Estimation with Optional Probability Regions using Parameter Grid Integration: Users Guide (Beta Edition).

Pierson, Jr., F.B., Robichaud, P.R., Spaeth, K.E., and Moffet, C.A. 2003. Impacts of fire on hydrology and erosion in steep mountain big sagebrush communities. In: Proceedings of the First Interagency Conference on Research in the Watersheds., Benson, AZ, p. 625-630.

Pierson, F.B., Robichaud, P.R., Moffet, C.A., Spaeth, K.E., Williams, C.J., Hardegree, S.P., and Clark, P.E. (2008). Soil water repellency and infiltration in coarse-textured soils of burned and unburned sagebrush ecosystems. Catena 74:98-108.

Pope, B.F., Tasker, G.D., and Robbins, J.C., 2001, Estimating the magnitude and frequency of floods in rural basins of North Carolina—Revised: U.S. Geological Survey Water-Resources Investigations Report 01-4207, 44 p.

Radtke, K.W.H. (1983), *Living More Safely in the Chaparral-Urban Interface*, United States Department of Agriculture, Pacific Southwest Forest and Range Experimental Station.

Ralph, F. M., P. J. Neiman, and G. A. Wick, 2004: Satellite and CALJET aircraft observations of atmospheric rivers over the Eastern North Pacific Ocean during the winter of 1997/98. Mon. Wea. Rev., 132, 1721-1745.

Ralph, F. M., P. J. Neiman, G. A. Wick, S. I. Gutman, M. D. Dettinger, D. R. Cayan, and A. B. White, 2006: Flooding on California's Russian River: Role of atmospheric rivers. J. Geophys. Res. Lett., 33, doi:10.1029/2006GL026689.

Rao, A.R. and Hamed, K.H, 2000. Flood Frequency Analysis, CRC Press, p. 350.

Rawls, W.J., C.A. Onstad, and H.H. Richardson. 1980. Residue and tillage effects on SCS runoff curve numbers. Trans. ASAE 23:357–361

Rice, R.M. (1987), *The Hydrology of Chaparral Watersheds*, Pacific Southwest Forest and Range Experimental Station.

Robichaud, P.R. 2000. Fire effects on infiltration rates after prescribed fire in northern rocky mountain forest, USA. Journal of Hydrology 231-232:220-229.

Russell, S., Kenning, B., and Sunnell, G., 1979. Estimating Design Flows for Urban Drainage..ASCE Journal of the Hydraulics Division, Vol 105, No. HY1, pp 49.

Simpson, Larry. 1969. Los Angeles County Flood Control District *Hydrologic Report on the Storms of 1969*. 1969.

Spaeth, K. E.; Pierson, F. B.; Robichaud, P. R.; Moffet, C. A. (2007). *Hydrology, erosion, plant, and soil relationships after rangeland wildfire.* In: Sosebee, Ronald E.; Wester, David B.; Britton, Carlton M.; McArthur, E. Durant; Kitchen, Stanley G., comps. Proceedings: Shrubland dynamics -- fire and water; 2004 August 10-12; Lubbock, TX. Proceedings RMRS-P-47. Fort Collins, CO: U.S. Department of Agriculture, Forest Service, Rocky Mountain Research Station. 62-68.

Spreen, W. C., Determination of the Effect of Topography upon Precipitation, Trans. Am. Geophys. Union, vol. 28, no. 2, April 1947.

Stedinger, J.R., and G.D. Tasker, 1985. Regional hydrologic analysis, 1. Ordinary, weighted and generalized least squares compared, *Water Resour. Res.,* 21(9), p. 1421-32.

Stedinger, J.R., and G.D. Tasker, 1986a. Correction to 'Regional hydrologic analysis, 1. Ordinary, weighted and generalized least squares compared,' *Water Resources Research*, 22(5), p. 844.

Stedinger, J.R., and G.D. Tasker, 1986b. Regional hydrologic analysis, 2. Model error estimates, estimation of sigma, and log-Pearson Type 3 distributions, *Water Resources. Research*, 22(10), p. 1487-1499.

Stedinger, J.R., R. Surani, and R. Therivel, 1988. Max Users Guide: A Program for Flood Frequency Analysis using Systematic-Record, Historical, Botanical, Physical Paleohydrologic and Regional Hydrologic Information Using Maximum Likelihood Techniques, Department of Environmental Engineering, Cornell University.

Stedinger, J.R., R.M.Vogel, and E. Foufoula-Georgiou, 1993. Frequency Analysis of Extreme Events, Chapter 18, *Handbook of Hydrology*, D. Maidment (ed.), McGraw-Hill, Inc., New York.

Straub, T.D., Melching, C.S., Kocher, K.E. USGS Water Resources Investigations Report 00-4184, Equations for Estimating Clark Unit-Hydrograph Parameters for Small Rural Watersheds in Illinois, 2000.

Swain, R.E., Bowles, D., Ostenaa, D., 1998. A Framework for Characterization of Extreme Floods for Dam Safety Risk Assessments. Proceedings of the 1998 USCOLD Annual Lecture, Buffalo, New York. August 1998

Tasker, G.D., and Slade, R.M., 1994, An interactive regional regression approach to estimating flood quantiles, *in* Fontane, D.G., and Tuvel, H.N., eds.,

Water policy and management, solving the problems, Proceedings of the Twenty-First Annual Conference, May 23-26, 1994: Denver, Colo., Denver Society of American Society of Civil Engineers, p. 782-785.

Tasker, G.D., Hodge, S.A., and Barks, C.S., 1996, Region of influence regression for estimating the 50-year flood at ungaged sites: Water Resources Bulletin, v. 32, no. 1, p. 163-170.

U.S. Bureau of Reclamation (USBR, 1999): A framework for developing inputs for dam safety risk assessments, Part I - Framework, USBR, February 1999.
Wang, Q. (1997). LH Moments for statistical analysis of extreme events. Water Research 133(12): 2841-2848.

U.S. Army Corps of Engineers, Hydrologic Engineering Center. Sacramento 1967. Generalized Standard Project Rainflood Criteria, Southern California Coastal Streams.

US Army Corps of Engineers, Los Angeles, California District, 1987. Derivation of a rainfall-runoff model to compute n-year floods for Orange County Watersheds.

U.S. Army Corps of Engineers, Los Angeles, California District, 1944. "Hydrology, San Gabriel River and the Rio Hondo above Whittier Narrows Flood Control Basin"

United States Department of Agriculture (USDA), Wildland Fire in Ecosystems: Effects of Fire on Soil and Water. General Technical Report RMRS-GTR-42-Volume 4. September 2005.

Veenhuis, J. E. (2002). *Effects of wildfire on the hydrology of Capulin and Rito de Los Frijoles Canyons, Bandelier National Monument, New Mexico*. Ann Arbor, Michigan: University Of Michigan Library.

Vogel, R.M., McMahon, T.A., Chiew, F.H.S (1993) Flood Flow Frequency Selection in Australia, Journal of Hydrology, vol. 146, pp, 421-449

Vogel, R.M. and N.M. Fennessey, L moment diagrams should replace product moment diagrams, *Water Resour. Res., 29*(6), 1745-1752, 1993.

Walden, A. and Willardson, B.J. 2003. Development of Burn Policy Methodology (Santa Clara River Watershed Pilot Project), County of Los Angeles Department of Public Works Technical Report.

Walden, A. Willardson, B.J., Conkle, C. 2004. Development of Burn Policy Methodology, County of Los Angeles Department of Public Works Technical Report.

Wallis, J.R., Matalas, N.C., and Slack, J.R. 1974. Just a Moment!, Water Resources Research. 10(2), pp. 211-219.

Wells, W.G. (1987), *The Effects of Fire on the Generation of Debris Flows in Southern California*, Geologic Society of America Reviews in Engineering.

White, K. 2004. The 2000-2002 Forest Fires in the Western United States. Rosen Publishing Group.

Willardson, B., Prietto, J., and Conkle, C. Los Angeles County Rural and Mountain Hydrology Method. October 2004. Los Angeles County Department of Public Works.

Willardson, B., Walden, A., and Nasseri, I. PMP Soil Extension Curves. July 2004. Los Angeles County Department of Public Works.

Wilcox, B.P., M.K. Wood, and J.M. Tromble. 1988. Factors influencing infiltrability of semiarid mountain slopes. Journal of Range Management 41:197-206.

Wondzell, S. M., and J. G. King. 2003. Post-fire erosional processes in the Pacific Northwest and Rocky Mountain region. Forest Ecology and Management 178:75-87.

World Meteorological Organization (1969): Manual for Depth-Area-Duration Analysis of Storm Precipitation, WMO No. 237, Tech. Pap. 129, Geneva.

World Meteorological Organization (1986): Manual for estimation of probable maximum precipitation, Second Edition, Operational Hydrology Report No. 1, WMO -No. 332, Geneva.

Wright, H.A., and A.W. Bailey. 1982. Fire Ecology. John Wiley & Sons, New York.

Yevjevich, V., 1964a, Fluctuations of Wet and Dry Years, Part II, Analysis by Serial Correlation, Hydrology Paper No. 4, Colorado State University, Fort Collins Colorado.

Yevjevich, V. 1964b Misconceptions in Hydrology and their consequences, Water Resources Research Vol. 4, No. 2, pp. 225-232.

Yevjevich, V., 1971, Stochasticity in Geophysical and Hydrological Time Series, Nordic Hydrology, Vol. II, pp. 217-242.

Appendix A - Rain Gage Location and Record Length

Gage #	Station Name	Region	Elev.	Latitude	Longitude	Annual Average (in.)	Years of Record
5	Calabasas	F	924	34-09-24	118-38-14	17.85	80
6	Topanga Patrol Station	F	745	34-05-03	118-35-57	23.98	60
9	Sepulveda and Rayen	B	824	34-13-52	118-28-04	16.10	72
10	Bel Air Hotel	F	540	34-05-11	118-26-45	18.86	79
11	Upper Franklin Canyon Reservoir	F	867	34-07-10	118-24-35	19.15	80
13	North Hollywood - Lakeside	F	550	34-08-46	118-21-13	17.89	100
20	Girard Reservoir	F	986	34-09-07	118-36-36	18.34	80
21	Woodland Hills	F	875	34-10-14	118-35-33	15.64	95
23	Chatsworth Reservoir	B	900	34-13-44	118-37-18	15.77	82
25	Northridge - L.A.D.W.P.	B	810	34-13-52	118-32-28	15.39	86
28	San Fernando	B	967	34-16-36	118-28-06	16.95	46
32	Newhall - Soledad Div. Headquarters	G	1243	34-23-07	118-31-54	17.69	80
33	Pacoima Dam	G	1500	34-19-48	118-23-59	19.46	92
42	Redondo Beach City Hall	A	70	33-50-43	118-23-20	11.55	89
43	Palos Verdes Estates	A	216	33-47-58	118-23-29	12.36	80
44	Point Vicente Lighthouse	A	125	33-44-30	118-24-38	10.99	81
46	Big Tujunga Dam	D	2315	34-17-40	118-11-14	26.51	79
47	Clear Creek City School	D	3150	34-16-38	118-10-12	30.51	62
53	Colby's	D	3620	34-18-05	118-06-39	27.23	66
54	Loomis Ranch-Alder Creek	E	4325	34-20-55	118-02-54	18.15	56
57	Camp Hi Hill (Opids)	D	4250	34-15-18	118-05-41	37.76	89
60	Hogee's/Winter Creek	D	2400	34-12-29	118-01-55	33.24	68
63	Big Santa Anita Dam	D	1400	34-11-03	118-01-12	26.14	80
68	Sawpit Dam	D	1375	34-10-30	117-59-07	26.22	38
73	Glendora - Englewild Ridge	D	1165	34-09-22	117-50-57	21.92	65
78	Coldbrook Ranger Station	D	3280	34-17-26	117-50-26	26.52	68
82	Table Mountain	H	7420	34-22-56	117-40-39	16.51	82
83	Big Pines Recreation Park	H	6860	34-22-44	117-41-20	24.49	82
89	San Dimas Dam	D	1350	34-09-10	117-46-17	22.77	79
92	Claremont - Pomona College	C	1185	34-05-48	117-42-33	17.69	94
93	Claremont Police Station	C	1170	34-05-45	117-43-18	17.89	79
95	San Dimas - Fire Warden	C	955	34-06-26	117-48-19	17.76	82
96	Puddingstone Dam	C	1030	34-05-31	117-48-24	17.80	79
106	Whittier City Hall	A	300	33-58-57	118-02-50	14.27	79
107	Downey - Fire Department	A	110	33-55-48	118-08-47	14.23	82
108	El Monte Fire Department	C	275	34-04-30	118-02-30	16.67	80
109	West Arcadia	C	547	34-07-42	118-04-22	19.07	79
116	Inglewood Fire Station	A	125	33-57-53	118-21-22	13.32	71
120	Vincent Patrol Station	G	3135	34-29-17	118-08-27	8.68	79
124	Bouquet Canyon Reservoir	G	3050	34-35-14	118-21-45	16.06	51
125	San Francisquito Canyon Power House No. 2	G	2105	34-35-25	118-27-15	18.31	89
128	Elizabeth Lake - Warm Springs Camp	G	2075	34-36-28	118-33-40	17.93	40
134	Puddingstone Diversion	C	1160	34-07-52	117-46-55	19.23	70
140	Sawtelle - West L.A.	A	250	34-02-43	118-26-55	16.47	61
144	Sierra Madre Dam	D	1100	34-10-34	118-02-32	25.01	79
156	La Mirada - Standard Oil Company	A	75	34-08-59	118-01-00	13.36	86
157	El Segundo - Chevron Oil Company	A	150	33-54-57	118-25-05	12.49	59
158	Tanbark Flats	D	2750	34-12-20	117-45-40	27.23	48
167	Arcadia Pumping Plant No. 1	D	611	34-09-31	118-02-02	21.34	79
169	Sierra Madre Pumping Plant	D	700	34-09-47	118-02-21	22.14	82
170	Potrero Heights	C	285	34-02-32	118-04-44	16.60	40
172	Duarte	D	548	34-08-26	117-58-02	18.98	78
174	Glendora	C	930	34-07-43	117-49-08	19.69	84
175	La Canada Irrigation District	D	2020	34-13-39	118-12-40	24.84	83
176	Altadena - Rubio Canyon	D	1125	34-10-55	118-08-15	21.72	83
178	Azusa Valley Water Company	C	620	34-06-38	117-52-50	17.87	96
179	Bailey Debris Basin	D	1180	34-10-25	118-03-38	23.39	79
191	Los Angeles - Alcazar Yard	C	400	34-03-48	118-11-58	14.96	45
196	La Verne - Fire Station	C	1050	34-06-06	117-46-20	18.00	82
201	Hacienda Heights	C	875	33-59-40	117-59-28	17.96	49

Gage #	Station Name	Region	Elev.	Latitude	Longitude	Annual Average (in.)	Years of Record
210	Brand Park	B	1250	34-11-18	118-16-20	18.12	78
213	Los Angeles Hancock Park	A	200	34-03-52	118-21-17	15.69	61
216	Glendale - Andree	B	615	34-09-54	118-15-01	17.77	81
223	Big Dalton Dam	D	1587	34-10-06	117-48-36	26.21	78
225	Montana Ranch - Lakewood	A	47	33-50-35	118-07-09	12.63	92
227	San Gabriel - Bruington - Orton	C	472	34-06-18	118-06-32	18.82	78
228	Beverly Hills City Hall	F	250	34-06-00	118-23-40	17.47	82
235	Henniger Flats	D	2550	34-11-38	118-05-17	27.51	78
237	Stone Canyon Reservoir	F	865	34-06-21	118-27-13	20.70	82
238	Hollywood Reservoir	F	720	34-07-04	118-19-53	17.21	78
241	Long Beach - City Hall	A	116	33-46-12	118-11-32	11.66	57
250	Acton Camp	G	2625	34-27-02	118-11-55	10.00	77
251	La Crescenta	D	1440	34-13-20	118-14-40	23.83	77
252	Castaic Dam	G	1150	34-29-53	118-36-53	16.40	77
255	Mt. San Antonio College - Spadra	C	720	34-02-41	117-50-19	16.78	77
259	Chatsworth - Twin Lakes	B	1275	34-16-43	118-35-41	18.02	60
261	Acton - Escondido Canyon	G	2960	34-29-42	118-16-22	10.32	110
269	Diamond Bar Fire Station	C	870	33-59-50	117-48-55	16.80	79
277	Sawmill Mountain	H	3700	34-43-15	118-35-00	22.09	72
280	Flintridge-Sacred Heart	C	1600	34-10-54	118-11-08	22.10	59
283	Crystal Lake-East Pine Flat	E	5370	34-19-02	117-50-28	35.53	55
287	Glendora - City Hall	D	785	34-08-09	117-51-52	21.06	78
291	Los Angeles - 96th and Central	A	121	33-56-56	118-15-17	13.83	60
292	Encino Reservoir	F	1075	34-08-56	118-30-57	18.53	79
293	Los Angeles Reservoir	B	1150	34-17-18	118-28-54	18.10	79
294	Sierra Madre - Mira Monte Pumping Plant	D	985	34-10-11	118-02-51	24.67	77
298	Gorman - Sheriff	G	3835	34-47-47	118-51-27	12.39	69
299	Little Rock - Schwab	H	2800	34-32-12	117-58-43	6.99	77
303	Haines Canyon	D	3419	34-16-03	118-15-02	6.96	79
304	Mendenhall Ridge	D	3770	34-20-37	118-18-02	31.58	56
306	Zuma Beach	F	15	34-01-15	118-49-42	15.25	77
321	Pine Canyon Patrol Station	H	3286	34-40-24	118-25-45	18.65	71
322	Munz Valley Ranch	H	2600	34-42-50	118-21-15	10.65	77
334	Cogswell Dam	D	2300	34-14-37	117-57-35	34.17	75
336	Silver Lake Reservoir	A	445	34-06-08	118-15-54	16.23	77
338	Mt. Wilson Observatory	D	5709	34-14-07	118-04-28	36.53	74
342	Upland - Chappel	C	1610	34-7-33	117-40-52	18.55	63
347	Baldwin Park Experimental Station	C	386	34-05-36	117-57-40	17.57	54
352	Lechuza Patrol Station	F	1620	34-04-38	118-52-47	22.42	51
355	Los Angeles City College	A	310	34-05-14	118-17-28	14.03	62
356	Spadra - Lanterman Hospital	C	690	34-02-31	117-48-35	16.29	87
372	San Francisquito Power House No. 2	G	1580	34-32-02	118-31-27	16.92	77
373	Briggs Terrace	D	2200	34-14-17	118-13-27	27.01	74
377	Lake Sherwood Estates	F	960	34-08-26	118-52-31	18.32	66
379	San Gabriel - East Fork	D	1600	34-14-09	117-48-18	26.04	70
387	Covina City Yard	C	508	34-05-02	117-53-57	16.96	73
388	Paramount - County Fire Department	A	80	33-53-50	118-10-02	14.77	72
390	Morris Dam	D	1210	34-10-53	117-52-43	25.82	77
391	Montebello - Fire Department	A	250	34-01-08	118-06-15	15.16	70
395	Olive View Sanitarium	G	1425	34-19-29	118-26-55	20.45	73
402	Cedar Springs	E	6780	34-21-21	117-52-34	29.50	71
405	Soledad Canyon	G	2150	34-26-23	118-17-33	14.41	71
406	West Azusa	C	505	34-06-53	117-54-56	18.18	71
409	Pyramid Reservoir	G	2505	34-40-34	118-46-47	16.42	71
415	Signal Hill - City Hall	A	140	33-47-49	118-10-03	12.22	51
423	Angeles Forest - Aliso Cyn. (Wagon Wheel)	E	3920	34-24-57	118-05-26	18.56	70
425	San Gabriel Dam	D	1481	34-12-19	117-51-38	28.72	72
433	Fair Oaks Debris Basin	D	1585	34-12-15	118-08-18	22.50	48
434	Agoura	F	800	34-08-08	118-45-08	17.84	69
435	Monte Nido	F	600	34-04-41	118-41-35	22.06	41
436	Hansen Dam	B	1110	34-16-08	118-23-59	15.50	69
444	Rolling Hills - South Coast Botanical Garden	A	400	33-47-00	118-20-35	14.68	51
445	Live Oak Dam	C	1516	34-08-02	117-44-38	17.90	55

Gage #	Station Name	Region	Elev.	Latitude	Longitude	Annual Average (in.)	Years of Record
446	Aliso Canyon - Oat Mountain	B	2367	34-18-53	118-33-25	22.85	68
447	Carbon Canyon	F	50	34-02-18	118-38-56	16.01	66
449	Eaton Wash Dam	D	880	34-10-06	118-05-33	20.76	25
453	Devils Gate Dam	C	980	34-10-53	118-10-27	19.05	31
455	Lancaster - State Hwy. Maintenance Station	H	2395	34-40-57	118-08-02	7.11	67
458	Zuma Canyon Patrol Station	F	115	34-01-10	118-47-46	14.73	36
462	Los Angeles -Hillcrest Country Club	A	185	34-02-54	118-24-06	16.31	70
465	Sepulveda Dam	B	683	34-10-06	118-28-11	16.21	68
466	Pacoima Canyon - Dutch Louie	G	3220	34-21-07	118-20-38	22.97	42
471	Little Tujunga - Gold Creek	D	2750	34-18-57	118-18-02	18.08	25
477	Santa Anita - Spring Camp	D	4655	34-12-52	117-58-56	32.12	29
482	Los Angeles - U.S.C.	A	208	34-01-14	118-17-15	14.27	69
488	Kagel Canyon Patrol Station	D	1450	34-17-45	118-22-30	16.95	64
492	Chilao - State Highway Maintenance Station	E	5275	34-19-05	118-00-30	22.42	63
493	Sand Canyon - MacMillan Ranch	G	1805	34-23-17	118-24-50	17.00	53
497	Claremont - Slaughter	C	1350	34-07-35	117-43-55	19.12	69
498	Dark Canyon Trail - Angeles Crest Highway	D	2800	34-15-21	118-11-45	25.66	45
517	Lewis Ranch	H	4615	34-25-12	117-53-11	13.08	39
542	Fairmont	H	3050	34-42-15	118-25-40	15.40	79
564	Llano	H	3390	34-29-13	117-50-02	7.41	90
565	Long Beach - City Automatic	A	11	33-47-16	118-12-08	11.46	43
566	Long Beach #1	A	15	33-46-46	118-08-36	12.03	50
591	Santa Anita Reservoir	D	1250	34-11-20	118-06-17	23.67	32
598	Neenach - Check 43 - California D.W.R.	H	2965	34-47-40	118-37-15	10.12	64
610	Pasadena - City Hall	C	864	34-08-54	118-08-36	20.48	83
612	Pasadena - Chlorine Plant	D	1160	34-12-04	118-09-49	22.84	83
613	Pasadena Fire Station	C	779	34-07-15	118-08-05	19.54	68
619	San Antonio Canyon - Sierra Power House	D	3110	34-12-29	117-40-26	31.11	105
627	San Gabriel Canyon - power house	D	744	34-09-20	117-54-28	22.91	105
634	Santa Monica	A	94	34-00-43	118-29-27	14.38	80
680	Westwood (U.C.L.A.)	A	430	34-04-10	118-26-30	18.01	75
683	Sunset Ridge	D	2110	34-12-53	118-08-47	23.36	68
694	Big Tujunga Camp 15	D	1525	34-17-22	118-17-17	15.09	70
695	Tujunga Canyon - Vogel Flat	D	1850	34-17-12	118-13-32	28.66	72
716	Los Angeles - Ducommun Street	A	306	34-03-09	118-14-13	15.67	137
726	Angeles Crest Guard Station	D	2300	34-14-01	118-11-04	27.44	62
734	El Segundo - Curia	A	125	33-55-52	118-25-07	13.06	89
735	Bell Canyon - Platt Ranch	B	895	34-11-40	118-39-23	14.79	60
740	San Dimas Canyon - Fern No. 2	D	5200	34-11-48	117-41-45	27.96	52
741	San Dimas Canyon - Upper East Fork	D	2675	34-11-41	117-44-26	21.26	53
742	San Gabriel Fire Department	C	445	34-06-11	118-05-56	17.47	68
750	Palmdale - F.A.A. Airport	H	2528	34-37-20	118-05-00	6.29	61
755	Griffith Park - Little Canyon	F	900	34-07-32	118-16-58	16.10	42
757	Griffith Park - Fern Dell	F	750	34-07-12	118-18-20	17.38	42
758	Griffith Park Ranger Headquarters	F	455	34-8-10	118-17-02	15.80	37
759	Nichols Debris Basin	F	440	34-06-10	118-21-23	15.75	42
760	Studio City - Beeman Avenue	F	627	34-08-58	118-24-24	17.64	33
762	Upper Stone Canyon	F	943	34-07-27	118-27-15	19.75	42
767	Mandeville Canyon Road	F	1160	34-06-24	118-30-10	20.36	42
772	Los Angeles - Echo Park and Lucretia	A	475	34-05-02	118-15-11	14.51	42
783	Coon Canyon	D	1350	34-12-45	118-10-12	21.29	35
794	Lower Franklin Reservoir	F	585	34-05-43	118-24-40	17.25	59
795	Pasadena - Jourdan	C	705	34-08-52	118-05-14	19.69	59
796	Elysian Park - Fire Department	A	757	34-04-55	118-14-22	12.97	41
797	De Soto Reservoir	B	1127	34-16-17	118-35-12	17.43	59
801	Magic Mountain	G	4720	34-23-18	118-19-27	17.57	44
802	Eagle Rock Reservoir	C	970	34-08-47	118-11-20	18.16	55
807	Ascot Reservoir	C	620	34-04-46	118-11-14	17.12	53
1005	Mint Canyon Fire Station	G	2300	34-30-35	118-21-40	13.03	56
1006	San Pedro - City Reservoir	A	150	33-44-37	118-17-47	12.76	63
1008	La Fresa S.C.E. Company Substation	A	65	33-52-07	118-19-55	12.66	47
1012	Castaic junction	G	1005	34-26-18	118-36-43	12.80	60
1014	Rio Hondo Spreading Grounds	A	170	33-59-57	118-06-04	12.65	36

Gage #	Station Name	Region	Elev.	Latitude	Longitude	Annual Average (in.)	Years of Record
1017	Little Rock Creek Above Dam	H	3280	34-28-41	118-01-24	9.16	49
1029	Tujunga - Mill Creek Summit Ranger Stat	E	4990	34-23-22	118-04-49	18.67	58
1035	Whittier - Wood	A	280	33-59-52	118-03-10	14.80	31
1037	Arcadia - Arboretum	C	565	34-08-48	118-02-59	19.42	57
1041	Santa Fe Dam	C	427	34-07-04	117-58-24	17.29	58
1051	Canoga Park - Pierce College	B	800	34-10-51	118-34-23	16.78	56
1058	Palmdale	H	2595	34-35-17	118-05-31	6.96	54
1062	Buckhorn Flat	E	6760	34-20-44	117-55-08	30.16	42
1070	Manhattan Beach	A	182	33-53-00	118-23-19	12.29	54
1071	Descanso Gardens	D	1325	34-12-07	118-12-46	22.11	58
1072	Little Tujunga Ranger Station	D	1275	34-17-37	118-21-38	15.32	39
1074	Little Gleason	D	5600	34-22-43	118-08-57	22.43	28
1075	Upper Wolfskill	D	3625	34-10-13	117-43-16	23.96	53
1076	Monte Cristo Ranger Station	D	3360	34-19-42	118-07-20	21.08	49
1078	Covina	C	975	34-04-10	117-50-47	16.13	36
1080	Bradbury Debris Basin	D	935	34-09-23	117-57-58	21.96	35
1081	Glendale - Gregg	B	1350	34-11-45	118-14-30	20.66	53
1087	Green - Verdugo Pumping Plant	B	1340	34-15-25	118-20-11	16.91	52
1088	La Habra Heights Mutual Water Co.	C	445	33-56-55	117-57-51	15.91	52
1093	Fullerton Airport	A	100	33-52-23	117-58-24	12.75	37
1095	Orange County Reservoir	C	660	33-56-07	117-52-58	14.56	53
1104	Bouquet Canyon at Texas Canyon	G	1760	34-30-35	118-27-00	14.13	36
1107	La Tuna Debris Basin	B	1160	34-14-13	118-19-37	16.24	32
1113	Dominguez Water Company	A	30	33-49-54	118-13-30	11.96	31
1114	Whittier Narrows Dam	C	239	34-01-29	118-05-02	15.18	51
1115	San Antonio Dam	D	2120	34-09-24	117-40-20	23.33	53
1126	Los Angeles - East Valley	B	780	34-12-30	118-24-35	15.92	50
1138	Mount Disappointment	D	5725	34-14-42	118-06-07	31.56	32
1140	Rosemead	C	305	34-04-53	118-03-55	17.31	37
1157	California State University - Northridge	B	890	34-14-17	118-31-48	14.21	25
1158	Torrance Municipal Airport	A	102	33-47-59	118-20-08	14.42	46
1159	Shortcut Canyon - West Fork	D	4425	34-15-55	118-04-08	35.00	13
1160	San Gabriel Canyon - West Fork Heliport	D	3200	34-15-02	118-01-30	34.61	26
1166	Mile High Ranch	G	5280	34-24-40	117-46-15	15.01	43
1170	Thousand Oaks Weather Station	F	805	34-10-44	118-51-01	16.65	38
1171	Camulos Ranch	G	725	34-24-22	118-45-21	18.77	37
1172	Piru Canyon Above Lake Piru	G	1120	34-30-48	118-45-24	20.85	36
1173	Tapo Canyon	B	1525	34-19-54	118-42-39	16.09	30
1177	Bard Reservoir	B	1010	34-14-32	118-49-41	15.19	26
1190	Pacoima Canyon - North Fork Ranger Station	G	4180	34-23-17	118-15-06	22.72	23
1191	Bear Divide	E	2700	34-21-35	118-23-37	25.92	36
1194	Santa Ynez Reservoir	A	735	34-04-23	118-33-59	21.16	34
1199	Cloudcroft Debris Basin	F	350	34-02-58	118-34-12	18.51	16
1212	Lancaster FSS/FAA	H	2340	34-44-00	118-13-00	7.32	33
1214	Encinal Canyon - Fire Station	F	175	34-02-52	118-52-07	13.97	12
1215	Santa Monica Canyon - Camp Kilpatrick	F	1775	34-06-45	118-49-52	19.04	12
1216	Rancho Palos Verdes	A	780	33-45-10	118-23-32	12.45	28
1217	Los Angeles Country Club	A	380	34-04-10	118-25-17	17.38	88
1222	Northridge-Garland	B	911	34-15-15	118-30-33	17.42	25
1223	Woodland Hills - Sherman	F	1035	34-10-06	118-38-57	17.53	35
1239	Malibu - Big Rock Mesa	F	725	34-02-34	118-37-16	16.10	22
1240	Pearblossom-CA D.W.R. Booster	G	3050	34-30-32	117-55-15	7.56	28
1242	Rocky Buttes	H	2540	34-38-60	117-51-48	4.50	19
1243	Redman	H	2360	34-45-52	117-55-30	5.54	22
1244	Lancaster Roper	H	2400	34-40-27	118-00-37	5.38	15
1245	Quartz Hill	H	2398	34-40-28	118-14-40	7.42	18
1246	Scott Ranch	H	2710	34-46-59	118-28-10	7.93	14
1247	North Lancaster	H	2310	34-45-41	118-07-30	4.90	16
1248	Mescal - Smith	H	3810	34-28-03	117-42-40	6.47	13
1249	Relay	H	3140	34-45-43	117-47-55	4.74	18
1250	Avek	H	2825	34-32-21	117-55-23	5.93	20
1251	Palos Verdes - Whites Point	A	100	33-42-50	118-19-02	10.39	22
1252	Palos Verdes Landfill	A	400	33-45-40	118-20-03	14.63	22

Gage #	Station Name	Region	Elev.	Latitude	Longitude	Annual Average (in.)	Years of Record
1253	Point Water Polution Control	A	40	33-48-11	118-16-58	12.29	22
1254	Long Beach Reclamation Plant	A	20	33-48-11	118-05-20	12.13	22
1255	Los Coyotes Reclamation Plant	A	70	33-53-05	118-06-24	12.98	22
1256	South Gate Transfer Station	A	100	33-56-40	118-09-56	12.45	21
1257	San Jose Creek Reclamation Plant	A	275	34-01-55	118-01-16	15.03	22
1258	Puente Hills Landfill	C	300	34-01-35	118-01-49	16.22	22
1259	Whittier Narrows Reclamation	C	225	34-03-59	118-03-54	14.31	22
1260	Spadra Landfill	C	700	34-02-36	117-49-50	16.40	22
1261	La Canada Reclamation Plant	D	1800	34-13-00	118-11-14	22.24	22
1262	Saugus Reclamation Plant	G	1150	34-24-48	118-32-23	13.78	22
1263	Valencia Reclamation Plant	G	1000	34-25-55	118-37-13	13.26	22
1264	Calabasas Landfill	F	800	34-08-25	118-42-35	18.30	22
1265	Scholl Canyon Landfill	F	1000	34-08-40	118-11-07	19.25	22
1266	Mission Canyon Landfill	C	1150	34-08-40	118-28-45	17.13	22
1267	Lancaster Reclamation Plant	H	2302	34-46-38	118-09-11	6.18	22
1268	Palmdale Reclamation Plant	H	2565	34-35-30	118-05-10	6.83	22
1271	Pomona Waste Reclamation Plant	C	786	34-03-18	117-47-34	16.30	22
1274	Whittier - Valna Drive	C	255	33-57-39	118-01-10	18.18	13
1277	Fremont Headquarters	C	450	34-05-06	118-08-56	16.84	12
1278	La Canada	D	1647	34-13-22	118-12-17	20.24	22

Appendix B - Rain Gage Statistics, PMPs, and AEPs

Station Number	Region	Statistical Data									HMR 58-59 24-hr PMP	PMP Frequency	Hershfield Estimate	Hershfield Frequency	Magnitued Difference
		Mean	St. Dev.	LCv	LCs	LCk	alpha	beta	Cv-mom	Ck-mom					
5	F	3.0919	0.9161	0.2963	0.2146	0.1035	1.3216	2.3290	0.2067	0.0499	23.15	10^6	29.25	10^8	2
6	F	4.5925	1.3372	0.2912	0.2737	0.1701	1.9291	3.4790	0.0942	0.0719	31.51	10^6	37.44	10^7	1
9	B	2.7030	0.7048	0.2608	0.2248	0.1399	1.0168	2.1160	0.4728	0.2005	21.00	10^8	23.19	10^9	1
10	F	3.2486	0.9228	0.2841	0.2665	0.1292	1.3314	2.4801	0.2669	0.2778	26.33	10^7	26.51	10^7	0
11	F	2.9916	0.8035	0.2686	0.2495	0.1401	1.1593	2.3225	0.3824	0.3898	25.65	10^8	24.41	10^8	0
13	F	3.0277	0.8420	0.2781	0.2080	0.1778	1.2148	2.3265	0.4652	1.1605	24.00	10^7	30.21	10^9	2
20	F	3.2229	0.9027	0.2801	0.1450	0.0244	1.3023	2.4712	0.1724	0.0382	24.10	10^7	26.82	10^8	1
21	F	2.5192	0.6528	0.2591	0.1390	0.0373	0.9418	1.9756	0.3428	-0.4431	22.87	10^9	21.65	10^9	0
23	B	2.5026	0.6056	0.2420	0.1371	0.1003	0.8737	1.9983	0.6429	0.6440	21.00	10^9	19.07	10^8	-1
25	B	2.4307	0.6443	0.2651	0.1937	0.0967	0.9295	1.8942	0.5795	0.2497	21.00	10^8	21.14	10^8	0
28	B	2.6435	0.7261	0.2747	0.2969	0.1710	1.0475	2.0388	0.5730	0.7021	21.00	10^7	21.47	10^8	1
32	G	3.1536	0.8534	0.2706	0.1761	0.0776	1.2313	2.4429	0.2082	-0.0300	22.68	10^7	26.87	10^8	1
33	G	2.7985	0.6694	0.2392	0.1868	0.1368	0.9658	2.2410	0.6576	1.1408	26.85	10^11	20.10	10^8	-3
42	A	1.8773	0.5046	0.2688	0.2157	0.1005	0.7280	1.4571	1.1703	0.4470	16.70	10^9	16.97	10^9	0
43	A	1.9562	0.5034	0.2573	0.2128	0.1169	0.7262	1.5370	1.3443	1.4714	15.48	10^8	16.73	10^9	1
44	A	1.8947	0.5232	0.2762	0.2520	0.1560	0.7549	1.4590	1.4510	2.3344	14.10	10^7	17.31	10^9	2
46	D	4.5209	1.3248	0.2930	0.2985	0.1976	1.9112	3.4177	0.0934	0.0632	40.72	10^8	37.58	10^7	-1
47	D	5.7168	1.7131	0.2997	0.2644	0.1653	2.4714	4.2902	0.0421	0.0229	44.27	10^7	43.29	10^6	-1
53	D	5.5842	1.8916	0.3387	0.3293	0.2099	2.7290	4.0090	0.0371	0.0254	45.85	10^6	50.03	10^7	1
54	E	3.2879	1.0899	0.3315	0.2548	0.1607	1.5724	2.3803	0.1465	0.0705	28.43	10^7	33.68	10^8	1
57	D	6.8934	1.9942	0.2893	0.2254	0.1810	2.8770	5.2328	0.0273	0.0157	48.00	10^6	46.78	10^6	0
60	D	6.5369	2.4738	0.3784	0.4652	0.3347	3.5689	4.4769	0.0171	0.0124	38.38	10^4	39.18	10^4	0
63	D	3.8828	1.1058	0.2848	0.2896	0.2209	1.5954	2.9619	0.2063	0.3231	31.00	10^7	30.25	10^7	0
68	D	4.1532	1.1059	0.2663	0.3146	0.2203	1.5954	3.2323	0.2128	0.3552	29.34	10^7	22.40	10^5	-2
73	D	3.4143	0.8250	0.2416	0.2927	0.2249	1.1902	2.7273	0.3716	0.3183	26.74	10^8	27.25	10^8	0
78	D	5.7094	1.3971	0.2447	0.1394	0.1276	2.0156	4.5459	0.0512	0.0156	40.35	10^7	34.35	10^6	-1
82	H	2.6333	0.7326	0.2782	0.1723	0.1274	1.0570	2.0232	0.3693	0.1513	28.96	10^11	23.82	10^8	-3
83	H	4.0071	1.0367	0.2587	0.2531	0.1924	1.4957	3.1437	0.1729	0.1298	29.83	10^7	31.66	10^8	1
89	D	3.2921	0.8897	0.2702	0.3036	0.2589	1.2835	2.5513	0.3496	0.5213	26.43	10^8	26.41	10^8	0
92	C	2.6517	0.6336	0.2389	0.2329	0.1444	0.9140	2.1241	0.7624	0.9028	20.38	10^8	20.27	10^8	0
93	C	2.6001	0.6117	0.2352	0.1920	0.1831	0.8824	2.0908	0.9256	2.0270	20.60	10^9	18.51	10^8	-1
95	C	2.7470	0.6779	0.2468	0.2470	0.1970	0.9780	2.1825	0.6547	0.8032	22.42	10^8	22.25	10^8	0
96	C	2.6209	0.6099	0.2327	0.2194	0.1991	0.8799	2.1130	0.9033	1.4976	21.46	10^9	19.50	10^8	-1
106	A	2.2501	0.5227	0.2323	0.1891	0.1587	0.7541	1.8149	1.3259	2.6949	18.05	10^9	16.50	10^8	-1
107	A	2.3857	0.5833	0.2445	0.1606	0.1187	0.8416	1.9000	0.7175	0.4309	16.62	10^7	19.49	10^9	2
108	C	2.6138	0.6327	0.2421	0.2649	0.2120	0.9128	2.0869	0.9823	2.1292	19.24	10^8	20.54	10^8	0
109	C	3.0006	0.8239	0.2746	0.2710	0.2167	1.1887	2.3145	0.6033	1.9012	22.03	10^7	34.20	10^11	4
116	A	2.2501	0.6191	0.2752	0.2093	0.1068	0.8932	1.7346	0.7094	0.4416	18.74	10^8	21.06	10^9	1
120	G	1.4603	0.3636	0.2490	0.2422	0.2266	0.5246	1.1575	3.9508	7.1893	13.00	10^9	13.46	10^10	1
124	G	2.3869	0.5660	0.2371	0.2710	0.2122	0.8165	1.9156	1.3060	2.9075	21.65	10^10	16.35	10^7	-3
125	G	2.5748	0.6465	0.2511	0.1743	0.1047	0.9327	2.0364	0.5178	0.0978	20.90	10^8	21.45	10^9	1
128	G	3.6370	0.9034	0.2484	0.1348	0.0762	1.3034	2.8847	0.1122	-0.0908	25.59	10^7	29.10	10^8	1
134	C	2.9000	0.7296	0.2516	0.1919	0.2401	1.0525	2.2633	0.4447	0.6080	23.85	10^8	23.36	10^8	0
140	A	2.8293	0.6501	0.2298	0.1239	0.1275	0.9380	2.2879	0.4216	0.1319	23.17	10^9	20.92	10^8	-1
144	D	3.6243	0.9492	0.2619	0.2104	0.1656	1.3695	2.8338	0.2633	0.3795	29.14	10^8	27.21	10^7	-1
156	A	2.2781	0.6323	0.2776	0.2585	0.0529	0.9122	1.7515	0.6384	0.1089	15.11	10^6	20.96	10^9	3
157	A	2.0625	0.5270	0.2555	0.2609	0.1345	0.7603	1.6236	1.3071	1.3200	18.31	10^9	17.57	10^9	0
158	D	4.9310	1.3614	0.2761	0.3662	0.2671	1.9641	3.7973	0.0976	0.0864	33.71	10^6	35.78	10^7	1
167	D	3.3527	0.8686	0.2591	0.2014	0.1416	1.2531	2.6293	0.2600	0.1385	25.73	10^8	28.08	10^8	0
169	D	3.2736	0.8709	0.2660	0.2471	0.1884	1.2565	2.5484	0.4099	0.8557	26.52	10^8	23.54	10^7	-1
170	C	2.6190	0.6691	0.2555	0.2119	0.1941	0.9653	2.0618	0.7992	1.7619	18.75	10^7	20.59	10^8	1
172	D	2.9429	0.8286	0.2816	0.0967	0.1288	1.1954	2.2416	0.1691	0.0879	22.01	10^7	25.67	10^8	1
174	C	3.0092	0.7086	0.2355	0.2467	0.2087	1.0222	2.4191	0.5193	0.4085	23.74	10^9	23.93	10^9	0
175	D	3.5906	0.9491	0.2643	0.1521	0.1084	1.3692	2.7712	0.1332	0.0111	35.91	10^10	29.31	10^8	-2
176	D	3.4512	0.9226	0.2673	0.2119	0.1307	1.3310	2.6829	0.2224	0.1263	29.66	10^8	28.52	10^8	0
178	C	2.8524	0.6550	0.2296	0.2523	0.2336	0.9449	2.3070	0.7622	1.0904	21.38	10^8	22.08	10^9	1
179	D	4.0960	1.1141	0.2720	0.2143	0.1445	1.6073	3.1682	0.1410	0.1103	28.78	10^6	31.77	10^7	1
191	C	2.4692	0.5396	0.2185	0.1770	0.0632	0.7785	2.0198	0.8649	-0.1421	19.81	10^9	18.79	10^9	0
196	C	2.7135	0.6879	0.2535	0.2007	0.2212	0.9924	2.1223	0.5624	0.7988	21.76	10^8	22.47	10^8	0
201	C	3.0592	0.7259	0.2373	0.2121	0.1698	1.0472	2.4547	0.5513	0.8062	18.58	10^6	22.25	10^8	2
210	B	3.4394	1.0205	0.2967	0.2831	0.2277	1.4722	2.5896	0.2403	0.3622	26.02	10^6	37.58	10^10	4
213	A	2.6795	0.6631	0.2475	0.1154	0.0403	0.9567	2.1273	0.3469	-0.1390	20.95	10^8	21.63	10^8	0
216	B	2.7848	0.7676	0.2756	0.2818	0.2352	1.1073	2.1456	0.6316	1.5929	25.37	10^9	20.78	10^7	-2
223	D	3.6940	0.8647	0.2341	0.1999	0.1913	1.2476	2.9739	0.2879	0.2731	29.63	10^9	26.22	10^8	-1
225	A	2.0832	0.5346	0.2566	0.1930	0.1429	0.7713	1.6379	1.0721	0.9647	14.43	10^7	18.19	10^9	2
227	C	3.0222	0.8637	0.2858	0.2957	0.2332	1.2461	2.3029	0.4640	1.0997	20.79	10^6	22.28	10^6	0
228	F	2.9335	0.7519	0.2563	0.1499	0.1491	1.0848	2.2793	0.2899	0.1746	24.86	10^9	24.73	10^8	-1
235	D	4.0679	1.1836	0.2910	0.2420	0.1547	1.7075	3.0823	0.1175	0.0697	32.95	10^7	34.91	10^8	1
237	F	3.3579	0.8211	0.2445	0.2020	0.1837	1.1846	2.6742	0.4282	0.8281	28.07	10^9	23.20	10^7	-2
238	F	2.5771	0.6192	0.2403	0.2214	0.2124	0.8933	2.0614	1.3024	5.0583	24.00	10^10	15.65	10^6	-4
241	A	2.0796	0.5560	0.2673	0.2380	0.1436	0.8021	1.6167	0.9935	0.4576	13.87	10^6	19.50	10^9	3
250	G	2.0468	0.5649	0.2760	0.2747	0.2193	0.8150	1.5764	1.2574	2.3095	15.56	10^7	16.30	10^7	0
251	D	3.8158	1.0680	0.2799	0.2296	0.1314	1.5408	2.9265	0.1574	0.1091	33.92	10^8	32.13	10^8	0
252	G	2.2853	0.5888	0.2576	0.1165	0.1591	0.8495	1.7741	0.4217	0.7722	18.15	10^8	19.05	10^8	0
255	C	2.4464	0.5240	0.2142	0.1917	0.1976	0.7559	2.0100	1.2340	2.4472	21.00	10^10	17.18	10^8	-2
259	B	2.8283	0.7261	0.2567	0.1935	0.1169	1.0476	2.2236	0.4287	0.2581	24.46	10^9	22.94	10^8	-1
261	G	1.7640	0.4939	0.2800	0.2124	0.1727	0.7126	1.3527	1.4274	1.3182	14.06	10^8	16.96	10^9	1
269	C	2.7399	0.7052	0.2574	0.1385	0.1651	1.0174	2.1759	0.3253	0.1837	21.00	10^9	23.42	10^9	0
277	H	3.4075	0.8507	0.2497	0.1865	0.1022	1.2274	2.6990	0.2451	0.1098	27.19	10^9	26.08	10^8	-1
280	C	3.9864	1.2153	0.3049	0.2325	0.1866	1.7533	2.9744	0.1297	0.1420	30.01	10^6	32.78	10^7	1
283	E	6.0942	1.6837	0.2763	0.2821	0.2369	2.4291	4.6921	0.0480	0.0310	43.89	10^7	41.98	10^6	-1
287	D	3.0760	0.7315	0.2378	0.2483	0.2470	1.0554	2.4668	0.5919	1.0115	23.58	10^8	23.52	10^8	0
291	A	2.5547	0.6767	0.2649	0.1882	0.0744	0.9763	1.9911	0.4616	0.0891	17.88	10^7	22.26	10^9	2
292	F	3.2161	0.8890	0.2764	0.1747	0.0694	1.2826	2.4758	0.1902	-0.0015	29.21	10^9	27.78	10^8	-1
293	B	2.6387	0.5697	0.2159	0.1770	0.1974	0.8219	2.1643	1.3922	4.7777	21.61	10^10	16.18	10^7	-3
294	D	3.6310	0.9430	0.2597	0.2135	0.1936	1.3604	2.8458	0.2975	0.5240	27.95	10^8	25.94	10^7	-1
298	G	2.0325	0.4818	0.2371	0.1614	0.1886	0.6951	1.6312	1.3694	1.6735	13.44	10^7	16.78	10^9	2
299	H	1.3409	0.3689	0.2751	0.2200	0.2362	0.5322	1.0202	4.8207	23.1259	9.97	10^7	11.42	10^8	1
303	D	3.3505	0.9365	0.2795	0.2998	0.1973	1.3511	2.5706	0.2550	0.1930	39.00	10^11	29.97	10^8	-3
304	D	6.4992	2.0239	0.3114	0.2504	0.1778	2.9199	4.8138	0.0354	0.0349	32.44	10^4	37.96	10^4	0

Station Number	Region	Statistical Data									HMR 58-59 24-hr PMP	PMP Frequency	Hershfield Estimate	Hershfield Frequency	Magnitued Difference
		Mean	St. Dev.	LCv	LCs	LCk	alpha	beta	Cv-mom	Ck-mom					
306	F	2.2664	0.6654	0.2936	0.1566	0.1327	0.9600	1.7028	0.3395	-0.0392	17.91	10^7	22.28	10^9	2
321	H	2.9910	0.8347	0.2791	0.1889	0.1062	1.2042	2.2959	0.2428	0.0264	22.48	10^7	27.13	10^8	1
322	H	1.9653	0.5652	0.2876	0.1893	0.0929	0.8154	1.4947	0.7394	-0.1330	13.09	10^6	19.40	10^9	3
334	D	6.7009	1.8967	0.2831	0.2976	0.1927	2.7363	5.1214	0.0369	0.0289	41.29	10^5	41.71	10^5	0
336	A	2.4686	0.6270	0.2540	0.2325	0.1674	0.9046	1.9464	1.0732	3.2714	21.58	10^9	17.23	10^7	-2
338	D	5.5848	1.6050	0.2874	0.2206	0.1388	2.3156	4.1895	0.0389	0.0126	22.56	10^3	44.40	10^7	4
342	C	2.9886	0.7089	0.2372	0.1956	0.1849	1.0227	2.3983	0.5075	0.5228	22.79	10^8	22.89	10^8	0
347	C	3.4304	1.1137	0.3247	0.3824	0.2518	1.6067	2.5030	0.1648	0.1357	19.72	10^4	34.00	10^8	4
352	F	3.8596	1.1069	0.2868	0.2048	0.1264	1.5970	2.9378	0.1112	0.0342	30.57	10^7	32.63	10^8	1
355	A	2.8839	0.7379	0.2559	0.1653	0.1375	1.0645	2.2694	0.5397	1.1872	20.89	10^7	20.29	10^7	0
356	C	2.6775	0.6578	0.2457	0.1825	0.1644	0.9490	2.1297	0.6557	0.9924	20.25	10^8	20.81	10^8	0
372	G	2.5157	0.6465	0.2570	0.1922	0.1211	0.9328	1.9773	0.6673	0.7935	17.64	10^7	20.89	10^8	1
373	D	4.1945	1.2043	0.2871	0.2256	0.1526	1.7374	3.1916	0.1054	0.0542	36.71	10^8	35.29	10^8	0
377	F	3.3085	0.8962	0.2709	0.2483	0.1395	1.2930	2.5622	0.2950	0.3064	31.55	10^9	26.86	10^8	-1
379	D	4.2747	1.0927	0.2556	0.1921	0.1426	1.5764	3.3648	0.1330	0.0772	33.00	10^8	30.64	10^7	-1
387	C	2.4217	0.5242	0.2164	0.1137	0.1886	0.7562	1.9622	0.6178	0.9246	20.50	10^10	18.32	10^9	-1
388	A	2.4203	0.6726	0.2779	0.2116	0.1251	0.9703	1.8372	0.4886	0.2438	16.04	10^6	22.00	10^9	3
390	D	3.8668	1.0175	0.2631	0.2488	0.2014	1.4679	3.0195	0.1822	0.1089	29.30	10^7	32.23	10^8	1
391	A	2.4315	0.6049	0.2488	0.1140	0.1157	0.8727	1.9090	0.4534	0.9178	18.42	10^8	19.34	10^8	0
395	G	2.9290	0.7533	0.2572	0.2450	0.1315	1.0868	2.3017	0.4139	0.2414	25.73	10^9	24.32	10^8	-1
402	E	4.5287	1.0730	0.2369	0.1411	0.0918	1.5480	3.6351	0.1110	0.0389	41.04	10^10	29.80	10^7	-3
405	G	2.6277	0.7695	0.2929	0.2314	0.1358	1.1102	1.9869	0.3679	0.1173	18.27	10^6	26.04	10^9	3
406	C	2.7055	0.6157	0.2276	0.1603	0.1803	0.8882	2.1928	0.9166	2.3424	20.77	10^9	18.03	10^7	-2
409	G	2.9537	0.7522	0.2547	0.1640	0.1316	1.0852	2.3273	0.3327	0.1374	23.58	10^8	24.37	10^8	0
415	A	2.4027	0.6956	0.2895	0.2511	0.1635	1.0035	1.8235	0.5760	0.5362	13.91	10^5	22.20	10^8	3
423	E	3.0900	0.8002	0.2590	0.2736	0.2057	1.1544	2.4237	0.4057	0.4409	20.66	10^6	24.95	10^8	2
425	D	5.2132	1.4130	0.2710	0.3144	0.2287	2.0385	4.0365	0.0904	0.0895	34.00	10^6	34.40	10^7	1
433	D	3.7437	1.0995	0.2937	0.1983	0.0406	1.5862	2.8281	0.0986	-0.0266	34.51	10^8	33.72	10^8	0
434	F	3.3166	0.9558	0.2882	0.1384	0.0489	1.3789	2.5207	0.1199	-0.0530	29.69	10^8	30.04	10^8	0
435	F	3.8858	0.9834	0.2531	0.1657	0.1087	1.4187	3.0669	0.1610	0.0720	33.00	10^9	29.25	10^8	-1
436	B	2.4043	0.6823	0.2838	0.1616	0.0687	0.9844	1.8361	0.3764	-0.1632	21.20	10^8	22.53	10^9	1
444	A	2.4442	0.7158	0.2929	0.2448	0.1419	1.0327	1.8481	0.6084	0.9869	14.92	10^5	20.47	10^7	2
445	C	3.3465	1.0348	0.3092	0.2750	0.1604	1.4930	2.4847	0.1854	0.1220	23.83	10^6	28.69	10^7	1
446	B	3.4715	0.9600	0.2765	0.2214	0.1263	1.3850	2.6720	0.2121	0.1608	29.26	10^8	27.26	10^7	-1
447	F	2.5765	0.6484	0.2517	0.2040	0.1002	0.9354	2.0366	0.5909	0.3244	23.09	10^9	20.72	10^8	-1
449	D	3.1768	1.0681	0.3362	0.2278	0.0900	1.5410	2.2873	0.1194	-0.0167	28.09	10^7	33.09	10^8	1
453	C	3.2271	1.0320	0.3198	0.1450	0.1390	1.4889	2.3677	0.1129	0.0160	30.10	10^8	30.87	10^8	0
455	H	1.3645	0.4416	0.3236	0.3209	0.2500	0.6371	0.9968	3.3462	14.2536	8.18	10^4	12.49	10^7	3
458	F	2.7029	0.7651	0.2831	0.2085	0.0574	1.1038	2.0657	0.3111	-0.0663	18.00	10^6	24.52	10^8	2
462	A	2.8003	0.7146	0.2552	0.2075	0.1186	1.0310	2.2052	0.4182	0.1260	22.16	10^8	23.89	10^9	1
465	B	2.8732	0.7968	0.2773	0.1885	0.0827	1.1495	2.2097	0.2710	-0.0375	24.00	10^8	26.28	10^9	1
466	G	4.0105	1.1656	0.2906	0.1985	0.0843	1.6816	3.0399	0.0868	-0.0156	30.60	10^7	36.28	10^8	1
471	D	3.8905	1.3060	0.3357	0.2520	0.0490	1.8841	2.8029	0.0639	-0.0204	28.71	10^5	39.41	10^8	3
477	D	6.7134	2.3934	0.3565	0.3317	0.1550	3.4530	4.7203	0.0164	0.0061	41.50	10^4	51.05	10^5	1
482	A	2.3330	0.6307	0.2703	0.1377	0.0875	0.9099	1.7803	0.3780	-0.1170	19.32	10^8	21.10	10^9	1
488	D	2.3672	0.5345	0.2258	0.2036	0.1755	0.7711	1.9221	1.2051	1.7755	23.97	10^12	17.26	10^8	-4
492	E	4.1927	1.3740	0.3277	0.1846	0.1727	1.9823	3.0485	0.0727	0.0496	41.17	10^8	34.83	10^6	-2
493	G	3.0750	0.7025	0.2285	0.0536	0.0515	1.0135	2.4900	0.1417	-0.3198	30.84	10^12	22.90	10^8	-4
497	C	2.7319	0.6035	0.2209	0.1866	0.2273	0.8706	2.2293	0.9553	1.9785	23.21	10^10	19.43	10^8	-2
498	D	5.0579	1.6709	0.3304	0.3121	0.1671	2.4106	3.6664	0.0433	0.0147	40.52	10^6	45.46	10^7	1
517	H	3.0792	1.0082	0.3274	0.2257	0.1008	1.4546	2.2396	0.1629	0.0491	28.22	10^7	30.16	10^8	1
542	H	2.5576	0.7019	0.2744	0.2197	0.1558	1.0126	1.9731	0.5594	0.7064	18.62	10^7	21.91	10^8	1
564	H	1.3857	0.3525	0.2544	0.2056	0.1971	0.5086	1.0803	4.5967	17.7096	12.19	10^9	11.75	10^9	0
565	A	2.1715	0.5681	0.2616	0.2100	0.1696	0.8196	1.6984	1.1098	1.9302	13.97	10^6	16.88	10^8	2
566	A	2.0642	0.5295	0.2565	0.1817	0.0976	0.7639	1.6232	0.9575	0.3111	13.72	10^6	17.55	10^9	3
591	D	3.2859	0.7967	0.2424	0.0872	0.1162	1.1493	2.6225	0.1586	-0.0542	31.61	10^10	25.53	10^8	-2
598	H	1.6237	0.5209	0.3208	0.1203	0.1181	0.7515	1.2078	0.7277	0.0927	12.02	10^6	17.73	10^9	3
610	C	3.1578	0.7769	0.2460	0.1714	0.1254	1.1208	2.5109	0.3318	0.2111	25.66	10^8	24.41	10^8	0
612	D	3.4892	0.9627	0.2759	0.2046	0.1180	1.3889	2.6875	0.1999	0.1296	33.43	10^9	29.40	10^8	-1
613	C	3.0222	0.8133	0.2691	0.2157	0.1275	1.1733	2.3450	0.3082	0.1253	22.60	10^7	26.09	10^8	1
619	D	4.8849	1.2734	0.2607	0.2117	0.1557	1.8371	3.8244	0.0952	0.0761	40.29	10^8	39.54	10^8	0
627	D	3.5914	0.8495	0.2365	0.2582	0.2320	1.2256	2.8839	0.3024	0.1944	24.85	10^7	24.27	10^7	0
634	A	2.3408	0.6066	0.2591	0.1804	0.1535	0.8751	1.8087	0.5490	0.1863	20.95	10^9	20.66	10^9	0
680	A	2.9260	0.7611	0.2601	0.1611	0.0619	1.0981	2.2922	0.2627	-0.1343	24.92	10^8	24.88	10^8	0
683	D	3.4300	1.1108	0.3238	0.2501	0.1878	1.6025	2.4820	0.1452	0.1047	37.18	10^9	32.65	10^8	-1
694	D	3.1683	0.9358	0.2954	0.3142	0.1820	1.3501	2.3890	0.3160	0.4962	28.50	10^8	24.34	10^7	-1
695	D	4.7658	1.5096	0.3168	0.2905	0.1776	2.1779	3.5087	0.0611	0.0308	39.00	10^7	42.65	10^7	0
716	A	2.4261	0.6248	0.2575	0.2121	0.1154	0.9014	1.9058	0.8299	1.5444	19.69	10^8	22.23	10^9	1
726	D	3.8410	1.3863	0.3609	0.1873	0.1873	1.9999	2.8410	0.0535	0.0248	37.97	10^7	39.20	10^7	0
734	A	2.0091	0.5567	0.2771	0.2303	0.1578	0.8031	1.5455	1.0806	1.3834	18.52	10^9	18.07	10^8	-1
735	B	2.5282	0.7346	0.2906	0.1774	0.0833	1.0598	1.9164	0.3391	-0.0070	21.65	10^8	23.44	10^8	0
740	D	6.3069	2.0881	0.3311	0.3592	0.2058	3.0124	4.5680	0.0325	0.0304	40.57	10^5	37.94	10^4	-1
741	D	2.9178	0.9970	0.3417	-0.0921	0.0468	1.4384	4.4036	0.0053	0.0033	37.39	10^9	23.40	10^5	-4
742	C	2.7246	0.7138	0.2620	0.1876	0.1552	1.0298	2.1028	0.4330	0.4477	20.64	10^7	23.10	10^8	1
750	H	1.1250	0.3415	0.3036	0.1344	0.1422	0.4927	0.8263	2.7740	1.2236	8.46	10^6	12.26	10^10	4
755	F	2.6506	0.7167	0.2704	0.1467	0.0859	1.0340	2.0537	0.3532	0.0889	24.00	10^9	21.92	10^8	-1
757	F	2.4322	0.6712	0.2760	0.1733	0.0684	0.9684	1.8732	0.4024	-0.2105	24.00	10^9	22.05	10^9	0
758	F	2.7963	0.7312	0.2615	0.1288	0.0558	1.0549	2.1874	0.2314	-0.2886	24.00	10^8	24.86	10^9	1
759	F	2.8756	0.6935	0.2412	0.0792	0.0316	1.0005	2.2981	0.1733	-0.4472	24.00	10^9	23.49	10^9	0
760	F	2.9831	0.8919	0.2990	0.2188	0.0567	1.2867	2.2404	0.1868	-0.0990	24.37	10^7	29.06	10^9	2
762	F	3.3906	0.9912	0.2923	0.1986	0.0922	1.4300	2.5651	0.1582	0.0343	28.06	10^7	29.01	10^8	1
767	F	3.8517	1.0194	0.2647	0.1855	0.1301	1.4707	3.0028	0.1516	0.0593	30.00	10^7	29.77	10^7	0
772	A	2.4436	0.6254	0.2559	0.1077	0.0535	0.9023	1.9228	0.4327	0.0696	20.58	10^8	19.35	10^8	0
783	D	4.2456	1.4291	0.3366	0.2630	0.0588	2.0617	3.0555	0.0518	-0.0102	35.24	10^6	44.91	10^8	2
794	F	2.6347	0.6104	0.2317	0.1006	0.0714	0.8806	2.1264	0.3042	-0.5728	25.66	10^11	21.13	10^9	-2
795	C	3.0152	0.7724	0.2562	0.1843	0.1091	1.1144	2.3719	0.3286	0.1160	25.13	10^8	24.29	10^8	0
796	A	2.1572	0.5888	0.2729	0.1879	0.1899	0.8495	1.6669	1.2468	3.6298	20.46	10^9	14.02	10^6	-3
797	B	2.6639	0.6431	0.2414	0.1301	0.1042	0.9278	2.1284	0.3991	-0.1942	22.39	10^9	21.68	10^9	0
801	G	3.7097	1.1730	0.3162	0.3388	0.2386	1.6922	2.7329	0.1521	0.1551	31.06	10^7	28.10	10^6	-1
802	C	2.5867	0.6150	0.2378	0.2087	0.0999	0.8873	2.0746	0.7200	0.5595	25.04	10^11	19.43	10^8	-3
807	C	2.4981	0.5363	0.2147	0.1377	0.0247	0.7737	2.0515	0.6062	-1.0517	20.31	10^10	18.42	10^9	-1
1005	G	1.8304	0.4687	0.2561	0.2085	0.0580	0.6762	1.4400	1.2872	-0.7599	15.38	10^8	16.54	10^9	1
1006	A	1.9943	0.4891	0.2452	0.1597	0.2329	0.7056	1.5693	1.6432	5.0417	13.96	10^7	15.36	10^8	1

Station Number	Region	Statistical Data									HMR 58-59 24-hr PMP	PMP Frequency	Hershfield Estimate	Hershfield Frequency	Magnitued Difference
		Mean	St. Dev.	LCv	LCs	LCk	alpha	beta	Cv-mom	Ck-mom					
1008	A	2.4196	0.9237	0.3818	0.5628	0.4807	1.3326	1.6504	0.2112	0.4397	16.88	10^4	8.29	10^3	-1
1012	G	2.2480	0.5788	0.2575	0.1420	0.0368	0.8350	1.7660	0.4873	-0.5704	19.34	10^8	19.49	10^9	1
1014	A	2.2084	0.5058	0.2290	0.2067	0.1505	0.7297	1.7872	1.8469	5.3419	18.07	10^9	13.16	10^6	-3
1017	H	1.7724	0.5285	0.2982	0.2394	0.1639	0.7624	1.3323	1.2273	1.1288	15.98	10^8	17.15	10^9	1
1029	E	2.9334	0.7637	0.2603	0.1697	0.0823	1.1017	2.2975	0.2675	-0.1263	23.33	10^8	25.36	10^9	1
1035	A	2.4417	0.5186	0.2124	0.1921	0.1965	0.7482	2.0098	1.7772	5.5507	18.22	10^9	12.86	10^6	-3
1037	C	3.0207	0.7685	0.2544	0.2069	0.1461	1.1088	2.3807	0.4313	0.4985	24.17	10^8	23.46	10^8	0
1041	C	2.7633	0.6668	0.2413	0.1225	0.0962	0.9619	2.2080	0.4412	0.3625	20.41	10^8	20.56	10^8	0
1051	B	2.8541	0.7831	0.2744	0.1591	0.0704	1.1297	2.2020	0.2618	-0.0330	22.57	10^7	25.15	10^8	1
1058	H	1.1976	0.3027	0.2527	0.0793	0.1169	0.4367	0.9455	2.3715	-5.6724	10.46	10^9	11.12	10^10	1
1062	E	5.5954	1.6315	0.2916	0.3221	0.2022	2.3537	4.2368	0.0527	0.0291	42.61	10^7	43.11	10^7	0
1070	A	1.8659	0.4746	0.2544	0.2030	0.1418	0.6847	1.4707	1.5113	1.8714	17.66	10^10	15.63	10^8	-2
1071	D	3.2195	0.8580	0.2665	0.2124	0.1121	1.2378	2.5050	0.2517	0.0815	32.44	10^10	26.56	10^8	-2
1072	D	2.6895	0.6878	0.2557	0.2193	0.1207	0.9923	2.1167	0.5580	0.4652	24.34	10^9	21.19	10^8	-1
1074	D	3.8175	1.6223	0.4250	0.3019	0.1173	2.3404	2.4666	0.0432	0.0060	33.07	10^5	48.30	10^8	3
1075	D	5.9187	2.1376	0.3612	0.3722	0.2032	3.0839	4.1386	0.0248	0.0128	33.10	10^4	53.02	10^6	2
1076	D	3.4759	0.9587	0.2758	0.2830	0.1890	1.3832	2.6775	0.2291	0.1487	32.10	10^9	29.51	10^8	-1
1078	C	2.6723	0.5821	0.2178	0.2468	0.2173	0.8398	2.1875	1.1107	2.0585	21.00	10^9	16.31	10^7	-2
1080	D	3.6965	0.9076	0.2455	0.2194	0.1573	1.3094	2.9406	0.2262	0.0754	25.08	10^7	29.65	10^8	1
1081	B	3.1085	0.8218	0.2644	0.1630	0.0989	1.1856	2.4241	0.2548	0.0815	30.19	10^10	25.37	10^8	-2
1087	B	2.5624	0.6207	0.2422	0.0917	0.1486	0.8955	2.0160	0.3718	0.3305	26.23	10^11	20.68	10^9	-2
1088	C	2.6002	0.6449	0.2480	0.0610	0.1382	0.9304	2.0347	0.3323	0.5321	17.86	10^7	20.05	10^8	1
1093	A	2.1278	0.4555	0.2140	0.1727	0.1567	0.6571	1.7485	1.9699	5.0441	14.28	10^8	13.25	10^7	-1
1095	C	2.4044	0.5918	0.2461	0.1549	0.0999	0.8538	1.9116	0.5689	-0.2633	18.01	10^8	20.26	10^9	1
1104	G	1.7669	0.5271	0.2983	-0.0464	0.1489	0.7604	1.3847	0.1777	0.4783	15.44	10^8	19.10	10^10	2
1107	B	2.8888	0.8527	0.2952	0.2474	0.1001	1.2302	2.1786	0.2984	0.1871	30.85	10^10	24.60	10^7	-3
1113	A	2.6239	0.8680	0.3308	0.1942	0.1609	1.2522	1.9011	0.2546	0.1360	15.05	10^4	27.36	10^8	4
1114	C	2.4335	0.5792	0.2380	0.0867	0.0948	0.8356	1.9512	0.4758	0.0439	18.51	10^8	18.72	10^8	0
1115	D	3.3265	0.8075	0.2427	0.2369	0.2554	1.1650	2.6540	0.3875	0.4753	27.01	10^9	24.34	10^8	-1
1126	B	2.5670	0.6826	0.2659	0.1430	0.0537	0.9847	1.9986	0.3638	-0.0974	20.76	10^8	22.01	10^8	0
1138	D	6.1669	1.7644	0.2861	0.1255	0.0389	2.5455	4.6976	0.0235	0.0068	47.91	10^7	41.63	10^6	-1
1140	C	2.6016	0.6224	0.2393	0.0907	-0.0285	0.8980	2.0833	0.2295	-0.9366	19.63	10^8	21.70	10^9	1
1157	B	2.3938	0.5583	0.2332	0.1956	0.1342	0.8055	1.9288	1.0110	1.0564	21.00	10^10	16.87	10^8	-2
1158	A	2.3124	0.5598	0.2421	0.1076	0.0215	0.8077	1.8462	0.4498	-0.7840	8.00	10^3	19.11	10^9	6
1159	D	6.8800	1.6139	0.2346	-0.0194	0.0986	2.3284	5.5360	-0.0071	-0.0075	47.52	10^7	48.60	10^8	1
1160	D	5.6852	1.2478	0.2195	0.3201	0.1908	1.8002	4.6461	0.1179	0.0825	42.67	10^9	32.27	10^6	-3
1166	G	2.5133	0.8164	0.3248	0.1151	0.1363	1.1778	1.7796	0.1395	-0.0664	23.77	10^8	27.20	10^9	1
1170	F	2.7967	0.7417	0.2652	0.1753	0.0892	1.0701	2.1790	0.3470	0.0398	24.95	10^9	23.58	10^8	-1
1171	G	2.8103	0.7711	0.2744	0.2243	0.0423	1.1125	2.1681	0.2829	-0.1905	24.00	10^8	26.51	10^9	1
1172	G	3.0809	0.8345	0.2709	0.1345	0.0562	1.2039	2.4631	0.0987	-0.1489	24.94	10^8	29.83	10^9	1
1173	B	2.6685	0.6603	0.2475	0.2063	0.0707	0.9527	2.1186	0.4573	-0.2610	25.53	10^10	22.75	10^9	-1
1177	B	2.0777	0.6301	0.3033	0.1225	0.0648	0.9091	1.6287	0.2732	-0.3397	21.30	10^9	23.15	10^10	1
1190	G	4.3395	1.3017	0.3000	0.3130	0.1039	1.8780	3.2555	0.0777	-0.0041	33.50	10^6	47.85	10^10	4
1191	E	3.4647	0.7809	0.2254	0.1277	0.0735	1.1266	2.8144	0.2012	-0.1779	32.16	10^11	26.01	10^8	-3
1194	A	3.0118	0.7110	0.2361	0.0897	0.1510	1.0258	2.3664	0.1735	0.1743	28.49	10^11	23.14	10^8	-3
1199	F	2.7267	0.6333	0.2323	0.1709	0.1874	0.9137	2.1993	0.5432	0.2900	23.91	10^10	19.40	10^8	-2
1212	H	1.3581	0.4342	0.3197	0.1398	0.1277	0.6265	2.7303	0.2067	0.0499	8.09	10^3	15.01	10^8	5
1214	F	2.1400	0.4778	0.2233	-0.0593	0.2417	0.6893	4.1946	0.0942	0.0719	20.53	10^10	17.52	10^8	-2
1215	F	2.8200	0.7889	0.2797	0.1648	0.2626	1.1381	2.0460	0.4728	0.2005	37.51	10^13	24.60	10^8	-5
1216	A	1.6232	0.4440	0.2735	0.1713	0.1293	0.6405	2.6219	0.3824	0.3898	14.38	10^7	13.05	10^7	0
1217	A	2.9194	0.8055	0.2759	0.1871	0.1406	1.1621	2.3570	0.4652	1.1605	24.36	10^8	24.92	10^8	0
1222	B	2.4532	0.6765	0.2758	0.1895	0.0271	0.9760	2.6595	0.1724	0.0382	21.00	10^8	22.69	10^8	0
1223	F	2.6954	0.7970	0.2957	0.1798	0.1012	1.1498	1.8555	0.3428	-0.4431	22.08	10^7	25.07	10^8	1
1239	F	2.4155	0.5918	0.2450	0.1608	0.3094	0.8538	2.0097	0.6429	0.6440	23.58	10^10	17.10	10^7	-3
1240	G	1.3811	0.4891	0.3541	0.2222	0.1224	0.7056	2.0234	0.5795	0.2497	11.05	10^5	16.50	10^8	3
1242	H	0.9132	0.2573	0.2818	0.0903	-0.0003	0.3712	2.4292	0.5730	0.7021	8.00	10^6	10.04	10^8	2
1243	H	0.9082	0.3202	0.3525	0.1899	0.0389	0.4619	2.8870	0.2082	-0.0300	8.00	10^4	11.29	10^7	3
1244	H	0.8420	0.2481	0.2946	0.2790	0.3390	0.3579	2.5919	0.6576	1.1408	8.00	10^6	4.46	10^3	-3
1245	H	1.4583	0.5538	0.3798	0.2399	0.0480	0.7990	1.4161	1.1703	0.4470	11.63	10^5	19.83	10^10	5
1246	H	1.7200	0.6110	0.3552	0.1793	-0.0107	0.8815	1.4474	1.3443	1.4714	10.36	10^4	22.59	10^10	6
1247	H	0.9069	0.2673	0.2947	0.2112	0.1150	0.3856	1.6721	1.4510	2.3344	8.00	10^7	8.20	10^7	0
1248	H	1.1615	0.4119	0.3546	0.0323	-0.0311	0.5943	4.1778	0.0934	0.0632	11.56	10^5	15.59	10^8	3
1249	H	0.9367	0.2725	0.2910	0.1117	0.0726	0.3932	5.4898	0.0421	0.0229	8.00	10^3	9.79	10^4	1
1250	H	0.9980	0.3201	0.3207	0.1832	0.2158	0.4618	5.3177	0.0371	0.0254	8.48	10^3	9.04	10^3	0
1251	A	1.5016	0.3788	0.2523	-0.2098	0.0599	0.5465	2.9724	0.1465	0.0705	13.91	10^8	16.20	10^10	2
1252	A	2.1845	0.6581	0.3013	0.1511	0.0909	0.9495	6.3453	0.0273	0.0157	14.97	10^3	23.12	10^7	4
1253	A	1.9653	0.4958	0.2523	0.1304	0.5471	0.7153	6.1241	0.0171	0.0124	14.98	10^5	9.47	10^3	-2
1254	A	1.9873	0.5653	0.2845	0.2304	0.2660	0.8155	3.4120	0.2063	0.3231	13.69	10^5	13.63	10^5	0
1255	A	2.0659	0.5594	0.2708	0.1630	-0.0114	0.8071	3.6873	0.2128	0.3552	15.46	10^6	20.20	10^8	2
1256	A	1.8624	0.5490	0.2948	0.1937	0.1031	0.7920	2.9571	0.3716	0.3183	17.02	10^7	18.98	10^8	1
1257	A	2.4900	0.6813	0.2736	-0.0038	-0.0596	0.9828	5.1421	0.0512	0.0156	18.80	10^6	25.28	10^8	2
1258	C	2.6000	0.6171	0.2374	-0.0316	0.0482	0.8903	2.1194	0.3693	0.1513	18.67	10^8	22.02	10^9	1
1259	C	2.2491	0.6262	0.2784	0.0712	0.0568	0.9035	3.4856	0.1729	0.1298	19.04	10^7	21.86	10^8	1
1260	C	2.7109	0.7258	0.2677	0.0574	0.1050	1.0472	2.6877	0.3496	0.5213	21.00	10^7	23.43	10^8	1
1261	D	3.2695	0.9061	0.2771	0.1061	0.0119	1.3073	1.8971	0.7624	0.9028	34.91	10^10	29.88	10^9	-1
1262	G	2.4582	0.6780	0.2758	0.0788	0.0464	0.9781	2.0356	0.9256	2.0270	19.92	10^7	22.10	10^8	1
1263	G	2.3164	0.7197	0.3107	0.2067	0.1400	1.0383	2.1477	0.6547	0.8032	21.72	10^8	22.19	10^8	0
1264	F	3.1895	1.0196	0.3197	0.1516	0.0764	1.4710	1.7718	0.9033	1.4976	27.00	10^7	29.87	10^8	1
1265	F	2.8941	0.7858	0.2715	0.1698	0.2004	1.1336	1.5958	1.3259	2.6949	25.08	10^8	17.59	10^6	-2
1266	C	3.0491	0.8096	0.2655	0.0692	0.0227	1.1680	1.7115	0.7175	0.4309	29.59	10^10	23.51	10^8	-2
1267	H	1.0881	0.4225	0.3883	0.2301	0.1558	0.6095	2.2619	0.9823	2.1292	8.00	10^4	14.31	10^8	4
1268	H	1.1218	0.3426	0.3054	0.1333	0.1482	0.4942	2.7154	0.6033	1.9012	9.27	10^5	12.28	10^8	3
1271	C	2.5259	0.6350	0.2514	0.0646	0.0883	0.9160	1.7214	0.7094	0.4416	19.18	10^8	21.10	10^9	1
1274	C	2.4579	0.7005	0.2850	0.1584	0.0041	1.0106	0.8769	3.9508	7.1893	17.71	10^7	24.52	10^10	3
1277	C	2.4258	0.5434	0.2240	0.1051	0.0632	0.7840	1.9344	1.3060	2.9075	20.33	10^10	21.49	10^10	0
1278	D	3.8429	1.2619	0.3284	0.3257	0.1216	1.8206	1.5240	0.5178	0.0978	35.13	10^8	38.13	10^8	0

Station Number	Region	Recurrence Interval for 24-hr Rainfall (inches)															
		10-yr	25-yr	50-yr	100-yr	200-yr	500-yr	1,000-yr	10^4-yr	10^5-yr	10^6-yr	10^7-yr	10^8-yr	10^9-yr	10^10-yr	10^11-yr	10^12-yr
5	F	5.30	6.56	7.49	8.41	9.33	10.54	11.46	14.50	17.54	20.59	23.63	26.67	29.72	32.76	35.80	38.85
6	F	7.82	9.65	11.01	12.35	13.70	15.47	16.80	21.25	25.69	30.13	34.57	39.01	43.46	47.90	52.34	56.78
9	B	4.40	5.37	6.08	6.79	7.50	8.43	9.14	11.48	13.82	16.16	18.51	20.85	23.19	25.53	27.87	30.21
10	F	5.48	6.74	7.67	8.60	9.53	10.75	11.68	14.74	17.81	20.87	23.94	27.00	30.07	33.14	36.20	39.27
11	F	4.93	6.03	6.85	7.66	8.46	9.53	10.33	13.00	15.67	18.34	21.01	23.68	26.35	29.02	31.68	34.35
13	F	5.06	6.21	7.07	7.91	8.76	9.87	10.72	13.51	16.31	19.11	21.91	24.70	27.50	30.30	33.09	35.89
20	F	5.40	6.64	7.55	8.46	9.37	10.56	11.47	14.47	17.46	20.46	23.46	26.46	29.46	32.46	35.46	38.45
21	F	4.09	4.99	5.65	6.31	6.96	7.83	8.48	10.65	12.82	14.99	17.15	19.32	21.49	23.66	25.83	28.00
23	B	3.96	4.79	5.41	6.02	6.63	7.43	8.03	10.05	12.06	14.07	16.08	18.09	20.10	22.12	24.13	26.14
25	B	3.99	4.87	5.52	6.17	6.82	7.67	8.31	10.46	12.60	14.74	16.88	19.02	21.16	23.30	25.44	27.58
28	B	4.40	5.39	6.13	6.86	7.59	8.55	9.27	11.69	14.10	16.51	18.92	21.34	23.75	26.16	28.57	30.98
32	G	5.21	6.38	7.25	8.11	8.96	10.09	10.95	13.78	16.62	19.45	22.29	25.12	27.96	30.79	33.63	36.46
33	G	4.41	5.33	6.01	6.68	7.36	8.24	8.91	11.14	13.36	15.58	17.81	20.03	22.26	24.48	26.70	28.93
42	A	3.10	3.79	4.30	4.81	5.31	5.98	6.49	8.16	9.84	11.51	13.19	14.87	16.54	18.22	19.90	21.57
43	A	3.17	3.86	4.37	4.88	5.38	6.05	6.55	8.23	9.90	11.57	13.24	14.91	16.59	18.26	19.93	21.60
44	A	3.16	3.87	4.40	4.93	5.46	6.15	6.67	8.41	10.15	11.89	13.63	15.36	17.10	18.84	20.58	22.32
46	D	7.72	9.53	10.88	12.21	13.54	15.29	16.62	21.02	25.42	29.82	34.22	38.62	43.02	47.43	51.83	56.23
47	D	9.85	12.20	13.93	15.66	17.38	19.65	21.36	27.05	32.74	38.43	44.12	49.82	55.51	61.20	66.89	72.58
53	D	10.15	12.74	14.66	16.56	18.46	20.97	22.86	29.14	35.43	41.71	48.00	54.28	60.56	66.85	73.13	79.42
54	E	5.92	7.41	8.52	9.61	10.71	12.15	13.24	16.86	20.48	24.10	27.72	31.34	34.97	38.59	42.21	45.83
57	D	11.71	14.43	16.46	18.47	20.47	23.11	25.10	31.73	38.35	44.98	51.60	58.23	64.85	71.48	78.10	84.73
60	D	12.51	15.89	18.40	20.89	23.38	26.65	29.13	37.35	45.57	53.78	62.00	70.22	78.44	86.65	94.87	103.09
63	D	6.55	8.06	9.19	10.30	11.41	12.87	13.98	17.66	21.33	25.00	28.68	32.35	36.02	39.70	43.37	47.04
68	D	6.82	8.34	9.46	10.57	11.68	13.15	14.25	17.93	21.60	25.27	28.95	32.62	36.29	39.97	43.64	47.32
73	D	5.41	6.53	7.37	8.20	9.03	10.12	10.95	13.69	16.43	19.17	21.91	24.65	27.39	30.13	32.87	35.61
78	D	9.08	10.99	12.41	13.82	15.22	17.07	18.47	23.11	27.75	32.39	37.03	41.68	46.32	50.96	55.60	60.24
82	H	4.40	5.40	6.15	6.89	7.62	8.59	9.32	11.76	14.19	16.63	19.06	21.49	23.93	26.36	28.79	31.23
83	H	6.51	7.93	8.98	10.02	11.06	12.44	13.47	16.92	20.36	23.81	27.25	30.70	34.14	37.58	41.03	44.47
89	D	5.44	6.66	7.56	8.46	9.35	10.53	11.42	14.37	17.33	20.28	23.24	26.19	29.15	32.11	35.06	38.02
92	C	4.18	5.05	5.69	6.33	6.96	7.80	8.44	10.54	12.65	14.75	16.86	18.96	21.07	23.17	25.28	27.38
93	C	4.08	4.91	5.53	6.15	6.76	7.57	8.19	10.22	12.25	14.28	16.31	18.35	20.38	22.41	24.44	26.47
95	C	4.38	5.31	6.00	6.68	7.36	8.26	8.94	11.19	13.44	15.69	17.95	20.20	22.45	24.70	26.95	29.21
96	C	4.09	4.93	5.55	6.16	6.77	7.58	8.19	10.22	12.24	14.27	16.30	18.32	20.35	22.37	24.40	26.43
106	A	3.51	4.23	4.76	5.28	5.81	6.50	7.02	8.76	10.50	12.23	13.97	15.71	17.44	19.18	20.91	22.65
107	A	3.79	4.59	5.18	5.77	6.36	7.13	7.71	9.65	11.59	13.53	15.46	17.40	19.34	21.28	23.22	25.15
108	C	4.14	5.01	5.65	6.29	6.92	7.76	8.39	10.49	12.60	14.70	16.80	18.90	21.00	23.10	25.21	27.31
109	C	4.99	6.12	6.95	7.78	8.61	9.70	10.53	13.26	16.00	18.74	21.47	24.21	26.95	29.69	32.42	35.16
116	A	3.74	4.59	5.22	5.84	6.46	7.28	7.90	9.96	12.02	14.07	16.13	18.19	20.25	22.30	24.36	26.42
120	G	2.34	2.84	3.20	3.57	3.94	4.42	4.78	5.99	7.20	8.40	9.61	10.82	12.03	13.24	14.44	15.65
124	G	3.75	4.53	5.10	5.67	6.24	6.99	7.56	9.44	11.32	13.20	15.08	16.96	18.84	20.72	22.60	24.48
125	G	4.14	5.02	5.68	6.33	6.98	7.83	8.48	10.63	12.77	14.92	17.07	19.22	21.37	23.51	25.66	27.81
128	G	5.82	7.05	7.97	8.88	9.79	10.98	11.89	14.89	17.89	20.89	23.89	26.89	29.90	32.90	35.90	38.90
134	C	4.63	5.63	6.37	7.11	7.84	8.80	9.53	11.96	14.38	16.80	19.23	21.65	24.08	26.50	28.92	31.35
140	A	4.40	5.29	5.95	6.60	7.26	8.12	8.77	10.93	13.09	15.25	17.41	19.57	21.73	23.89	26.04	28.20

Station Number	Region	Recurrence Interval for 24-hr Rainfall (inches)															
		10-yr	25-yr	50-yr	100-yr	200-yr	500-yr	1,000-yr	10^4-yr	10^5-yr	10^6-yr	10^7-yr	10^8-yr	10^9-yr	10^10-yr	10^11-yr	10^12-yr
144	D	5.92	7.21	8.18	9.13	10.09	11.34	12.29	15.45	18.60	21.75	24.91	28.06	31.21	34.37	37.52	40.67
156	A	3.80	4.67	5.31	5.95	6.58	7.42	8.05	10.15	12.25	14.35	16.45	18.56	20.66	22.76	24.86	26.96
157	A	3.33	4.06	4.59	5.12	5.65	6.35	6.88	8.63	10.38	12.13	13.88	15.63	17.38	19.13	20.88	22.63
158	D	8.22	10.08	11.46	12.83	14.20	16.00	17.36	21.89	26.41	30.93	35.45	39.98	44.50	49.02	53.54	58.07
167	D	5.45	6.64	7.52	8.39	9.27	10.42	11.29	14.17	17.06	19.94	22.83	25.71	28.60	31.48	34.37	37.26
169	D	5.38	6.57	7.45	8.33	9.20	10.36	11.23	14.12	17.01	19.91	22.80	25.69	28.59	31.48	34.37	37.27
170	C	4.23	5.15	5.83	6.50	7.17	8.06	8.73	10.95	13.18	15.40	17.62	19.84	22.07	24.29	26.51	28.73
172	D	4.93	6.07	6.91	7.74	8.57	9.67	10.50	13.25	16.00	18.76	21.51	24.26	27.01	29.77	32.52	35.27
174	C	4.72	5.69	6.41	7.12	7.83	8.77	9.48	11.83	14.19	16.54	18.90	21.25	23.60	25.96	28.31	30.66
175	D	5.85	7.15	8.11	9.07	10.02	11.28	12.23	15.38	18.53	21.69	24.84	27.99	31.15	34.30	37.45	40.60
176	D	5.68	6.94	7.88	8.81	9.73	10.95	11.88	14.94	18.01	21.07	24.14	27.20	30.27	33.33	36.40	39.46
178	C	4.43	5.33	5.99	6.65	7.31	8.18	8.83	11.01	13.19	15.36	17.54	19.71	21.89	24.06	26.24	28.42
179	D	6.79	8.31	9.44	10.56	11.68	13.16	14.27	17.97	21.67	25.37	29.07	32.78	36.48	40.18	43.88	47.58
191	C	3.77	4.51	5.06	5.60	6.14	6.86	7.40	9.19	10.98	12.78	14.57	16.36	18.15	19.95	21.74	23.53
196	C	4.36	5.30	5.99	6.69	7.38	8.29	8.98	11.26	13.55	15.83	18.12	20.40	22.69	24.97	27.26	29.54
201	C	4.81	5.80	6.54	7.27	8.00	8.96	9.69	12.10	14.51	16.92	19.33	21.74	24.16	26.57	28.98	31.39
210	B	5.90	7.30	8.33	9.36	10.39	11.74	12.76	16.15	19.54	22.93	26.32	29.71	33.10	36.49	39.88	43.27
213	A	4.28	5.19	5.86	6.53	7.19	8.07	8.74	10.94	13.14	15.34	17.55	19.75	21.95	24.16	26.36	28.56
216	B	4.64	5.69	6.47	7.24	8.01	9.03	9.79	12.34	14.89	17.44	19.99	22.54	25.09	27.64	30.19	32.74
223	D	5.78	6.96	7.84	8.71	9.58	10.73	11.59	14.46	17.34	20.21	23.08	25.95	28.83	31.70	34.57	37.45
225	A	3.37	4.11	4.65	5.19	5.72	6.43	6.97	8.74	10.52	12.29	14.07	15.85	17.62	19.40	21.17	22.95
227	C	5.11	6.29	7.17	8.04	8.90	10.05	10.91	13.78	16.65	19.52	22.39	25.26	28.13	31.00	33.86	36.73
228	F	4.72	5.75	6.51	7.27	8.02	9.02	9.77	12.27	14.77	17.27	19.76	22.26	24.76	27.26	29.76	32.25
235	D	6.92	8.54	9.75	10.94	12.13	13.69	14.88	18.81	22.74	26.67	30.60	34.54	38.47	42.40	46.33	50.26
237	F	5.34	6.46	7.30	8.12	8.95	10.03	10.86	13.58	16.31	19.04	21.77	24.50	27.22	29.95	32.68	35.41
238	F	4.07	4.92	5.55	6.17	6.79	7.61	8.23	10.29	12.35	14.40	16.46	18.52	20.57	22.63	24.69	26.74
241	A	3.42	4.18	4.75	5.31	5.86	6.60	7.16	9.00	10.85	12.70	14.54	16.39	18.24	20.09	21.93	23.78
250	G	3.41	4.18	4.76	5.33	5.89	6.64	7.21	9.08	10.96	12.84	14.71	16.59	18.47	20.34	22.22	24.09
251	D	6.39	7.85	8.94	10.01	11.09	12.50	13.57	17.12	20.67	24.21	27.76	31.31	34.86	38.40	41.95	45.50
252	G	3.69	4.49	5.09	5.68	6.27	7.05	7.64	9.60	11.55	13.51	15.47	17.42	19.38	21.33	23.29	25.25
255	C	3.71	4.43	4.96	5.49	6.01	6.71	7.23	8.97	10.71	12.45	14.19	15.93	17.68	19.42	21.16	22.90
259	B	4.58	5.57	6.31	7.04	7.77	8.73	9.46	11.87	14.28	16.70	19.11	21.52	23.93	26.35	28.76	31.17
261	G	2.96	3.63	4.13	4.63	5.13	5.78	6.27	7.92	9.56	11.20	12.84	14.48	16.12	17.76	19.40	21.04
269	C	4.47	5.43	6.15	6.86	7.56	8.50	9.20	11.55	13.89	16.23	18.57	20.92	23.26	25.60	27.95	30.29
277	H	5.46	6.62	7.49	8.35	9.20	10.33	11.18	14.00	16.83	19.66	22.48	25.31	28.13	30.96	33.79	36.61
280	C	6.92	8.58	9.82	11.04	12.26	13.87	15.08	19.12	23.16	27.20	31.23	35.27	39.31	43.35	47.38	51.42
283	E	10.16	12.46	14.17	15.87	17.56	19.79	21.47	27.06	32.66	38.25	43.84	49.44	55.03	60.62	66.22	71.81
287	D	4.84	5.84	6.58	7.32	8.06	9.02	9.76	12.19	14.62	17.05	19.48	21.91	24.34	26.77	29.20	31.63
291	A	4.19	5.11	5.80	6.48	7.16	8.06	8.73	10.98	13.23	15.48	17.73	19.97	22.22	24.47	26.72	28.97
292	F	5.36	6.58	7.48	8.38	9.27	10.45	11.33	14.29	17.24	20.20	23.15	26.10	29.05	32.01	34.96	37.91
293	B	4.01	4.79	5.37	5.95	6.52	7.27	7.84	9.73	11.63	13.52	15.41	17.30	19.20	21.09	22.98	24.87
294	D	5.91	7.20	8.15	9.10	10.05	11.30	12.24	15.38	18.51	21.64	24.77	27.91	31.04	34.17	37.30	40.44
298	G	3.20	3.85	4.34	4.83	5.31	5.95	6.43	8.03	9.63	11.23	12.84	14.44	16.04	17.64	19.24	20.84
299	H	2.22	2.72	3.10	3.47	3.84	4.33	4.70	5.92	7.15	8.37	9.60	10.82	12.05	13.27	14.50	15.72

Station Number	Region	Recurrence Interval for 24-hr Rainfall (inches)															
		10-yr	25-yr	50-yr	100-yr	200-yr	500-yr	1,000-yr	10^4-yr	10^5-yr	10^6-yr	10^7-yr	10^8-yr	10^9-yr	10^10-yr	10^11-yr	10^12-yr
303	D	5.61	6.89	7.84	8.79	9.73	10.97	11.90	15.01	18.13	21.24	24.35	27.46	30.57	33.68	36.79	39.90
304	D	11.38	14.15	16.21	18.25	20.28	22.96	24.98	31.71	38.43	45.15	51.88	58.60	65.32	72.05	78.77	85.49
306	F	3.86	4.77	5.45	6.12	6.79	7.67	8.33	10.54	12.75	14.97	17.18	19.39	21.60	23.81	26.02	28.23
321	H	5.01	6.15	6.99	7.84	8.67	9.78	10.61	13.39	16.16	18.93	21.71	24.48	27.25	30.02	32.80	35.57
322	H	3.33	4.10	4.68	5.25	5.81	6.56	7.13	9.00	10.88	12.76	14.64	16.51	18.39	20.27	22.15	24.02
334	D	11.28	13.87	15.80	17.71	19.61	22.12	24.02	30.32	36.62	42.93	49.23	55.53	61.83	68.13	74.43	80.73
336	A	3.98	4.84	5.48	6.11	6.74	7.57	8.19	10.28	12.36	14.44	16.53	18.61	20.69	22.78	24.86	26.94
338	D	9.40	11.60	13.22	14.84	16.45	18.58	20.18	25.52	30.85	36.18	41.51	46.84	52.18	57.51	62.84	68.17
342	C	4.70	5.67	6.39	7.10	7.81	8.75	9.46	11.82	14.17	16.53	18.88	21.24	23.59	25.95	28.30	30.66
347	C	6.12	7.64	8.77	9.89	11.01	12.49	13.60	17.30	21.00	24.70	28.40	32.10	35.80	39.50	43.20	46.90
352	F	6.53	8.05	9.17	10.28	11.39	12.86	13.97	17.65	21.32	25.00	28.68	32.35	36.03	39.71	43.39	47.06
355	A	4.66	5.67	6.42	7.17	7.91	8.88	9.62	12.07	14.53	16.98	19.43	21.88	24.33	26.78	29.23	31.68
356	C	4.27	5.16	5.83	6.50	7.16	8.03	8.68	10.87	13.05	15.24	17.43	19.61	21.80	23.98	26.17	28.35
372	G	4.08	4.96	5.62	6.27	6.92	7.77	8.42	10.57	12.72	14.86	17.01	19.16	21.31	23.45	25.60	27.75
373	D	7.10	8.75	9.97	11.18	12.39	13.99	15.19	19.19	23.19	27.20	31.20	35.20	39.20	43.20	47.20	51.20
377	F	5.47	6.70	7.61	8.51	9.41	10.60	11.49	14.47	17.45	20.43	23.40	26.38	29.36	32.33	35.31	38.29
379	D	6.91	8.41	9.52	10.62	11.71	13.16	14.25	17.88	21.51	25.14	28.77	32.40	36.03	39.66	43.29	46.92
387	C	3.66	4.38	4.91	5.44	5.97	6.66	7.19	8.93	10.67	12.41	14.15	15.89	17.63	19.37	21.12	22.86
388	A	4.02	4.94	5.62	6.30	6.98	7.87	8.54	10.77	13.01	15.24	17.48	19.71	21.95	24.18	26.41	28.65
390	D	6.32	7.71	8.75	9.77	10.79	12.14	13.16	16.54	19.92	23.30	26.68	30.06	33.44	36.82	40.20	43.58
391	A	3.87	4.70	5.31	5.92	6.53	7.33	7.94	9.95	11.96	13.97	15.98	17.99	20.00	22.00	24.01	26.02
395	G	4.75	5.78	6.54	7.30	8.06	9.05	9.81	12.31	14.81	17.32	19.82	22.32	24.82	27.33	29.83	32.33
402	E	7.12	8.59	9.68	10.76	11.83	13.25	14.33	17.89	21.46	25.02	28.59	32.15	35.71	39.28	42.84	46.41
405	G	4.49	5.54	6.32	7.09	7.87	8.89	9.66	12.21	14.77	17.33	19.88	22.44	24.99	27.55	30.11	32.66
406	C	4.19	5.03	5.66	6.28	6.90	7.71	8.33	10.37	12.42	14.46	16.51	18.55	20.60	22.65	24.69	26.74
409	G	4.77	5.80	6.56	7.32	8.07	9.07	9.82	12.32	14.82	17.32	19.82	22.32	24.82	27.32	29.81	32.31
415	A	4.08	5.03	5.74	6.44	7.14	8.06	8.76	11.07	13.38	15.69	18.00	20.31	22.62	24.93	27.24	29.55
423	E	5.02	6.12	6.93	7.73	8.54	9.60	10.40	13.06	15.71	18.37	21.03	23.69	26.35	29.00	31.66	34.32
425	D	8.62	10.56	11.99	13.41	14.83	16.70	18.12	22.81	27.51	32.20	36.89	41.59	46.28	50.97	55.67	60.36
433	D	6.40	7.90	9.02	10.12	11.23	12.68	13.78	17.44	21.09	24.74	28.39	32.05	35.70	39.35	43.00	46.66
434	F	5.62	6.93	7.90	8.86	9.82	11.09	12.04	15.22	18.40	21.57	24.75	27.92	31.10	34.27	37.45	40.62
435	F	6.26	7.60	8.60	9.59	10.58	11.88	12.87	16.13	19.40	22.67	25.93	29.20	32.47	35.73	39.00	42.27
436	B	4.05	4.98	5.68	6.36	7.05	7.95	8.64	10.90	13.17	15.44	17.70	19.97	22.24	24.50	26.77	29.04
444	A	4.17	5.15	5.88	6.60	7.32	8.26	8.98	11.36	13.74	16.11	18.49	20.87	23.25	25.63	28.00	30.38
445	C	5.84	7.26	8.31	9.35	10.39	11.76	12.80	16.24	19.67	23.11	26.55	29.99	33.42	36.86	40.30	43.74
446	B	5.79	7.10	8.08	9.04	10.01	11.28	12.24	15.43	18.62	21.81	25.00	28.19	31.37	34.56	37.75	40.94
447	F	4.14	5.03	5.69	6.34	6.99	7.85	8.50	10.65	12.81	14.96	17.11	19.27	21.42	23.58	25.73	27.88
449	D	5.76	7.22	8.30	9.38	10.45	11.86	12.93	16.48	20.03	23.58	27.13	30.67	34.22	37.77	41.32	44.87
453	C	5.72	7.13	8.18	9.22	10.25	11.62	12.65	16.08	19.51	22.94	26.37	29.79	33.22	36.65	40.08	43.51
455	H	2.43	3.03	3.48	3.93	4.37	4.96	5.40	6.86	8.33	9.80	11.26	12.73	14.20	15.67	17.13	18.60
458	F	4.55	5.60	6.37	7.14	7.91	8.92	9.69	12.23	14.77	17.32	19.86	22.40	24.94	27.48	30.02	32.57
462	A	4.53	5.50	6.23	6.95	7.67	8.61	9.33	11.70	14.08	16.45	18.82	21.20	23.57	25.95	28.32	30.69
465	B	4.80	5.89	6.69	7.50	8.30	9.35	10.15	12.80	15.44	18.09	20.74	23.38	26.03	28.68	31.32	33.97
466	G	6.82	8.42	9.60	10.78	11.95	13.49	14.66	18.53	22.40	26.27	30.14	34.02	37.89	41.76	45.63	49.50

Station Number	Region	Recurrence Interval for 24-hr Rainfall (inches)															
		10-yr	25-yr	50-yr	100-yr	200-yr	500-yr	1,000-yr	10^4-yr	10^5-yr	10^6-yr	10^7-yr	10^8-yr	10^9-yr	10^10-yr	10^11-yr	10^12-yr
471	D	7.04	8.83	10.15	11.47	12.78	14.51	15.82	20.16	24.49	28.83	33.17	37.51	41.85	46.19	50.52	54.86
477	D	12.49	15.76	18.19	20.60	23.01	26.18	28.57	36.52	44.47	52.43	60.38	68.33	76.28	84.23	92.18	100.13
482	A	3.83	4.69	5.33	5.97	6.60	7.43	8.07	10.16	12.26	14.35	16.45	18.54	20.64	22.73	24.83	26.92
488	D	3.66	4.39	4.93	5.47	6.01	6.71	7.25	9.02	10.80	12.57	14.35	16.13	17.90	19.68	21.45	23.23
492	E	7.51	9.39	10.78	12.17	13.55	15.37	16.74	21.31	25.87	30.43	35.00	39.56	44.13	48.69	53.26	57.82
493	G	4.77	5.73	6.44	7.15	7.86	8.79	9.49	11.82	14.16	16.49	18.83	21.16	23.49	25.83	28.16	30.49
497	C	4.19	5.01	5.63	6.23	6.84	7.64	8.24	10.25	12.25	14.26	16.26	18.27	20.27	22.28	24.28	26.29
498	D	9.09	11.38	13.07	14.76	16.43	18.65	20.32	25.87	31.42	36.97	42.52	48.07	53.62	59.17	64.72	70.28
517	H	5.51	6.89	7.92	8.93	9.94	11.28	12.29	15.64	18.99	22.34	25.68	29.03	32.38	35.73	39.08	42.43
542	H	4.25	5.21	5.92	6.63	7.34	8.27	8.97	11.30	13.63	15.96	18.29	20.63	22.96	25.29	27.62	29.95
564	H	2.22	2.71	3.06	3.42	3.77	4.24	4.59	5.76	6.94	8.11	9.28	10.45	11.62	12.79	13.96	15.13
565	A	3.54	4.32	4.90	5.47	6.04	6.79	7.36	9.25	11.13	13.02	14.91	16.80	18.68	20.57	22.46	24.34
566	A	3.34	4.07	4.60	5.14	5.67	6.37	6.90	8.66	10.42	12.18	13.94	15.70	17.45	19.21	20.97	22.73
591	D	5.21	6.30	7.11	7.91	8.71	9.76	10.56	13.21	15.85	18.50	21.15	23.79	26.44	29.09	31.73	34.38
598	H	2.90	3.61	4.14	4.66	5.19	5.88	6.40	8.13	9.86	11.59	13.32	15.05	16.78	18.51	20.24	21.97
610	C	5.03	6.10	6.88	7.67	8.45	9.48	10.25	12.83	15.41	18.00	20.58	23.16	25.74	28.32	30.90	33.48
612	D	5.81	7.13	8.11	9.08	10.04	11.32	12.28	15.48	18.68	21.88	25.07	28.27	31.47	34.67	37.87	41.06
613	C	4.99	6.10	6.92	7.74	8.56	9.64	10.45	13.15	15.85	18.55	21.26	23.96	26.66	29.36	32.06	34.76
619	D	7.96	9.70	10.99	12.28	13.55	15.24	16.51	20.74	24.98	29.21	33.44	37.67	41.90	46.13	50.36	54.59
627	D	5.64	6.80	7.67	8.52	9.37	10.50	11.35	14.17	16.99	19.82	22.64	25.46	28.28	31.10	33.93	36.75
634	A	3.78	4.61	5.22	5.83	6.44	7.25	7.85	9.87	11.88	13.90	15.91	17.93	19.94	21.96	23.97	25.99
680	A	4.76	5.80	6.58	7.34	8.11	9.12	9.88	12.41	14.93	17.46	19.99	22.52	25.05	27.58	30.10	32.63
683	D	6.09	7.61	8.74	9.85	10.97	12.44	13.55	17.24	20.93	24.62	28.31	32.00	35.69	39.38	43.07	46.76
694	D	5.43	6.71	7.66	8.60	9.54	10.78	11.71	14.82	17.93	21.04	24.15	27.26	30.37	33.48	36.59	39.69
695	D	8.41	10.47	12.01	13.53	15.04	17.04	18.55	23.57	28.58	33.60	38.61	43.63	48.64	53.66	58.67	63.69
716	A	3.93	4.79	5.42	6.05	6.68	7.51	8.13	10.21	12.28	14.36	16.43	18.51	20.59	22.66	24.74	26.81
726	D	7.34	9.24	10.64	12.04	13.43	15.27	16.66	21.26	25.87	30.47	35.08	39.68	44.29	48.89	53.50	58.10
734	A	3.35	4.11	4.68	5.24	5.80	6.54	7.09	8.94	10.79	12.64	14.49	16.34	18.19	20.04	21.89	23.74
735	B	4.30	5.31	6.05	6.79	7.53	8.50	9.24	11.68	14.12	16.56	19.00	21.44	23.88	26.32	28.76	31.20
740	D	11.35	14.20	16.32	18.43	20.52	23.29	25.38	32.31	39.25	46.19	53.12	60.06	67.00	73.93	80.87	87.80
741	D	7.64	9.00	10.02	11.02	12.02	13.34	14.34	17.65	20.96	24.28	27.59	30.90	34.21	37.52	40.84	44.15
742	C	4.42	5.40	6.12	6.84	7.56	8.50	9.22	11.59	13.96	16.33	18.70	21.07	23.44	25.81	28.19	30.56
750	H	1.94	2.40	2.75	3.09	3.44	3.89	4.23	5.36	6.50	7.63	8.77	9.90	11.04	12.17	13.31	14.44
755	F	4.38	5.36	6.09	6.81	7.53	8.48	9.20	11.58	13.96	16.34	18.72	21.10	23.48	25.86	28.24	30.63
757	F	4.05	4.97	5.65	6.33	7.00	7.89	8.56	10.79	13.02	15.25	17.48	19.71	21.94	24.17	26.40	28.63
758	F	4.56	5.56	6.30	7.04	7.77	8.74	9.47	11.90	14.33	16.76	19.19	21.62	24.05	26.48	28.91	31.34
759	F	4.55	5.50	6.20	6.90	7.60	8.51	9.21	11.51	13.82	16.12	18.42	20.73	23.03	25.34	27.64	29.94
760	F	5.14	6.36	7.26	8.16	9.05	10.24	11.13	14.09	17.05	20.02	22.98	25.94	28.91	31.87	34.83	37.79
762	F	5.78	7.14	8.15	9.14	10.14	11.45	12.44	15.74	19.03	22.32	25.61	28.91	32.20	35.49	38.79	42.08
767	F	6.31	7.71	8.74	9.77	10.79	12.14	13.16	16.55	19.93	23.32	26.71	30.09	33.48	36.87	40.25	43.64
772	A	3.95	4.81	5.44	6.07	6.70	7.53	8.16	10.23	12.31	14.39	16.47	18.54	20.62	22.70	24.78	26.85
783	D	7.70	9.65	11.10	12.54	13.97	15.87	17.30	22.04	26.79	31.54	36.29	41.03	45.78	50.53	55.28	60.02
794	F	4.11	4.94	5.56	6.18	6.79	7.60	8.21	10.24	12.26	14.29	16.32	18.35	20.38	22.40	24.43	26.46
795	C	4.88	5.94	6.72	7.50	8.27	9.30	10.07	12.64	15.20	17.77	20.33	22.90	25.47	28.03	30.60	33.16

Station Number	Region	Recurrence Interval for 24-hr Rainfall (inches)															
		10-yr	25-yr	50-yr	100-yr	200-yr	500-yr	1,000-yr	10^4-yr	10^5-yr	10^6-yr	10^7-yr	10^8-yr	10^9-yr	10^10-yr	10^11-yr	10^12-yr
796	A	3.58	4.38	4.98	5.57	6.17	6.95	7.53	9.49	11.45	13.40	15.36	17.31	19.27	21.23	23.18	25.14
797	B	4.22	5.10	5.75	6.40	7.04	7.89	8.54	10.67	12.81	14.95	17.08	19.22	21.35	23.49	25.63	27.76
801	G	6.54	8.15	9.34	10.52	11.69	13.25	14.42	18.32	22.22	26.11	30.01	33.91	37.80	41.70	45.59	49.49
802	C	4.07	4.91	5.54	6.16	6.77	7.59	8.20	10.25	12.29	14.33	16.38	18.42	20.46	22.50	24.55	26.59
807	C	3.79	4.53	5.07	5.61	6.15	6.86	7.40	9.18	10.96	12.74	14.52	16.30	18.09	19.87	21.65	23.43
1005	G	2.96	3.60	4.08	4.55	5.02	5.64	6.11	7.67	9.23	10.78	12.34	13.90	15.45	17.01	18.57	20.13
1006	A	3.16	3.83	4.32	4.82	5.31	5.95	6.44	8.07	9.69	11.32	12.94	14.57	16.19	17.82	19.44	21.07
1008	A	4.65	5.91	6.85	7.78	8.71	9.93	10.85	13.92	16.99	20.06	23.13	26.20	29.27	32.33	35.40	38.47
1012	G	3.65	4.44	5.02	5.61	6.19	6.95	7.53	9.46	11.38	13.30	15.22	17.15	19.07	20.99	22.92	24.84
1014	A	3.43	4.12	4.63	5.14	5.65	6.32	6.83	8.51	10.19	11.87	13.55	15.23	16.91	18.59	20.27	21.95
1017	H	3.05	3.77	4.31	4.84	5.37	6.07	6.60	8.35	10.11	11.87	13.62	15.38	17.13	18.89	20.64	22.40
1029	E	4.78	5.82	6.60	7.37	8.13	9.14	9.91	12.44	14.98	17.52	20.06	22.59	25.13	27.67	30.20	32.74
1035	A	3.69	4.40	4.93	5.45	5.97	6.66	7.18	8.90	10.62	12.35	14.07	15.79	17.51	19.24	20.96	22.68
1037	C	4.88	5.93	6.71	7.48	8.25	9.27	10.04	12.59	15.15	17.70	20.25	22.80	25.36	27.91	30.46	33.02
1041	C	4.37	5.28	5.96	6.63	7.30	8.19	8.85	11.07	13.28	15.50	17.71	19.93	22.14	24.36	26.57	28.79
1051	B	4.74	5.82	6.61	7.40	8.18	9.22	10.01	12.61	15.21	17.81	20.41	23.01	25.61	28.22	30.82	33.42
1058	H	1.93	2.34	2.65	2.95	3.26	3.66	3.96	4.97	5.97	6.98	7.98	8.99	10.00	11.00	12.01	13.01
1062	E	9.53	11.77	13.42	15.06	16.70	18.86	20.49	25.92	31.34	36.75	42.17	47.59	53.01	58.43	63.85	69.27
1070	A	3.01	3.66	4.14	4.62	5.10	5.73	6.20	7.78	9.35	10.93	12.51	14.08	15.66	17.24	18.81	20.39
1071	D	5.29	6.46	7.33	8.20	9.06	10.20	11.06	13.91	16.76	19.61	22.46	25.31	28.16	31.01	33.86	36.71
1072	D	4.35	5.29	5.99	6.68	7.37	8.28	8.97	11.26	13.54	15.83	18.11	20.39	22.68	24.96	27.25	29.53
1074	D	7.73	9.95	11.60	13.23	14.86	17.01	18.63	24.02	29.41	34.80	40.19	45.58	50.97	56.36	61.75	67.14
1075	D	11.08	14.00	16.17	18.32	20.47	23.30	25.44	32.54	39.64	46.74	53.84	60.95	68.05	75.15	82.25	89.35
1076	D	5.79	7.10	8.07	9.04	10.00	11.27	12.23	15.42	18.60	21.79	24.97	28.16	31.34	34.53	37.71	40.90
1078	C	4.08	4.87	5.46	6.05	6.63	7.41	7.99	9.92	11.86	13.79	15.72	17.66	19.59	21.52	23.46	25.39
1080	D	5.89	7.13	8.05	8.96	9.88	11.08	11.99	15.00	18.02	21.03	24.05	27.06	30.08	33.09	36.11	39.12
1081	B	5.09	6.22	7.05	7.88	8.70	9.79	10.61	13.34	16.07	18.80	21.53	24.26	26.99	29.72	32.45	35.18
1087	B	4.03	4.88	5.51	6.14	6.76	7.58	8.20	10.26	12.33	14.39	16.45	18.51	20.57	22.63	24.70	26.76
1088	C	4.13	5.01	5.67	6.31	6.96	7.82	8.46	10.60	12.75	14.89	17.03	19.17	21.32	23.46	25.60	27.74
1093	A	3.23	3.85	4.31	4.77	5.23	5.83	6.29	7.80	9.31	10.83	12.34	13.85	15.37	16.88	18.39	19.90
1095	C	3.83	4.64	5.24	5.84	6.43	7.22	7.81	9.78	11.74	13.71	15.67	17.64	19.60	21.57	23.54	25.50
1104	G	3.10	3.82	4.35	4.88	5.41	6.11	6.64	8.39	10.14	11.89	13.64	15.39	17.14	18.89	20.65	22.40
1107	B	4.95	6.11	6.98	7.84	8.69	9.82	10.68	13.51	16.34	19.18	22.01	24.84	27.67	30.51	33.34	36.17
1113	A	4.72	5.91	6.79	7.66	8.53	9.68	10.55	13.43	16.32	19.20	22.08	24.97	27.85	30.73	33.62	36.50
1114	C	3.83	4.62	5.21	5.79	6.38	7.14	7.72	9.65	11.57	13.49	15.42	17.34	19.27	21.19	23.11	25.04
1115	D	5.28	6.38	7.20	8.01	8.82	9.89	10.70	13.38	16.07	18.75	21.43	24.11	26.80	29.48	32.16	34.84
1126	B	4.21	5.15	5.84	6.53	7.21	8.12	8.80	11.07	13.34	15.60	17.87	20.14	22.41	24.67	26.94	29.21
1138	D	10.43	12.84	14.63	16.41	18.18	20.51	22.28	28.14	34.00	39.87	45.73	51.59	57.45	63.31	69.17	75.03
1140	C	4.10	4.96	5.59	6.21	6.84	7.66	8.29	10.35	12.42	14.49	16.56	18.63	20.69	22.76	24.83	26.90
1157	B	3.74	4.51	5.07	5.63	6.19	6.93	7.49	9.35	11.20	13.06	14.91	16.77	18.62	20.48	22.33	24.19
1158	A	3.66	4.43	5.00	5.56	6.12	6.86	7.43	9.29	11.14	13.00	14.86	16.72	18.58	20.44	22.30	24.16
1159	D	10.78	12.98	14.62	16.25	17.87	20.00	21.62	26.98	32.34	37.70	43.07	48.43	53.79	59.15	64.51	69.87
1160	D	8.70	10.40	11.67	12.93	14.18	15.83	17.08	21.23	25.37	29.52	33.66	37.81	41.95	46.10	50.24	54.39
1166	G	4.43	5.55	6.38	7.20	8.02	9.10	9.91	12.63	15.34	18.05	20.76	23.48	26.19	28.90	31.61	34.32

Station Number	Region	Recurrence Interval for 24-hr Rainfall (inches)															
		10-yr	25-yr	50-yr	100-yr	200-yr	500-yr	1,000-yr	10^4-yr	10^5-yr	10^6-yr	10^7-yr	10^8-yr	10^9-yr	10^10-yr	10^11-yr	10^12-yr
1170	F	4.59	5.60	6.35	7.10	7.85	8.83	9.57	12.03	14.50	16.96	19.43	21.89	24.35	26.82	29.28	31.75
1171	G	4.67	5.73	6.51	7.29	8.06	9.08	9.85	12.41	14.98	17.54	20.10	22.66	25.22	27.78	30.35	32.91
1172	G	5.17	6.31	7.16	8.00	8.84	9.94	10.78	13.55	16.32	19.10	21.87	24.64	27.41	30.18	32.96	35.73
1173	B	4.26	5.17	5.84	6.50	7.16	8.04	8.70	10.89	13.09	15.28	17.47	19.67	21.86	24.05	26.25	28.44
1177	B	3.67	4.54	5.18	5.81	6.44	7.28	7.91	10.00	12.09	14.19	16.28	18.37	20.47	22.56	24.65	26.75
1190	G	7.48	9.26	10.58	11.89	13.20	14.92	16.23	20.55	24.88	29.20	33.52	37.85	42.17	46.50	50.82	55.15
1191	E	5.35	6.42	7.21	8.00	8.78	9.81	10.60	13.19	15.78	18.38	20.97	23.57	26.16	28.76	31.35	33.94
1194	A	4.67	5.65	6.37	7.09	7.80	8.74	9.45	11.81	14.18	16.54	18.90	21.26	23.62	25.99	28.35	30.71
1199	F	4.26	5.12	5.76	6.40	7.04	7.88	8.51	10.61	12.72	14.82	16.93	19.03	21.13	23.24	25.34	27.45
1212	H	4.14	4.73	5.17	5.61	6.05	6.62	7.06	8.50	9.94	11.39	12.83	14.27	15.71	17.16	18.60	20.04
1214	F	5.75	6.40	6.88	7.37	7.84	8.48	8.96	10.54	12.13	13.72	15.30	16.89	18.48	20.07	21.65	23.24
1215	F	4.61	5.69	6.49	7.28	8.07	9.12	9.91	12.53	15.15	17.77	20.39	23.01	25.63	28.25	30.87	33.49
1216	A	4.06	4.67	5.12	5.57	6.01	6.60	7.05	8.52	10.00	11.47	12.95	14.42	15.90	17.37	18.84	20.32
1217	A	4.97	6.07	6.89	7.70	8.51	9.58	10.38	13.06	15.74	18.41	21.09	23.76	26.44	29.11	31.79	34.47
1222	B	4.86	5.78	6.47	7.15	7.83	8.72	9.40	11.65	13.90	16.14	18.39	20.64	22.89	25.13	27.38	29.63
1223	F	4.44	5.53	6.34	7.14	7.94	9.00	9.80	12.45	15.09	17.74	20.39	23.04	25.68	28.33	30.98	33.63
1239	F	3.93	4.74	5.34	5.94	6.53	7.31	7.91	9.87	11.84	13.81	15.77	17.74	19.70	21.67	23.64	25.60
1240	G	3.61	4.28	4.78	5.27	5.76	6.41	6.90	8.52	10.15	11.77	13.40	15.02	16.65	18.27	19.89	21.52
1242	H	3.26	3.62	3.88	4.14	4.40	4.74	4.99	5.85	6.70	7.56	8.41	9.27	10.12	10.98	11.83	12.69
1243	H	3.93	4.36	4.69	5.01	5.33	5.76	6.08	7.14	8.20	9.27	10.33	11.40	12.46	13.52	14.59	15.65
1244	H	3.40	3.74	3.99	4.24	4.49	4.82	5.06	5.89	6.71	7.54	8.36	9.19	10.01	10.83	11.66	12.48
1245	H	3.21	3.97	4.53	5.09	5.65	6.38	6.93	8.78	10.61	12.45	14.29	16.13	17.97	19.81	21.65	23.49
1246	H	3.43	4.27	4.89	5.50	6.12	6.92	7.54	9.57	11.60	13.63	15.66	17.68	19.71	21.74	23.77	25.80
1247	H	2.54	2.91	3.18	3.45	3.71	4.07	4.34	5.22	6.11	7.00	7.89	8.78	9.66	10.55	11.44	12.33
1248	H	5.52	6.08	6.50	6.91	7.33	7.87	8.28	9.65	11.02	12.39	13.76	15.12	16.49	17.86	19.23	20.60
1249	H	6.37	6.75	7.02	7.30	7.57	7.93	8.21	9.11	10.02	10.92	11.83	12.73	13.64	14.54	15.45	16.35
1250	H	6.36	6.79	7.12	7.44	7.76	8.19	8.51	9.57	10.63	11.70	12.76	13.82	14.89	15.95	17.01	18.08
1251	A	4.20	4.72	5.10	5.49	5.87	6.37	6.75	8.01	9.26	10.52	11.78	13.04	14.30	15.56	16.82	18.07
1252	A	8.48	9.38	10.05	10.71	11.37	12.25	12.90	15.09	17.28	19.46	21.65	23.84	26.02	28.21	30.39	32.58
1253	A	7.73	8.41	8.92	9.41	9.91	10.57	11.06	12.71	14.36	16.01	17.65	19.30	20.95	22.59	24.24	25.89
1254	A	5.25	6.02	6.59	7.16	7.73	8.48	9.05	10.92	12.80	14.68	16.56	18.43	20.31	22.19	24.07	25.95
1255	A	5.50	6.27	6.84	7.40	7.96	8.70	9.26	11.12	12.98	14.84	16.70	18.55	20.41	22.27	24.13	25.99
1256	A	4.74	5.49	6.05	6.60	7.15	7.88	8.43	10.25	12.08	13.90	15.72	17.55	19.37	21.19	23.02	24.84
1257	A	7.35	8.29	8.98	9.66	10.35	11.25	11.93	14.19	16.46	18.72	20.98	23.25	25.51	27.77	30.04	32.30
1258	C	4.12	4.97	5.59	6.22	6.83	7.65	8.27	10.32	12.37	14.42	16.47	18.52	20.57	22.62	24.67	26.72
1259	C	5.52	6.38	7.01	7.64	8.27	9.10	9.73	11.81	13.89	15.97	18.05	20.13	22.21	24.29	26.37	28.45
1260	C	5.04	6.04	6.77	7.50	8.23	9.19	9.92	12.33	14.74	17.15	19.57	21.98	24.39	26.80	29.21	31.62
1261	D	4.84	6.08	7.00	7.91	8.82	10.02	10.93	13.94	16.95	19.96	22.97	25.98	28.99	32.00	35.01	38.02
1262	G	4.24	5.16	5.85	6.53	7.22	8.11	8.79	11.04	13.30	15.55	17.80	20.05	22.30	24.56	26.81	29.06
1263	G	4.48	5.47	6.20	6.92	7.65	8.60	9.32	11.71	14.10	16.49	18.88	21.27	23.66	26.06	28.45	30.84
1264	F	5.08	6.48	7.51	8.54	9.56	10.91	11.93	15.32	18.71	22.09	25.48	28.87	32.26	35.64	39.03	42.42
1265	F	4.15	5.22	6.02	6.81	7.60	8.64	9.43	12.04	14.65	17.26	19.87	22.48	25.09	27.70	30.31	32.92
1266	C	4.34	5.45	6.27	7.08	7.90	8.97	9.78	12.47	15.16	17.85	20.54	23.23	25.92	28.61	31.30	33.99
1267	H	3.63	4.21	4.64	5.07	5.49	6.05	6.47	7.88	9.28	10.68	12.09	13.49	14.89	16.30	17.70	19.10

Station Number	Region	Recurrence Interval for 24-hr Rainfall (inches)															
		10-yr	25-yr	50-yr	100-yr	200-yr	500-yr	1,000-yr	10^4-yr	10^5-yr	10^6-yr	10^7-yr	10^8-yr	10^9-yr	10^10-yr	10^11-yr	10^12-yr
1268	H	3.83	4.30	4.64	4.99	5.33	5.79	6.13	7.27	8.41	9.54	10.68	11.82	12.96	14.09	15.23	16.37
1271	C	3.78	4.65	5.30	5.94	6.57	7.41	8.05	10.16	12.27	14.38	16.49	18.60	20.70	22.81	24.92	27.03
1274	C	3.15	4.11	4.82	5.53	6.23	7.16	7.86	10.18	12.51	14.84	17.17	19.49	21.82	24.15	26.47	28.80
1277	C	3.70	4.44	4.99	5.54	6.09	6.81	7.35	9.15	10.96	12.77	14.57	16.38	18.18	19.99	21.79	23.60
1278	D	5.62	7.35	8.63	9.90	11.17	12.84	14.10	18.29	22.48	26.68	30.87	35.06	39.25	43.44	47.64	51.83

Appendix C - Los Angeles Soil Equations and Variables

Equations for Los Angeles Soil Type Undeveloped Runoff Coefficient Curves		
Soil Number	**Equation #**	**Equation Used To Model Soil Curve**
1	0	
2	7121	y^2=(a+cx)/(1+bx)
3	7111	y^(0.5)=(a+cx)/(1+bx)
4	7121	y^2=(a+cx)/(1+bx)
5	7121	y^2=(a+cx)/(1+bx)
6	7104	lny = (a + cx + ex ^ 2) / (1 + bx + dx ^ 2 + fx ^ 3)
7	7104	lny = (a + cx + ex ^ 2) / (1 + bx + dx ^ 2 + fx ^ 3)
8	7121	y^2=(a+cx)/(1+bx)
9	7301	y^2=(a+cx^2)/(1+bx^2)
10	7301	y^2=(a+cx^2)/(1+bx^2)
11	7121	y^2=(a+cx)/(1+bx)
12	7207	y=(a+clnx+e(lnx)^2+g(lnx)^3+i(lnx)^4)/(1+blnx+d(lnx)^2+f(lnx)^3+h(lnx)^4)
13	7113	y^(0.5)=(a+cx+ex^2)/(1+bx+dx^2)
14	7121	y^2=(a+cx)/(1+bx)
15	7111	y^(0.5)=(a+cx)/(1+bx)
16	7104	lny = (a + cx + ex ^ 2) / (1 + bx + dx ^ 2 + fx ^ 3)
17	7121	y^2=(a+cx)/(1+bx)
18	7104	lny = (a + cx + ex ^ 2) / (1 + bx + dx ^ 2 + fx ^ 3)
19	7104	lny = (a + cx + ex ^ 2) / (1 + bx + dx ^ 2 + fx ^ 3)
20	7111	y^(0.5)=(a+cx)/(1+bx)
21	7111	y^(0.5)=(a+cx)/(1+bx)
22	7121	y^2=(a+cx)/(1+bx)
23	7111	y^(0.5)=(a+cx)/(1+bx)
24	7101	lny=(a+cx)/(1+bx)
25	7113	y^(0.5)=(a+cx+ex^2)/(1+bx+dx^2)
26	7101	lny=(a+cx)/(1+bx)
27	7111	y^(0.5)=(a+cx)/(1+bx)
28	7103	lny = (a + cx + ex ^ 2) / (1 + bx + dx ^ 2)
29	7121	y^2=(a+cx)/(1+bx)
30	7121	y^2=(a+cx)/(1+bx)
31	7121	y^2=(a+cx)/(1+bx)
32	7104	lny = (a + cx + ex ^ 2) / (1 + bx + dx ^ 2 + fx ^ 3)
33	7113	y^(0.5)=(a+cx+ex^2)/(1+bx+dx^2)
34	7104	lny = (a + cx + ex ^ 2) / (1 + bx + dx ^ 2 + fx ^ 3)
35	7113	y^(0.5)=(a+cx+ex^2)/(1+bx+dx^2)
36	7104	lny = (a + cx + ex ^ 2) / (1 + bx + dx ^ 2 + fx ^ 3)
37	7121	y^2=(a+cx)/(1+bx)
38	7121	y^2=(a+cx)/(1+bx)
39	7121	y^2=(a+cx)/(1+bx)
40	7121	y^2=(a+cx)/(1+bx)
41	7111	y^(0.5)=(a+cx)/(1+bx)
42	7121	y^2=(a+cx)/(1+bx)
43	7111	y^(0.5)=(a+cx)/(1+bx)
44	7121	y^2=(a+cx)/(1+bx)
45	7121	y^2=(a+cx)/(1+bx)
46	7101	lny=(a+cx)/(1+bx)
47	7104	lny = (a + cx + ex ^ 2) / (1 + bx + dx ^ 2 + fx ^ 3)
48	7121	y^2=(a+cx)/(1+bx)
49	7121	y^2=(a+cx)/(1+bx)
50	7104	lny = (a + cx + ex ^ 2) / (1 + bx + dx ^ 2 + fx ^ 3)
51	7121	y^2=(a+cx)/(1+bx)

Equations for Los Angeles Soil Type Undeveloped Runoff Coefficient Curves		
Soil Number	**Equation #**	**Equation Used To Model Soil Curve**
52	7101	lny=(a+cx)/(1+bx)
53	7121	y^2=(a+cx)/(1+bx)
54	7121	y^2=(a+cx)/(1+bx)
55	7111	y^(0.5)=(a+cx)/(1+bx)
56	7113	y^(0.5)=(a+cx+ex^2)/(1+bx+dx^2)
57	7104	lny = (a + cx + ex ^ 2) / (1 + bx + dx ^ 2 + fx ^ 3)
58	7121	y^2=(a+cx)/(1+bx)
59	7121	y^2=(a+cx)/(1+bx)
60	7111	y^(0.5)=(a+cx)/(1+bx)
61	7111	y^(0.5)=(a+cx)/(1+bx)
62	7121	y^2=(a+cx)/(1+bx)
63	7121	y^2=(a+cx)/(1+bx)
64	7111	y^(0.5)=(a+cx)/(1+bx)
65	7121	y^2=(a+cx)/(1+bx)
66	7103	lny = (a + cx + ex ^ 2) / (1 + bx + dx ^ 2)
67	7121	y^2=(a+cx)/(1+bx)
68	7111	y^(0.5)=(a+cx)/(1+bx)
69	7111	y^(0.5)=(a+cx)/(1+bx)
70	7121	y^2=(a+cx)/(1+bx)
71	7121	y^2=(a+cx)/(1+bx)
72	7111	y^(0.5)=(a+cx)/(1+bx)
73	7101	lny=(a+cx)/(1+bx)
74	7104	lny = (a + cx + ex ^ 2) / (1 + bx + dx ^ 2 + fx ^ 3)
75	7111	y^(0.5)=(a+cx)/(1+bx)
76	7121	y^2=(a+cx)/(1+bx)
77	7121	y^2=(a+cx)/(1+bx)
78	7121	y^2=(a+cx)/(1+bx)
79	7121	y^2=(a+cx)/(1+bx)
80	7121	y^2=(a+cx)/(1+bx)
81	7121	y^2=(a+cx)/(1+bx)
82	7111	y^(0.5)=(a+cx)/(1+bx)
83	7121	y^2=(a+cx)/(1+bx)
84	7111	y^(0.5)=(a+cx)/(1+bx)
85	7121	y^2=(a+cx)/(1+bx)
86	7104	lny = (a + cx + ex ^ 2) / (1 + bx + dx ^ 2 + fx ^ 3)
87	7111	y^(0.5)=(a+cx)/(1+bx)
88	7301	y^2=(a+cx^2)/(1+bx^2)
89	7121	y^2=(a+cx)/(1+bx)
90	7121	y^2=(a+cx)/(1+bx)
91	7121	y^2=(a+cx)/(1+bx)
92	7121	y^2=(a+cx)/(1+bx)
93	7111	y^(0.5)=(a+cx)/(1+bx)
94	7121	y^2=(a+cx)/(1+bx)
95	7121	y^2=(a+cx)/(1+bx)
96	7111	y^(0.5)=(a+cx)/(1+bx)
97	7121	y^2=(a+cx)/(1+bx)
98	7113	y^(0.5)=(a+cx+ex^2)/(1+bx+dx^2)
99	7121	y^2=(a+cx)/(1+bx)
100	7121	y^2=(a+cx)/(1+bx)
101	7121	y^2=(a+cx)/(1+bx)
102	7121	y^2=(a+cx)/(1+bx)
103	7121	y^2=(a+cx)/(1+bx)
104	7121	y^2=(a+cx)/(1+bx)

Equations for Los Angeles Soil Type Undeveloped Runoff Coefficient Curves		
Soil Number	**Equation #**	**Equation Used To Model Soil Curve**
105	7113	y^(0.5)=(a+cx+ex^2)/(1+bx+dx^2)
106	7121	y^2=(a+cx)/(1+bx)
107	7121	y^2=(a+cx)/(1+bx)
108	5076	y=a+bx+clnx+d/x+elnx/x^2
109	7121	y^2=(a+cx)/(1+bx)
110	7121	y^2=(a+cx)/(1+bx)
111	7121	y^2=(a+cx)/(1+bx)
112	7121	y^2=(a+cx)/(1+bx)
113	7121	y^2=(a+cx)/(1+bx)
114	7121	y^2=(a+cx)/(1+bx)
115	7121	y^2=(a+cx)/(1+bx)
116	7121	y^2=(a+cx)/(1+bx)
117	7121	y^2=(a+cx)/(1+bx)
118	7121	y^2=(a+cx)/(1+bx)
119	7111	y^(0.5)=(a+cx)/(1+bx)
120	7121	y^2=(a+cx)/(1+bx)
121	7101	y^2=(a+cx)/(1+bx)
122	7111	y^(0.5)=(a+cx)/(1+bx)
123	7121	y^2=(a+cx)/(1+bx)
124	7111	y^(0.5)=(a+cx)/(1+bx)
125	7111	y^(0.5)=(a+cx)/(1+bx)
126	7121	y^2=(a+cx)/(1+bx)
127	7111	y^(0.5)=(a+cx)/(1+bx)
128	7121	y^2=(a+cx)/(1+bx)
129	7111	y^(0.5)=(a+cx)/(1+bx)
130	7101	lny=(a+cx)/(1+bx)
131	7101	lny=(a+cx)/(1+bx)
132	7113	y^(0.5)=(a+cx+ex^2)/(1+bx+dx^2)
133	7111	y^(0.5)=(a+cx)/(1+bx)
134	7103	lny = (a + cx + ex ^ 2) / (1 + bx + dx ^ 2)
135	7121	y^2=(a+cx)/(1+bx)
136	7121	y^2=(a+cx)/(1+bx)
137	7111	y^(0.5)=(a+cx)/(1+bx)
138	7111	y^(0.5)=(a+cx)/(1+bx)
139	7121	y^2=(a+cx)/(1+bx)
140	7111	y^(0.5)=(a+cx)/(1+bx)
141	7111	y^(0.5)=(a+cx)/(1+bx)
142	7121	y^2=(a+cx)/(1+bx)
143	7111	y^(0.5)=(a+cx)/(1+bx)
144	7111	y^(0.5)=(a+cx)/(1+bx)
145	7121	y^2=(a+cx)/(1+bx)
146	7111	y^(0.5)=(a+cx)/(1+bx)
147	7111	y^(0.5)=(a+cx)/(1+bx)
148	7111	y^(0.5)=(a+cx)/(1+bx)
149	7121	y^2=(a+cx)/(1+bx)
150	7111	y^(0.5)=(a+cx)/(1+bx)
151	7101	lny=(a+cx)/(1+bx)
152	7111	y^(0.5)=(a+cx)/(1+bx)
153	7111	y^(0.5)=(a+cx)/(1+bx)
154	7121	y^2=(a+cx)/(1+bx)
155	7111	y^(0.5)=(a+cx)/(1+bx)
156	7104	lny = (a + cx + ex ^ 2) / (1 + bx + dx ^ 2 + fx ^ 3)
157	7101	lny=(a+cx)/(1+bx)

Equations for Los Angeles Soil Type Undeveloped Runoff Coefficient Curves		
Soil Number	**Equation #**	**Equation Used To Model Soil Curve**
158	7121	y^2=(a+cx)/(1+bx)
159	7301	y^2=(a+cx^2)/(1+bx^2)
160	7111	y^(0.5)=(a+cx)/(1+bx)
161	7301	y^2=(a+cx^2)/(1+bx^2)
162	7111	y^(0.5)=(a+cx)/(1+bx)
163	7121	y^2=(a+cx)/(1+bx)
164	7121	y^2=(a+cx)/(1+bx)
165	7121	y^2=(a+cx)/(1+bx)
166	7111	y^(0.5)=(a+cx)/(1+bx)
167	7111	y^(0.5)=(a+cx)/(1+bx)
168	7103	lny = (a + cx + ex ^ 2) / (1 + bx + dx ^ 2)
169	7206	y=(a+clnx+e(lnx)^2+g(lnx)^3)/(1+blnx+d(lnx)^2+f(lnx)^3+h(lnx)^4)
170	7121	y^2=(a+cx)/(1+bx)
171	7111	y^(0.5)=(a+cx)/(1+bx)
172	7111	y^(0.5)=(a+cx)/(1+bx)
173	7121	y^2=(a+cx)/(1+bx)
174	7301	y^2=(a+cx^2)/(1+bx^2)
175	7121	y^2=(a+cx)/(1+bx)
176	7121	y^2=(a+cx)/(1+bx)
177	7121	y^2=(a+cx)/(1+bx)
178	7301	y^2=(a+cx^2)/(1+bx^2)
179	6503	y=a+b/x+c/x^2+d/x^3+e/x^4+f/x^5
180	6503	y=a+b/x+c/x^2+d/x^3+e/x^4+f/x^5

Variable Values for Soil Equations											
Soil Number	Equation #	a	b	c	d	e	f	g	h	I	r^2
1	0	1	1	1							1.00000
2	7121	-0.17633	1.593751	1.563581							0.99938
3	7111	-0.26585	1.020726	1.002159							0.99640
4	7121	-0.35359	0.998362	0.842516							0.99913
5	7121	-0.31361	0.591028	0.64949							0.98956
6	7104	0.926019	-4.74247	0.512265	1.547259	0.128667	-0.72932				0.99576
7	7104	1.03981	-2.47959	0.430427	0.522188	0.181086	-0.29275				0.99982
8	7121	-0.7034	3.595607	3.660972							0.98420
9	7301	-0.01823	0.388625	0.388591							0.99369
10	7301	-0.02533	0.054486	0.054056							0.99986
11	7121	-0.20702	0.925756	0.866257							0.99597
12	7207	0.838788	0.015599	0.14191	-0.25313	-0.22218	0.199584	0.148416	0.077472	0.087118	0.99990
13	7113	0.485917	-0.88055	-0.80604	1.282425	1.273691					0.98558
14	7121	-0.88832	0.952268	1.01229							0.99849
15	7111	0.09347	0.394854	0.43546							0.99407
16	7104	2.270091	-5.34482	0.413844	0.355194	0.004958	-0.36847				0.99952
17	7121	-0.60229	1.994134	2.067107							0.99782
18	7104	1.917591	-0.98587	-0.65383	0.251328	0.066101	-0.02155				0.99996
19	7104	-8.06405	2.346291	2.329367	-0.7529	-0.28892	0.120037				0.99968
20	7111	0.089485	1.401219	1.321083							0.97692
21	7111	-0.24023	1.112068	1.110003							0.99882
22	7121	-0.2011	0.629961	0.532956							0.99569
23	7111	-0.35313	2.721951	2.708109							0.99894
24	7101	1.524583	-1.23847	0.265669							0.98654
25	7113	0.816097	-6.0355	-4.52695	-2.11529	-2.13289					0.98495
26	7101	1.18716	-0.51054	0.304367							0.99991
27	7111	-0.38779	1.405725	1.403433							0.99692
28	7103	-6.73971	3.699219	-0.28631	0.529542	-0.10771					0.99965
29	7121	-0.3222	1.915728	1.879016							0.99845
30	7121	-0.17292	0.277815	0.230073							0.99957
31	7121	-0.66454	0.823249	0.642119							0.99891
32	7104	-5.16666	6.333169	1.846287	-2.24398	-0.20708	0.242492				0.99977
33	7113	0.894461	-2.47474	-1.31747	-1.09669	-1.11616					0.99941
34	7104	4.647189	-14.1089	-0.50109	3.848682	0.108967	-0.63255				0.99966
35	7113	1.036576	-0.82607	-0.68304	-0.00754	-0.01031					0.99964
36	7104	1.563328	-9.88187	3.884946	-2.42593	-0.12359	-1.21023				0.99899
37	7121	-0.21471	0.303237	0.297844							0.99702
38	7121	-0.3111	0.611538	0.57438							0.99853
39	7121	-0.30973	1.341471	1.323278							0.99185
40	7121	-0.35157	1.445868	1.403807							0.99925
41	7111	1.162749	-0.57633	-0.50487							0.99612
42	7121	-0.17283	0.694161	0.657637							0.99889
43	7111	-0.00039	0.822611	0.832838							0.99817
44	7121	-0.27662	1.928851	1.976142							0.98095
45	7121	-0.52987	0.422639	0.272543							0.99955
46	7101	-7.05987	1.349253	-0.149							0.99989
47	7104	-7.47164	8.09195	2.863042	-3.12147	-0.38183	0.455186				0.99769
48	7121	-0.21283	0.276513	0.319804							0.99773
49	7121	-0.15311	0.575583	0.621904							0.99693
50	7104	2.436585	-11.3862	0.792021	4.113916	0.706937	-3.74759				0.99605
51	7121	-0.23698	0.547755	0.508675							0.99120
52	7101	1.120466	-0.39647	0.104928							0.99977
53	7121	-0.078	0.153448	0.153194							0.99730
54	7121	-0.22393	0.456116	0.492931							0.99193
55	7111	-0.12911	1.666474	1.709978							0.99755
56	7113	0.950549	-2.99107	-5.43808	14.25232	13.85576					0.99509
57	7104	5.539023	-3.02442	-1.78409	0.887479	0.157787	-0.07503				1.00000
58	7121	-0.17684	0.351015	0.364264							0.99861
59	7121	-0.31204	0.913362	0.960437							0.99248
60	7111	2.201668	-3.8424	-3.06139							0.99965
61	7111	1.003242	-0.34255	-0.27752							0.99940
62	7121	-0.23006	0.28715	0.332417							0.99849
63	7121	-0.19164	0.414344	0.418853							0.98861
64	7111	-0.14106	3.800284	3.752774							0.99866
65	7121	-0.20231	1.563764	1.594836							0.99310
66	7103	0.817378	-4.36942	2.873715	-1.68999	-0.01373					0.99567
67	7121	-0.17929	0.335238	0.271005							0.99858
68	7111	-0.05199	1.774242	1.754059							0.99941
69	7111	0.153169	0.973038	0.92871							0.99625
70	7121	-0.34767	1.559153	1.104718							0.98398
71	7121	-0.30886	1.334045	1.309846							0.98920
72	7111	-3.11184	10.88026	10.92241							0.99975

Variable Values for Soil Equations											
Soil Number	Equation #	a	b	c	d	e	f	g	h	I	r^2
73	7101	3.037562	-2.97172	0.023129							0.99958
74	7104	-5.226	2.615638	1.807644	-0.93535	-0.19359	0.103489				0.99950
75	7111	-0.53503	1.507953	1.517645							0.99958
76	7121	-0.05854	0.141327	0.127285							0.99973
77	7121	-0.43257	1.218341	1.212743							0.99938
78	7121	-0.14129	0.260512	0.270429							0.99880
79	7121	-0.25077	0.678669	0.682973							0.99592
80	7121	-0.14972	0.356844	0.363691							0.98494
81	7121	-0.29129	0.900655	0.937258							0.99714
82	7111	-0.48119	2.750924	2.711505							0.99944
83	7121	-0.08958	0.865378	0.833193							0.99870
84	7111	-0.18255	1.176908	1.213199							0.99957
85	7121	-0.23821	0.178792	0.198102							0.98685
86	7104	9.164816	-3.73643	-4.12985	1.516429	0.549094	-0.19211				0.99993
87	7111	-0.51078	1.895164	1.85594							0.99835
88	7301	-0.032	0.097937	0.090772							0.99766
89	7121	-0.19911	0.804718	0.634796							0.98868
90	7121	-0.16361	1.137931	1.087174							0.99929
91	7121	-0.19328	1.364425	1.123025							0.99819
92	7121	-0.2749	1.883646	1.59838							0.99817
93	7111	-0.10144	2.532178	2.46317							0.99787
94	7121	-0.50631	2.753189	2.577929							0.99769
95	7121	-0.30551	1.674588	1.453369							0.99628
96	7111	2.62744	-2.1986	-2.044							0.99967
97	7121	-0.23357	0.921451	0.752114							0.99447
98	7113	4.728384	-27.1952	-26.2065	0.263442	0.230694					0.99986
99	7121	-0.42278	1.679189	1.533421							0.99454
100	7121	-0.22005	0.370169	0.344632							0.99445
101	7121	-0.17017	0.483516	0.28565							0.99717
102	7121	-0.39096	1.469722	1.336977							0.99852
103	7121	-0.16936	0.625108	0.592526							0.98625
104	7121	-0.23806	0.342255	0.338673							0.99434
105	7113	-0.1231	2.377948	2.05399	0.155122	0.172742					0.99998
106	7121	-0.07117	0.083205	0.049056							0.99928
107	7121	-0.18949	1.023084	0.911876							0.99498
108	5076	0.722918	-0.00413	0.104359	-0.0183	0.000648					0.99376
109	7121	-0.27502	1.164275	0.945645							0.99761
110	7121	-0.22463	2.728585	2.303038							0.99280
111	7121	-0.23397	0.738702	0.626834							0.99542
112	7121	-0.36979	1.534761	1.366674							0.99884
113	7121	-0.12223	0.53681	0.539764							0.99698
114	7121	-0.06847	0.172146	0.220944							0.99912
115	7121	-0.16777	0.931937	0.848147							0.99436
116	7121	-0.31384	0.593471	0.449594							0.99716
117	7121	-0.22708	2.670206	2.406053							0.99922
118	7121	-0.2986	0.553248	0.534206							0.99680
119	7111	-0.78645	2.102349	2.077522							0.99989
120	7121	-0.23258	0.379638	0.377706							0.99687
121	7101	2.548093	-0.6065	-0.00177							0.99687
122	7111	-0.48241	1.512111	1.498407							0.99937
123	7121	-0.08958	0.865378	0.833193							0.99870
124	7111	-0.58884	0.908819	0.945697							0.99955
125	7111	3.765367	-1.77789	-1.77855							0.99968
126	7121	-0.16072	0.196708	0.249184							0.99656
127	7111	-0.98132	1.384513	1.387817							0.99943
128	7121	-0.16128	0.056925	0.112624							0.99861
129	7111	-0.31019	0.831849	0.875288							0.99989
130	7101	1.724393	-1.10516	0.567941							0.99931
131	7101	2.753268	-0.65922	-0.0152							0.99989
132	7113	0.618507	-0.43843	-0.30274	0.059019	0.040978					0.99789
133	7111	-0.99458	7.610285	7.392733							0.99916
134	7103	0.734487	-1.40246	1.280321	-0.20884	-0.06307					0.99960
135	7121	-0.46291	1.426285	1.299167							0.99962
136	7121	-0.32778	0.17629	0.15399							0.99710
137	7111	-0.74858	5.101834	4.918566							0.99820
138	7111	2.223014	-3.2469	-3.00713							0.99926
139	7121	-0.09317	0.795792	0.834859							0.98869
140	7111	2.033186	-3.77982	-3.62744							0.99891
141	7111	3.000035	-7.50953	-7.07691							0.99571
142	7121	-0.3911	0.770765	0.758231							0.99770
143	7111	1.979302	-1.97868	-1.75384							0.99949
144	7111	2.201742	-2.65442	-2.48094							0.99964

Variable Values for Soil Equations											
Soil Number	**Equation #**	**a**	**b**	**c**	**d**	**e**	**f**	**g**	**h**	**I**	**r^2**
145	7121	-0.18403	0.086771	0.072601							0.99938
146	7111	2.227199	-4.61527	-4.26122							0.99931
147	7111	2.374798	-3.8579	-3.76932							0.99892
148	7111	2.43999	-4.65481	-4.19483							0.99934
149	7121	-0.39136	0.308415	0.249037							0.99785
150	7111	1.66488	-1.3231	-1.21243							0.99894
151	7101	1.461268	-5.96472	0.506332							0.99894
152	7111	2.161202	-6.48316	-6.34241							0.99985
153	7111	1.098016	-0.71985	-0.64236							0.98888
154	7121	-0.49177	1.567197	1.341695							0.99850
155	7111	0.125437	0.97437	1.013629							0.98080
156	7104	-5.09836	2.275417	1.583413	-0.46665	-0.22416	0.11392				0.99997
157	7101	0.317883	-0.90488	0.325791							0.99459
158	7121	-0.11735	0.208051	0.229303							0.99582
159	7301	-0.01777	0.184157	0.132798							0.99431
160	7111	-0.74243	0.811688	0.869775							0.99889
161	7301	-0.02405	0.034239	0.033256							0.99677
162	7111	-0.39972	3.958879	4.008661							0.99134
163	7121	-0.21955	1.948176	1.776642							0.99867
164	7121	-0.16591	0.52419	0.449189							0.98693
165	7121	-0.1991	0.478604	0.494051							0.99132
166	7111	-0.27059	0.172781	0.177443							0.99912
167	7111	-0.12781	4.487394	4.523759							0.99470
168	7103	0.411537	-0.5853	-0.0294	0.093342	-0.03956					0.99713
169	7206	0.401362	-0.71059	-0.1824	-0.14451	-0.16481	0.227429	0.110204	-0.02525		0.99990
170	7121	-0.17965	0.402536	0.057745							0.99828
171	7111	0.016043	1.457684	1.380061							0.99897
172	7111	-0.13315	0.743136	0.795422							0.99865
173	7121	0.927961	-0.95899	-0.44697							0.99925
174	7301	-0.05698	0.246421	0.182184							0.99913
175	7121	-0.95157	1.147857	0.985331							0.98999
176	7121	-0.16832	0.67324	0.724939							0.99756
177	7121	-0.28507	0.953902	0.950439							0.99927
178	7301	-0.39482	0.107509	0.095313							0.98448
179	6503	0.765302	0.070856	1.251185	-23.9843	55.25434	-39.046				0.99977
180	6503	0.933928	0.044485	-2.80072	4.231886	-2.45987	0.493216				0.99958

Appendix D - LACDPW Style Analysis by Grid Level

Percent	Watershed Size = 0.10 sq. mi. Grid				
	Original Data		Actual		Conditional
Burned	Histogram	pdf	CDF	Excedence	Excedence
0%	2884925				
1%-10%	67208	0.2037	0.2037	0.7963	0.0817
10%-20%	59098	0.1791	0.3829	0.6171	0.0633
20%-30%	32776	0.0994	0.4822	0.5178	0.0531
30%-40%	34722	0.1053	0.5875	0.4125	0.0423
40%-50%	34676	0.1051	0.6926	0.3074	0.0315
50%-60%	4803	0.0146	0.7072	0.2928	0.0300
60%-70%	7057	0.0214	0.7286	0.2714	0.0279
70%-80%	28775	0.0872	0.8158	0.1842	0.0189
80%-90%	28195	0.0855	0.9013	0.0987	0.0101
90%-100%	32572	0.0987	1.0000	0.0000	0.0000
Unburned	89.74%				
Burned	10.26%				

Percent	Watershed Size = 0.25 sq. mi. Grid				
	Original Data		Actual		Conditional
Burned	Histogram	pdf	CDF	Excedence	Excedence
0%	1218821				
1%-10%	61196	0.4394	0.4394	0.5606	0.0575
10%-20%	29232	0.2099	0.6493	0.3507	0.0360
20%-30%	15814	0.1136	0.7629	0.2371	0.0243
30%-40%	10391	0.0746	0.8375	0.1625	0.0167
40%-50%	7726	0.0555	0.8930	0.1070	0.0110
50%-60%	1596	0.0115	0.9045	0.0955	0.0098
60%-70%	1203	0.0086	0.9131	0.0869	0.0089
70%-80%	3633	0.0261	0.9392	0.0608	0.0062
80%-90%	4567	0.0328	0.9720	0.0280	0.0029
90%-100%	3903	0.0280	1.0000	0.0000	0.0000
Unburned	89.75%				
Burned	10.25%				

Percent	Watershed Size = 1.0 sq. mi. Grid				
	Original Data		Actual		Conditional
Burned	Histogram	pdf	CDF	Excedence	Excedence
0%	338127				
1%-10%	23555	0.4795	0.4795	0.5205	0.0660
10%-20%	7623	0.1552	0.6347	0.3653	0.0463
20%-30%	4110	0.0837	0.7183	0.2817	0.0357
30%-40%	3262	0.0664	0.7847	0.2153	0.0273
40%-50%	2906	0.0592	0.8439	0.1561	0.0198
50%-60%	940	0.0191	0.8630	0.1370	0.0174
60%-70%	1093	0.0222	0.8853	0.1147	0.0146
70%-80%	1766	0.0359	0.9212	0.0788	0.0100
80%-90%	1873	0.0381	0.9593	0.0407	0.0052
90%-100%	1997	0.0407	1.0000	0.0000	0.0000
Unburned	87.31%				
Burned	12.69%				

Percent	Watershed Size = 4.0 sq. mi. Grid				
	Original Data		Actual		Conditional
Burned	Histogram	pdf	CDF	Excedence	Excedence
0%	93883				
1%-10%	12348	0.6495	0.6495	0.3505	0.0590
10%-20%	2361	0.1242	0.7736	0.2264	0.0381
20%-30%	1190	0.0626	0.8362	0.1638	0.0276
30%-40%	840	0.0442	0.8804	0.1196	0.0201
40%-50%	678	0.0357	0.9161	0.0839	0.0141
50%-60%	334	0.0176	0.9336	0.0664	0.0112
60%-70%	319	0.0168	0.9504	0.0496	0.0084
70%-80%	321	0.0169	0.9673	0.0327	0.0055
80%-90%	326	0.0171	0.9844	0.0156	0.0026
90%-100%	296	0.0156	1.0000	0.0000	0.0000
Unburned	83.16%				
Burned	16.84%				

Percent	Watershed Size = 16.0 sq. mi. Grid				
	Original Data		Actual		Conditional
Burned	Histogram	pdf	CDF	Excedence	Excedence
0%	25945				
1%-10%	6431	0.7787	0.7787	0.2213	0.0534
10%-20%	786	0.0952	0.8738	0.1262	0.0305
20%-30%	372	0.0450	0.9189	0.0811	0.0196
30%-40%	202	0.0245	0.9433	0.0567	0.0137
40%-50%	163	0.0197	0.9631	0.0369	0.0089
50%-60%	86	0.0104	0.9735	0.0265	0.0064
60%-70%	75	0.0091	0.9826	0.0174	0.0042
70%-80%	52	0.0063	0.9889	0.0111	0.0027
80%-90%	46	0.0056	0.9944	0.0056	0.0013
90%-100%	46	0.0056	1.0000	0.0000	0.0000
Unburned	75.85%				
Burned	24.15%				

Percent	Watershed Size = 25.0 sq. mi. Grid				
	Original Data		Actual		Conditional
Burned	Histogram	pdf	CDF	Excedence	Excedence
0%	16632				
1%-10%	5231	0.8095	0.8095	0.1905	0.0533
10%-20%	562	0.0870	0.8965	0.1035	0.0290
20%-30%	249	0.0385	0.9350	0.0650	0.0182
30%-40%	145	0.0224	0.9574	0.0426	0.0119
40%-50%	105	0.0162	0.9737	0.0263	0.0074
50%-60%	53	0.0082	0.9819	0.0181	0.0051
60%-70%	47	0.0073	0.9892	0.0108	0.0030
70%-80%	29	0.0045	0.9937	0.0063	0.0018
80%-90%	18	0.0028	0.9964	0.0036	0.0010
90%-100%	23	0.0036	1.0000	0.0000	0.0000
Unburned	72.02%				
Burned	27.98%				

Percent	Watershed Size = 64.0 sq. mi. Grid				
	Original Data		Actual		Conditional
Burned	Histogram	pdf	CDF	Excedence	Excedence
0%	7844				
1%-10%	3241	0.8597	0.8597	0.1403	0.0455
10%-20%	268	0.0711	0.9308	0.0692	0.0225
20%-30%	110	0.0292	0.9599	0.0401	0.0130
30%-40%	58	0.0154	0.9753	0.0247	0.0080
40%-50%	39	0.0103	0.9857	0.0143	0.0046
50%-60%	20	0.0053	0.9910	0.0090	0.0029
60%-70%	10	0.0027	0.9936	0.0064	0.0021
70%-80%	10	0.0027	0.9963	0.0037	0.0012
80%-90%	6	0.0016	0.9979	0.0021	0.0007
90%-100%	8	0.0021	1.0000	0.0000	0.0000
Unburned	67.54%				
Burned	32.46%				

Percent	Watershed Size = 100.0 sq. mi. Grid				
	Original Data		Actual		Conditional
Burned	Histogram	pdf	CDF	Excedence	Excedence
0%	4196				
1%-10%	2435	0.8791	0.8791	0.1209	0.0481
10%-20%	184	0.0664	0.9455	0.0545	0.0217
20%-30%	70	0.0253	0.9708	0.0292	0.0116
30%-40%	38	0.0137	0.9845	0.0155	0.0062
40%-50%	23	0.0083	0.9928	0.0072	0.0029
50%-60%	9	0.0032	0.9960	0.0040	0.0016
60%-70%	7	0.0025	0.9986	0.0014	0.0006
70%-80%	3	0.0011	0.9996	0.0004	0.0001
80%-90%	1	0.0004	1.0000	0.0000	0.0000
90%-100%	0	0.0000	1.0000	0.0000	0.0000
Unburned	60.24%				
Burned	39.76%				

Percent Burned	Watershed Size = 256.0 sq. mi. Grid				
	Original Data		Actual		Conditional
	Histogram	pdf	CDF	Excedence	Excedence
0%	2479				
1%-10%	1580	0.8886	0.8886	0.1114	0.0465
10%-20%	119	0.0669	0.9556	0.0444	0.0186
20%-30%	44	0.0247	0.9803	0.0197	0.0082
30%-40%	23	0.0129	0.9933	0.0067	0.0028
40%-50%	5	0.0028	0.9961	0.0039	0.0016
50%-60%	1	0.0006	0.9966	0.0034	0.0014
60%-70%	5	0.0028	0.9994	0.0006	0.0002
70%-80%	1	0.0006	1.0000	0.0000	0.0000
80%-90%	0	0.0000	1.0000	0.0000	0.0000
90%-100%	0	0.0000	1.0000	0.0000	0.0000
Unburned	58.23%				
Burned	41.77%				

Percent Burned	Watershed Size = 400.0 sq. mi. Grid				
	Original Data		Actual		Conditional
	Histogram	pdf	CDF	Excedence	Excedence
0%	1139				
1%-10%	1087	0.9189	0.9189	0.0811	0.0413
10%-20%	60	0.0507	0.9696	0.0304	0.0155
20%-30%	26	0.0220	0.9915	0.0085	0.0043
30%-40%	7	0.0059	0.9975	0.0025	0.0013
40%-50%	2	0.0017	0.9992	0.0008	0.0004
50%-60%	1	0.0008	1.0000	0.0000	0.0000
60%-70%	0	0.0000	1.0000	0.0000	0.0000
70%-80%	0	0.0000	1.0000	0.0000	0.0000
80%-90%	0	0.0000	1.0000	0.0000	0.0000
90%-100%	0	0.0000	1.0000	0.0000	0.0000
Unburned	49.05%				
Burned	50.95%				

Percent Burned	Watershed Size = 1024.0 sq. mi. Grid				
	Original Data		Actual		Conditional
	Histogram	pdf	CDF	Excedence	Excedence
0%	1103				
1%-10%	877	0.9126	0.9126	0.0874	0.0407
10%-20%	62	0.0645	0.9771	0.0229	0.0107
20%-30%	14	0.0146	0.9917	0.0083	0.0039
30%-40%	4	0.0042	0.9958	0.0042	0.0019
40%-50%	3	0.0031	0.9990	0.0010	0.0005
50%-60%	1	0.0010	1.0000	0.0000	0.0000
60%-70%	0	0.0000	1.0000	0.0000	0.0000
70%-80%	0	0.0000	1.0000	0.0000	0.0000
80%-90%	0	0.0000	1.0000	0.0000	0.0000
90%-100%	0	0.0000	1.0000	0.0000	0.0000
Unburned	53.44%				
Burned	46.56%				

Percent Burned	Watershed Size = 1600.0 sq. mi. Grid				
	Original Data		Actual		Conditional
	Histogram	pdf	CDF	Excedence	Excedence
0%	624				
1%-10%	501	0.9330	0.9330	0.0670	0.0310
10%-20%	23	0.0428	0.9758	0.0242	0.0112
20%-30%	5	0.0093	0.9851	0.0149	0.0069
30%-40%	5	0.0093	0.9944	0.0056	0.0026
40%-50%	1	0.0019	0.9963	0.0037	0.0017
50%-60%	1	0.0019	0.9981	0.0019	0.0009
60%-70%	1	0.0019	1.0000	0.0000	0.0000
70%-80%	0	0.0000	1.0000	0.0000	0.0000
80%-90%	0	0.0000	1.0000	0.0000	0.0000
90%-100%	0	0.0000	1.0000	0.0000	0.0000
Unburned	53.75%				
Burned	46.25%				

Fire Factor Histograms by Percentage Burned													
Percent Burned	Area (mi^2) Level	0.10 0	0.25 1	1 2	4 3	16 4	25 5	65 6	100 7	256 8	400 9	1024 10	1600 11
0%		2884925	1218821	338127	93883	25945	16632	7844	4196	2479	1139	1103	624
1%-10%		67208	61196	23555	12348	6431	5231	3241	2435	1580	1087	877	501
10%-20%		59098	29232	7623	2361	786	562	268	184	119	60	62	23
20%-30%		32776	15814	4110	1190	372	249	110	70	44	26	14	5
30%-40%		34722	10391	3262	840	202	145	58	38	23	7	4	5
40%-50%		34676	7726	2906	678	163	105	39	23	5	2	3	1
50%-60%		4803	1596	940	334	86	53	20	9	1	1	1	1
60%-70%		7057	1203	1093	319	75	47	10	7	5	0	0	1
70%-80%		28775	3633	1766	321	52	29	10	3	1	0	0	0
80%-90%		28195	4567	1873	326	46	18	6	1	0	0	0	0
90%-100%		32572	3903	1997	296	46	23	8	0	0	0	0	0
Total Records		3214807	1358082	387252	112896	34204	23094	11614	6966	4257	2322	2064	1161
Unburned		89.74%	89.75%	87.31%	83.16%	75.85%	72.02%	67.54%	60.24%	58.23%	49.05%	53.44%	53.75%
Burned		10.26%	10.25%	12.69%	16.84%	24.15%	27.98%	32.46%	39.76%	41.77%	50.95%	46.56%	46.25%

Fire Factor Probability Density Functions													
Percent Burned	Area (mi^2) Level	0.10 0	0.25 1	1 2	4 3	16 4	25 5	65 6	100 7	256 8	400 9	1024 10	1600 11
0%													
1%-10%		0.2037	0.4394	0.4795	0.6495	0.7787	0.8095	0.8597	0.8791	0.8886	0.9189	0.9126	0.9330
10%-20%		0.1791	0.2099	0.1552	0.1242	0.0952	0.0870	0.0711	0.0664	0.0669	0.0507	0.0645	0.0428
20%-30%		0.0994	0.1136	0.0837	0.0626	0.0450	0.0385	0.0292	0.0253	0.0247	0.0220	0.0146	0.0093
30%-40%		0.1053	0.0746	0.0664	0.0442	0.0245	0.0224	0.0154	0.0137	0.0129	0.0059	0.0042	0.0093
40%-50%		0.1051	0.0555	0.0592	0.0357	0.0197	0.0162	0.0103	0.0083	0.0028	0.0017	0.0031	0.0019
50%-60%		0.0146	0.0115	0.0191	0.0176	0.0104	0.0082	0.0053	0.0032	0.0006	0.0008	0.0010	0.0019
60%-70%		0.0214	0.0086	0.0222	0.0168	0.0091	0.0073	0.0027	0.0025	0.0028	0.0000	0.0000	0.0019
70%-80%		0.0872	0.0261	0.0359	0.0169	0.0063	0.0045	0.0027	0.0011	0.0006	0.0000	0.0000	0.0000
80%-90%		0.0855	0.0328	0.0381	0.0171	0.0056	0.0028	0.0016	0.0004	0.0000	0.0000	0.0000	0.0000
90%-100%		0.0987	0.0280	0.0407	0.0156	0.0056	0.0036	0.0021	0.0000	0.0000	0.0000	0.0000	0.0000
Cumulative Value		1.0000	1.0000	1.0000	1.0000	1.0000	1.0000	1.0000	1.0000	1.0000	1.0000	1.0000	1.0000

Fire Factor Cumulative Probability Distribution													
Percent Burned	Area (mi^2) Level	0.10 0	0.25 1	1 2	4 3	16 4	25 5	65 6	100 7	256 8	400 9	1024 10	1600 11
0%													
1%-10%		0.2037	0.4394	0.4795	0.6495	0.7787	0.8095	0.8597	0.8791	0.8886	0.9189	0.9126	0.9330
10%-20%		0.3829	0.6493	0.6347	0.7736	0.8738	0.8965	0.9308	0.9455	0.9556	0.9696	0.9771	0.9758
20%-30%		0.4822	0.7629	0.7183	0.8362	0.9189	0.9350	0.9599	0.9708	0.9803	0.9915	0.9917	0.9851
30%-40%		0.5875	0.8375	0.7847	0.8804	0.9433	0.9574	0.9753	0.9845	0.9933	0.9975	0.9958	0.9944
40%-50%		0.6926	0.8930	0.8439	0.9161	0.9631	0.9737	0.9857	0.9928	0.9961	0.9992	0.9990	0.9963
50%-60%		0.7072	0.9045	0.8630	0.9336	0.9735	0.9819	0.9910	0.9960	0.9966	1.0000	1.0000	0.9981
60%-70%		0.7286	0.9131	0.8853	0.9504	0.9826	0.9892	0.9936	0.9986	0.9994	1.0000	1.0000	1.0000
70%-80%		0.8158	0.9392	0.9212	0.9673	0.9889	0.9937	0.9963	0.9996	1.0000	1.0000	1.0000	1.0000
80%-90%		0.9013	0.9720	0.9593	0.9844	0.9944	0.9964	0.9979	1.0000	1.0000	1.0000	1.0000	1.0000
90%-100%		1.0000	1.0000	1.0000	1.0000	1.0000	1.0000	1.0000	1.0000	1.0000	1.0000	1.0000	1.0000

Fire Factor Exceedance Probability Distribution													
Percent Burned	Area (mi^2) Level	0.10 0	0.25 1	1 2	4 3	16 4	25 5	65 6	100 7	256 8	400 9	1024 10	1600 11
0%													
1%-10%		0.7963	0.5606	0.5205	0.3505	0.2213	0.1905	0.1403	0.1209	0.1114	0.0811	0.0874	0.0670
10%-20%		0.6171	0.3507	0.3653	0.2264	0.1262	0.1035	0.0692	0.0545	0.0444	0.0304	0.0229	0.0242
20%-30%		0.5178	0.2371	0.2817	0.1638	0.0811	0.0650	0.0401	0.0292	0.0197	0.0085	0.0083	0.0149
30%-40%		0.4125	0.1625	0.2153	0.1196	0.0567	0.0426	0.0247	0.0155	0.0067	0.0025	0.0042	0.0056
40%-50%		0.3074	0.1070	0.1561	0.0839	0.0369	0.0263	0.0143	0.0072	0.0039	0.0008	0.0010	0.0037
50%-60%		0.2928	0.0955	0.1370	0.0664	0.0265	0.0181	0.0090	0.0040	0.0034	0.0000	0.0000	0.0019
60%-70%		0.2714	0.0869	0.1147	0.0496	0.0174	0.0108	0.0064	0.0014	0.0006	0.0000	0.0000	0.0000
70%-80%		0.1842	0.0608	0.0788	0.0327	0.0111	0.0063	0.0037	0.0004	0.0000	0.0000	0.0000	0.0000
80%-90%		0.0987	0.0280	0.0407	0.0156	0.0056	0.0036	0.0021	0.0000	0.0000	0.0000	0.0000	0.0000
90%-100%		0.0000	0.0000	0.0000	0.0000	0.0000	0.0000	0.0000	0.0000	0.0000	0.0000	0.0000	0.0000

Appendix E - Grid Frequency Analysis of Fire Factors by Size

Grid Level 0 - 0.1 Square Miles												
Probability	Recurrence Interval	Fire Factor Frequency Using Extreme Value Probability Distributions				Fire Factor Frequency Using Plotting Position Distributions						Percentile Analysis
p	T	Normal	Log-Normal	LP3	Gumbel	Weibull	California	Cunnane	Gringorton	Adamowski	Hazen	
0.990	1.01	-0.32127	0.00616		-0.11226	0.00142	0.00142	0.00142	0.00142	0.00142	0.00142	0.0007
0.800	1.25	0.131	0.060		0.138	0.10000	0.10000	0.10000	0.10000	0.10000	0.10000	0.1000
0.500	2	0.388	0.215		0.338	0.31000	0.31000	0.31000	0.31000	0.31000	0.31000	0.3100
0.200	5	0.645	0.779		0.607	0.72000	0.72000	0.72000	0.72000	0.72000	0.72000	0.7200
0.100	10	0.779	1.526		0.786	0.90000	0.90000	0.90000	0.90000	0.90000	0.90000	0.9000
0.040	25	0.922	3.124		1.011	0.90000	0.90000	0.90000	0.90000	0.90000	0.90000	0.9000
0.020	50	1.014	4.964		1.178	0.97360	0.97360	0.97355	0.97354	0.97357	0.97354	0.9738
0.010	100	1.097	7.528		1.344	1.00000	1.00000	1.00000	1.00000	1.00000	1.00000	1.0000
0.005	200	1.173	11.021		1.510	1.00000	1.00000	1.00000	1.00000	1.00000	1.00000	1.0000
0.002	500	1.266	17.490		1.728	1.00000	1.00000	1.00000	1.00000	1.00000	1.00000	1.0000
0.001	1000	1.330	24.182		1.893	1.00000	1.00000	1.00000	1.00000	1.00000	1.00000	1.0000
0.0001	10000	1.522	63.191		2.440	1.00000	1.00000	1.00000	1.00000	1.00000	1.00000	1.0000

Grid Level 1 - 0.25 Square Miles												
Probability	Recurrence Interval	Fire Factor Frequency Using Extreme Value Probability Distributions				Fire Factor Frequency Using Plotting Position Distributions						Percentile Analysis
p	T	Normal	Log-Normal	LP3	Gumbel	Weibull	California	Cunnane	Gringorton	Adamowski	Hazen	
0.990	1.01	-0.36029	0.00376	0.00060	-0.15048	0.000302	0.00030	0.00030	0.00030	0.00030	0.00030	0.0004
0.800	1.25	0.094	0.043	0.058	0.100	0.071297	0.07130	0.07130	0.07130	0.07130	0.07130	0.0719
0.500	2	0.352	0.172	0.268	0.301	0.257560	0.25756	0.25756	0.25756	0.25756	0.25756	0.2599
0.200	5	0.609	0.688	0.651	0.572	0.720000	0.72000	0.72000	0.72000	0.72000	0.72000	0.7200
0.100	10	0.744	1.418	0.850	0.751	0.900000	0.90000	0.90000	0.90000	0.90000	0.90000	0.9000
0.040	25	0.887	3.067	1.010	0.977	0.902007	0.90201	0.90200	0.90200	0.90201	0.90200	0.9035
0.020	50	0.980	5.048	1.080	1.145	1.000000	1.00000	1.00000	1.00000	1.00000	1.00000	1.0000
0.010	100	1.064	7.903	1.124	1.312	1.000000	1.00000	1.00000	1.00000	1.00000	1.00000	1.0000
0.005	200	1.140	11.910	1.152	1.478	1.000000	1.00000	1.00000	1.00000	1.00000	1.00000	1.0000
0.002	500	1.233	19.579		1.697	1.000000	1.00000	1.00000	1.00000	1.00000	1.00000	1.0000
0.001	1000	1.297	27.748		1.862	1.000000	1.00000	1.00000	1.00000	1.00000	1.00000	1.0000
0.0001	10000	1.490	78.020		2.412	1.000000	1.00000	1.00000	1.00000	1.00000	1.00000	1.0000

Grid Level 2 - 1.0 Square Miles												
Probability	Recurrence Interval	Fire Factor Frequency Using Extreme Value Probability Distributions				Fire Factor Frequency Using Plotting Position Distributions						Percentile Analysis
p	T	Normal	Log-Normal	LP3	Gumbel	Weibull	California	Cunnane	Gringorton	Adamowski	Hazen	
0.990	1.01	-0.39497	0.00044	0.00009	-0.21557	0.00005	0.00005	0.00005	0.00005	0.00005	0.00005	0.0001
0.800	1.25	-0.006	0.010	0.013	-0.001	0.01181	0.01181	0.01181	0.01181	0.01181	0.01181	0.0118
0.500	2	0.214	0.063	0.092	0.171	0.09999	0.09999	0.09999	0.09999	0.09999	0.09999	0.1000
0.200	5	0.434	0.375	0.380	0.402	0.40000	0.40000	0.40000	0.40000	0.40000	0.40000	0.4000
0.100	10	0.549	0.955	0.659	0.555	0.68190	0.68191	0.68188	0.68187	0.68189	0.68187	0.6819
0.040	25	0.672	2.591	1.045	0.749	0.90000	0.90000	0.90000	0.90000	0.90000	0.90000	0.9000
0.020	50	0.751	4.937	1.324	0.892	0.90000	0.90000	0.90000	0.90000	0.90000	0.90000	0.9000
0.010	100	0.823	8.818	1.579	1.035	1.00000	1.00000	1.00000	1.00000	1.00000	1.00000	1.0000
0.005	200	0.888	14.993	1.806	1.177	1.00000	1.00000	1.00000	1.00000	1.00000	1.00000	1.0000
0.002	500	0.967	28.524		1.364	1.00000	1.00000	1.00000	1.00000	1.00000	1.00000	1.0000
0.001	1000	1.022	44.787		1.505	1.00000	1.00000	1.00000	1.00000	1.00000	1.00000	1.0000
0.0001	10000	1.187	170.653		1.975	1.00000	1.00000	1.00000	1.00000	1.00000	1.00000	1.0000

Grid Level 3 - 4.0 Square Miles												
Probability	Recurrence Interval	Fire Factor Frequency Using Extreme Value Probability Distributions				Fire Factor Frequency Using Plotting Position Distributions						Percentile Analysis
p	T	Normal	Log-Normal	LP3	Gumbel	Weibull	California	Cunnane	Gringorton	Adamowski	Hazen	
0.990	1.01	-0.35422	0.00015	0.00005	-0.20963	0.00003	0.00003	0.00003	0.00003	0.00003	0.00003	0.0000
0.800	1.25	-0.041	0.004	0.005	-0.037	0.00438	0.00438	0.00438	0.00438	0.00438	0.00438	0.0044
0.500	2	0.136	0.029	0.038	0.102	0.04046	0.04047	0.04046	0.04046	0.04046	0.04046	0.0405
0.200	5	0.314	0.195	0.202	0.288	0.21915	0.21916	0.21915	0.21915	0.21915	0.21915	0.2192
0.100	10	0.407	0.529	0.423	0.412	0.43820	0.43822	0.43815	0.43814	0.43817	0.43814	0.4382
0.040	25	0.506	1.531	0.844	0.568	0.71791	0.71793	0.71770	0.71768	0.71777	0.71765	0.7180
0.020	50	0.570	3.040	1.255	0.683	0.87749	0.87752	0.87698	0.87697	0.87713	0.87697	0.8775
0.010	100	0.627	5.635	1.735	0.798	0.90000	0.90000	0.90000	0.90000	0.90000	0.90000	0.9000
0.005	200	0.680	9.914	2.276	0.912	1.00000	1.00000	1.00000	1.00000	1.00000	1.00000	1.0000
0.002	500	0.743	19.658		1.063	1.00000	1.00000	1.00000	1.00000	1.00000	1.00000	1.0000
0.001	1000	0.788	31.774		1.177	1.00000	1.00000	1.00000	1.00000	1.00000	1.00000	1.0000
0.0001	10000	0.921	131.934		1.556	1.00000	1.00000	1.00000	1.00000	1.00000	1.00000	1.0000

Grid Level 4 - 16.0 Square Miles												
Probability	Recurrence Interval	Fire Factor Frequency Using Extreme Value Probability Distributions				Fire Factor Frequency Using Plotting Position Distributions						Percentile Analysis
p	T	Normal	Log-Normal	LP3	Gumbel	Weibull	California	Cunnane	Gringorton	Adamowski	Hazen	
0.990	1.01	-0.27813	0.00007	0.00003	-0.17227	0.00003	0.00003	0.00003	0.00003	0.00003	0.00003	0.0000
0.800	1.25	-0.049	0.002	0.002	-0.046	0.00191	0.00191	0.00191	0.00191	0.00191	0.00191	0.0019
0.500	2	0.081	0.014	0.017	0.056	0.01694	0.01695	0.01694	0.01694	0.01694	0.01694	0.0170
0.200	5	0.211	0.096	0.099	0.192	0.11082	0.11084	0.11081	0.11081	0.11081	0.11081	0.1109
0.100	10	0.279	0.262	0.226	0.283	0.24737	0.24738	0.24732	0.24731	0.24734	0.24731	0.2474
0.040	25	0.351	0.770	0.505	0.397	0.47384	0.47386	0.47376	0.47376	0.47379	0.47374	0.4739
0.020	50	0.398	1.543	0.818	0.481	0.64483	0.64485	0.64454	0.64451	0.64464	0.64446	0.6449
0.010	100	0.440	2.885	1.230	0.565	0.78697	0.78700	0.78589	0.78585	0.78603	0.78579	0.7870
0.005	200	0.479	5.116	1.748	0.649	0.90000	0.90000	0.90000	0.90000	0.90000	0.90000	0.9000
0.002	500	0.526	10.240		0.760	1.00000	1.00000	1.00000	1.00000	1.00000	1.00000	1.0000
0.001	1000	0.558	16.661		0.843	1.00000	1.00000	1.00000	1.00000	1.00000	1.00000	1.0000
0.0001	10000	0.655	70.550		1.121	1.00000	1.00000	1.00000	1.00000	1.00000	1.00000	1.0000

Grid Level 5 - 25.0 Square Miles												
Probability	Recurrence Interval	Fire Factor Frequency Using Extreme Value Probability Distributions				Fire Factor Frequency Using Plotting Position Distributions						Percentile Analysis
p	T	Normal	Log-Normal	LP3	Gumbel						0.0000	
0.990	1.01	-0.24811	0.00006	0.00002	-0.15480	0.00002	0.00002	0.00002	0.00002	0.00002	0.00002	0.0000
0.800	1.25	-0.046	0.002	0.002	-0.043	0.00178	0.00178	0.00178	0.00178	0.00178	0.00178	0.0018
0.500	2	0.069	0.012	0.015	0.046	0.01393	0.01394	0.01393	0.01393	0.01393	0.01393	0.0139
0.200	5	0.183	0.080	0.083	0.166	0.08972	0.08973	0.08971	0.08971	0.08971	0.08971	0.0897
0.100	10	0.243	0.220	0.183	0.246	0.19960	0.19966	0.19940	0.19938	0.19947	0.19935	0.1997
0.040	25	0.307	0.646	0.388	0.347	0.40339	0.40341	0.40332	0.40332	0.40333	0.40332	0.4034
0.020	50	0.348	1.294	0.602	0.421	0.55910	0.55912	0.55872	0.55868	0.55885	0.55863	0.5591
0.010	100	0.385	2.418	0.869	0.495	0.69895	0.69896	0.69847	0.69847	0.69855	0.69845	0.6990
0.005	200	0.419	4.285	1.187	0.569	0.83668	0.83668	0.83658	0.83657	0.83662	0.83656	0.8367
0.002	500	0.460	8.571		0.667	0.96122	0.96123	0.96009	0.95998	0.96049	0.95981	0.9612
0.001	1000	0.489	13.939		0.740	1.00000	1.00000	1.00000	1.00000	1.00000	1.00000	1.0000
0.0001	10000	0.575	58.936		0.985	1.00000	1.00000	1.00000	1.00000	1.00000	1.00000	1.0000

Grid Level 6 - 64.0 Square Miles												
Probability	Recurrence Interval	Fire Factor Frequency Using Extreme Value Probability Distributions				Fire Factor Frequency Using Plotting Position Distributions						Percentile Analysis
p	T	Normal	Log-Normal	LP3	Gumbel	Weibull	California	Cunnane	Gringorton	Adamowski	Hazen	
0.990	1.01	-0.20100	0.00005	0.00003	-0.12693	0.00002	0.00002	0.00002	0.00002	0.00002	0.00002	0.0000
0.800	1.25	-0.041	0.001	0.001	-0.038	0.00132	0.00133	0.00132	0.00132	0.00132	0.00132	0.0013
0.500	2	0.050	0.009	0.010	0.033	0.01050	0.01051	0.01050	0.01050	0.01050	0.01050	0.0105
0.200	5	0.141	0.057	0.058	0.128	0.06098	0.06100	0.06097	0.06096	0.06097	0.06096	0.0610
0.100	10	0.189	0.150	0.134	0.191	0.13701	0.13701	0.13673	0.13670	0.13687	0.13664	0.1370
0.040	25	0.240	0.422	0.307	0.271	0.29374	0.29379	0.29330	0.29326	0.29345	0.29320	0.2938
0.020	50	0.272	0.824	0.507	0.330	0.43881	0.43884	0.43747	0.43734	0.43796	0.43713	0.4389
0.010	100	0.302	1.505	0.780	0.389	0.55801	0.55806	0.55748	0.55743	0.55766	0.55736	0.5581
0.005	200	0.329	2.611	1.141	0.448	0.72000	0.72000	0.72000	0.72000	0.72000	0.72000	0.7200
0.002	500	0.361	5.091		0.525	0.90000	0.90000	0.89775	0.89730	0.89935	0.89661	0.9000
0.001	1000	0.384	8.132		0.584	0.92188	0.92190	0.91560	0.91501	0.91766	0.91413	0.9219
0.0001	10000	0.452	32.607		0.778							1.0000

Grid Level 7 - 100.0 Square Miles												
Probability	Recurrence Interval	Fire Factor Frequency Using Extreme Value Probability Distributions				Fire Factor Frequency Using Plotting Position Distributions						Percentile Analysis
p	T	Normal	Log-Normal	LP3	Gumbel	Weibull	California	Cunnane	Gringorton	Adamowski	Hazen	
0.990	1.01	-0.16120	0.00004	0.00002	-0.10128	0.00001	0.00001	0.00001	0.00001	0.00001	0.00001	0.0000
0.800	1.25	-0.031	0.001	0.001	-0.030	0.00129	0.00129	0.00129	0.00129	0.00129	0.00129	0.0013
0.500	2	0.042	0.008	0.009	0.028	0.00913	0.00917	0.00913	0.00913	0.00913	0.00913	0.0092
0.200	5	0.116	0.049	0.051	0.105	0.05203	0.05206	0.05198	0.05198	0.05200	0.05197	0.0521
0.100	10	0.154	0.131	0.113	0.156	0.11752	0.11754	0.11748	0.11748	0.11750	0.11746	0.1175
0.040	25	0.195	0.370	0.246	0.221	0.24199	0.24201	0.24180	0.24177	0.24187	0.24174	0.2420
0.020	50	0.222	0.725	0.393	0.269	0.35052	0.35053	0.35008	0.35003	0.35026	0.34995	0.3505
0.010	100	0.245	1.328	0.583	0.316	0.45249	0.45266	0.45093	0.45082	0.45132	0.45066	0.4528
0.005	200	0.267	2.309	0.818	0.364	0.53393	0.53397	0.53112	0.53084	0.53211	0.53042	0.5340
0.002	500	0.294	4.515		0.426	0.63733	0.63738	0.62998	0.62959	0.63134	0.62901	0.6374
0.001	1000	0.312	7.227		0.473	0.74175	0.74179	0.71667	0.71384	0.72660	0.70958	0.7418
0.0001	10000	0.367	29.147		0.630							0.8141

Grid Level 8 - 256.0 Square Miles												
Probability	Recurrence Interval	Fire Factor Frequency Using Extreme Value Probability Distributions				Fire Factor Frequency Using Plotting Position Distributions						Percentile Analysis
p	T	Normal	Log-Normal	LP3	Gumbel	Weibull	California	Cunnane	Gringorton	Adamowski	Hazen	
0.990	1.01	-0.13312	0.00006	0.00003	-0.08255	0.00002	0.00002	0.00002	0.00002	0.00002	0.00002	0.0000
0.800	1.25	-0.024	0.001	0.002	-0.022	0.00151	0.00151	0.00151	0.00151	0.00151	0.00151	0.0015
0.500	2	0.038	0.008	0.010	0.026	0.01057	0.01060	0.01057	0.01057	0.01057	0.01057	0.0106
0.200	5	0.101	0.050	0.051	0.092	0.05168	0.05170	0.05165	0.05165	0.05166	0.05164	0.0517
0.100	10	0.133	0.125	0.106	0.135	0.10662	0.10666	0.10651	0.10651	0.10652	0.10651	0.1067
0.040	25	0.168	0.336	0.210	0.189	0.20702	0.20705	0.20680	0.20677	0.20688	0.20674	0.2071
0.020	50	0.190	0.634	0.315	0.230	0.28874	0.28880	0.28665	0.28628	0.28794	0.28572	0.2889
0.010	100	0.210	1.125	0.441	0.270	0.34223	0.34224	0.34192	0.34189	0.34203	0.34185	0.3423
0.005	200	0.228	1.899	0.586	0.310	0.48052	0.48057	0.47686	0.47649	0.47814	0.47594	0.4806
0.002	500	0.251	3.584		0.363	0.61556	0.61559	0.60951	0.60915	0.61126	0.60861	0.6156
0.001	1000	0.266	5.595		0.402	0.63804	0.63807	0.63087	0.63066	0.63162	0.63034	0.6381
0.0001	10000	0.313	20.954		0.535							0.7363

Grid Level 9 - 400.0 Square Miles												
Probability	Recurrence Interval	Fire Factor Frequency Using Extreme Value Probability Distributions				Fire Factor Frequency Using Plotting Position Distributions						Percentile Analysis
p	T	Normal	Log-Normal	LP3	Gumbel	Weibull	California	Cunnane	Gringorton	Adamowski	Hazen	
0.990	1.01	-0.10184	0.00304	0.00439	-0.06288	0.00001	0.00001	0.00001	0.00001	0.00001	0.00001	0.0000
0.800	1.25	-0.017	0.013	0.013	-0.016	0.00127	0.00128	0.00128	0.00128	0.00128	0.00128	0.0013
0.500	2	0.030	0.031	0.028	0.021	0.00916	0.00918	0.00916	0.00916	0.00916	0.00916	0.0092
0.200	5	0.078	0.071	0.068	0.071	0.04090	0.04093	0.04087	0.04087	0.04087	0.04087	0.0410
0.100	10	0.103	0.109	0.114	0.104	0.08405	0.08406	0.08380	0.08376	0.08392	0.08371	0.0841
0.040	25	0.130	0.174	0.204	0.146	0.15385	0.15403	0.15267	0.15263	0.15281	0.15257	0.1542
0.020	50	0.147	0.235	0.303	0.178	0.21794	0.21796	0.21761	0.21758	0.21773	0.21753	0.2180
0.010	100	0.163	0.308	0.440	0.209	0.28734	0.28736	0.28645	0.28636	0.28676	0.28623	0.2874
0.005	200	0.177	0.395	0.626	0.239	0.34825	0.34826	0.34784	0.34780	0.34798	0.34773	0.3483
0.002	500	0.194	0.533		0.280	0.42965	0.42965	0.42950	0.42948	0.42955	0.42946	0.4297
0.001	1000	0.206	0.658		0.311	0.48489	0.48494	0.46667	0.46485	0.47305	0.46212	0.4850
0.0001	10000	0.242	1.228		0.413							0.5541

Grid Level 10 - 1024.0 Square Miles												
Probability	Recurrence Interval	Fire Factor Frequency Using Extreme Value Probability Distributions				Fire Factor Frequency Using Plotting Position Distributions						Percentile Analysis
p	T	Normal	Log-Normal	LP3	Gumbel	Weibull	California	Cunnane	Gringorton	Adamowski	Hazen	
0.990	1.01	-0.10267	0.00007	0.00002	-0.06329	0.00003	0.00004	0.00004	0.00004	0.00004	0.00004	0.0000
0.800	1.25	-0.017	0.001	0.002	-0.016	0.00140	0.00141	0.00140	0.00140	0.00140	0.00140	0.0014
0.500	2	0.031	0.008	0.010	0.022	0.00925	0.00926	0.00925	0.00925	0.00925	0.00925	0.0093
0.200	5	0.079	0.041	0.043	0.072	0.04283	0.04285	0.04282	0.04281	0.04282	0.04281	0.0429
0.100	10	0.105	0.101	0.080	0.106	0.08783	0.08788	0.08765	0.08763	0.08771	0.08761	0.0879
0.040	25	0.132	0.262	0.142	0.148	0.14655	0.14664	0.14573	0.14565	0.14602	0.14552	0.1467
0.020	50	0.149	0.483	0.195	0.180	0.21444	0.21446	0.21399	0.21389	0.21417	0.21374	0.2145
0.010	100	0.165	0.840	0.252	0.211	0.27428	0.27442	0.27181	0.27181	0.27182	0.27180	0.2746
0.005	200	0.179	1.392	0.312	0.242	0.35260	0.35284	0.34739	0.34726	0.34782	0.34708	0.3531
0.002	500	0.196	2.569		0.283	0.45089	0.45098	0.44136	0.44049	0.44439	0.43919	0.4511
0.001	1000	0.208	3.948		0.314	0.48598	0.48549	0.47749	0.47567	0.48387	0.47294	0.4962
0.0001	10000	0.245	14.114		0.418	0.04860						0.5550

Grid Level 11 - 1600.0 Square Miles												
Probability	Recurrence Interval	Fire Factor Frequency Using Extreme Value Probability Distributions				Fire Factor Frequency Using Plotting Position Distributions						Percentile Analysis
p	T	Normal	Log-Normal	LP3	Gumbel	Weibull	California	Cunnane	Gringorton	Adamowski	Hazen	
0.990	1.01	-0.10649	0.00170	0.00236	-0.06592	0.00012	0.00013	0.00012	0.00012	0.00012	0.00012	0.0001
0.800	1.25	-0.019	0.009	0.009	-0.017	0.00230	0.00230	0.00230	0.00230	0.00230	0.00230	0.0023
0.500	2	0.031	0.022	0.021	0.021	0.01001	0.01005	0.01001	0.01001	0.01001	0.01001	0.0101
0.200	5	0.081	0.056	0.055	0.074	0.04949	0.04962	0.04949	0.04949	0.04949	0.04949	0.0498
0.100	10	0.107	0.092	0.095	0.108	0.07606	0.07606	0.07606	0.07606	0.07606	0.07606	0.0761
0.040	25	0.135	0.154	0.178	0.152	0.13526	0.13555	0.13257	0.13230	0.13350	0.13190	0.1358
0.020	50	0.153	0.215	0.271	0.185	0.21043	0.21081	0.20316	0.20243	0.20569	0.20134	0.2112
0.010	100	0.169	0.291	0.400	0.217	0.32375	0.32375	0.32375	0.32375	0.32375	0.32354	0.3238
0.005	200	0.184	0.383	0.579	0.249	0.39958	0.39962	0.39657	0.39622	0.39781	0.39568	0.3996
0.002	500	0.202	0.536		0.291	0.46972	0.46998	0.41685	0.41156	0.43535	0.40469	0.4702
0.001	1000	0.214	0.677		0.323			0.51693	0.51164	0.53547	0.50369	0.5706
0.0001	10000	0.251	1.357		0.430							0.6617